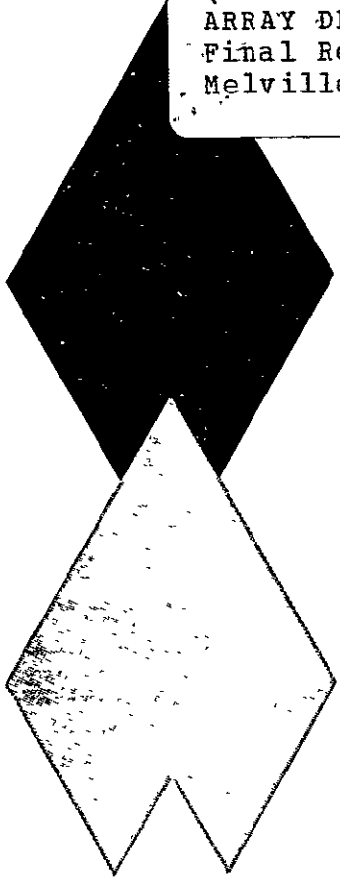


NASA CR-152460

Copy #3

(NASA-CR-152460) ADAPTIVE MULTIBEAM PHASED ARRAY DESIGN FOR A SPACELAB EXPERIMENT Final Report (Airborne Instruments Lab., Melville, N.Y.) 296 p HC A13/MF A01	N77-20150 Unclas CSCL 22A G3/16 . 24599
---	---



ADAPTIVE MULTIBEAM PHASED ARRAY
DESIGN FOR A SPACELAB EXPERIMENT

THOMAS T. NOJI

AIL, a Division of Cutler-Hammer
Walt Whitman Road
Melville, New York 11746

MARCH 1977
Final Report

PREPARED FOR:
GODDARD SPACE FLIGHT CENTER
Greenbelt, Maryland 20771



TECHNICAL REPORT STANDARD TITLE PAGE

1. Report No.		2. Government Accession No.		3. Recipient's Catalog No.	
4. Title and Subtitle ADAPTIVE MULTIBEAM PHASED ARRAY DESIGN FOR A SPACELAB EXPERIMENT				5. Report Date MARCH 1977	
				6. Performing Organization Code	
7. Author(s) T. T. Noji, S. Fass, A. M. Fuoco and C. D. Wang				8. Performing Organization Report No. C751	
9. Performing Organization Name and Address AIL, a Division of Cutler-Hammer Walt Whitman Road Melville, New York 11746				10. Work Unit No.	
				11. Contract or Grant No. NAS5-23469	
				13. Type of Report and Period Covered FINAL REPORT	
12. Sponsoring Agency Name and Address: National Aeronautics and Space Administration Goddard Space Flight Center Greenbelt, Maryland 20771				14. Sponsoring Agency Code	
15. Supplementary Notes					
16. Abstract <p>This final report describes the parametric tradeoff analyses and design for an Adaptive Multibeam Phased Array (AMPA) for a Spacelab experiment. This AMPA Experiment System was designed with particular emphasis to maximize channel capacity and minimize implementation and cost impacts for future austere Maritime and Aeronautical users, operating with a low gain hemispherical coverage antenna element, low effective radiated power (ERP), and low antenna gain-to-system noise temperature ratio (G/T_s).</p> <p>The AMPA Experiment System has been designed to provide two (2) independently steerable adaptive beams on receive and two (2) independently steerable beams on transmit. On receive each beam can operate in the pointed, fully adaptive or directed-adaption modes; and on transmit, each beam can operate in the pointed, or open loop beam and null forming modes that uses user ephemeris data to point the main beam on the desired user and places spatial pattern nulls on co-channel users. In addition, the Experiment System can operate in a pseudoretrodirective mode on transmit, using received signal information to point the main beam to the desired user and place spatial pattern nulls on co-channel users.</p> <p>The Experiment System can operate in a simplex mode on receive as well as transmit to service four (4) independent users, or full duplex to provide two-way communication to two (2) users. The system can also operate in a bentpipe mode to provide a direct user-to-user link.</p> <p>In addition, as a by-product, the AMPA Experiment System can provide (1) direction finding capability for a search and rescue mission, (2) high resolution readout of closely spaced signal sources, as for data collection or future wrist transceiver operators, and (3) orbital antenna test range to evaluate large ground based antennas.</p>					
17. Key Words Adaptive Phased Array Spacelab Experiment Multibeam Array			18. Distribution Statement		
19. Security Classif. (of this report) Unclassified		20. Security Classif. (of this page) Unclassified		21. No. of Pages 294	22. Price

PREFACE

The objectives of this study are to establish the requirements and design for an L-band communication experiment, based upon the requirements for an Adaptive Multibeam Phased Array (AMPA) for an operational Maritime and Aeronautical Satellite system located in geostationary orbit. The L-band communication experiment will be conducted on one or more lower orbit Spacelab mission(s) and will incorporate the key performance, design and implementation approaches that will evaluate the viability of AMPA for the operational system. Particular emphasis was given to maximizing the channel capacity and to minimizing the implementation and cost impacts to the user terminal. The operational system tradeoff analyses have shown that an array of 32 high gain elements in space with all beam and signal processor functions located on the ground could support austere user terminals having low gain, hemispherical coverage elements. In addition, the tradeoff analysis has shown (1) a thinned array as compared to a fully filled array provides improved resolution to resolve signals and closely spaced interference sources, (2) improved spatial dispersion of intermodulation products, and (3) improved direction finding accuracy to locate signal sources.

These key parameters from the operational system were then scaled for the AMPA design for a Spacelab experiment. However, rather than high gain elements, the AMPA Experiment System uses 32 low gain, hemispherical coverage elements that provides horizon-to-horizon coverage, or approximately +70 degrees, as seen from the Spacelab orbital altitude. The array has been designed as a variable aperture array, so that meaningful experiment results could be obtained as a function of aperture sizes for application in the design of future operational systems.

In addition, the Experiment System has been designed to provide the same effective radiated power and have the same receiver front end as required for the operational system, so that the design could be subsequently applied for an experiment at either Spacelab or geostationary altitudes.

The Experiment System has been designed as two subsystems, Pallet and Spacelab Module subsystems, to represent the Spaceborne and Ground based segments of the Beam Process on Ground approach. The system will provide 2 independently steerable adaptive beams on receive, operating in the pointed, fully adaptive and directed-adaption modes; and to provide 2 independently steerable beams on transmit, operating in the pointed and open loop beam and null-forming modes, using user ephemeris data to point a beam to the desired user, and spatial nulls to co-channel users. Furthermore, the system can operate pseudo-retrodirective on transmit, using measured signal location data to point the beam on the desired user and spatial nulls on interference sources.

The Experiment System can operate in the simplex (one-way communication) mode with 4 independent user terminals, or operate in the full duplex (2-way communication) mode with 2 independent users. In addition, the Experiment System can operate in the bentpipe mode to provide direct user-to-user communication.

As a by-product, the Experiment System can provide (1) high resolution capability to resolve 2 closely spaced sources such as for data collection or for future personalized wrist transceiver operators, (2) direction finding capability to locate signal geolocation as required for a search and rescue mission, and (3) orbital test range to evaluate the performances of large ground based antennas.

The Experiment System weighs 235 kg and requires 383 watts of prime power, exclusive of the digital processor network.

The study has shown the viability and practicality of an AMPA system for a Spacelab Experiment. It is recommended that a hardware system be designed, developed and flight tested to fully evaluate the achievable performances for the AMPA Experiment System and to develop and establish a design base that could be applied in the design of future satellite systems in geostationary orbit to service and support the austere Maritime and Aeronautical users.

TABLE OF CONTENTS

<u>SECTION</u>	<u>TITLE</u>	<u>PAGE</u>
1.0	INTRODUCTION AND SUMMARY	1-1
2.0	DESIGN REQUIREMENTS	2-1
3.0	OPERATIONAL SYSTEM	3-1
3.1	General	3-1
3.2	Link Analysis for Operational System	3-3
3.3	Adaptive Approaches	3-4
3.3.1	General	3-4
3.4	Operational System Design	3-10
4.0	SPACELAB EXPERIMENT SYSTEM TRADEOFF ANALYSIS AND DESIGN	4-1
4.1	General Experiment System Considerations	4-1
4.1.1	Key Operational System Parameters to Scale for Spacelab Experiment	4-3
4.1.2	Experiment System Link Analysis	4-14
4.1.3	Dynamic Signal Environment	4-22
4.1.4	Description of the AMPA Experiment System	4-25
4.1.4.1	General	4-25
4.1.4.2	Detailed Block Diagram	4-28
4.1.4.3	AMPA Experiment System Family Tree	4-33
4.2	Pallet Mounted Subsystem	4-36
4.2.1	Array Assembly	4-36
4.2.1.1	General	4-36
4.2.1.2	Element Design	4-36
4.2.1.3	Array Design	4-42
4.2.2	Transmitter/Receiver Unit	4-60
4.2.2.1	General	4-60
4.2.2.2	Transmitter Module Design	4-60
4.2.2.2.1	Overall Description	4-60
4.2.2.2.2	Tradeoff Analysis	4-63
4.2.2.2.3	Detailed Design	4-66
4.2.2.3	Receiver Module Design	4-68
4.2.2.3.1	Overall Description	4-68
4.2.2.3.2	Tradeoff Analysis	4-72
4.2.2.3.3	Detailed Design	4-74
4.2.2.4	Power Monitor Sampling Switch	4-77
4.2.2.5	Layout	4-77
4.2.3	Frequency Source	4-79
4.2.3.1	General	4-79
4.2.3.2	Tradeoff Analysis - Phased Locked Loop Vs. Multiplier	4-79

TABLE OF CONTENTS (cont'd)

<u>SECTION</u>	<u>TITLE</u>	<u>PAGE</u>
4.2.3.3	Design	4-81
4.2.4	Power Conditioner	4-85
4.2.4.1	General	4-85
4.2.5	Pallet Mounted Subsystem Layout	4-86
4.2.5.1	Recommended Hard Mounted Configuration	4-86
4.2.5.2	Alternate Hard Mounted Configuration	4-86
4.2.5.3	Optional Erectable Configuration	4-86
4.3	Spacelab Module Mounted Subsystem	4-93
4.3.1	Receiver Processor Unit	4-93
4.3.1.1	General	4-93
4.3.1.2	Tradeoffs	4-96
4.3.1.3	Design of the Beam Forming Network Subassembly	4-105
4.3.1.4	Design of the Channel Downconverter Subassemblies and the Sampling Switch	4-105
4.3.1.5	Design of the Correlator Processor Subassembly	4-108
4.3.1.6	Design of the Array Divider and Array Summer Matrices	4-113
4.3.1.7	Design of the Doppler Processor Subassembly	4-114
4.3.1.8	Modem Subassembly	4-119
4.3.1.9	Data Conditioner	4-121
4.3.1.10	Adaptive Processor Layout	4-125
4.3.2	Transmitter Beam Processor Assembly	4-127
4.3.2.1	Overall Description	4-127
4.3.2.2	Transmitter Beam Processor	4-127
4.3.2.2.1	General	4-127
4.3.2.2.2	Tradeoff Analysis	4-130
4.3.2.2.3	Detailed Design	4-131
4.3.2.3	IM Simulator	4-133
4.3.2.3.1	General	4-133
4.3.2.3.2	Tradeoffs	4-138
4.3.2.3.3	Design of the IM Simulator	4-140
4.3.2.4	Summer/Amplifier Matrix	4-142
4.3.3	Digital Processor Network	4-145
4.3.3.1	General	4-145
4.3.3.2	Tradeoffs	4-147
4.3.3.3	Design	4-149
4.3.3.4	Layout	4-150
4.3.4	Interface Logic Assembly	4-151
4.3.4.1	General	4-151
4.3.4.2	Tradeoffs	4-151
4.3.4.3	Design	4-151
4.3.4.4	Layout	4-153
4.3.5	Frequency Source	4-155
4.3.5.1	General	4-155
4.3.5.2	Frequency Generation - Tradeoff Analysis	4-155

TABLE OF CONTENTS (cont'd)

<u>SECTION</u>	<u>TITLE</u>	<u>PAGE</u>
	4.3.5.3 Design	4-157
	4.3.5.4 Layout	4-159
	4.3.6 AMPA Control Unit	4-160
	4.3.6.1 General	4-160
	4.3.6.2 Tradeoffs	4-160
	4.3.6.3 Design	4-160
	4.3.6.3.1 Ground-Based Unit	4-160
	4.3.6.3.2 Spaceborne Unit	4-162
	4.3.7 Power Conditioner	4-164
	4.3.7.1 General	4-164
	4.3.7.2 Tradeoffs	4-166
	4.3.7.2.1 Type of Power Supply	4-166
	4.3.7.2.2 Single or Dual Outputs	4-167
	4.3.7.3 Design	4-169
	4.3.8 Spacelab Module Mounted Subsystem Layout	4-171
	4.3.9 Thermal Analysis of the AMPA Experiment System	4-173
	4.3.9.1 General	4-173
	4.3.9.2 Heat Generating Pallet Mounted Equipment	4-173
	4.3.9.3 Passive Pallet Mounted Equipment	4-173
	4.3.9.4 Spacelab Module Subsystem	4-174
5.0	EXPERIMENT PLAN	5-1
5.1	General	5-1
5.2	Communication Experiments	5-1
5.2.1	General	5-1
5.2.2	Simplex and Full Duplex Modes	5-4
5.2.3	Bentpipe Mode	5-9
5.2.4	Frequency Reuse Experiment	5-9
5.2.5	IM Spatial Dispersion Experiment	5-12
5.3	Direction Finding Experiment	5-15
5.4	Resolution Experiment	5-17
5.5	Orbital Antenna Test Range Experiment	5-19
6.0	IDENTIFICATION OF PROBLEM AREAS	6-1
7.0	ESTIMATED SCHEDULE AND COST FOR THE HARDWARE EXECUTION PHASE	7-1
8.0	PROGRAM RECOMMENDATION AND SUMMARY	8-1

TABLE OF CONTENTS (cont'd)

		<u>PAGE</u>
APPENDIX A	Design Guidelines Used for an Advanced Operational AMPA System in Geostationary Orbit	A-1
APPENDIX B	System Analyses for an Advanced Operation Satellite Relay System to support Future Maritime and Aeronautical Users	B-1
APPENDIX C	Weight and Power Tradeoff Analysis for the AMPA Experiment System as a Function of the Number of Beams and Number of Array Elements	C-1

LIST OF ILLUSTRATIONS

<u>Figure</u>	<u>Title</u>	<u>Page</u>
1-1	AMPA Experiment System	1-7
3.3-1	Simplified 32 Element Gradient Adaptive Processor	3-5
3.3-2	Advanced Operational System Concept	3-11
4.1-1	Dwell Time as a Function of Signal Offset From Flight Path	4-2
4.1-2	Array Characteristics for Spacelab Experiment	4-6
4.1-3	Experiment Requirements	4-7
4.1-4	AMPA Cost Vs. Number of Beams	4-12
4.1-5	System Noise Temperature Geometry for Return Link	4-16
4.1-6	System Noise Temperature Geometry for Forward Link	4-17
4.1-7	CNR Requirements in Tandem Link	4-21
4.1-8	Spatial Geometry of AMPA and Signal Source	4-23
4.1-9	Signal/Array - Relative Angular Rate of Motion	4-24
4.1-10	AMPA Experiment System	4-26
4.1-11	Block Diagram of AMPA Experiment System	4-29
4.1-12	AMPA Experiment System Family Tree	4-34
4.2-1	Components of Pallet Subsystem	4-37
4.2-2	Achievable Coverage	4-40
4.2-3	Modified Flared Cone Turnstile Antenna Design	4-43
4.2-4	Flared Cone Turnstile Antenna Pattern	4-44
4.2-5	Variable Aperture 32 Element Instrument Array	4-45
4.2-6	Array Characteristics for Spacelab Experiment	4-46
4.2-7	Principal Cardinal Plane Pattern for Filled Array	4-47
4.2-8	Variable Aperture : Wine Rack Concept	4-49
4.2-9	Variable Aperture : Umbrella Concept	4-50
4.2-10	Variable Aperture : Variable Iris Concept	4-51
4.2-11	Variable Aperture : Flex Rib Concept	4-52
4.2-12	Variable Aperture Phased Array - Electrically Switched	4-54
4.2-13	Principal Cardinal Plane Pattern - Variable Aperture Phased Array (Aperture Size Factor = 1.0)	4-55
4.2-14	Principal Cardinal Plane Pattern - Variable Aperture Phased Array (Aperture Size Factor = 2.0)	4-56
4.2-15	Principal Cardinal Plane Pattern - Variable Aperture Phased Array (Aperture Size Factor = 3.0)	4-57
4.2-16	Principal Cardinal Plane Pattern - Variable Aperture Phased Array (Aperture Size Factor = 4.23)	4-58
4.2-17	Array Performance Vs. Aperture Size Factor	4-59
4.2-18	Transmitter Module Block Diagram	4-61
4.2-19	Receiver Module Block Diagram	4-69
4.2-20	Antenna Element and Transmitter/Receiver Module	4-78
4.2-21	Pallet Frequency Source Block Diagram	4-82
4.2-22	Pallet Equipment - Switched Aperture Phased Array	4-87
4.2-23	Pallet Equipment - Variable Aperture Phased Array	4-88
4.2-24	Pallet Equipment - Filled Array Configuration	4-89
4.2-25	Pallet Equipment - Thinned Array Configuration	4-90
4.2-26	Optional Erectable AMPA Array Configuration	4-91

LIST OF ILLUSTRATIONS (cont.)

<u>Figure</u>	<u>Title</u>	<u>Page</u>
4.3-1	Components of Spacelab Module Subsystem	4-94
4.3-2	AMPA Adaptive Receiver Processor	4-95
4.3-3	Signal Scenario for Dynamic Environment Simulation	4-98
4.3-4	Adaptive Performance Vs. Process Speeds - No RFI	4-100
4.3-5	Adaptive Performance Vs. Process Speeds with Three RFI's	4-101
4.3-6	Adaptive Performance Vs. Number of Bits with Three RFI's for the Dynamic Environment	4-104
4.3-7	Dual Weighting Network Design	4-106
4.3-8	Correlator Processor & Downconverter Subassemblies	4-111
4.3-9	Doppler Processor Subassembly	4-115
4.3-10	Doppler Tracking Loop and Data Demodulator for BPSK	4-117
4.3-11	Doppler Tracking Loop for NBFM Voice	4-118
4.3-12	Modem Subassembly	4-120
4.3-13	Data Conditioner Interfaces	4-122
4.3-14	AMPA Data Conditioner	4-124
4.3-15	Adaptive Processor (Two Drawers)	4-126
4.3-16	Transmitter Beam Processor	4-128
4.3-17	Signal Scenario for Intermodulation Analysis	4-136
4.3-18	Spatial Dispersion of IM Products - 10 Signal Case	4-137
4.3-19	Spatial Dispersion of IM Products - 20 Signal Case	4-139
4.3-20	IM Simulator Block Diagram	4-141
4.3-21	Transmitter Processor/IM Simulator	4-143
4.3-22	Transmitter Processor and Frequency Source	4-144
4.3-23	Digital Processor Network Functional Block Diagram	4-146
4.3-24	Minimal Logic Weighting Network Interface	4-152
4.3-25	Interface Logic	4-154
4.3-26	Spacelab Frequency Source Block Diagram	4-158
4.3-27	Scenario Test Signal Generators	4-161
4.3-28	Front Panel Ground Based Control Unit	4-163
4.3-29	Spacelab Human Interface	4-165
4.4-30	Power Conditioner Block Diagram	4-170
4.3-31	Spacelab Module Subsystem Layout	4-172
5.1	Experiment Scenario (Example)	5-2
5.2	Communication Experiment Simplex Mode	5-5
5.3	Typical AMPA User Signal Scenario for Communication Experiment	5-6
5.4	Signal Scenario for Bentpipe Mode Experiment	5-10
5.5	Frequency Reuse by Zones	5-11
5.6	IM Experiment	5-14
5.7	Search and Rescue	5-16
5.8	Resolution Experiment with AMPA	5-18
5.9	Orbital Antenna Test Range Experiment	5-20
7.1	AMPA Experiment System-Hardware Execution Phase	7-2

LIST OF TABLES

<u>Table</u>	<u>Title</u>	<u>Page</u>
2-1	Design Requirements for Spacelab Mounted AMPA Experiment System	2-2
2-2	Candidate List of Spacelab AMPA Experiments	2-6
3-1	Key Operational System Requirements for an Advanced Maritime and Aeronautical Satellite Relay System	3-3
3.3-1	Comparison of Array Steering Algorithms	3-9
4.1-1	AMPA Scaling for Experiment	4-4
4.1-2	Number of Transmit Channels	4-9
4.1-3	Weight and Power Requirements for Spacelab Multiple Beam Experiment Using 32 Element Array	4-10
4.1-4	AMPA Spacelab Link Requirements	4-19
4.2-1	Candidate Element Types	4-41
4.2-2	Transmitter Module Performance Characteristics	4-62
4.2-3	Receiver Module Performance Characteristics	4-71
4.2-4	Frequency Source Performance Characteristics	4-83
4.3-1	Performance Vs. Weighting Network Resolution for the Static Environment	4-103
4.3-2	Characteristics for Bi-Phase Attenuator for Weighting Networks	4-107
4.3-3	Characteristics for Bandpass and Band Reject Filters	4-109
4.3-4	Characteristics for the Channel Sampling Switch	4-110
4.3-5	Characteristics of Correlator	4-112
4.3-6	Transmitter Beam Processor Performance Characteristics	4-129
4.3-7	Candidate Digital Processors for AMPA	4-148
4.3-8	Frequency Source Performance Characteristics	4-156
4.3-9	Comparison of Dissipative and Switching Regulators	4-168
5-1	List of Simplex and Full Duplex Communications Experiments	5-8
7-1	Estimated Cost for the AMPA Experiment System	7-3

1.0 INTRODUCTION AND SUMMARY

This study (NASA Contract No. NAS5-23469) has shown the viability of conducting an experiment on Spacelab missions to investigate and to evaluate an adaptive multibeam phased array (AMPA). This AMPA experiment has been based on a conceptual system approach that meets future Maritime and Aeronautical Satellite System needs with particular emphasis to maximize service capacity and overall cost effectiveness. The results of the AMPA experiment will provide a vital technology base that minimizes the risk, schedule and cost to realize an advanced operational system in geostationary orbit to service and support the expected high traffic density of the future.

• General Features

This study has shown that, by placing a high gain antenna in space, the user terminals can operate with a low cost, low gain hemispherical coverage element. This element requires no stabilization, minimal structure support, no gimbaled antenna pedestal mount nor an antenna drive system to continuously point its beam to the satellite relay system, as required for the four foot dish used on current MARISAT terminals. Not only is the antenna cost savings significant on a user terminal, but when multiplied by the thousands of expected users, the overall user terminal cost saving rises sharply. On the other hand, the increased complexity and cost added to the relay repeater system is relatively small since only a few relay systems are required.

The small antenna requirement makes the satellite relay system available to the smaller, austere users as well; not just the large tonnage vessels as in the current MARISAT system. It also provides a significantly larger number of channels for an aeronautical application than can be accommodated in the currently planned AEROSAT program. From both implementation as well as cost impact, the operating system, using the AMPA concept, is more universally suited to servicing and supporting the vast majority of potential users.

The AMPA concept for the geostationary applications performs all beam and signal processing functions on the ground; consequently, the spaceborne segment is essentially a bentpipe (turnaround) repeater and independent of the number of beams except for the transmitter. Using the beam process on

ground approach, the geostationary AMPA system provides 50 or more simultaneous beams on receive as well as on transmit for a typical spacecraft payload capacity of 182 kg (400 lbs.) and 1.6 kilowatt of prime power.

The AMPA Experiment System* has been scaled to meet the key design parameters and to evaluate the key performance criteria essential to the design of the conceptual system operating in geostationary system. Key design parameters for scaling are:

- Same number of elements in the array (32)
- Same receiver front end with 2 dB noise figure
- Radiate the same transmit power per beam (+8.2 dBw)

Designing the RF front end of the Experiment System, except for the array elements, to be compatible with the Spacelab and geostationary application provides the flexibility to use these components for an AMPA experiment at either altitude. Since the array elements provide different coverages (18 versus 160 degrees), the same elements cannot be used at both altitudes.

Rather than using 50 or more beams as in the conceptual operational system, the Experimental System will be designed for two independently steerable beams on receive as well as on transmit, as being a cost effective method to demonstrate the design as well as the achievable performance of the adaptive multibeam phased array. The two beams on receive and transmit will also be compatible with the estimated size, weight and prime power constraint for the Spacelab experiment.

This study has assumed that the total Maritime or Aeronautical operating frequency spectrum is serviced with three operational satellite systems, typically located over the Pacific, Atlantic and Indian Oceans for nearly global coverage. Each satellite covers one-third of the allocated spectrum, assumed to be 7.5 MHz for this study's purposes.

*The phrase "AMPA Experiment System" is used as shorthand for the AMPA System for a Spacelab Experiment.

- Potential Experiments

The key modes of operation to be tested in flight, and other experiments to be conducted are:

- Receive Modes of Operation

- Pointed Beam
- Directed-Adaption
- Fully Adaptive

- Transmit Modes of Operation

- Linear Amplifier
- Saturated Amplifier
- Pointed Beam
- Open Loop Beam and Null Forming
- Closed loop (retrodirective) Beam Forming

- Communication Experiments

- Point-to-Point (simplex, full duplex, and bentpipe)
- Frequency Reuse
- Automatic Acquisition and Track
- Spatial Dispersion of Intermodulation Products
- Direction Finding for Search and Rescue Experiment
- Multi-user Resolution Experiment (Data Collection and Personalized Wrist Radio)
- Orbital Pattern Measurement Experiment

- Adaptive Operation

The Experiment System is designed to operate with three adaptive algorithms on receive and two on transmit. On receive the Experiment System can operate in the pointed, fully adaptive or directed-adaption modes. In the pointed mode, the beam is steered to a desired user, using known user ephemeris data, and the digital processor will track the user during the contact period using known Spacelab angular velocity. The pointed mode does not

place spatial nulls in the direction of undesired interference signals (RFI sources) and is useful only in signal environments containing no RFI. It is used in the experiment primarily as a reference to compare the achievable performances of the other algorithms.

The fully adaptive algorithm uses a unique user signature (CW tone(s) used for experiment) to identify the desired signal; all other received signals being considered interferences or RFI's. The adaptive algorithm uses this unique signature to acquire and track the desired user, while nulling all others in order to maximize the signal-to-interference plus noise ratio $[S/(I+N)]$.

The directed-adaptation algorithm combines the pointed and fully adaptive algorithm, using a pseudo signal (by software) that steers the beam to a desired location while an adaptive algorithm continuously nulls all RFI's. This mode is particularly powerful since it:

- Provides a means to increase received signal level of the desired signal
- Provides a search and scan capability while simultaneously nulling all RFI's.
- Reduces acquisition time by initially steering the beam in the approximate area of the desired signal; or localizes the area wherein the desired signal is located, and considers all other co-channel signals as RFI's.

All three modes of adaptive algorithm have been implemented in the Experiment System design.

On transmit, pointed and open loop beam and null forming algorithms are used. The pointed mode is the same as on receive. The open loop beam and null forming mode is pseudo-adaptive, and is conducted open loop, using known or measured user (desired and interferers) geo-position data to point a main beam on the desired signal and nulls on the RFI's. The geo-position data may be available from known user ephemeris information, or measured from the Spacelab, using a direction finding technique described herein. The known or measured user and Spacelab geo-position data, as well

as array geometry are inputs to an Omniscient Solution algorithm that computes the theoretical "ideal" solution that optimizes the $S/(I+N)$. The outputs of the Omniscient Solution are the inputs to the weighting networks that steer and shape the beam. The purpose of including this mode in the experiment is to determine how "well" can this function be performed open loop. It is important to recognize, however, that deep nulls are not always necessary. For example, a suppression of only 10-15 dB in the direction of a co-channel receiver may be adequate to reduce the interference below his threshold level.

Alternatively, a closed loop fully adaptive retrodirective mode was considered on transmit, using received signal information to form a beam on transmit. This approach requires true phase or time delay measurement on receive in order to prevent beam distortion and beam squint on transmit, resulting in array gain loss of 5 or more dB's at scan limits. The implementation impact for time delay measurement would be considerable; consequently, the closed loop approach has not been included for the AMPA Experiment system.

- Array Element

A 32 element array is employed on the AMPA Experiment System, using modified NASA developed flared-cone turnstile elements that conservatively provide +4.2 dBi gain on peak and +2.2 dBi on the horizon, (+70 degrees). Horizon coverage elements were selected in order to increase the available maximum dwell time on a desired user signal to approximately 10 minutes rather than 1.6 minutes for a reduced +40 degree coverage element as recommended in the RFP Work Statement. The increased coverage provides more time to conduct meaningful AMPA experiments as well as better utilization of the Experiment payload.

- Array Aperture

The study has also shown the impact of using a thinned array as compared to a fully filled array (elements spaced as close as possible with non-overlapping effective apertures). Parametric tradeoff analysis by means of computer simulations have shown the achievable improvements in performance with increased aperture sizes, viz:

- Increased resolution (narrower beams)
- Greater Spatial Dispersion of Intermodulation (IM) products.
- Improved Direction Finding Accuracy

that make it highly desirable to use the largest aperture size, commensurate with implementation on the Pallet Structure.

The array has been designed for the largest size aperture that could be packaged within the maximum allowable payload dimensions of the Orbiter's payload bay without folding the array. As a first estimate, this has resulted in a hard mounted configuration with an effective array aperture of 2.24 meter by 2.24 meter or 4.23 times the filled array aperture. This permits implementation on the First Spacelab Mission that does not allow an erectable platform, as well as on subsequent missions where erection may be permissible. As an option, however, an erectable design has also been shown that rotates the array 90 degrees for stowage and erects the array with an Astro-mast for operation. This configuration allows the array to clear all the Orbiter's structural obstruction and provides a truly horizon coverage in all directions. In addition, rotating the array 90 degrees makes it possible to increase the effective aperture size of the array to approximately 3 meter by 3 meter for even greater improvements in achievable resolution, IM spatial dispersion and direction finding.

- Pallet and Module Mounted Subsystems

The AMPA Experiment System is divided into two subsystems; a Pallet Subsystem containing the 32 element array, multichannel transceiver, frequency source and power conditioner; and the Spacelab Module Subsystem containing the transmitter and receiver beam processors, signal processors and digital processor. These two subsystems correspond to the space and ground segment portions, respectively, of the conceptual operational system in geostationary orbit. Layouts of the subsystems are shown in Figure 1-1.

- Communication Subsystem

The spaceborne AMPA Experiment System provides an ERP of +8.2 dBw per beam or +11.2 dBw for the two beams, and a receiving sensitivity (antenna gain-

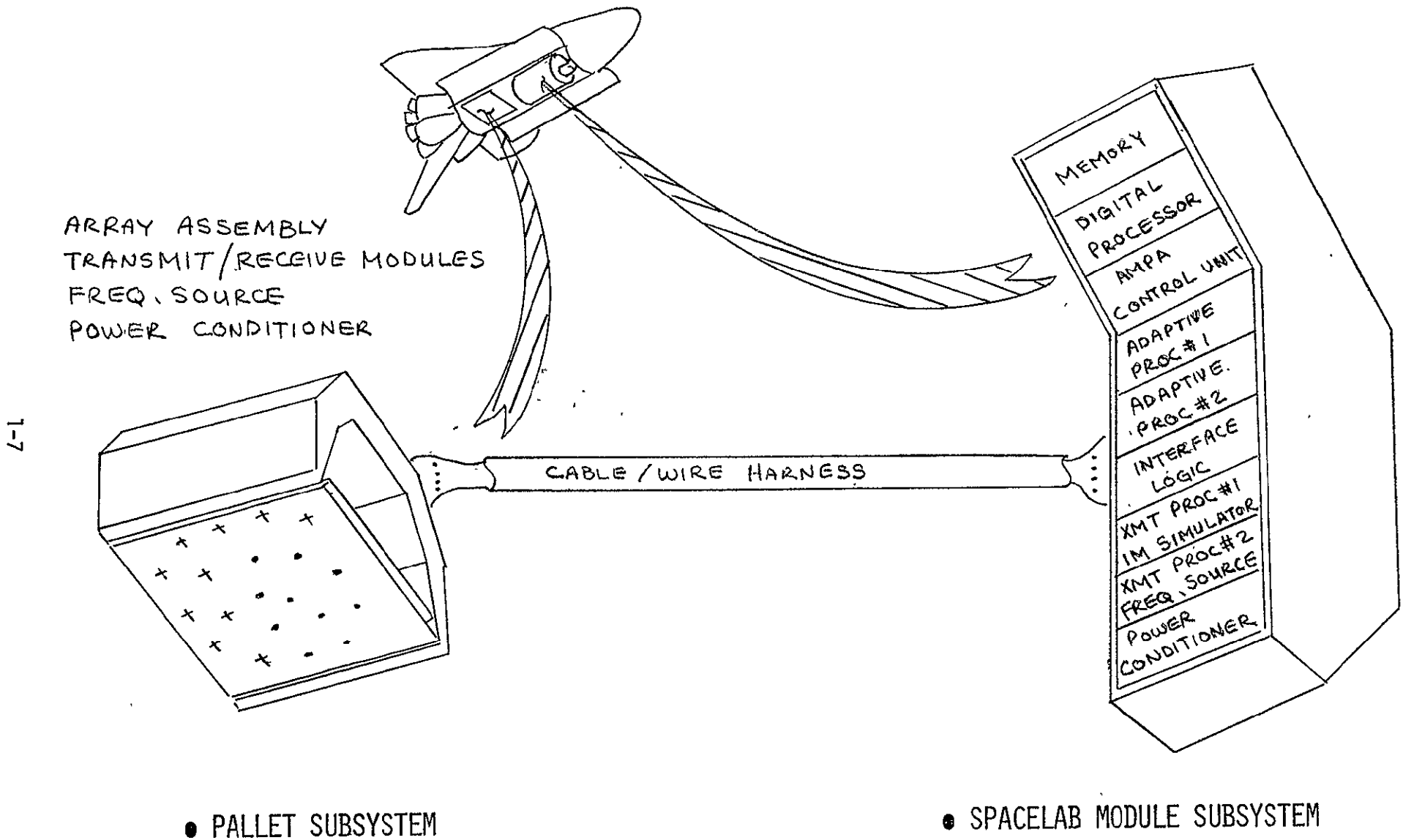


FIGURE 1-1. AMPA EXPERIMENT SYSTEM

to-system noise temperature ratio = G/T_S) of minus 9 dB/°K. The Experiment System supports users with an ERP of +8 dBw and G/T_S of minus 29.9°K. This provides a forward (AMPA-to-user) and return (user-to-AMPA) link system margins of +5.4 dB and +6.3 dB, respectively, for Maritime type users, and +12.4 dB and +13.3 dB, respectively, for Aeronautical type users. The additional system margins for Aeronautical type users are used to provide the additional tandem link carrier-to-noise ratio (CNR) capabilities required for the bentpipe mode (direct user-to-user link without Modem function).

The return link signal is received in one of two 50 kHz channels, at nominally 1640 MHz. The signal is filtered, preamplified in a low noise bipolar transistor amplifier with a 2 dB noise figure and downconverted to 70 MHz in the Pallet Mounted Receiver Module. A Surface Acoustical Wave (SAW) filter is used to reduce the receive band to 2.5 MHz before the signal is sent to the Spacelab Module Subsystem for adaptive beam and signal processing.

On the Module Subsystem, the return link data from each receiver module is divided into two separate adaptive receiver processors. Each processor provides a customized beam for a desired user, operating in either the pointed, directed-adaption or fully adaptive modes. A Doppler Processor subassembly is used to compensate for the doppler frequency shift of +38 kHz maximum for NBFM voice as well as for 4.8 kbps BPSK signals. The output of the array is demodulated, detected and formatted (data conditioned) for recording on the on-board Payload Recorder or for relay to the ground by way of the Orbiter's TDRS multiple access link.

In the forward link, all information to be transmitted to a user originates from the ground (except in the bentpipe mode), and relayed to the Spacelab by way of the TDRSS link. On the Experiment System the forward link information is formatted into analog voice or 4.8 kbps PCM data for modulating a 70 MHz carrier. The 70 MHz IF signal is then inputted to a Transmit Beam Processor where all beam forming functions are performed, in either pointed or open loop beam and null forming modes. All beam and null forming and/or pointing requirements are computed with the aid of a digital processor that uses known user ephemeris data, array geometry and Spacelab geo-position to compute the required inputs to the beam forming-weighting networks.

- IM Simulator

The forward link signal from the two Transmit Beam Processors are combined with eight additional signals from an IM Simulator. The eight IM signals are pointed in fixed random directions. The two variable plus eight fixed beams provide a total of 10 beams that are used to evaluate the achievable spatial dispersion with the AMPA array. This IM experiment is a very significant experiment because it provides a basis to establish the operating level for the L-Band transmitter amplifier, operating nominally with 3 dB back-off. The more spatial dispersion achievable in the array means less back-off required in the L-band amplifier; and hence higher RF-to-DC conversion efficiency. Ultimately, for an operational system in geostationary orbit, this can be translated to mean increased channel capacity. Ten contiguous 50 kHz channels have been selected for the two variable plus eight fixed transmit signals, resulting in the most severe channel allocation for IM rejection. With spatial dispersion of IM products with a phased array, more channels will be available and provide better spectrum utilization, as well as improved RF-to-DC power conversion efficiency.

At the transmitter module, the IF signal is upconverted to nominally 1540 MHz and amplified to provide a total array transmit power output of +8.2 dBw per beam. The L-band amplifier will also be designed to operate with other than the nominal 3 dB back-off to better conduct an experiment to evaluate the achievable IM suppression in the power amplifier as compared to spatial dispersion of IM products with a phased array. This will provide a significant technology base for the design of the operational system for geostationary application that most efficiently and effectively utilizes the payload capacity.

- Packaging

The SpaceLab Module Subsystems are located in eight drawers that mount in one of the on-board experiment racks, and are laid out for easy access during the development, contractor system test, integration test at NASA, and for in-flight tests.

The combined outputs from the Transmitter Beam Processor is hardwire connected to the Pallet Mounted Transmitter Module through approximately 18.3 meter (60 ft.) of IF cables.

- Instrument Weight and Power

The total Spacelab mounted AMPA Experiment System weighs 235 kg and requires 383 watts of prime power, exclusive of the Digital Processor Network. This network has not been included in this study due to the indefinite status and availability of the on-board Experiment Computer to meet AMPA's high speed computation requirements. However, tradeoff analyses have been conducted of:

- Modifying the on-board computer with external add-on capabilities to meet AMPA requirements
- Using a dedicated AMPA digital processor

Modification of the on-board computer is more economical but requires its availability full time during AMPA experiments.

- Schedule and Cost

An overall hardware execution phase has been estimated to require 18 months at the contractor, maximally using existing technology developed in previous hardware systems; and an additional three months for Spacelab system integration at NASA. An ROM cost for the AMPA Experiment System has been estimated at \$3900K, exclusive of the Digital Processor Network.

- Conclusion

In summary, the study has shown a viable, AMPA Experiment System that can be flown on a Spacelab mission that provides a valuable technology data base and operational experience for an advanced satellite relay system operating in geostationary orbit to support future Maritime and/or Aeronautical users. This Experiment System will demonstrate a vastly increased user support capacity and system availability to austere users in a manner that can save many millions of dollars in these and related systems. In particular, the experiment will demonstrate:

- A 32 element array in space that can operate with a low gain hemispherical coverage element on the user terminal.
- Two independently steerable beams on receive that adaptively steers the main beam on a desired user while placing RFI's in spatial pattern nulls in order to maximize the output $S/(I+N)$.

- Two independently steerable beams on transmit that open loop form beams on the desired user and spatial pattern nulls on RFI's, using known or measured geo-position data of the signal sources.
- The viability of remote beam forming on transmit as well as on receive.
- The advantages of employing large adaptive thinned arrays to provide:
 - High resolution that allows operation of a desired user in close vicinity to interference sources, and
 - Improved spatial dispersion of IM products with a phased array.

In addition, the study has shown other system by-products which allow the AMPA Experiment System configuration to be used for other experiments that can provide technology advancements in:

- Direction Finding for Search and Rescue
- Multi-user Resolution Experiment to resolve signals for advanced Data Collection and/or future personalized Wrist Radio systems.
- Orbital Pattern Measurement to measure antenna performances of large ground based antennas.

2.0 DESIGN REQUIREMENTS

The design requirements for the AMPA Experiment System are based on an advanced satellite relay system, enveloping the AMPA concept, and operating in geostationary orbit to support future austere Maritime and Aeronautical users. The advanced system has been designed with emphasis to maximize channel capacity and to minimize user terminal implementation and cost impacts. Key design and performance requirements for the advanced operational system have been scaled for application on the AMPA Experiment System to be flown on Spacelab mission(s). The AMPA Experiment System has been designed to operate with user terminals having:

- Antenna gain ≥ -2 dBi over a hemisphere
- ERP $\geq +8$ dBw
- $G/T_S \geq -29.9$ dB/ $^{\circ}$ K

and to provide an output carrier-to-noise density (C/N_0) of +53 dB-Hz to support Maritime type users and C/N_0 of +46 dB-Hz to support Aeronautical type users. The resultant requirements for the Spacelab AMPA Experiment System are summarized in Table 2-1.

Table 2-2 shows a list of candidate AMPA experiments to be conducted from the Spacelab.

TABLE 2-1. DESIGN REQUIREMENTS FOR SPACELAB MOUNTED AMPA EXPERIMENT SYSTEM

PARAMETERS	REQUIREMENTS
A. System	
<ul style="list-style-type: none"> ● Approach 	<ul style="list-style-type: none"> ○ Remotely located beam and signal processors (array, receiver and transmitter front ends located on Pallet structure and all beam, signal and data processors located in Spacelab Module)
<ul style="list-style-type: none"> ● Frequency <ul style="list-style-type: none"> ○ Return (User-to-AMPA) ○ Forward (AMPA-to-User) 	<ul style="list-style-type: none"> ○ 1640 \pm1.25 MHz ○ 1540 \pm1.25 MHz
<ul style="list-style-type: none"> ● Coverage 	<ul style="list-style-type: none"> ○ Horizon-to-horizon (\approx+70 degrees as seen from the Spacelab at an orbital altitude of 400 km)
<ul style="list-style-type: none"> ● Input Signal Format <ul style="list-style-type: none"> ○ Information ○ Pilot 	<ul style="list-style-type: none"> ○ NBFM voice or 4.8 kbps PCM-BPSK data ○ Unique CW tone(s) or code for each user
<ul style="list-style-type: none"> ● Number of Beams <ul style="list-style-type: none"> ○ Receive ○ Transmit 	<ul style="list-style-type: none"> ○ Two (2) independently steerable beams ○ Two (2) independently steerable beams
<ul style="list-style-type: none"> ● Receive-Adaptive Algorithm <ul style="list-style-type: none"> ○ Pointed Beam ○ Fully Adaptive ○ Directed Adaptive 	<ul style="list-style-type: none"> ○ Non-adapted, open loop acquisition and track ○ Automatic acquisition and track with spatial nulling of RFI ○ Pointed beams with adaptive spatial nulling of RFI
<ul style="list-style-type: none"> ● Transmit-Adaptive Algorithm <ul style="list-style-type: none"> ○ Pointed Beam ○ Open Loop Beam and Null Forming ○ Retrodirected 	<ul style="list-style-type: none"> ○ Open loop pointing and tracking ○ Open loop beam and null forming using user ephemeris data ○ Open loop beamforming based on measured received phases
<ul style="list-style-type: none"> ● Modes of Operation <ul style="list-style-type: none"> ○ Simplex ○ Full Duplex ○ Bentpipe 	<ul style="list-style-type: none"> ○ User-to-AMPA ○ AMPA-to-user ○ User-to-user (with MODEM function performed on AMPA) ○ User-to-user (direct turnaround without demodulation and remodulation)
<ul style="list-style-type: none"> ● Data Handling <ul style="list-style-type: none"> ○ Received Signal (User-to-AMPA) 	<ul style="list-style-type: none"> ○ Demodulate, detect and format received signal from user for recording on the on-board Spacelab Payload Recorder or for retransmission to ground by way of the Orbiter's TDRSS transceiver.

TABLE 2-1. (continued)

PARAMETERS	REQUIREMENTS
<ul style="list-style-type: none"> o Transmit Signal (AMPA-to-User) ● Performance Monitor ● Size, Weight and Power <ul style="list-style-type: none"> o Weight o Power o Size <ul style="list-style-type: none"> - Pallet Subsystem - Spacelab Module Subsystem 	<ul style="list-style-type: none"> o Format transmit signal (digitized NBFM voice or 4.8 kbps PCM data) received from ground by way of Orbiter's TDRSS transceiver for retransmission to the ultimate user o Monitor and record AMPA performance to evaluate: <ul style="list-style-type: none"> - time required for acquisition and lock-on to desired signal - signal quality - rejection or cancellation of interference sources o 250 KG exclusive of digital processor network o 400 watts o On one Pallet structure o Not to exceed one standard experiment rack
<p><u>B. Array</u></p>	<ul style="list-style-type: none"> o Variable aperture o Horizon-to-horizon ($\pm 70^\circ$) o 32 o Common transmit/receive o LHCP on receive RHCP on transmit o 19.2 dBi (Peak) 17.0 dBi ($\pm 70^\circ$) o Variable from fully filled array to thinned array with effective array aperture of 2.24 meter by 2.24 meter o ≈ 4 to 17 degrees o Hard mounted on a Pallet structure
<p><u>C. Receiver</u></p>	<ul style="list-style-type: none"> o 2.5 MHz o -10.0 dB/K o 35 dB o Two independently steerable beams (operated in pointed, fully adaptive and directed-adaption modes) o 70 MHz

TABLE 2-1. (continued)

PARAMETERS	REQUIREMENTS
<u>C. Receiver (contd.)</u> <ul style="list-style-type: none"> ● Channel Assignment ● Quality <ul style="list-style-type: none"> ○ Spurious Response ○ LO Leakage ○ Image Rejection ○ Phase Noise ○ Amplitude Linearity ○ Phase Linearity 	<ul style="list-style-type: none"> ○ Two adjacent 50 kHz channels in mid-band ○ ≤ -70 dB ○ ≤ -120 dB ○ ≥ -120 dB ○ ≤ 5 degrees (10 Hz - 1 kHz) ○ $\leq +0.3$ dB ○ $\leq +5$ degrees
<u>D. Transmitter</u> <ul style="list-style-type: none"> ● Type ● Radiated Power ● Number of Beams ● Beam Processing Frequency ● Channel Assignment ● Quality <ul style="list-style-type: none"> ○ Spurious Outputs ○ LO Leakage ○ Third Order IM Rejection ○ Phase Noise ○ Amplitude Linearity ○ Phase Linearity 	<ul style="list-style-type: none"> ○ Distributed power amplifier (class C with variable "back-off") ○ 8.2 dBW per beam ○ Two independently steerable beams (operated in pointed or open loop beam and null forming modes), and eight fixed beams for IM simulation ○ 70 MHz ○ 10 contiguous 50 kHz channels in mid-band, with two steerable channels located in the middle ○ ≤ -90 dB ○ ≤ -90 dBm ○ ≥ -14 dB ○ < 3 degrees (10 Hz - 1 kHz) ○ $\leq +0.2$ dB ○ $\leq +2$ degrees
<u>E. Doppler Processor</u>	<ul style="list-style-type: none"> ○ Compensate received signals for doppler frequency shifts of ± 38 kHz maximum
<u>F. Modem/Data Conditioner</u>	<ul style="list-style-type: none"> ○ Demodulate input signal and format baseband signal for recording on Spacelab Payload Recorder or for retransmission to ground via TDRSS link ○ Format input data/information from ground station for modulating 70 MHz carrier for retransmission to user ○ Direct turnaround of return-link user signal to forward-link user at 70 MHz for bentpipe mode

TABLE 2-1. (continued)

PARAMETERS	REQUIREMENTS
<u>G. Control Unit</u>	<ul style="list-style-type: none"> o Must provide control to de-energize system in emergency and to reload software in core memory for algorithm and executive functions
<u>H. Digital Processor</u>	<ul style="list-style-type: none"> o Must process all candidate array algorithms for receive and transmit beams and all executive control and read-out functions
<u>I. Type of Parts</u> <ul style="list-style-type: none"> ● Parts Selection <ul style="list-style-type: none"> o MIL- Parts o Commercial ● Design ● System Thermal Test 	<ul style="list-style-type: none"> o 100% screening of critical electrical parts and 100% burn-in of active devices o Derate guidelines as per NASA-GSFC Spec. #PPL 12 as far as possible o Thermal cycling for 168-200 hours (operating)
<u>J. Workmanship</u>	<ul style="list-style-type: none"> o MIL-STD-454
<u>K. Environment</u> <ul style="list-style-type: none"> ● Thermal-Operating <ul style="list-style-type: none"> o On Pallet o In Module ● Thermal-Non-operating <ul style="list-style-type: none"> o On Pallet o In Module ● Vibration ● Shock ● Acoustic 	<ul style="list-style-type: none"> o 0^o - 50^oC o 0^o - 50^oC o As per Spacelab Payload Accommodation Handbook ESA Ref. No. SLP/2104, dated May 1976

TABLE 2-2. CANDIDATE LIST OF SPACELAB
AMPA EXPERIMENTS

● Communication	User-to-AMPA and AMPA-to-user
● Bentpipe Mode	Direct user-to-user via AMPA
● Frequency Reuse	Demonstrate frequency reuse with co-channel users on return and forward link directions
● Spatial Dispersion of IM	Demonstrate effectiveness of spatial dispersion of IM products with an array
● Direction Finding	Demonstrate location accuracy for search and rescue mission
● Resolution	Demonstrate resolvability of closely spaced signal sources
● Orbital Test Range	Demonstrate use of AMPA antenna system for measuring performance of large ground based antennas

3.0 OPERATIONAL SYSTEM

3.1 GENERAL

This section summarizes the results of a detailed parametric analyses (included in Appendix B) for an advanced operational satellite relay system, enveloping the AMPA concept to support future multiple access Maritime and Aeronautical users. This advanced system approach has been used to develop the basic design requirements for the AMPA Experiment System to be flown on a Spacelab mission (s).

Since the potential users of the advanced operational system may number in thousands, prime emphasis has been given to overall system cost effectiveness commensurate with minimizing the cost impact on the user terminals by placing additional capabilities on the spaceborne relay repeater system. For example, the implementation cost for the current MARISAT user exceeds \$50,000. If the user terminal cost can be reduced by 50 per cent, the user terminal cost savings will be tens of millions (dependent upon the number of eventual users). More significantly, however, minimizing the user cost impact will ultimately make the relay repeater system more available, attractive and useful to the potential subscribers.

By placing a high gain antenna on the spaceborne relay repeater system, the user can use a low gain antenna element that reduces the need to employ a high gain steerable antenna as required by the present MARISAT users. The present MARISAT users employ a 4 foot parabolic reflector that requires a large protective radome, stabilized mounting platform as well as electronic sensors and drive to steer the beam to the MARISAT spaceborne repeater. Not only is the implementation cost expensive, but it limits the system utilization to large tonnage vessels, and excludes support for the smaller tonnage vessels. The operational AMPA system (for geostationary orbit) will permit the user terminal to be designed to use a low cost and low gain hemispherical coverage element that requires no stabilization mount or steering electronics on aircraft and simple gravity stabilized mounts on ships.

Three operational AMPA satellite systems have been assumed to provide global coverage; typically located over the Pacific, Atlantic and Indian Oceans to cover the major traffic lanes. For study purposes, it has been assumed that

each of the satellite systems would cover one-third of the allocated L-band frequency spectrum to service the Maritime or Aeronautical users, or approximately 2.5 MHz in the return (user-to-satellite) and forward (satellite-to-user) directions. This will provide a maximum of fifty contiguous 50 kHz channels in the return as well as forward directions per satellite system.

Although the allocated L-band frequency spectrum dedicated to Maritime and Aeronautical service should be clear of interference emitters (referred to herein as RFI), the AMPA system will be designed to spatially null intentional or unintentional interference emitters falling within a desired user channel. More importantly, however, the use of an adaptive nulling system makes it possible to employ frequency reuse by using spatial discrimination rather than polarization discrimination to reuse the same frequency, thus allowing more than 50 return channels.

An array also has an inherent advantage over a single antenna system (such as a parabolic reflector, lens, etc.) to provide spatial dispersion of intermodulation products generated in the final transmitter amplifier. More significantly, the inherent spatial dispersion achieved with an array allows the final L-band amplifiers to be designed with reduced backoff for higher RF-to-DC power efficiency.

A filled array (elements located as close as possible without overlapping their effective aperture) vs thinned array has also been considered. The thinned array provides equal peak gain as the filled array, but introduces higher sidelobes. However, the high sidelobes are not a problem in an adaptive array, since adaptive spatial nulling of interference sources automatically minimizes their impact. In addition, the thinned array provides improved resolution to operate near interference sources. Also, simulation results have shown that spatial dispersion of IM products improves rapidly as the array aperture is increased. On the other hand, the beam pointing requirements (particularly on transmit) as well as the implementation impact increases as the array dimensions are increased, thus placing constraints on the maximum aperture size that is practical to employ.

3.2 LINK ANALYSIS FOR OPERATIONAL SYSTEM

A link analysis for the advanced operational system is based upon the following characteristics (see Appendix A) envisioned for future Maritime and Aeronautical users:

PARAMETER		MARITIME USER	AERONAUTICAL USER
● C/N ₀	dB-Hz	+53.0	+46.0
● ERP	dBw	+21.0	+23.0
● G/T _S	dB/°K	-20.0	-26.0

A link analysis has shown that an array with 32 high gain elements in space can support the users. The key system requirements are summarized in Table 3-1.

TABLE 3-1. KEY OPERATIONAL SYSTEM REQUIREMENTS FOR AN ADVANCED MARITIME AND AERONAUTICAL SATELLITE RELAY SYSTEM

PARAMETER		MARITIME	AERONAUTICAL
● Voice C/No	dB-Hz	+53	+46
● User			
● ERP	dBw	+17.7	+10.7
● G/T _S	dB/°K	-20	-26
● Satellite			
● P _T /beam	dBw	+8.2	+7.2
● G/T _S (element)	dB	-10.6	-10.6
● # Elements		32	32
● Array Gain (peak)	dB _i	33.5	33.5
● Element Gain (peak)	dB _i	18.4	18.4

3.3 ADAPTIVE APPROACHES

3.3.1 General

Figure 3.3-1 is a simplified functional block diagram of an adaptive array system typical of that required for the AMPA experiments. Parameters such as the number of elements, their gains, channel sampling requirements, number of correlator processors, digital process speed, and adaptive convergence techniques are all a function of the adaptive algorithm and its implementation.

The function of the adaptive processor is to provide the optimum combination of weighting vectors to tailor the summed output effective antenna pattern for a given application; more specifically for the AMPA system to put the main beam on the desired signal while placing interference signals (or RFI's) into spatial array pattern nulls. To do this, an algorithm implemented on a digital processor uses measureables provided by the hardware and/or information supplied from other shuttle systems to compute the requisite weights. The nature of the algorithm used depends on the mode of operation. For adaptive nulling or tracking, such as would be desirable in the communication experiments, iterative or recursive algorithms are used and the correlator readings provide a closed loop measure of performance. In beam pointing applications, the algorithm provides open loop transformations from look angle to weight settings. For the purposes of algorithm discussion, the word adaptive applies to the nature of the steering. Open loop pointing is not adaptive in this sense.

The adaptive array steering algorithm described herein is based on maximization of the signal-to-interference plus noise ratio $[S/(I+N)]$ through an ability to distinguish the desired signal from its interferers. This separation is accomplished by utilizing a unique waveform property such as frequency or pseudorandom noise encoding. The requirement for separation is implicit in the driving function:

$$\frac{\sigma Z}{\sigma \omega_j} = q = k \frac{V_{S\epsilon} V_{Si}^*}{|V_{S\epsilon}|^2} - \frac{\sum_j (V_{I\epsilon j} \cdot V_{Ij i}) + \eta_\epsilon \cdot \eta_j}{\sum_j |V_{I\epsilon j}|^2 + |\eta_\epsilon|^2}$$

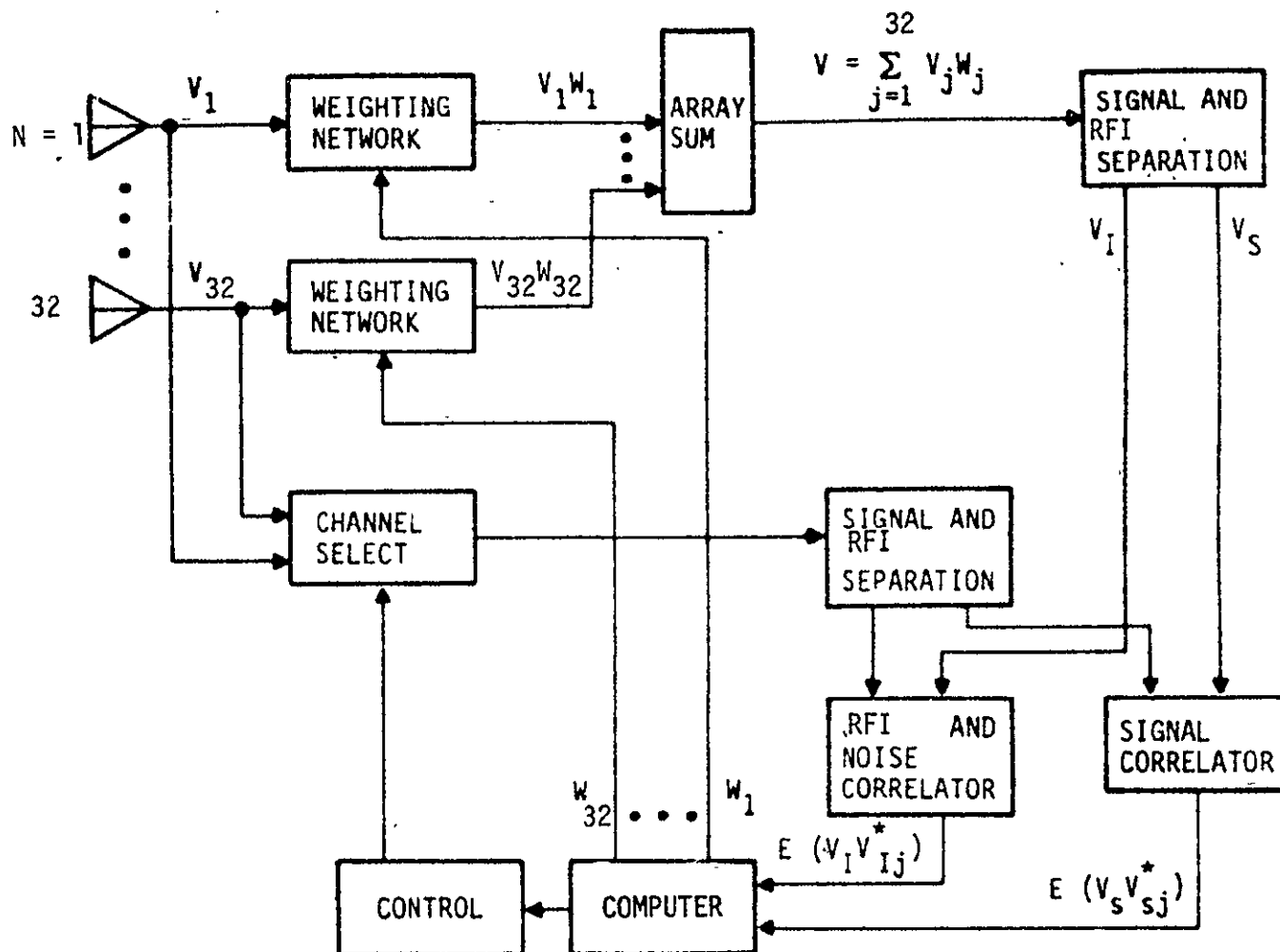


FIGURE 3.3-1. SIMPLIFIED 32 ELEMENT GRADIENT ADAPTIVE PROCESSOR

Where Z is an intermediate function with a maximum at a maximum of the $S/(I+N)$ and q_i represents the slope of this function with respect to a change in the complex weighting of the i^{th} element of the array. The remaining terms represent measurables if the signal and interfezers can be separated -

$$\begin{aligned}
 V_{S\epsilon} \cdot V_{Si}^* &= \text{desired signal correlation between summed output and } i^{\text{th}} \text{ element} \\
 |V_{S\epsilon}|^2 &= \text{desired signal summed output power} \\
 \sum_j (V_{I\epsilon j} \cdot V_{Iji}^*) + \eta_\epsilon \cdot \eta_i &= \text{total correlations of interfezers and thermal noise output in } i^{\text{th}} \text{ element} \\
 \sum_j |V_{I\epsilon j}|^2 + |\eta_\epsilon|^2 &= \text{total summed output interference power}
 \end{aligned}$$

This separation need not be perfect since both simulation and hardware demonstration have shown that a 6 to 10 dB $S/(I+N)$ at the signal correlator output is sufficient for rapid and reliable convergence. As the use of the word convergence implies, the algorithm is iterative and closed loop. Since it deals only with weight changes and not the absolute magnitude of the weights, the technique is extremely tolerant of the properties of the weighting networks. In addition, it is driving to a zero of the derivative function and thus linearity is necessary only over a very small incremental region. These factors are representative of the advantage of the fully adaptive technique - relative insensitivity to the operating environment in regard to array variables.

The disadvantage of the algorithm is obviously that, especially during acquisition, sufficient RF processing gain may not be available to produce a positive $S/(I+N)$ at the signal correlation output. In this event, other techniques such as pointed, omniscient, and directed solution could be employed to enhance adaption. In each case, the tradeoff for less knowledge of desired signal waveform is increased knowledge of array parameters, as well as the relative locations of the user and the array platforms.

● Pointed Mode

The oldest and most conceptually straightforward solution is to electronically point the array in the direction of the desired user without regard to interfering

signals. A situation where this is adequate is the multiple access portions of the NASA design for the Tracking and Data Relay Satellite System. Here, sufficient gain is provided by the pointed beam to allow acquisition of the user PN code. This, in turn, permits the array to enter the fully adaptive mode for tracking. Even this simple technique requires sufficient knowledge of element placement and weighting network parameters to produce a phase front in a given direction if a search of a relatively large spatial volume is to be avoided. The basic problem, however, is that flexibility in sidelobe shaping to reduce interference is lost, since the adaptive capability is solely used for tracking (closed and open loop).

● Omniscient Solution

To counter this difficulty, another technique called the Omniscient Solution was developed that provides the optimum theoretical solution. This is of little practical utility in most cases since the presumption is that the entire signal environment is known, that is, the location of all desired and interfering signals and their relative strengths together with the spatial and electrical properties of the array. With this much information, it is possible to compute the proper element weightings to produce the optimum $S/(I+N)$ in a single step by a matrix inversion technique. This technique provides an excellent reference, however, to determine how well convergence has been achieved with an adaptive algorithm.

● Directed Adaption. Mode

As a more practical solution to the interference problem, a directed adaption algorithm has been developed and demonstrated at AIL. Its name is derived from the fact that the position of the beam peak is directed while signals away from this direction are adaptively nulled. Returning to the driving function for the fully adaptive algorithm, it can be seen that if the phase distribution of the desired signal is known (based on a known position and array parameter) the proper signal correlations can be calculated).

These calculated correlations represent the outputs that the hardware signal correlator would have provided if a desired signal of sufficient strength were present from the given direction. By inserting this pseudo-

signal into the algorithm calculation, the gain in this direction is maintained while measured interference correlation values are used for adaptive nulling.

The directed-adaption algorithm also has a very powerful application for AMPA. On transmit AMPA beam could be directed to a known desired user, while nulls could simultaneously be placed on other co-channel users (such as in frequency reuse application) whose locations are usually known. Even though this open loop null steering technique may not place perfect deep nulls on these co-channel users, nulls of 10-15 dB may provide sufficient improvement. It is recommended that AMPA include this capability into the AMPA Experiment System.

In summary, a comparison of the array steering algorithm is shown in Table 3.3-1.

Computer simulations of achievable performances for the fully adaptive and omniscient solution algorithm are shown in Appendix B.

TABLE 3.3-1 COMPARISON OF ARRAY STEERING ALGORITHMS

TECHNIQUE	ADVANTAGES	DISADVANTAGES
Pointed Beam	Fastest Acquisition (one lookup operation)	No specific sidelobe nulling Requires tracking data Requires array calibration
Omniscient Solution	Fast acquisition for small number of elements Provides interference nulling	Computation time and memory increases rapidly with array size (matrix inversion) Requires complete knowledge of operating environment
Directed- Adaption	Does not require signal waveform information Provides adaptive nulling of interferers	Requires tracking data Gain on user dependent on degree of user position and array calibration accuracies Acquisition time depends on interference scenario-gain in user direction
Fully Adaptive	User tracking automatic Provides maximum SIR Least dependence on array and spatial parameters	Acquisition requires unique user waveform or frequency (matched filter)

3.4 OPERATIONAL SYSTEM DESIGN

Two key parametric tradeoff analyses were conducted to determine the optimum adaptive multibeam system approach that maximizes the channel capacity and minimizes the user implementation and cost impacts. These key tradeoffs are:

- Location of the beam processors (i.e., ground based vs. spaceborne)
- Type of array (filled vs. thinned array)

The result of the trade has shown (details included in Appendix B) that a Beam Process on Ground approach increases the channel capacity over the Beam Process in Space approach by 7.1 times as shown below for a candidate spacecraft having a payload weight and prime power capacity of 182 kg and 1.6 kw, respectively:

APPROACH	# BEAMS	WT-KG	PWR-KW
● Beam Process on Ground	50	77	1.6
● Beam Process in Space	7	182	0.69

In addition, the filled vs. thinned array tradeoff analysis has shown that a thinned array approach is desirable since it provides:

- Improved resolution as a result of its narrower beamwidth to spatially null close-in interferers (high grating lobes produced by a thinned array is not a problem with adaptive spatial nulling of interfezers).
- Improved spatial dispersion of intermodulation products as the array size is increased.

Consequently, the advanced operational system design is a 32 element thinned array with all beam processor functions performed on the ground as illustrated in Figure 3.3-2.

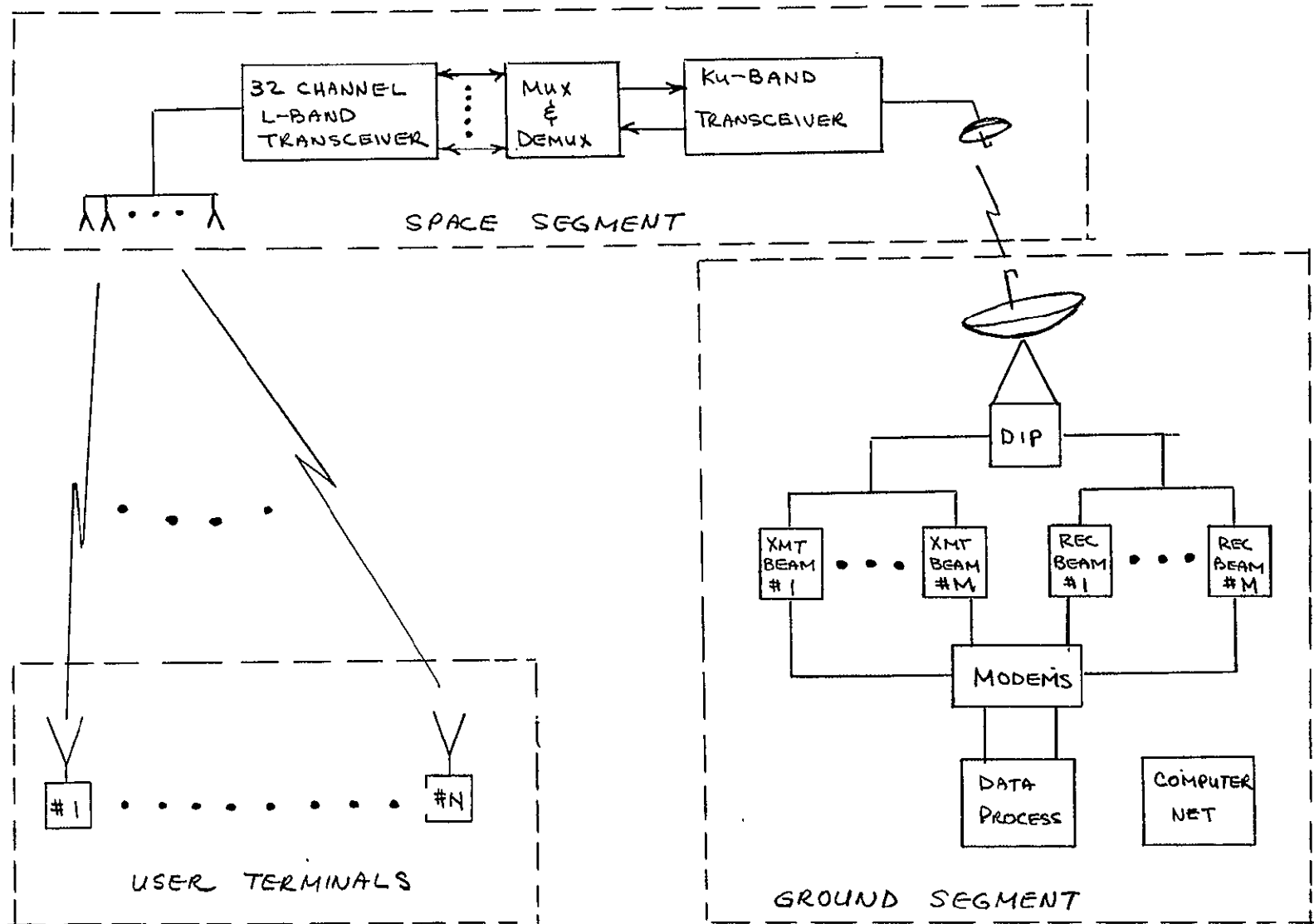


FIGURE 3.3-2. ADVANCED OPERATIONAL SYSTEM CONCEPT

4.0 SPACELAB EXPERIMENT SYSTEM TRADEOFF ANALYSIS AND DESIGN

4.1 GENERAL EXPERIMENT SYSTEM CONSIDERATIONS

The AMPA Experiment System will be designed to provide coverage or field-of-view (FOV) out to the horizon (FOV \approx ± 70 degrees), rather than limiting the FOV to ± 40 degrees (AMPA work statement requirement). This increased coverage will increase the maximum available dwell time on a user from 1.59 minutes to approximately 10.18 minutes when the user is located on the Orbiter's flight path. More importantly for users located off the flight path, the dwell time is significantly increased by increasing the FOV. This is so because the dwell time is reduced further by the cosine of the azimuthal angular displacement of the user from the flight path as shown in Figure 4.1-1. For example, for the FOV = ± 40 degree case with the user located at scan limit, and for azimuthal offset angles greater than 50 degrees, the dwell time is reduced to less than 1 minute which provides inadequate dwell time to conduct useful experiments. By comparison, the dwell time for 70 degree FOV is approximately 6.5 minutes. In addition, the increased FOV of ± 70 degrees will allow greater flexibility to locate cooperating user terminals for the experiment and will allow terminals to be used in multiple spacecraft passes.

Although the full horizon-to-horizon coverage may not always be available, due to blockage of the spacecraft structure and multipath, it is recommended that the array be designed to provide a FOV of ± 70 degrees. Furthermore, in order to minimize multipath reflection signals, the array will be designed with circular polarization to minimize reflected signals that are reflected with the reverse sense.

Increasing the coverage from ± 40 to ± 70 degrees increases the doppler frequency shift from ± 27 kHz to ± 38 kHz; however, this increase will have minimal impact on the design of the doppler processor.

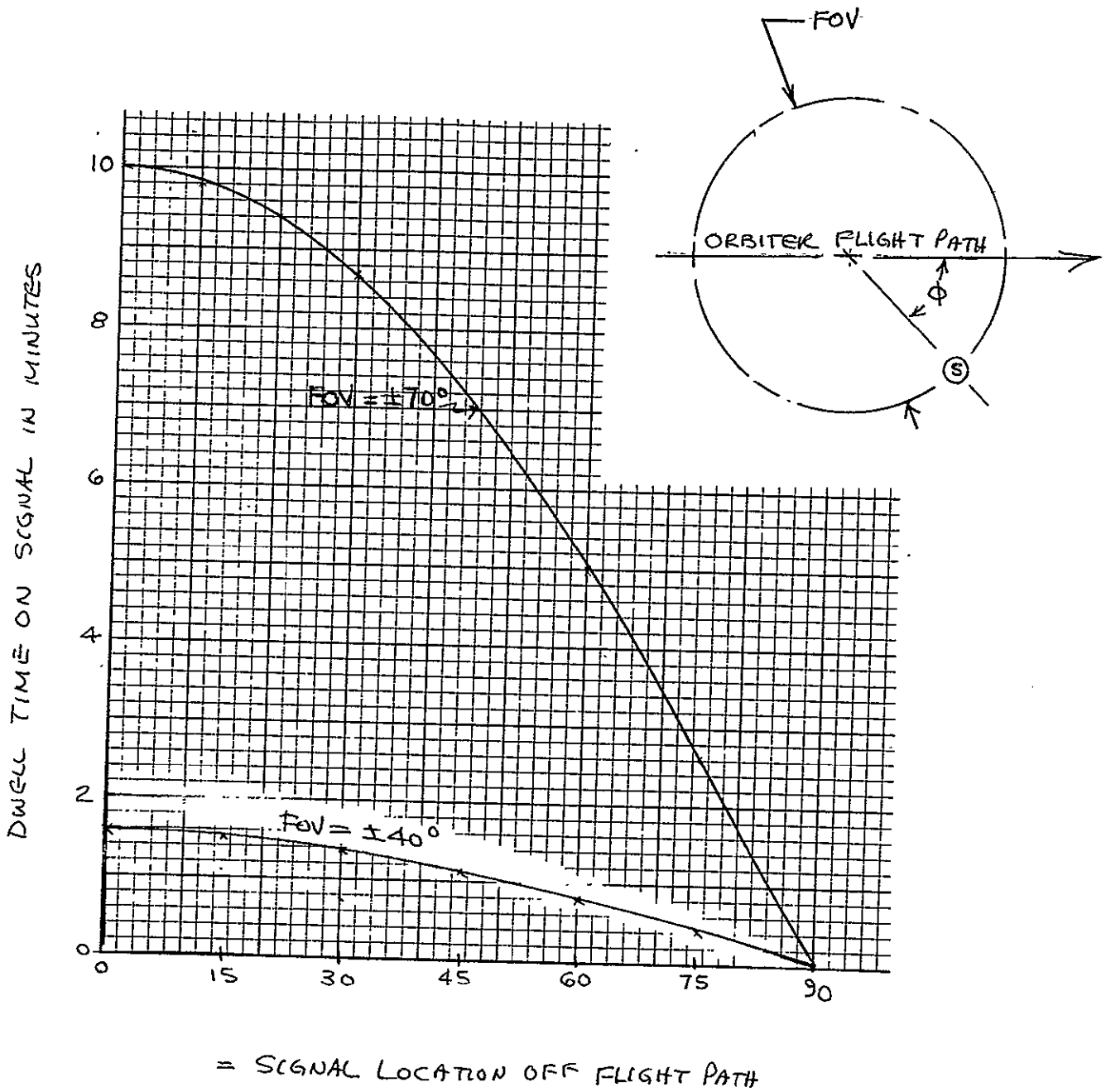


FIGURE 4.1-1 DWELL TIME AS A FUNCTION OF SIGNAL OFFSET FROM FLIGHT PATH

4.1.1 Key Operational System Parameters to Scale for Spacelab Experiment

The operational system analysis has shown that a 32 element array with beam processors located on the ground provides the best solution to meeting the future needs for servicing the multiple access Maritime and Aeronautical users, using an adaptive multibeam phased array. This system concept then is used as a basis to establish the design requirements for the AMPA experiment to be conducted on the Spacelab mission. The experiment system is functionally the same as the operational system except that both space and ground segments are located on the Spacelab and the space-to-ground link has been replaced with RF cables. The space segment is located on the pallet structure and the ground segment is located within the Spacelab module.

The key parameters to be considered for scaling the operational geostationary system to the Spacelab Experiment antenna system as summarized in Table 4.1-1 are:

- Spot Size: Scaling the synchronous spot size of approximately 2094 km results in an experiment array beamwidth of 148 degrees, resulting in no spatial resolution.
- Beamwidth: Scaling the 3 degree geosynchronous beamwidth requires an experiment array aperture of 4.1 meter by 4.1 meter which is too large for mounting directly on the pallet structure and within the payload bay dimensions without folding the array.
- Array Gain: Scaling the array gain of 33.5 dBi (peak) requires approximately 851 elements for the experiment coverage requirement of ± 70 degrees. Adaptive multibeam array with 851 elements is neither practical, cost effective nor a meaningful demonstration for the operational system, and therefore it is not a recommended approach.
- Number of Elements: Scaling the number of elements provides excess C/N_0 than required, but provides the best simulation of the array size and implementation requirements of the operational system.

TABLE 4.1-1. AMPA SCALING FOR EXPERIMENT

GEOSYNCHRONOUS OPERATIONAL CHARACTERISTICS		SPACELAB AMPA EXPERIMENT REQUIREMENTS	COMMENTS
● SPOT SIZE	2094 KM	HPBW = 148°	INADEQUATE RESOLUTION
● BEAMWIDTH	≈ 3°	D = 4.1M	TOO LARGE
● ARRAY GAIN	33.5 DBI	851 ELEMENTS	TOO MANY ELEMENTS
● # ELEMENTS	32 (18.4 DBI ELEMENTS)	32 (4.2 DBI ELEMENTS)	EXCEEDS C/N ₀ REQ'D BUT BEST SCALES ARRAY SIZE
● C/N ₀	53 DB-HZ	10 ELEMENTS	TOO FEW ELEMENTS (DOES NOT SIMULATE ARRAY SIZE)

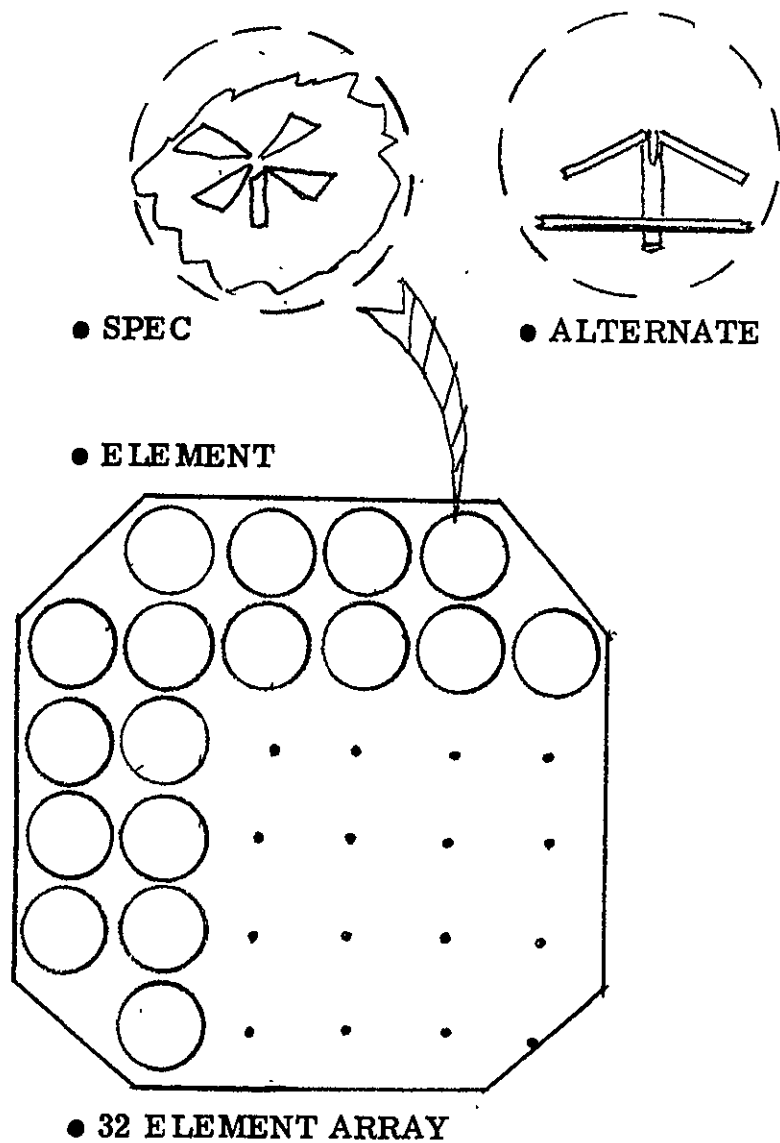
- o Carrier-to-Noise Density: Scaling the C/N_0 requires very few elements and does not simulate the intended purpose of the AMPA experiment to evaluate an adaptive multibeam phased array in space.

Therefore, it is recommended that the AMPA Experiment System scale the number of elements as the best option to evaluate and advance the technology for an adaptive multibeam phased array in space.

The resultant recommended 32 element array layout and characteristics are summarized in Figure 4.1-2. For hemispherical coverage, several types of element design have been considered as described subsequently in Section 4.2.1.

The key AMPA experiment parameters to be scaled from the operational systems are summarized in Figure 4.1-3. As indicated, a 32 element variable array is recommended for the experiment, providing a peak array gain of 19.2 dBi and variable HPBW of approximately 17 to 4 degrees, using 4.2 dBi elements with 160 degree field-of-view. In addition, since it will be most cost effective and efficient to design, develop, fly and test as much of the operational system design as possible, (within the constraints of available program funding) the transmit power per beam and the receive noise figure has been selected to be the same as the operational system; viz: 6.6 watts per beam and 2 dB, respectively.

The number of beams to be scaled has an implementation as well as cost impact. The implementation impact is constrained primarily by the allowable Spacelab weight and prime power that can be allocated for the experiment. Typical for the First Spacelab Mission, the total available payload weight and prime power are 5.1 kilograms and 2 kilowatts, respectively. Of these payload allowances, it is estimated that only a small portion will be available for the AMPA experiment. Of these allowances, it is estimated that the prime power will be the critical constraint, and limit the number of beams that can be scaled for the experiment.



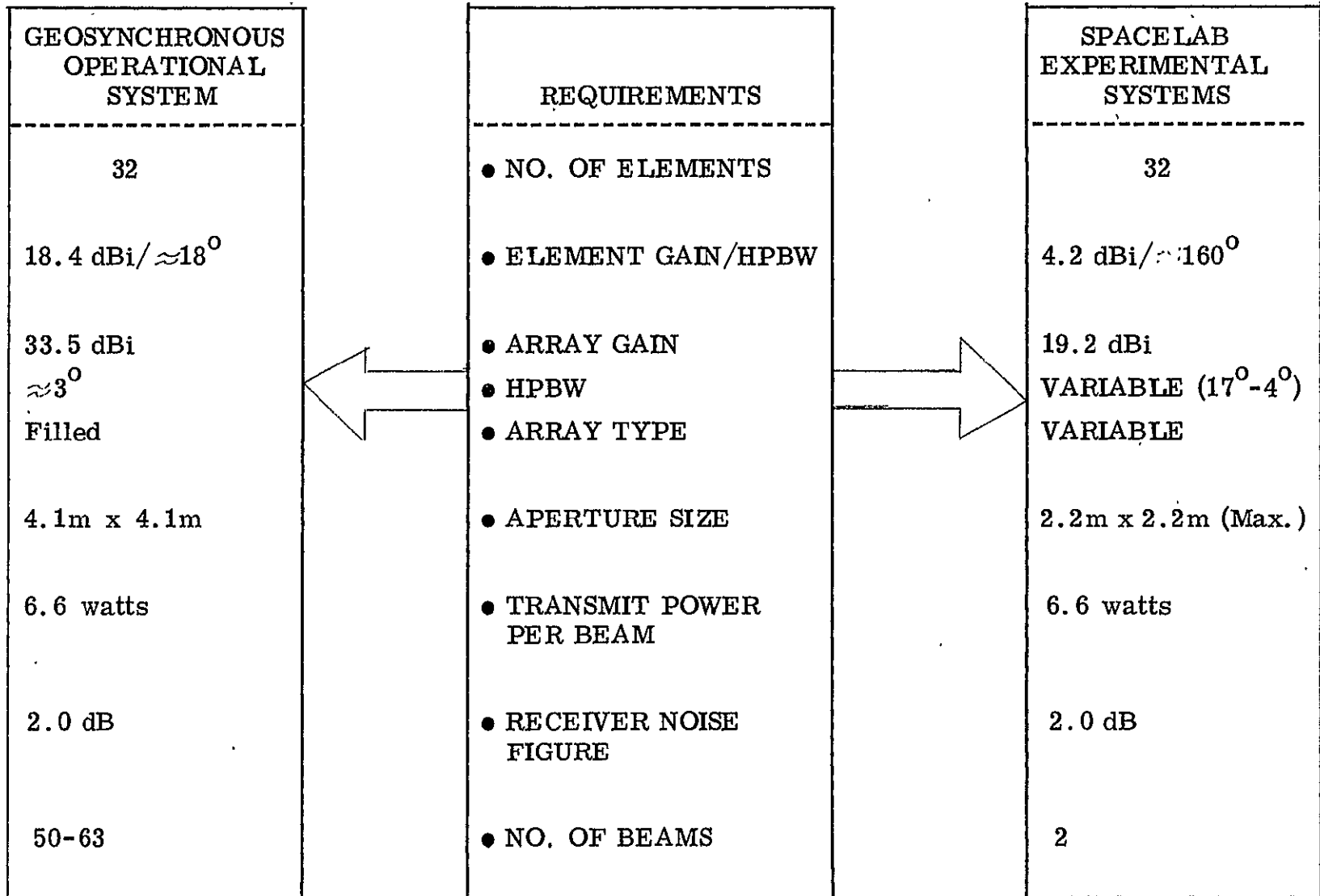
● ELEMENT CHARACTERISTICS (MODIFIED FLARED CONE TURNSTILE)

- HPBW $\approx 160^\circ$
- GAIN = 4.2 dBi (PEAK)
= 2.2 dBi ($\pm 70^\circ$)

● ARRAY CHARACTERISTICS

- HPBW $\approx 4^\circ - 17^\circ$
- GAIN = 19.2 dBi (PEAK)
= 17.0 dBi ($\pm 70^\circ$)

FIGURE 4.1-2. ARRAY CHARACTERISTICS FOR SPACELAB EXPERIMENT



4-7

FIGURE 4.1-3. EXPERIMENT REQUIREMENTS

Key design impact to scaling the number of beams is the L-band transmit amplifier. The amplifiers must be scaled to handle the total power for M transmit beams; i.e., in order to radiate the required 6.6 watts per beam from the 32 element array, each amplifier must be sized to radiate 6.6/32 watts or 210 milliwatts times the number of beams (M).

Although it would be desirable to size the transmit module to handle the number of transmit beams envisioned for the ultimate operational system, it would not be practical or cost effective for the experiment. Table 4.1-2 illustrates a preliminary estimate of the L-band transmit power requirements for an operational system with 50 transmit beams (or channels) resulting in a total array RF amplifier capacity of 587 watts and prime power requirement of 1467 watts. If we add the power required by the remaining on-board experiment electronic system of approximately 300 watts, nearly 1.8 kw will be required to implement the operational transmitter for the experiment. It is unlikely that 90 percent of the available Spacelab 2 kw prime power will be allocated for the AMPA experiment. Table 4.1-2 also shows that for 2 transmit beams that prime power can be reduced to a modest 124 watts for the transmitter and 444 watts total.

In order to provide a meaningful estimate of the implementation impact as a function of the number of array elements and the number of beams, a preliminary analysis of the AMPA Experiment system was conducted for 32, 64 and 128 array elements and for 2, 4 and 8 independently steerable receive and transmit beams. The tradeoff analysis is included in Appendix C, and the estimated total experiment system weight and prime power requirements are summarized in Table 4.1-3 for the 32 element array. The preliminary estimates shown in Table 4.1-3 indicates that the 2 beam system is probably more compatible with the total weight and prime powers that will be available for the AMPA experiment.

TABLE 4.1-2. NUMBER OF TRANSMIT CHANNELS

	Operational System	Experiment
- Radiated Power	= 6.6 W/Channel	6.6 W/Channel
- Total RF Power	= 50x6.6 (Chan) = 330 Watts	2x6.6 (Chan) = 13.2 W
- Amplifier Backoff**	= 1 dB	1 - 3 dB
- Array Intermod Dispersion**	= TBD	TBD*
- Line and Diplexer Loss	= 1.5 dB	1.5 dB
- Total Array RF Amplifier Capacity	= 587 Watts	37.2 Watts
- RF Power Per Array Element	= 18.3 Watts	1.2 Watts
- DC Power (40% Eff.)	= 1467 Watts	124 Watts (30% Eff.)

*Key Experimental Results

**Prichard, J. S., Spatial Dispersion of Intermodulation Products by Phased Array, dated October 1974, Presented at IEEE Canadian Communications and Power Conference, Montreal, Canada on 7, 8 November 1974

TABLE 4.1-3. WEIGHT AND POWER REQUIREMENTS FOR SPACELAB
 MULTIPLE BEAM EXPERIMENT USING 32 ELEMENT ARRAY

M BEAMS	TOTAL WEIGHT - KG *	TOTAL POWER - WATTS *
2	202	352
4	279	743
8	435	1774

Note:

*The analysis assumes a filled array and does not include:

- IM Simulator
- Data Conditioner
- Control Unit
- Digital Processor Network

The number of beams has also a large cost impact as illustrated in the relative cost estimate in Figure 4.1-4. The figure parametrically plots the estimated cost as a function of the number of beams for a 32 element array with a hardwire interconnection between the Pallet to the Spacelab Module subsystems. A system of two receive and two transmit beams is the minimum cost approach that still demonstrates the viability of operating multiple simultaneous beams without mutual interference.

In summary, from the prime power as well as cost considerations, it is recommended that 2 receive and 2 transmit beam systems be implemented for the Spacelab experiment. In general, the 2 receive and 2 transmit beams will be adequate to demonstrate the viability of the AMPA experiment system to:

- Demonstrate the concept for Beam Process on Ground
- Demonstrate adaptive acquisition and tracking of multiple austere users and to demonstrate adaptive nulling of interference emitters (intentional and/or unintentional)
- Demonstrate the concept for conducting transmit beam processor functions on the ground; i.e., evaluating the impact of phase errors in the transmit repeater, determine achievable pointing accuracies, and determine impact of phase errors in the transmit beams.
- Evaluate the impact of linear vs. Class C amplifiers for the L-band transmit amplifiers using the same power levels as for the operational system; and to evaluate intermodulation (IM) levels, back-off requirements (if necessary), amplifier phase errors; and to evaluate discrete channel usage to minimize the IM interference.

In summary, the Spacelab Experiment design and implementation considerations are:

- Approach - Simulation of Beam Process on Ground with both space and ground segments located on Spacelab

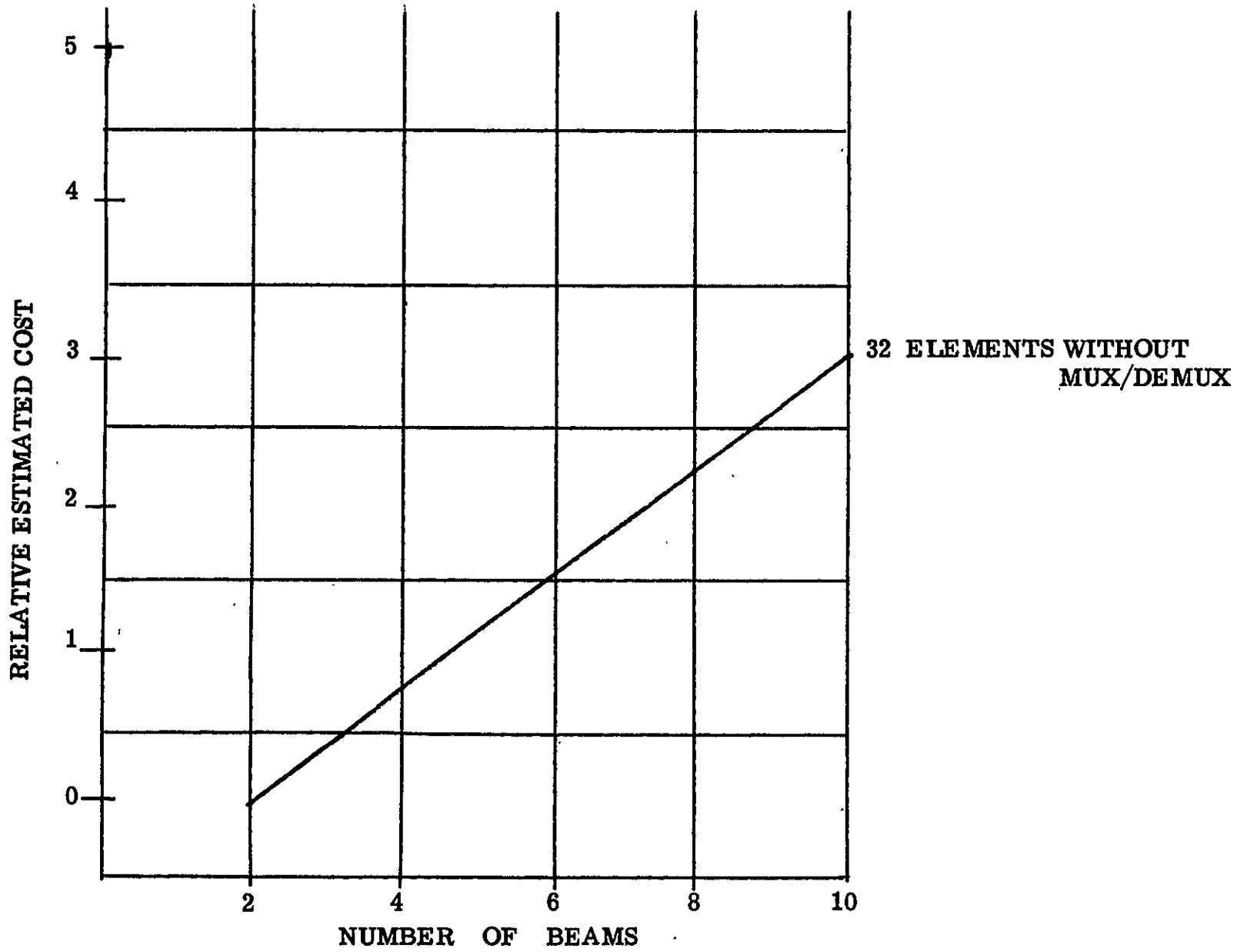


FIGURE 4.1-4. AMPA COST VS. NUMBER OF BEAMS

- Element Characteristics:
 - Gain = +4.2 dBi (peak)
 - HPBW \approx 160 degrees
 - Type = modified flared-cone turnstile using quadrature hybrid to provide LHCP on receive and RHCP on transmit
- Array Characteristics:
 - Common receive/transmit variable aperture array
 - Gain = +19.2 dBi peak
 - HPBW \approx 17 to 4 degrees (variable)
 - Aperture Size = Variable up to a maximum of 2.2 meter by 2.2 meter effective array aperture
- RF Front End Characteristics
 - Receiver Noise Figure = 2 dB
 - Modular construction per element including both receive front end and separate transmit amplifiers
- Number of Beams = 2 independently steerable adaptive receive and 2 independently steerable transmit beams (with open loop beam and null forming).
- Digital Processor = Independent dedicated digital processor to service AMPA; however, if the existing on-board Spacelab computer can be used, then this dedicated digital processor will not be required and will reduce AMPA cost, weight and power accordingly.
- Software = fixed beam, and adaptive beam algorithms for comparative operational evaluation.
- Hardwire interconnections between Pallet and Module equipments, rather than Mux/Demux networks in order to minimize implementation impact and cost.
- Data Recorder: The on-board Spacelab Pallet recorder will be used to record AMPA Experiment performance.

4.1.2 Experiment System Link Analysis

The AMPA Experiment System will be designed to support either narrowband frequency modulated (NBFM) voice or bi-phase shift keyed (BPSK) data at 4.8 kbps with a carrier-to-noise density (C/N₀) of +53 dB-Hz to support Maritime users or a C/N₀ of +46 dB-Hz to support Aeronautical users.

For the experiment, the communications link is primarily a simplex link between ground based user terminals (simulating a Maritime and/or Aeronautical user) and the AMPA experimental system located in orbit. All Modem functions on the signal to be transmitted to-or-received from the user will be performed by the Experiment system, even though the signal source or terminus may be on the ground (signals relayed to-or-from AMPA from the ground station by way of the Orbiter's TDRS multiple access system).

Link calculations for the forward (space-to-user) and return (user-to-space) links have been calculated using the expression:

$$C/N_0 = \frac{P_T G_T G_R \alpha_S}{K T_S M}$$

where:

P_T = transmitted power

G_T = transmit antenna gain

G_R = receive antenna gain

α_S = system losses including free space,
atmosphere, scan loss, polarization,
multipath and demodulation losses

K = Boltzman's Constant

T_S = system noise temperature

M = system design margin

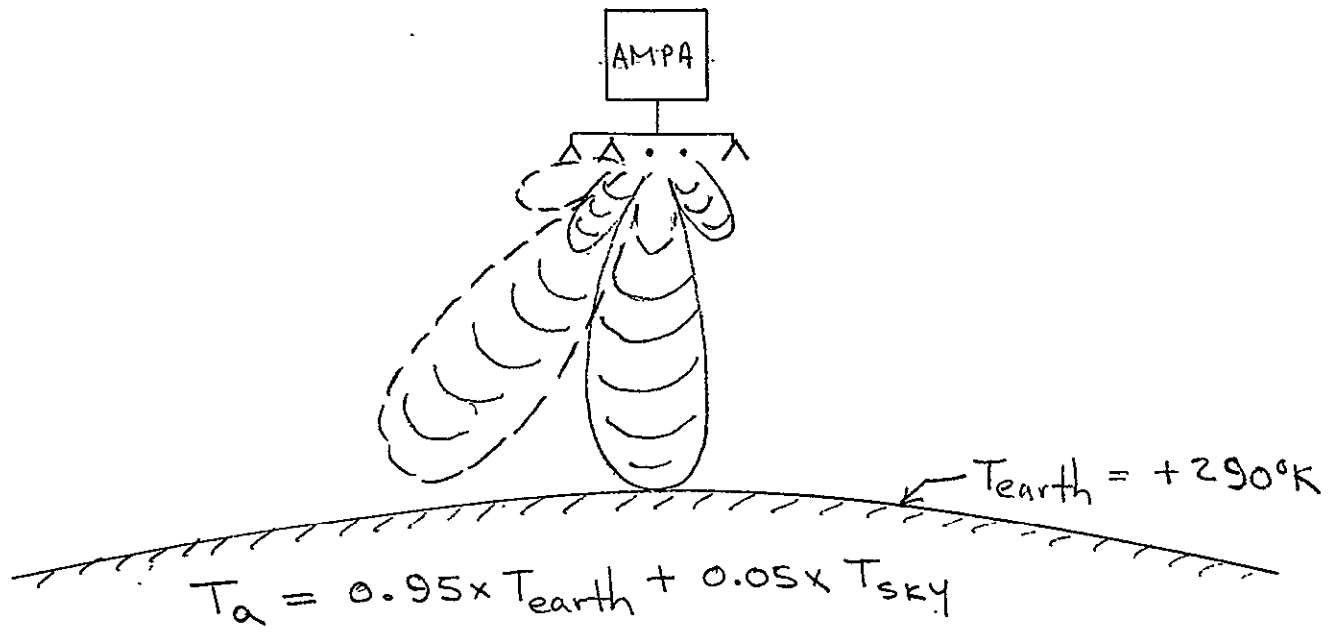
The atmospheric losses are negligible (≈ 0.16 dB), scan loss is due to electronically steering the array (2.2 dB at ± 70 degrees for the selected flared cone turnstile element), polarization loss has assumed to be 0.5 dB, multipath losses are estimated to be small (≈ 0.5 dB) for a circularly polarized antenna element since reflected signals reverse their sense of polarization (especially at low grazing angle), and 1.0 dB has been assumed for signal demodulation losses.

In the return link, the antenna and system noise temperatures have been computed using the geometry and expressions shown in Figure 4.1-5. A bi-polar transistor low noise amplifier with a 2 dB noise figure and gain (G_1) of 20 dB, line/component losses (L_1) of 1.5 dB ahead of the amplifier, and a mixer with a conversion loss of 7.5 dB has been assumed. The system noise temperature of 655°K or 28.2 dB-°K, result in a noise density (KT_S) of -170.4 dBm/Hz on the AMPA Experiment System.

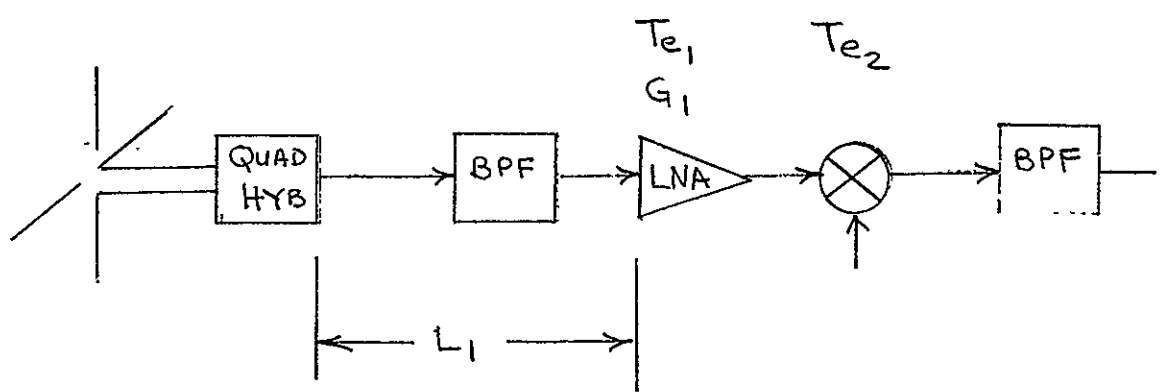
In the forward link, the ground terminal is assumed to have a low gain hemispherical coverage element, providing a cardioid shaped pattern as shown in Figure 4.1-6. This type of coverage can be achieved with a Kilgus Volute (or quadrifilar helical element*), providing conservatively -2 dBi gain on the horizon. Other potential elements to be considered include the flared cone-turnstile or a combination of a crossed dipole and a monopole; the crossed dipole providing zenith coverage and the monopole providing horizon coverage. The resultant antenna temperature as seen by this element is shown in Figure 4.1-6 to be 69°K. The ground receiver front end has been assumed to be approximately 20 feet from the antenna; therefore, the total component/line losses (L_1) ahead of the amplifier has been assumed to be 2.5 dB. Using a bi-polar transistor low noise amplifier with a noise figure of 2 dB and gain of 20 dB, and a mixer with a conversion loss of 7.5 dB, result in a system noise temperature of 621°K or 27.9 dB. The user's receiver noise density is then -170.7 dBm/Hz, and the $G/T_S = -29.9$ dB/°K.

* Kilgus C.C. Resonant Quadrifilar Helix Design, IEEE Transaction Antennas and Propagation, Vol AP-17, May 1969

$$T_{\text{sky}} \leq 30^{\circ}\text{K}$$



● ANTENNA NOISE TEMPERATURE

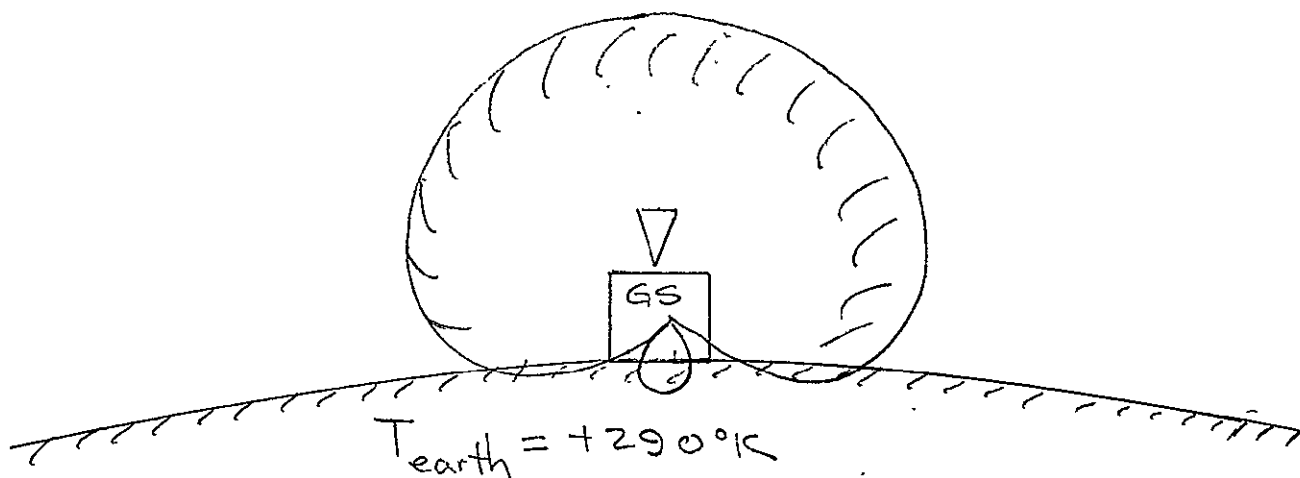


$$T_s = T_a + (L_1 - 1)T_0 + L_1 T_{e1} + \frac{L_1 T_{e2}}{G_1} + \dots$$

● SYSTEM NOISE TEMPERATURE

FIGURE 4.1-5. SYSTEM NOISE TEMPERATURE GEOMETRY FOR RETURN LINK

$$T_{\text{sky}} \leq 30^{\circ}\text{K}$$



$$T_a = 0.85 \times T_{\text{sky}} + 0.15 \times T_{\text{earth}} = 69^{\circ}\text{K}$$

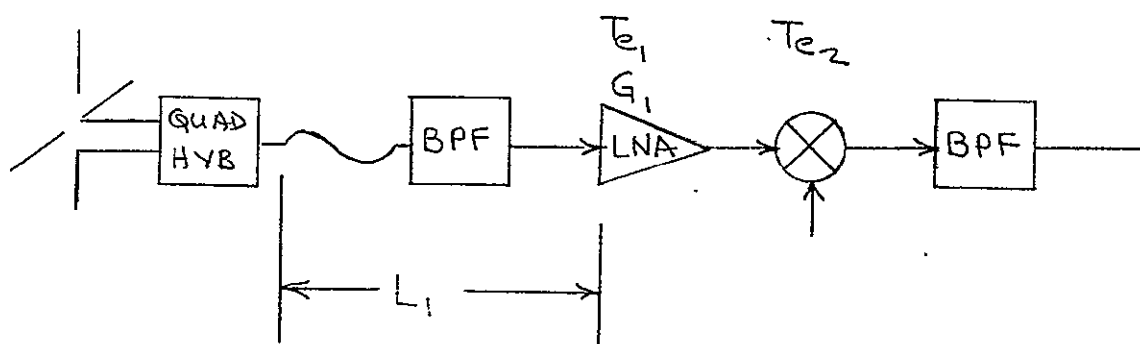


FIGURE 4.1-6. SYSTEM NOISE TEMPERATURE GEOMETRY FOR FORWARD LINK

The resultant link power budgets for the forward and return links have been computed as shown in Table 4.1-4, assuming a return link frequency of 1640 MHz and a forward link frequency of 1540 MHz.

The link budget shows that the required C/N₀ of +53 dB-Hz for the Maritime user is achieved in the forward link with a system margin of +5.4 dB, and in the return link with a system margin of +6.3 dB, assuming a user ERP of +8 dBw, or a transmit power of +10 dBw into the -2.0 dBi antenna. For the Aeronautical user requiring only a C/N₀ of +46 dB-Hz, the link margin increases by +7 dB to +12.4 dB and +13.3 dB in the forward and return links, respectively.

The additional system margin provided when operating with Aeronautical type users offers an opportunity to operate the AMPA Experiment System in the bentpipe repeater mode where the received signal from a user is simply frequency translated and returned to a second user without demodulation and modulation on the Spacelab. This bentpipe or tandem link mode requires a higher CNR in the forward link than considered previously. For the tandem link operation, the CNR required in the second link can be computed using the expression:

$$Q_0 = \frac{Q_1 Q_2}{Q_1 + Q_2 + 1}$$

where

Q_0 = required output CNR at the receiving user terminal

Q_1 = CNR required in the first link (user-to-space)

Q_2 = CNR required in the second link (space-to-user)

If we assume a CNR degradation ($\Delta Q = Q_0/Q_1$) in the AMPA repeater, the above expression can be rewritten as:

$$Q_2 = \frac{\Delta Q (1 + Q_1)}{(1 - \Delta Q)}$$

TABLE 4.1-4 AMPA SPACELAB LINK REQUIREMENTS

PARAMETERS		AMPA-TO-USER	USER-TO-AMPA
FREQUENCY	MHz	1540	1640
C/N ₀ Req'd.	dB/Hz	+53.0	+53.0
AMPA • ERP ⁽²⁾ • G _R /T _S ⁽³⁾	dBw dB/°K	+27.4	-9.0
USER • ERP ⁽⁴⁾ • G _R /T _S ⁽⁵⁾	dBw dB/°K	-29.9	+8.0
K ⁽⁶⁾ α _S	dBw/Hz/°K dB	-228.6 -167.7 ^(6.1)	-228.6 -168.3 ^(6.2)
C/N ₀ ⁽¹⁾ available	dB/Hz	58.4	59.3
SYSTEM MARGIN	dB	+5.4	+6.3

NOTE:

$$\frac{(1) C/N_0}{(1)} = \left(\frac{P_T G_T}{K} \right) \left(\frac{G_R}{T_S} \right) \frac{\alpha_S}{\text{Margin}}$$

(5) G_R = -2.0 dBi and T_S = +27.9 dB/°K

(2) ERP = P_TG_T = P_T (N × G_{e1})

where N = 32
 G_{e1} = +4.2 dBi

(3) G_R = +19.2 dBi and
 T_S = +28.2 dB/°K

(6) α_S = System losses (free spaces, atmospheric, scan loss, polarization, multipath demodulation)

(6.1) α_S = 163.4 + 0.16 + 2.2 + 0.5 +
 0.5 + 1.0 = 167.8 dB

(6.2) α_S = 163.9 + 0.16 + 2.2 + 0.5 +
 0.5 + 1.0 = 168.3 dB

} FOR MAXIMUM SLANT RANGE OF 2293 km

(4) ERP = P_TG_T

where P_T = +10 dBw
 G_T = -2.0 dBi

Allowing a ΔQ of 1 dB in the AMPA repeater, the above expression has been plotted in Figure 4.1-7 and shows that for an output Q_0 of +7 dB, that the first link must provide a Q_1 of +8 dB, and the second link must provide a Q_2 of +14.5 dB to operate with the forward link user on the horizon (range of 2293 km). If the user range was reduced to approximately 1200 km or less, then adequate CNR is available in the second link to provide the required output CNR of +7 dB with a +3 dB system margin.

This bentpipe mode of operation provides another useful AMPA experiment that can evaluate future operational concepts that may include direct user-to-user communications.

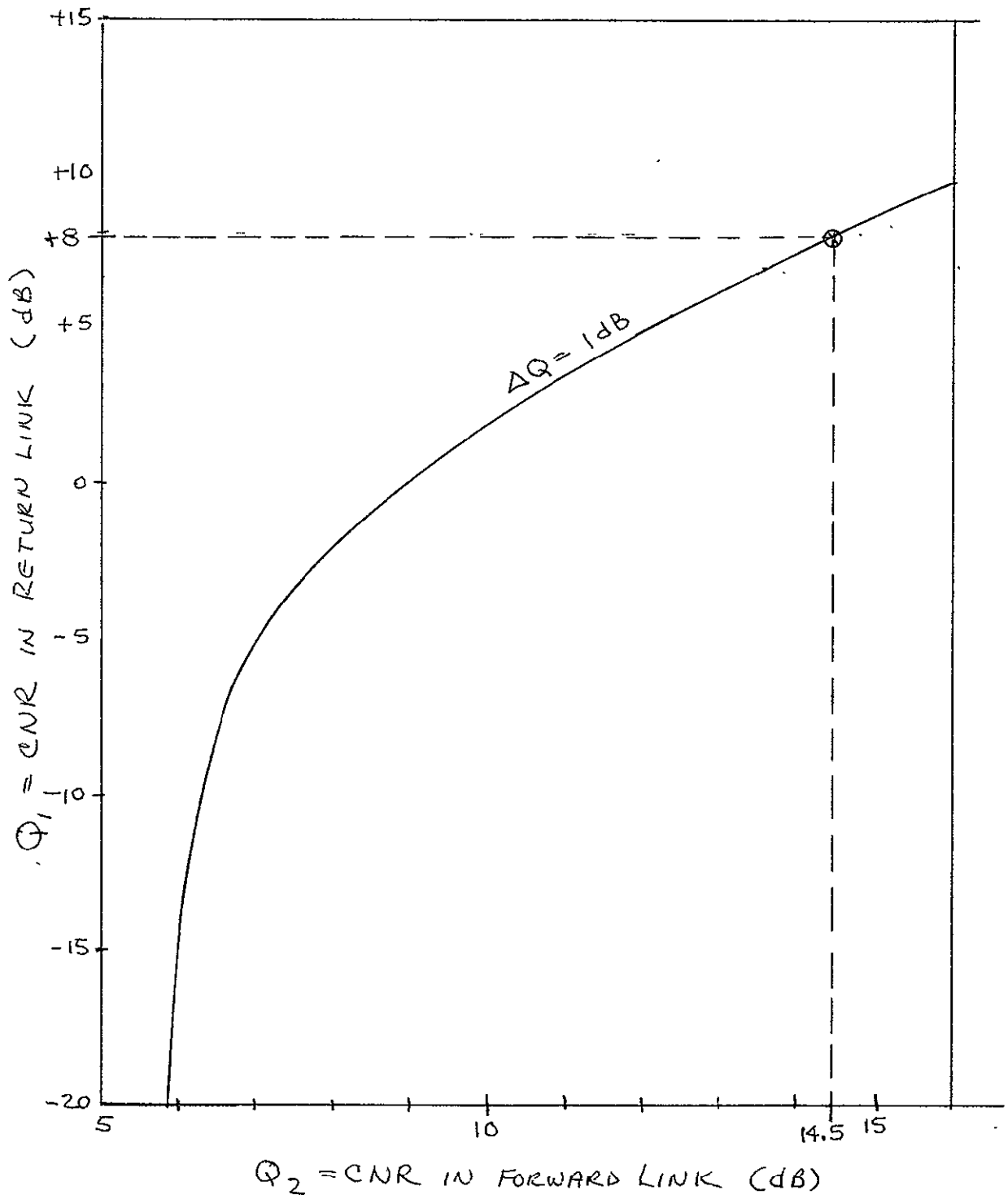


FIGURE 4.1-7. CNR REQUIREMENTS IN TANDEM LINK

4.1.3 Dynamic Signal Environment

The Spacelab is placed in a low circular earth orbit with a nominal altitude of 400 km, having an orbital period of approximately 92.6 minutes. For fixed user terminals, this causes a doppler frequency shift as well as a dynamically changing angular motion between the AMPA Experiment System and the signal sources. For signals on the horizon, the doppler frequency shift can be as high as ± 38 kHz which must be removed in order to track the desired NBFM voice or 4.8 kbps data.

The dynamically changing angular motion has a large impact on the adaptive system, since the adaptive algorithm uses historical data to determine its next adjustments to its beam processor networks. This motion is not too critical when no RFI's are present, since the adaptive processor need only place the relatively broad peak of the main beam on the desired signal; however, in the presence of RFI's, the adaptive processor must also maintain the RFI's in sharp nulls in order not to degrade the performance.

In order to evaluate the impact of the angular motion, the spatial geometry (shown in spherical coordinate system) as shown in Figure 4.1-8 has been used. The Spacelab is orbiting at a 400 km altitude in the y-z plane, and the signal(s) can be located anywhere on the earth's surface. The relative angular rate of motion has been calculated and plotted in Figure 4.1-9 as a function of the angular offset of a signal from the Spacelab flight path. As expected, the most severe case is when the Spacelab flies directly over the signal, reaching a maximum rate of 1.1 degree per second. This represents a very severe environment that requires a relatively high speed adaptive processing time in order to track a signal and maintain RFI's in spatial nulls.

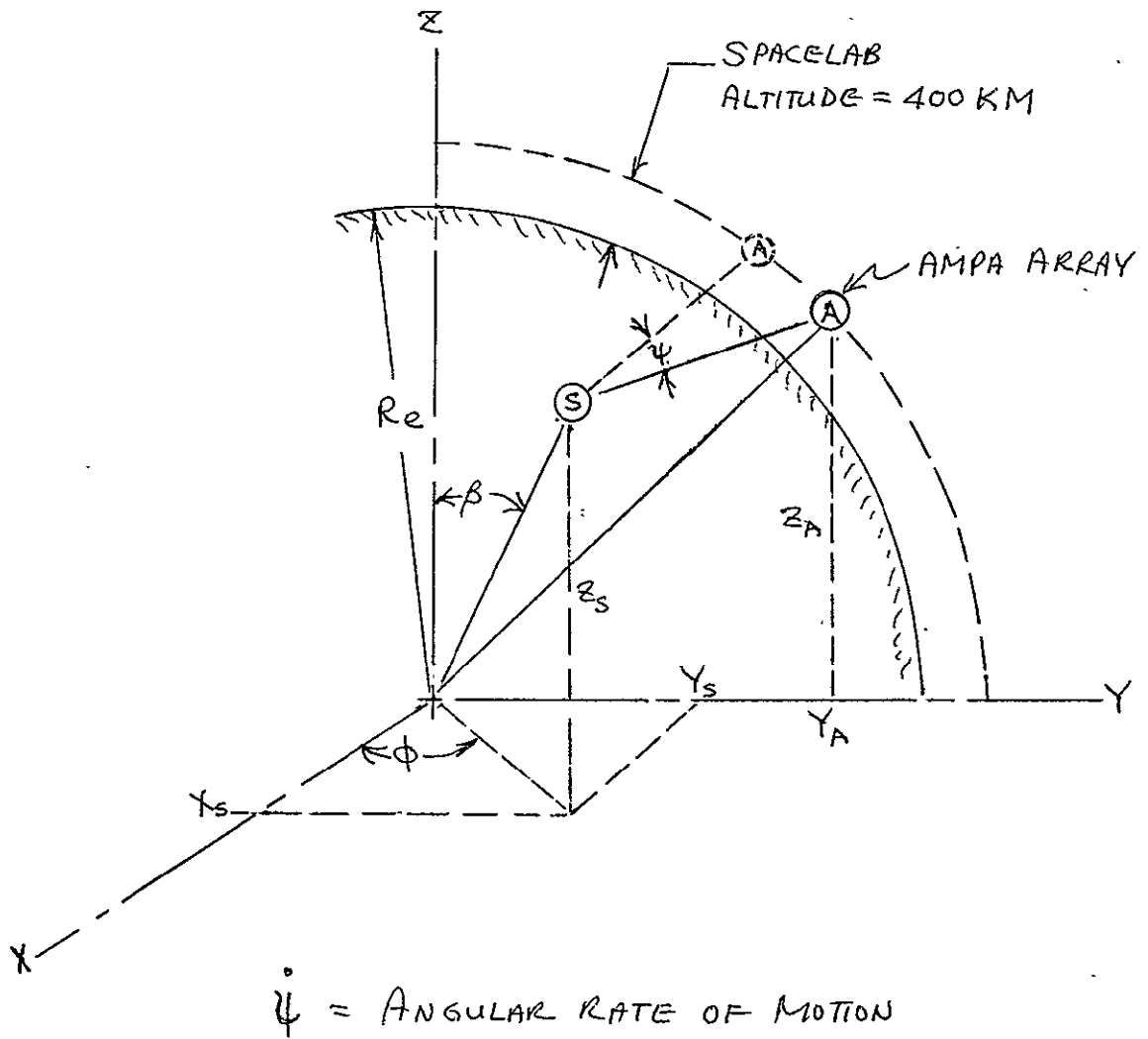
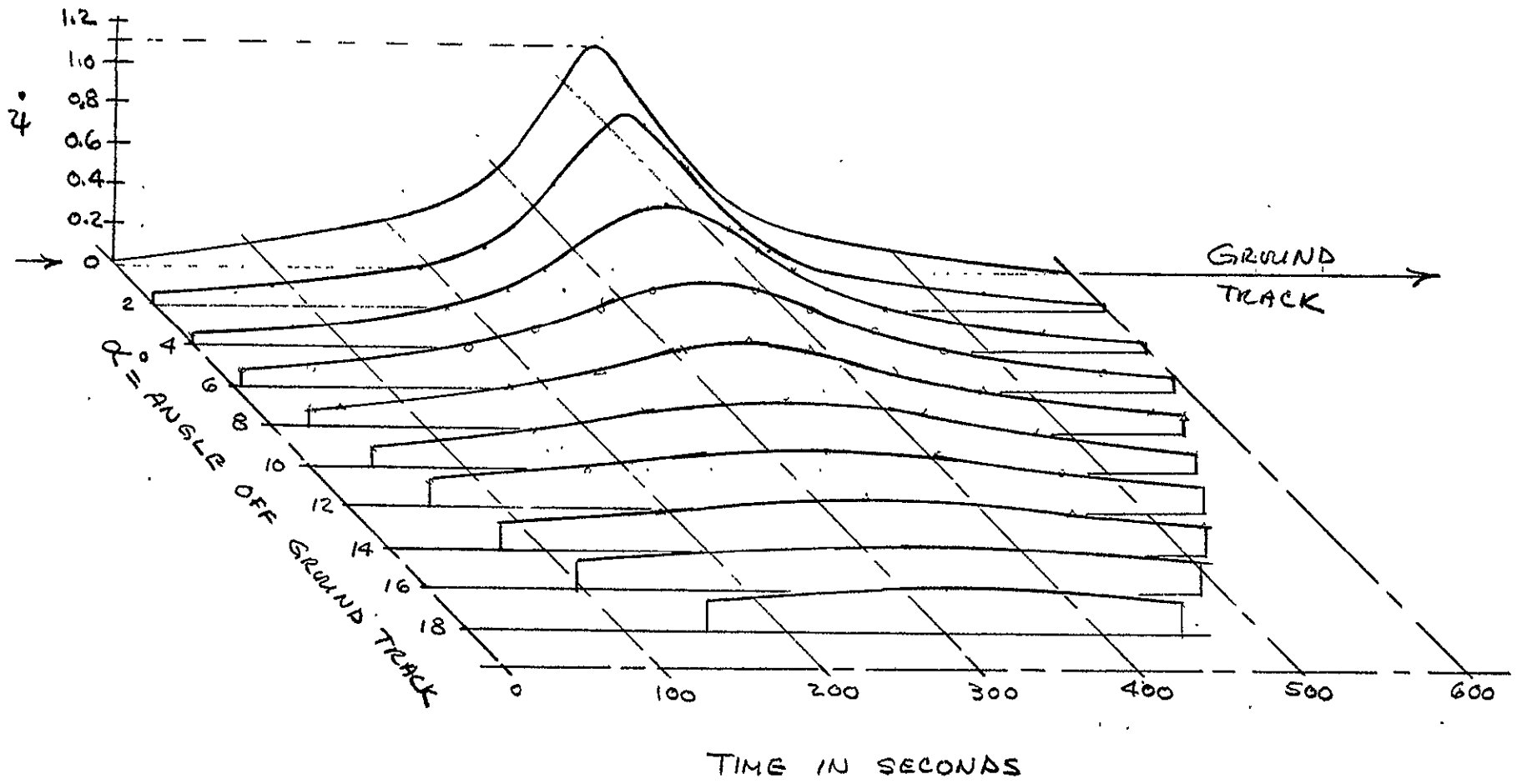


FIGURE 4.1-8. SPATIAL GEOMETRY OF AMPA AND SIGNAL SOURCE



NOTE:

- α = SIGNAL LOCATION OFF GROUND TRACK IN DEGREES
- $\dot{\psi}$ = ANGULAR RATE OF MOTION BETWEEN SIGNAL AND ARRAY

REV. 1 10/11/76

FIGURE 4.1-9. SIGNAL/ARRAY -- RELATIVE ANGULAR RATE OF MOTION

4.1.4 Description of the AMPA Experiment System

4.1.4.1 General

A simplified functional block diagram of the AMPA Experiment System is shown in Figure 4.1-10. The system is divided into two subsystems, viz., the Pallet Subsystem and the Spacelab Module Subsystem. The Pallet Subsystem includes the variable aperture array, multichannel transceiver, frequency source and power conditioner that represents the Spaceborne segment; and the Spacelab Module Subsystem includes the beam and signal processing networks, IM Simulator, frequency source, control unit, digital processor and power conditioner that represent the ground segment of the selected Beam Process on Ground Approach. The Pallet and Spacelab Module Subsystems are interconnected with a hardwire link.

● Dynamic Range

The signal is received nominally at 1640 MHz. The receiver input power level may be as low as minus 141.1 dBm, representing an Aeronautical type user ($C/N_0 = +46$ dB-Hz) located on the horizon, or as high as minus 116.7 dBm, representing a Maritime type user ($C/N_0 = +53$ dB-Hz) located directly below the Spacelab. If we include unintentional interferers (RFI's) with an RFI/S of +10 dB, the receiver sees an input signal dynamic range of approximately 35 dB.

● Operating Frequency

The Experiment System is designed to operate in 1640 ± 1.25 MHz frequency band in the return direction (user-to-AMPA) and in the 1540 ± 1.25 MHz frequency band in the forward direction (AMPA-to-user), forming two independently steerable beams in both directions. These 4 beams provide two full duplex communications links to two users, or 4 simplex communications links to four separate users. Although the experiment system has been designed to cover 2.5 MHz in both return and forward directions, the two 50 kHz operating channels in the return and forward links are fixed and preassigned in order to minimize the additional complexity and cost in the design of the pallet mounted Frequency Source. However, in order to fully evaluate the spatial dispersion of intermodulation products with the AMPA array, two adjacent transmit channels in the middle of the band are used, representing the most severe case if IM suppression were not achievable with a phased array.

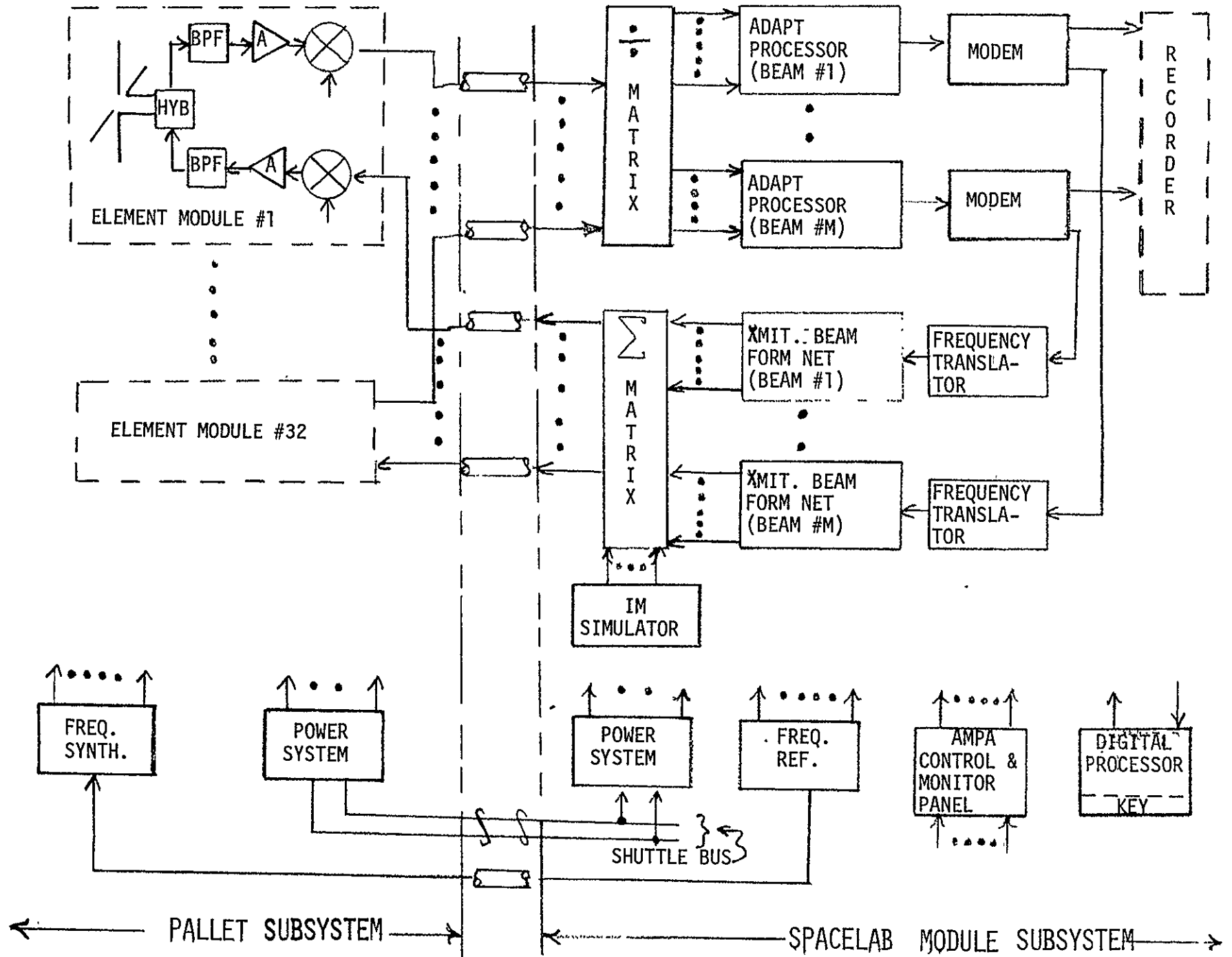


FIGURE 4.1-10. AMPA EXPERIMENT SYSTEM

● Modes of Operation

In addition to the full duplex and simplex modes of operation, the Experiment System has been designed to operate in the bentpipe mode that allows direct user-to-user communication without interfacing with the ground station. In this mode, the Experiment System is essentially a turn-around repeater, simply transmitting the received signal after frequency translation without demodulation and remodulation. Although this feature is not included in current MARISAT or planned for the forthcoming AEROSAT systems, this mode of operation can be realized with minimal implementation impact and has been included in the system design. This capability may be desirable in future satellite repeater systems, and the AMPA Experiment System provides a viable test bed to evaluate its usefulness and performance.

● On-Board Data Interface

All signals received from a user are demodulated and recorded on the on-board Spacelab Payload Recorder, and/or relayed, after demodulation to the TDRS Ground Station by way of Orbiter's TDRS multiple access transceiver. Conversely, all baseband signals to be transmitted to a user will be initiated from the TDRS Ground Station, relayed to the Spacelab by way of the same TDRSS link, and used to modulate a carrier at 20 MHz for subsequent retransmission to the ultimate receiver. In addition, all AMPA Experiment System housekeeping data and performance parameters will be recorded on the Payload Recorder and/or relayed to the ground by way of the TDRSS link. All system commands for changing the experiment mode of operation will be remotely initiated from the ground and relayed to the Experiment System by way of the TDRSS link.

● On-Board Command and Control Functions

The only command control functions available in the spaceborne AMPA Experiment System will be an over-ride power switch that can de-energize the Experiment system in case of emergency, and a Mass Memory (high speed paper tape reader) that can load the adaptive algorithms and executive routines into the core memory of the Digital Processor in the event that core memory content is destroyed during launch or in-flight transit phases. These functions are located on the AMPA control unit.

4.1.4.2 Detailed Block Diagram

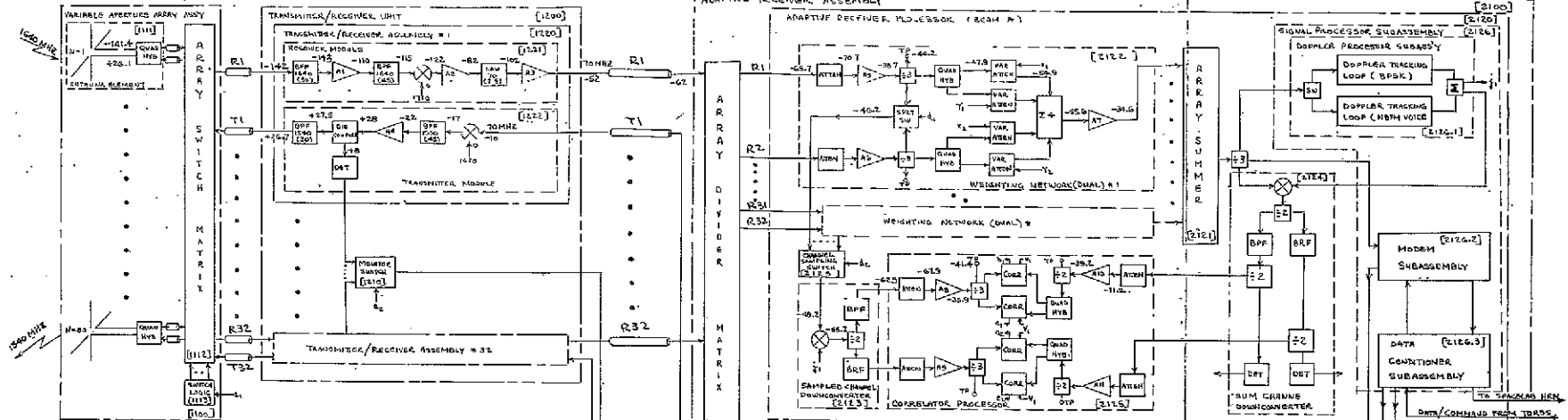
Figure 4.1-11 shows an overall detailed block diagram of the AMPA Experiment System and the frequency and power levels at the major junctions.

• Array Configuration

The signal is received by a variable switched array that can be varied from a fully filled array to a thinned array with an aperture size factor (thinned-to-filled aperture size ratio) of 4.23. The recommended system array is a switched aperture phased array whose aperture size factor can be varied in discrete steps of 1, 2, 3 and 4.23. The switched aperture array employs 80 elements; however, only 32 elements are used for any discrete aperture size. The elements are modified flared-cone turnstile elements fed by a quadrature hybrid that provides left hand circular polarization (LHCP) on receive and right hand circular polarization (RHCP) on transmit. Each element conservatively provides a peak gain of +4.2 dBi (dB above an ideal isotropic radiator) and +2.2 dBi at scan limits (± 70 degrees), resulting in a total array gain of +19.2 and +17.0 dBi on the peak and scan limits, respectively. The output of the array is fed to an array switch matrix that selects the 32 elements for the desired aperture size factor.

• Receiver Module

The received signal from each element is input to a receiver module that uses a low noise bi-polar transistor amplifier. This results in a system noise temperature of plus 28.2 dB-°K using an amplifier with a 2 dB noise figure. The receiver module effectively downconverts the output from the low noise amplifier to 70 MHz and uses a 2.5 MHz bandpass surface acoustical wave (SAW) filter to reject all out of band signals. The signal is amplified to a level of -52 dBm for transmission by hardwire (RG-188) to the Adaptive Receiver Processor located in the Spacelab Module. For the purposes of this study analysis, the hardwire link has been estimated to be as long as 18.3 meter (≈ 60 ft.) resulting in an insertion loss of approximately 10 dB at 70 MHz.



REPRODUCIBILITY OF THE ORIGINAL PAPER IS POOR

NOTES:

- ALL POWER LEVELS IN dBm
 - FOR FIXED APERTURE ARRAY
 - N = 32
 - ARRAY SWITCH MATRIX [1112]
 - SWITCH LOGIC [1113]
- NOT REQUIRED

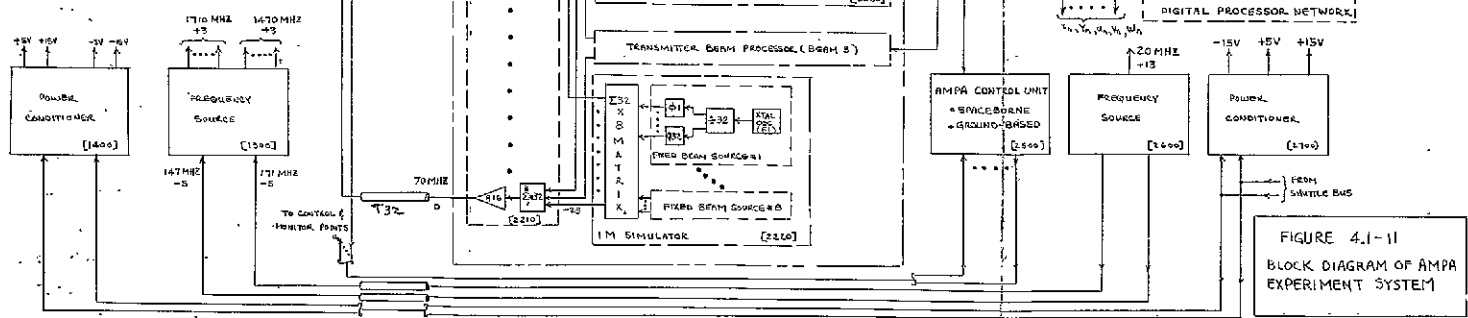


FIGURE 4.1-11
BLOCK DIAGRAM OF AMPA
EXPERIMENT SYSTEM

PALLET SUBSYSTEM SPACELAB MODULE SUBSYSTEM

• Algorithm - Pointed, Fully Adaptive and Directed-Adaption

The pointed mode is non-adaptive and simply steers the main beam to the desired user with no spatial nulling of RFI's. The fully adaptive mode uses a unique user waveform signature to provide automatic acquisition and track of a desired signal while simultaneously nulling all RFI's. The unique user signature can be a pseudo random noise (PN) code as used in the multiple access system for TDRSS, coded address as used in MARISAT, or simple CW tone(s). For the AMPA Experiment, a CW tone is used to minimize system complexity and cost.

The adaptive algorithm is a closed loop convergence process that uses historical and current correlator output data to determine the size and direction of the next step. Generally, convergence can be achieved in 5 to 10 iterations, dependent upon the complexity of the signal environment (number of signals, power levels, and spatial distribution). For the AMPA Experiment System, it is expected that convergence can be achieved in less than one second.

The directed-adaption mode is a combination of the pointed and fully adaptive modes. In this mode, a pseudo signal is used (via software) to initially point the main beam in the approximate vicinity of the desired signal while the adaptive algorithm nulls all RFI's. This mode is very powerful since it allows the main beam to be scanned in order to provide adequate input signal-to-interference plus noise ($S/(I+N)$) to initiate the doppler tracking loop and $S/(I+N)$ maximization process.

• Adaptive Receiver Processors

The 70 MHz signal from the 32 receiver modules are fed into one of two Adaptive Receiver Processors at a minus 62 dBm power level. Both processors can operate in the pointed, fully adaptive or in the directed-adaption modes.

The Adaptive Receiver Processor inputs the 32 signals (70 MHz) from the receiver modules and correlates the desired signal and interference signals from the individual channel and the array sum output. The outputs of the signal and interference correlators provide the measureables required by the adaptive algorithms to determine the inputs required to adjust the weighting network with the aid of the Digital Processor Network. Computer simulations have shown that a single correlator processor subassembly that sequentially

samples the 32 channel provides adequate adaptive process times in the dynamic environment of a moving array platform to maintain the required $S/(I+N)$ performance. Similarly, an 8 bit quantization level has been determined adequate for the AMPA environment.

- Signal Processor Assembly

The summed array output from the Adaptive Receiver Processor is then input to the Signal Processor Assembly. The Signal Processor Assembly includes 3 subassemblies:

- Doppler Processor
- Modem
- Data Conditioner

The Doppler Processor subassembly compensates for the doppler frequency shift for BPSK data or NBFM voice signal formats. The Modem subassembly demodulates and detects the signal for subsequent recording on the Payload Recorder or for relay to the ground by way of TDRSS; or modulates the baseband signals from ground for transmission to the ultimate user; and the data conditioner interfaces with the Modem Subassembly and the on-board High Rate Multiplexer (HRM) to condition the signal in the return as well as the forward link directions.

- Transmitter Beam Processors

In the forward link (or transmit) direction, the input to the Transmitter Beam Processor is a 70 MHz (plus 9 dBm) signal from the Modem subassembly. The source of this signal is from the ground by way of the TDRSS link, or a bentpipe turnaround signal from another user. There are two Transmit Beam Processors that provide two independently steerable transmit beams. All transmit beam forming function is performed remotely (i.e., remote from the array) at 70 MHz, using the same weighting network design used in the receiver beam processors. Each of the 32 channel weighted outputs then contain the beam steering and beam shaping information necessary to steer the beam to the desired user, and to place spatial nulls on co-channel receivers.

- IM Simulator

An IM simulator generates 8 additional weighted signal outputs that are combined with the 2 weighted signals from the two Transmitter Beam Processors that will allow assessment of spatial dispersion of IM products with a total of 10 signals for the AMPA array as a function of aperture size factor. A Summer/Amplifier Matrix combines the output for each respective channel from the two Transmitter Beam Processors and from an IM Simulator.

- Transmitter Modules

Each of the 32 outputs from the Summer/Amplifier Matrix is relayed at 70 MHz to the Transmitter Modules in the Pallet Subsystem through approximately 18.3 meter (60 ft.) of RG-188 coaxial cables at a power level of 0 dBm.

The 70 MHz transmit signal loses approximately 10 dB insertion loss in the RG-188, and inputs a minus 10 dBm signal into the Transmitter Module. The signal is upconverted to 1540 MHz, amplified to plus 28 dBm, fed through a directional coupler (used to monitor the power level), filtered, and fed to the array switching matrix that selects the appropriate array elements to be used (same as receive elements).

The L-band power amplifier is a Class C amplifier that operates nominally with a 3 dB backoff; however, its back-off is made adjustable with a variable attenuator in the Transmitter Beam Processor so that other back-off levels can be evaluated. This allows an empirical evaluation of the achievable IM suppression in the Class C amplifier versus the achievable spatial dispersion of IM products with the AMPA array as a function of aperture size factor.

Each of the L-band amplifiers has also been sized to provide a total array radiated power of 13.2 watts for the two beams, or a radiated power of 6.6 watts per beam. This sizes the transmit module output power per beam to be the same as for the advanced conceptual system operating in geostationary orbit, so that the knowledge gained in the design, development, test and flight of the Experiment System Transmitter Module will be applicable to the design of the geostationary operational system.

• Other Associated Support Assemblies

Other associated support assemblies in the Experiment System are the Frequency Sources and the Power Conditioners.

• Frequency Sources

The prime frequency reference is the Spacelab mounted Frequency Source. This source generates the 20 MHz at a plus 13 dBm power level required for the local oscillators in the Adaptive Receiver Processors as well as the 171 MHz and 147 MHz references used by the Pallet mounted Frequency Source. The 171 MHz and 147 MHz are then used as references to generate the 32 1470 MHz (at plus 3 dBm) local oscillator sources for the Transmitter Modules and the 32 1710 MHz (at plus 3 dBm) local oscillator sources for the Receiver Modules.

• Power Conditioners

The two Power Conditioners provide the regulated +5, +15 and -15 volts for the Pallet and Spacelab Module Subsystem from the Orbiter's basic prime power DC bus lines.

• Weight and Power Summary

The recommended AMPA Experiment System configuration weighs 235 kg and requires 383 watts of prime power, exclusive of the Digital Processor Network.

4.1.4.3 AMPA Experiment System Family Tree

The AMPA Experiment System has been designed and organized in a modular building block format that simplifies and eases the design, development, test and fabrication of "like" modules and subassemblies. Generally, building one and qualifying it will be representative of the other "like" units. The AMPA Experiment System Family Tree in Figure 4.1-12 shows the major assemblies and/or units of the system, viz:

- Pallet Structure
 - Variable Aperture Array Assembly
 - Transmitter/Receiver unit
 - Frequency Source
 - Power Conditioner

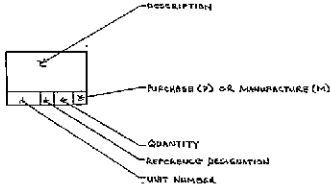
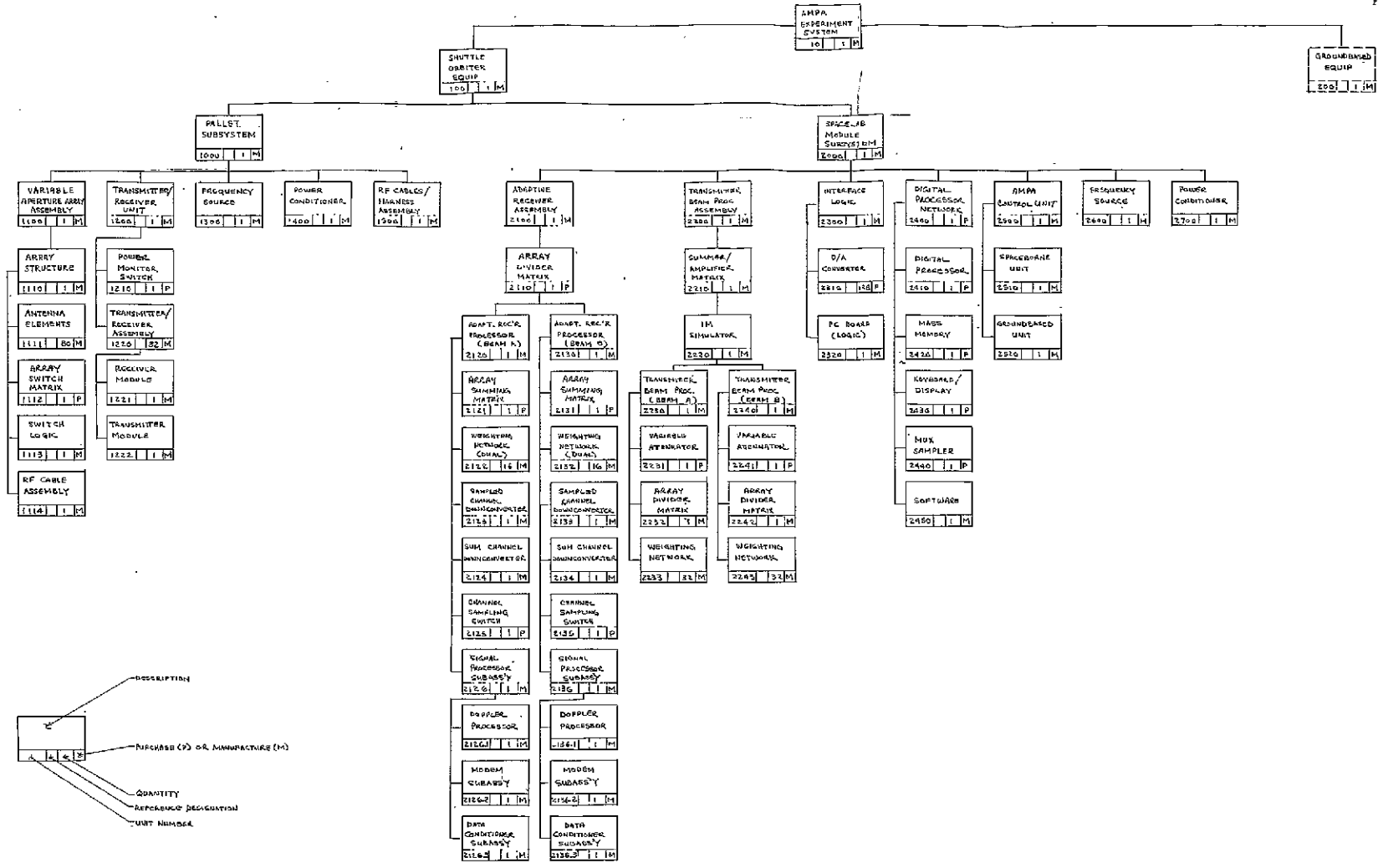


FIGURE 4-1-12
AMPA EXPERIMENT SYSTEM FAMILY TREE

- Spacelab Module Subsystem
 - Adaptive Receiver Assembly
 - Transmitter Beam Processor Assembly
 - Interface Logic Assembly
 - Digital Processor Network
 - Frequency Source
 - AMPA Control Unit
 - Power Conditioner

The Family Tree provides an excellent engineering and production tool that shows the breakdown of each major assembly and units into their modules and subassemblies. All blocks of the family tree are designated with unit numbers that correspond with its counterpart in the detailed system block diagram (Figure 4.1-11).

4.2 PALLET MOUNTED SUBSYSTEM

The components of the Pallet Subsystem are shown in Figure 4.2-1 and consist of a variable aperture array assembly, switch matrix, 32 transmitter modules, 32 receiver modules, frequency source and power conditioners. The Pallet Subsystem is interconnected with the Spacelab Module Subsystem by hardwires.

4.2.1 Array Assembly

4.2.1.1 General

The array assembly includes the antenna elements and array structure, which will be designed primarily for hard mounting on one of the pallet structures. Depending upon the pallet location in the orbiter's payload bay, the total field-of-view (FOV) of the array may be obstructed by the orbiter structure, as shown in Figure 4.2-2. Therefore, as an option, an alternate mounting concept using erectable Astro-mast that extends the array to clear all orbiter structure has also been included. This allows the array to be used during the First Spacelab Mission where hardware cannot be deployed external to the shuttle orbiter flight profile, or for subsequent Spacelab missions where the array may be erectable out of the payload bay in order to clear structural obstructions. Array erection out of the payload bay increases the experiment efficiency by providing coverage out to the horizon; thereby increasing the dwell time on a user as well as increasing the instantaneous coverage. On the other hand, the maximum doppler shift increases from approximately ± 27 kHz to ± 38 kHz; however, this will not significantly impact the design requirements for the doppler tracking network.

4.2.1.2 Element Design

Each element shall provide left hand circular polarization (LHCP) on receive and right hand circular polarization (RHCP) on transmit. In addition, as described in the previous section, each element will be designed to provide coverage out to the horizon or to approximately ± 70 degrees.

The simplest and most amenable element types meeting the above requirements are the dual polarized elements, such as the crossed dipoles or turnstile, fed by quadrature hybrid, as summarized in Table 4.2-1. The inputs to the hybrid are connected to the orthogonally polarized elements and the two outputs provide LHCP for receive and RHCP for transmit, respectively. A summary of the candidate turnstile element has been selected as showing the most promise, providing approximately 5.2 dBi gain on boresight and 2 dBi gain at ± 70 degrees. For design purposes, it has been estimated that this element will conservatively

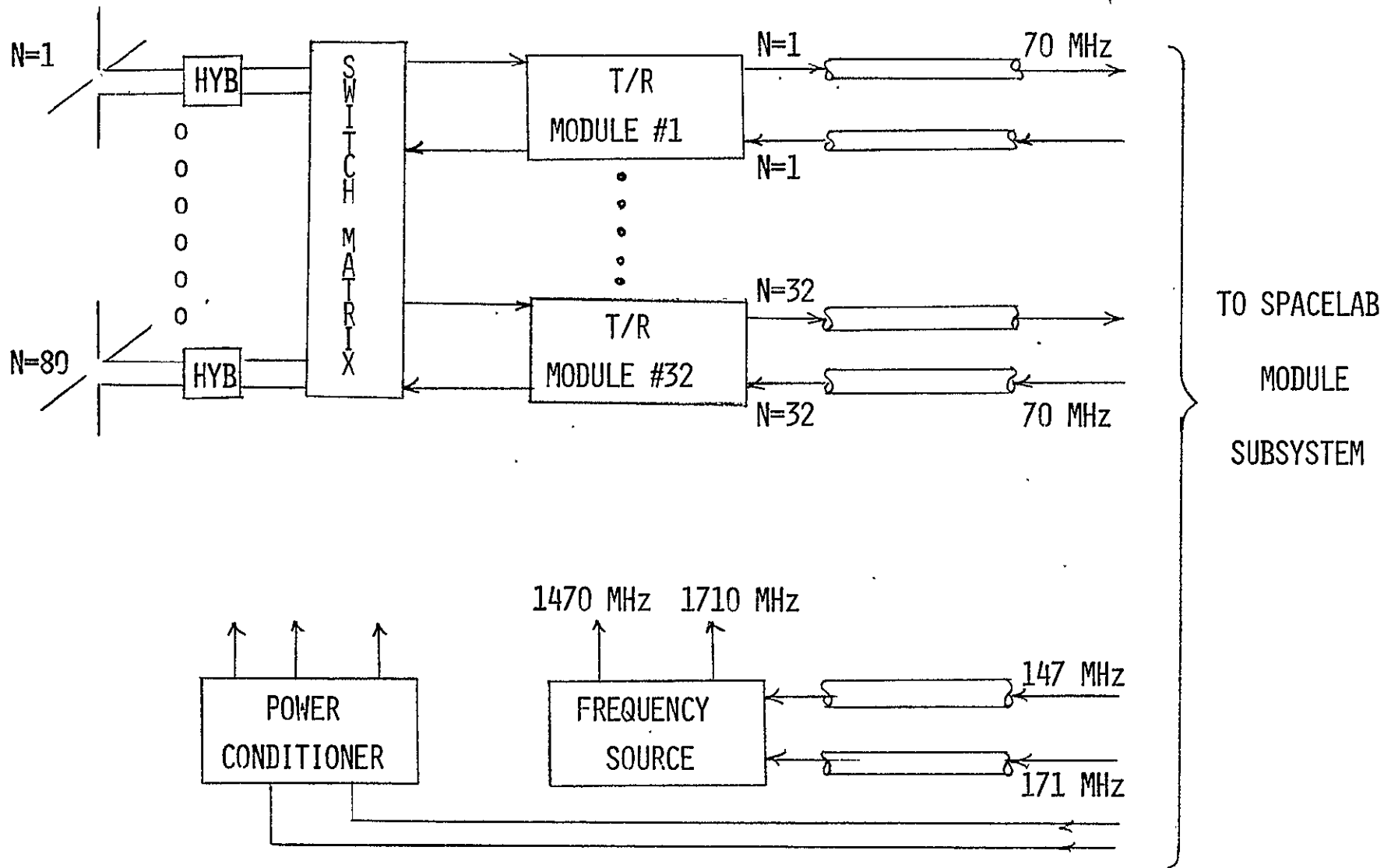


FIGURE 4.2-1 COMPONENTS OF PALLET SUBSYSTEM

A BLANK PAGE

A BLANK PAGE

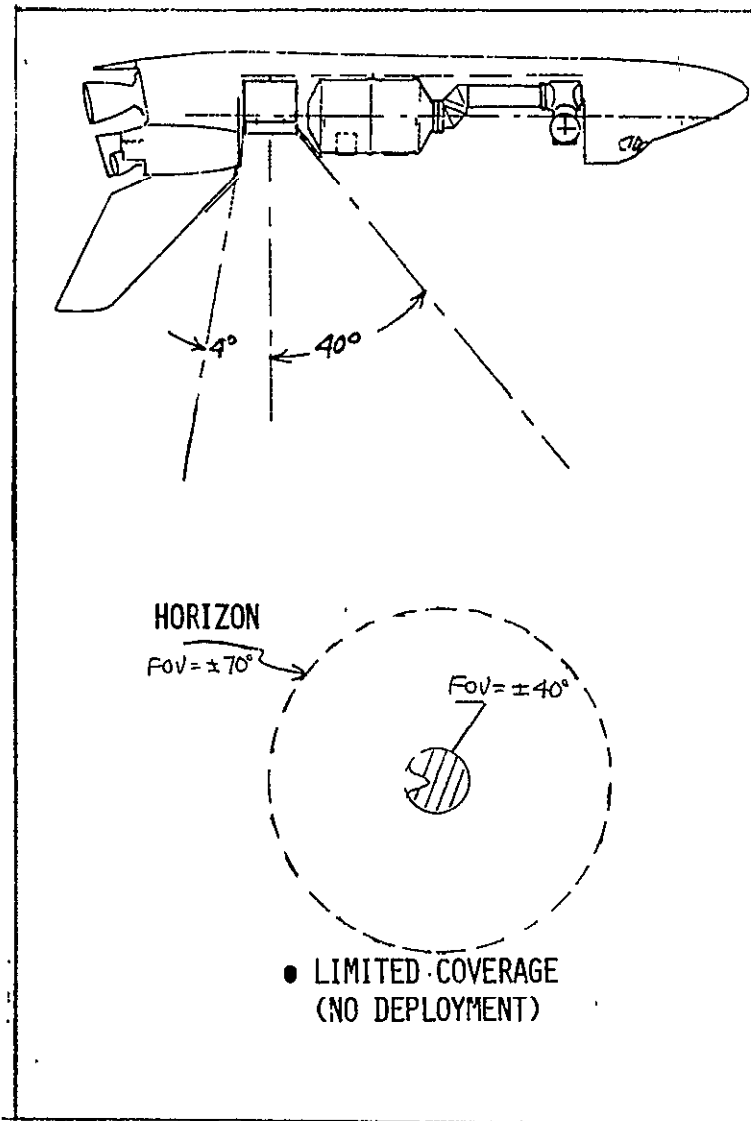
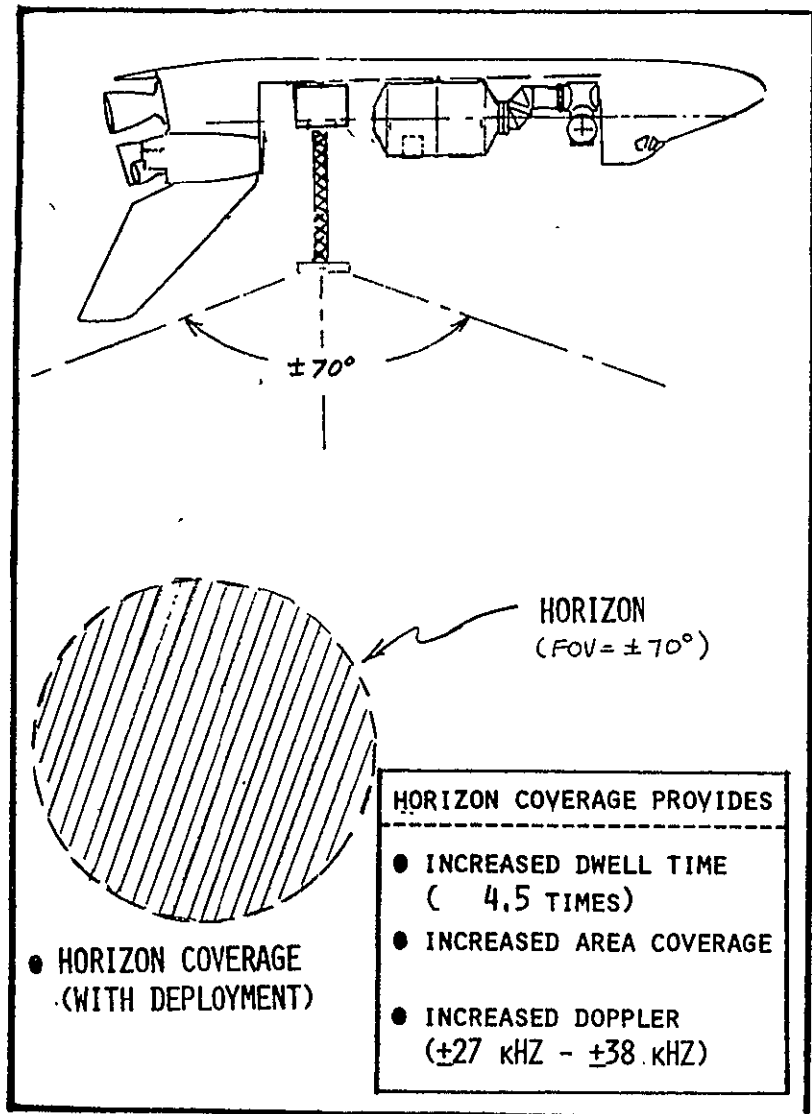
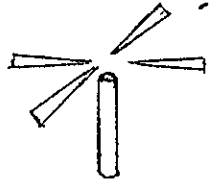
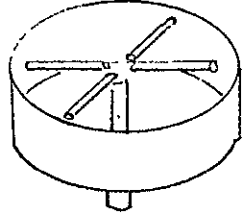
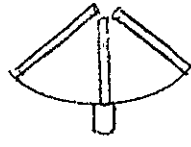
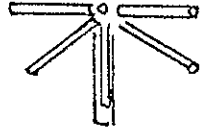
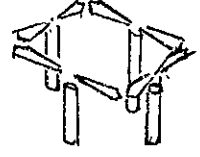


FIGURE 4.2-2. ACHIEVABLE COVERAGE

TABLE 4.2-1. CANDIDATE ELEMENT TYPES

PARAMETER	CROSSED DIPOLE OVER REFLECTOR ⁽¹⁾	CROSSED DIPOLE IN CAVITY ⁽²⁾	FLARED CONE TURNSTILE ⁽³⁾	TWO SUPERIMPOSED TURNSTILES ⁽⁴⁾	FOUR END LOADED DIPOLES ⁽⁵⁾
CONFIGURATION					
GAIN (dBi) ● AT 0° ● AT +70°	4.7 -3.0	6.0 2.0	5.2 3.0	4.5 0.5	4.7 -2.0
HPBW°	80	120.0	120.0	120.0	120.0
AXIAL RATIO (dB) ● AT 0°	1.5	1.5	1.3	2.0	1.2

- NOTES: (1) AIL Design
(2) Circularly Polarized Hemispheric Antenna, Rantec, MicroWaves, May 1964
(3) NASA Technical Brief, B73-10425, December 1973
(4) Two Communication Antennae for the Viking Lander Spacecraft, RCA, Moorestown, New Jersey
(5) AIL Design

provide a peak gain of 4.2 and 2.2 dBi (dB above an isotropic radiator) at scan limits, allowing for feed network losses and axial ratio losses.

The flared cone turnstile element design has been modified as shown in Figure 4.2-3 to provide independent outputs for the orthogonally polarized elements. The patterns in voltage ratios are shown for elevation cuts ($\theta = 0^\circ$, 45° , and 90°) and show excellent symmetrical coverage as shown in Figure 4.2-4.

4.2.1.3 Array Design

● General

The 32 element AMPA experiment array will be laid out so that its aperture can be varied from a fully filled array to a thinned array as shown in Figure 4.2-5, up to the maximum space allowable within the physical constraints of the shuttle orbiter payload bay without folding the array. For the purposes of this study, it has been estimated that adequate space for a 2.8 meter by 2.8 meter array structure will be available and a 2.24 meter by 2.24 meter array aperture. By implementing a variable aperture array, it will be possible to empirically:

- Assess the achievable spatial resolution to null interference emitters as a function of the aperture size factor, i.e., thinned-to-filled aperture size ratio.
- Evaluate the achievable spatial dispersion of IM products in a phased array as a function of the aperture size factor.
- Determine the beam pointing accuracy requirements in the receive and transmit beam weighting networks as a function of the aperture size factor.

● Filled Array

The 32 element array is laid out in a 6 x 6 square matrix array with the corner elements missing as shown in Figure 4.2-6 in its filled array configuration. For the filled array, the elements are spaced 0.565λ which represents approximately the minimum allowable element spacing with non-overlapping effective aperture for the recommended modified flare cone turnstile element. A typical single plane array pattern in the principal cardinal axis of the array has been synthesized with computer simulation for the case with uniform aperture illumination as shown in Figure 4.2-7, for the beam pointed on boresight. The resultant half power beamwidth (HPBW) is seen to be approximately 17 degrees and its sidelobe 15 dB below the peak of the main beam.

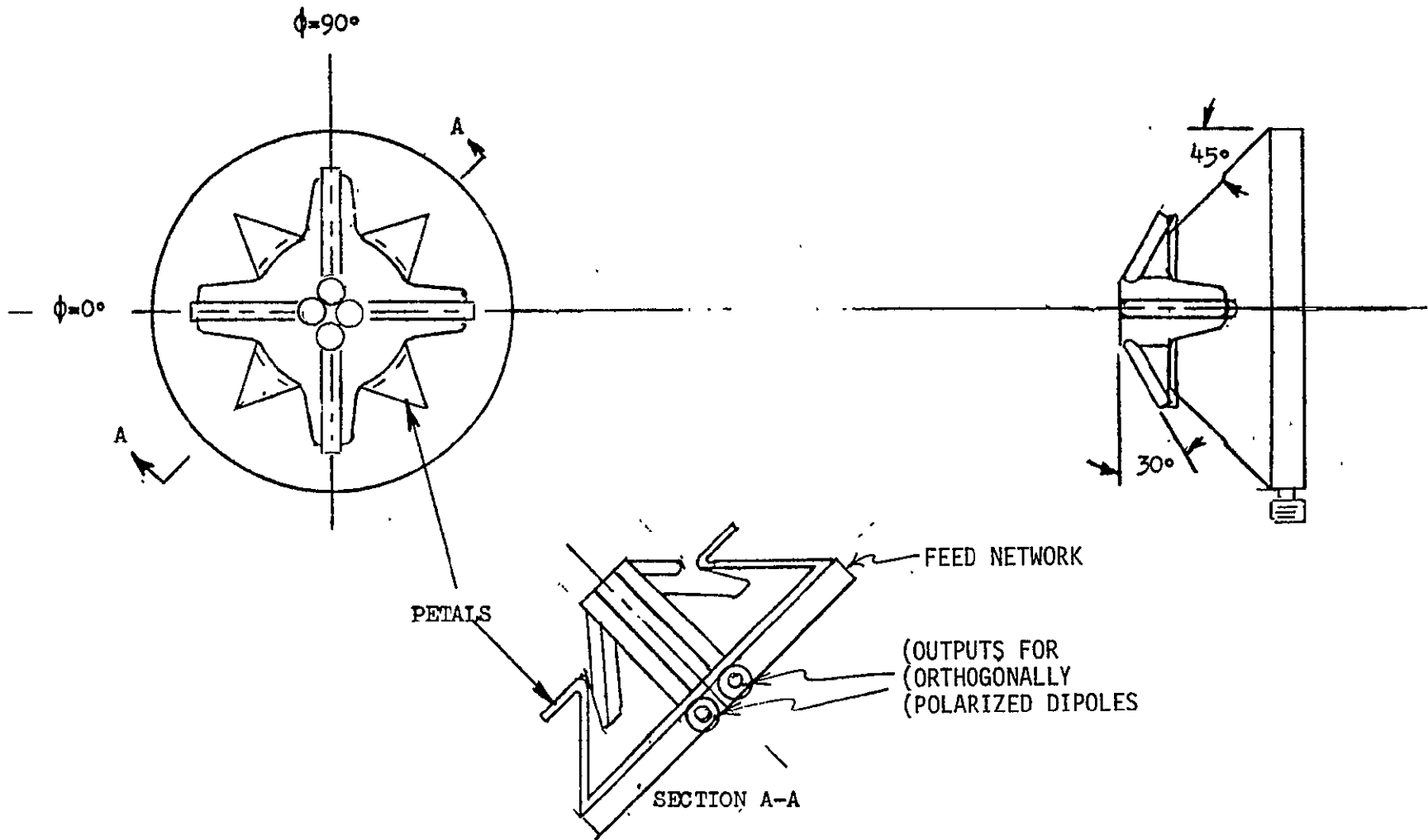


FIGURE 4.2-3. MODIFIED FLARED CONE TURNSTILE ANTENNA DESIGN

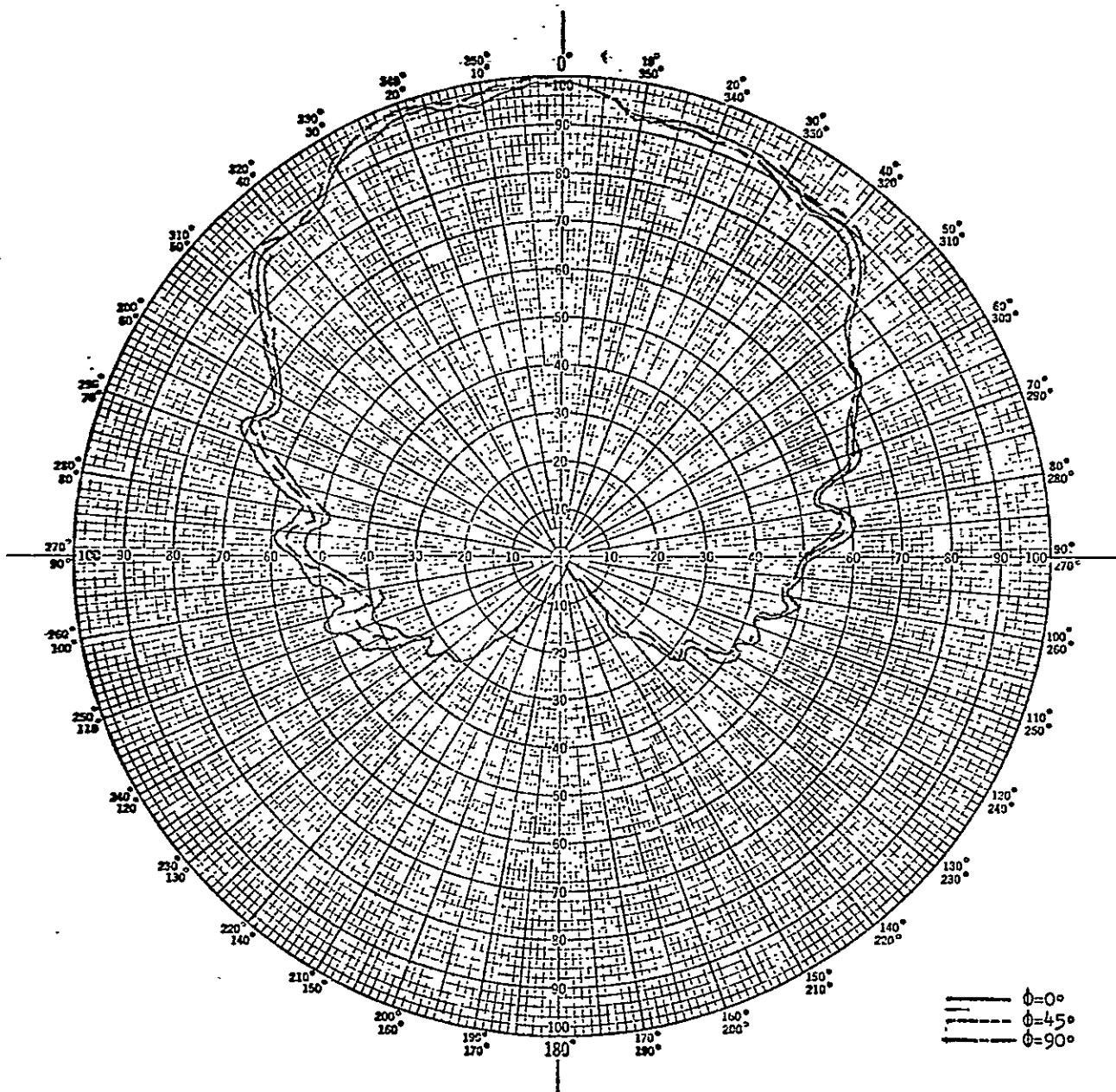
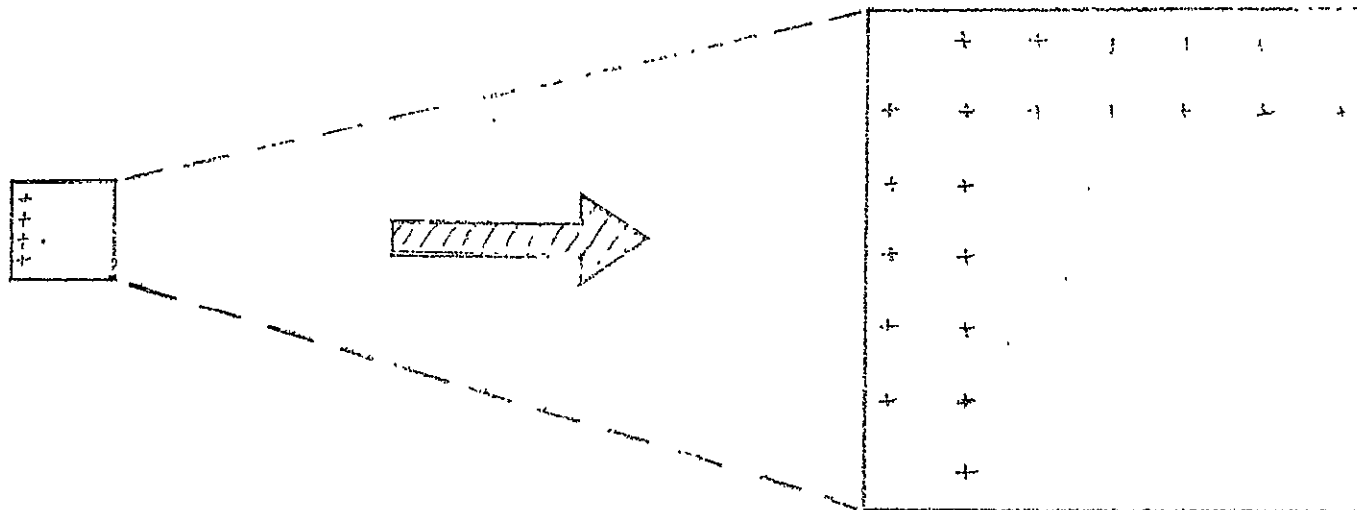


FIGURE 4.2-4. FLARED CONE TURNSTILE ANTENNA PATTERN



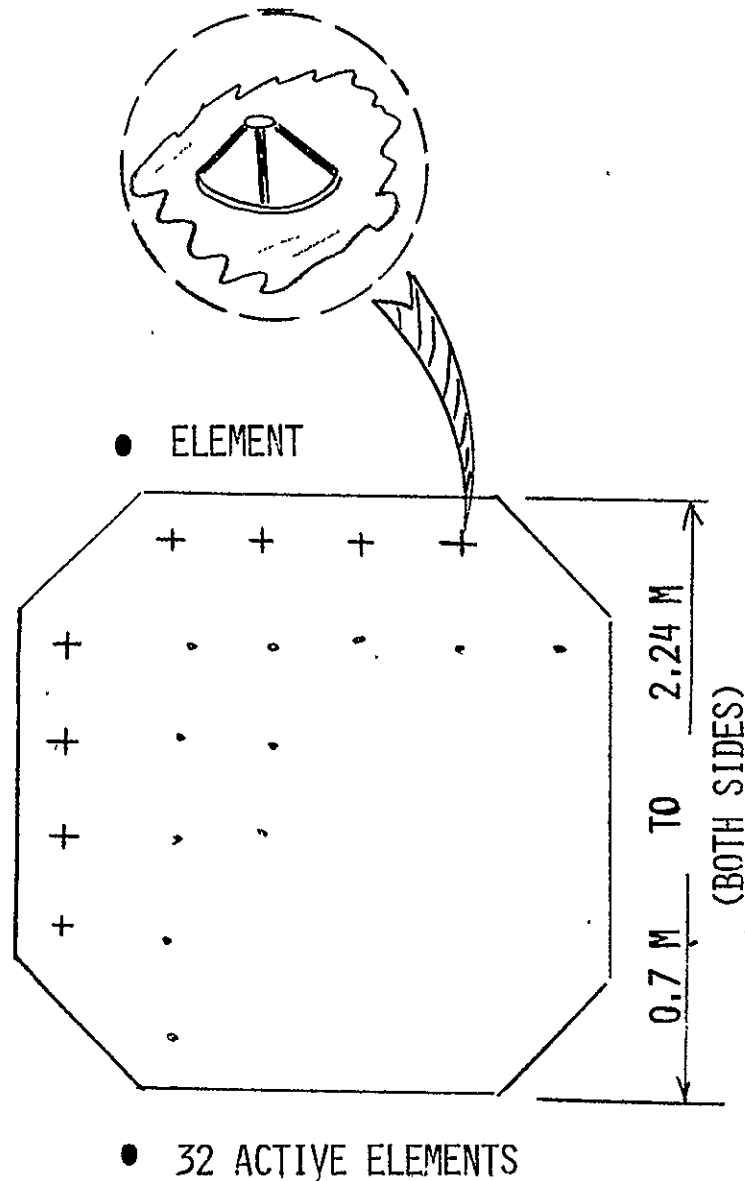
● ARRAY CHARACTERISTICS

PARAMETER	FILLED	THINNED
● APERTURE	0.7M x 0.7M	2.2M x 2.2M
● GAIN (0°)	+19.2 dBi	+19.2 dBi
● HPBW	$\approx +17^\circ$	$\approx 4^\circ$

● EXPERIMENT VALUE

- SPATIAL NULLING OF RFI'S
- IM SPATIAL DISPERSION
- DIRECTION FINDING

FIGURE 4.2-5. VARIABLE APERTURE 32 ELEMENT INSTRUMENT ARRAY



● ELEMENT CHARACTERISTICS (MODIFIED FLARED CONE TURNSTILE)

- HPBW $\approx 160^\circ$
- GAIN = 4.2 DBI (PEAK)
= 2.0 DBI ($\pm 70^\circ$)
- POLARIZATION = LHCP ON RECEIVE
= RHCP ON TRANSMIT

● ARRAY CHARACTERISTICS

- HPBW $\cdot 4^\circ - 17^\circ$
- GAIN = 19.2 DBI (PEAK)
= 17.0 DBI ($\pm 70^\circ$)
- VARIABLE APERTURE SIZE = 1, 2, 3,
& 4.23 TIMES FILLED ARRAY SIZE

FIGURE 4.2-6. ARRAY CHARACTERISTICS FOR SPACELAB EXPERIMENT

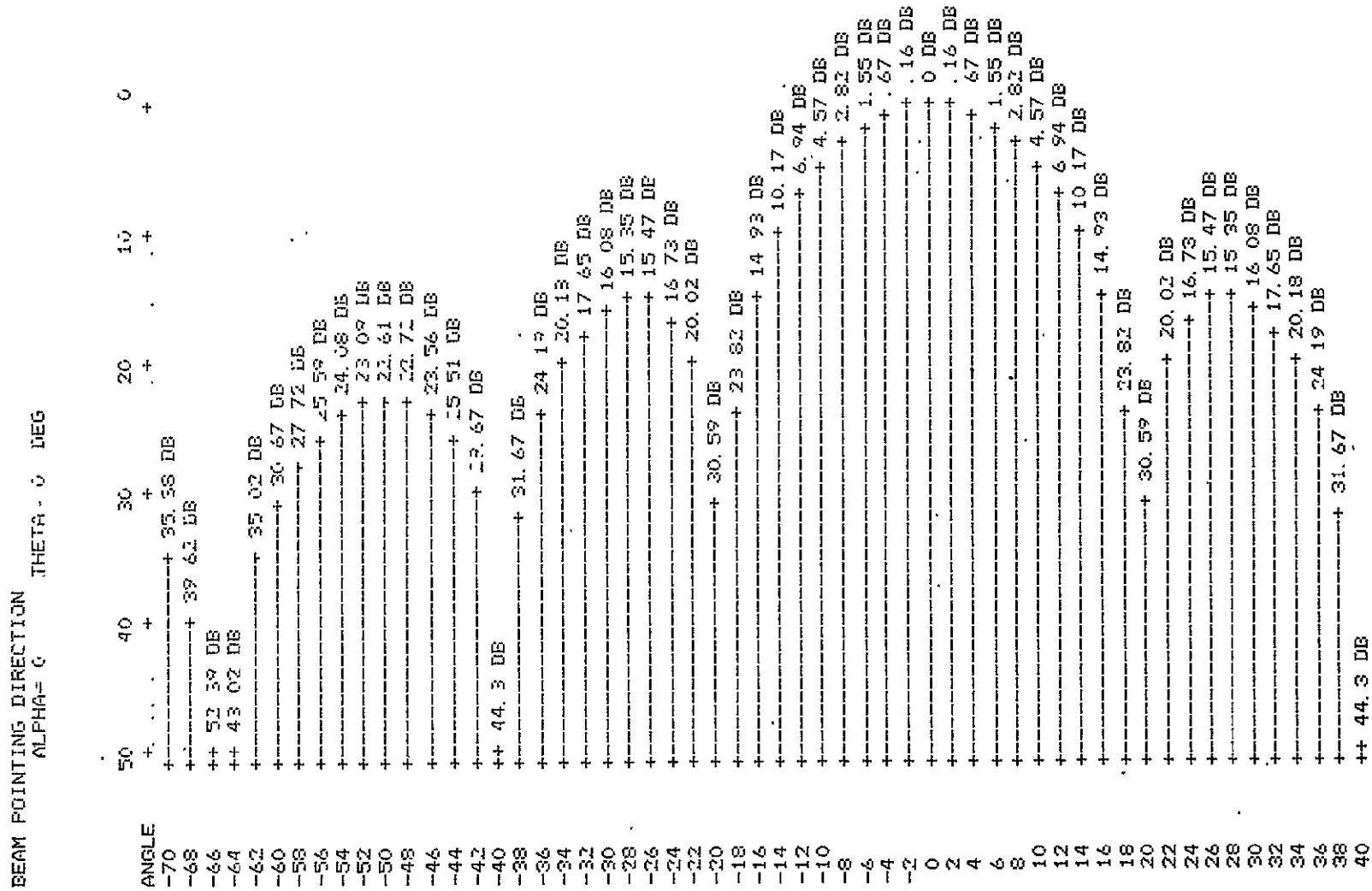


FIGURE 4.2-7. Principal Cardinal Plane Pattern For Filled Array

● Variable Aperture Array

Although no major effort has been expended during this study program to design in detail a variable aperture phased array (VAPA), several candidate approaches are described that can expand the filled array to a 2.2 meter by 2.2 meter aperture thinned array. The 2.2 meter constraint has been used as the largest fixed array that can be packaged on the pallet structure within the stowed payload bay dimensions of the shuttle orbiter.

Candidate concepts for the variable aperture array can be grouped into:

- Mechanical deployment concepts
- Electronic switching concepts

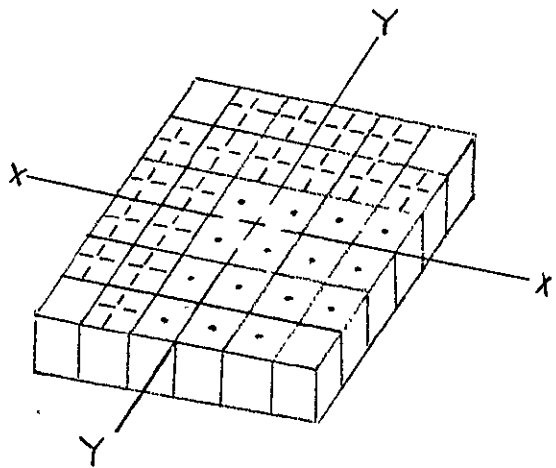
Several candidate mechanical deployment concepts have been considered for the variable aperture phased array as shown in Figures 4.2-8 through 4.2-11, viz:

- Wine rack concept
- Umbrella concept
- Variable Iris concept
- Flex rib concept

Of these, the first three concepts maintain a uniform element distribution as the array size is varied, whereas the flex rib concept results in a non-uniform distribution. However, the resultant performance is not expected to vary significantly whether uniform or non-uniform element distributions are used.

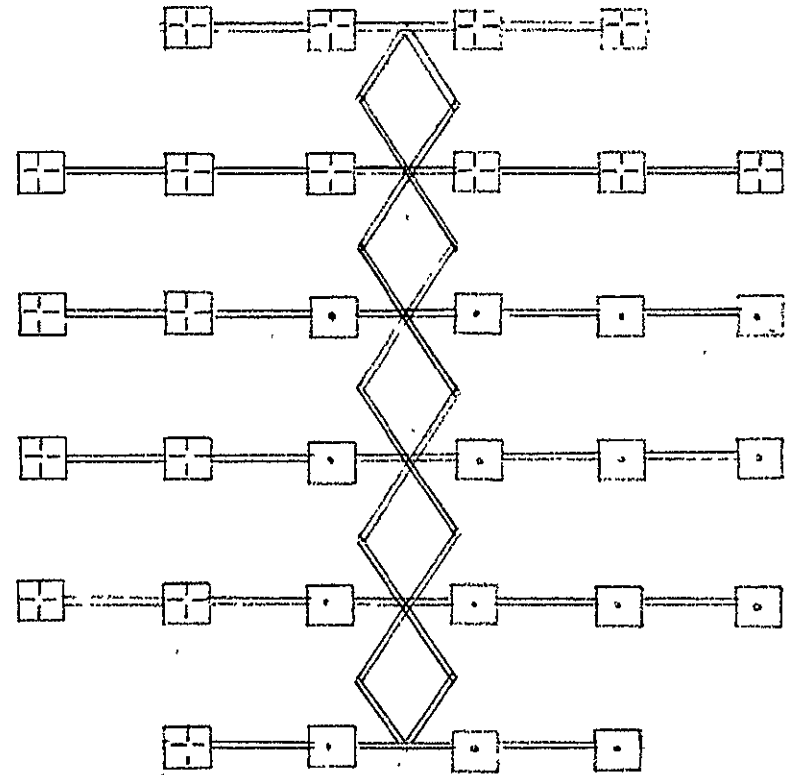
All of these mechanical concepts offer an excellent tool to provide a continuously variable aperture from a filled array to the maximum allowable thinned array.

Most promising of these concepts is the variable iris concept that employs two slotted templates, one fixed and the other rotatable. The element module has a shaft that fits into the appropriate slots in both plates. As the lower plate is rotated, the element modules are driven linearly outward in a radial direction until a maximum thinned array aperture of 2.24 meter by 2.24 meter is achieved. This variable iris concept offers a simple flat compact mechanism that can be remotely activated from within the Spacelab Module by using a motor to drive the lower rotatable template.



WINE RACKS
● 6 X-AXIS
● 1 Y-AXIS

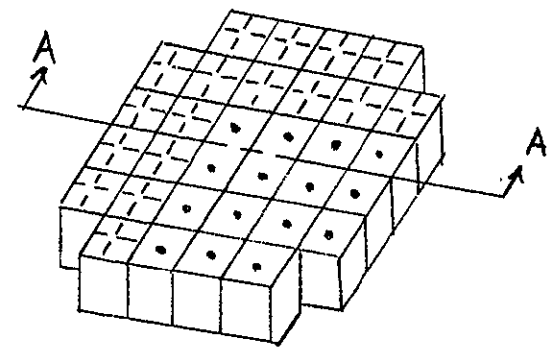
● FILLED ARRAY



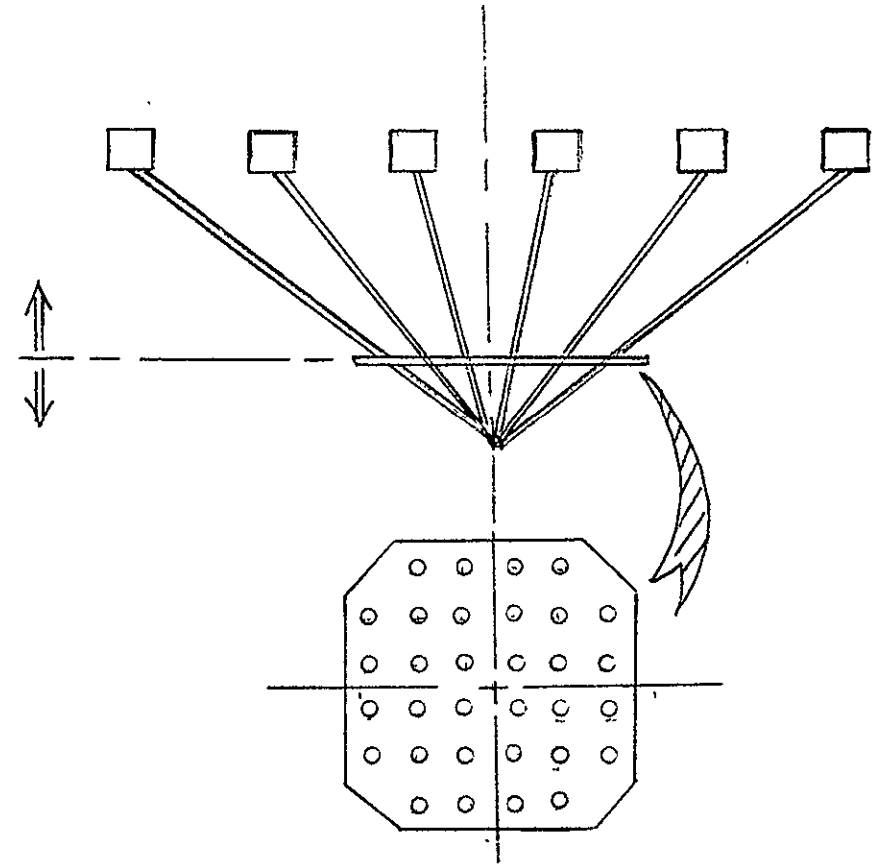
● THINNED ARRAY

FIGURE 4.2-8. VARIABLE APERTURE : WINE RACK CONCEPT

4-50



● FILLED ARRAY



● THINNED ARRAY
(SECTION A-A)

FIGURE 4.2-9. VARIABLE APERTURE ; UMBRELLA CONCEPT

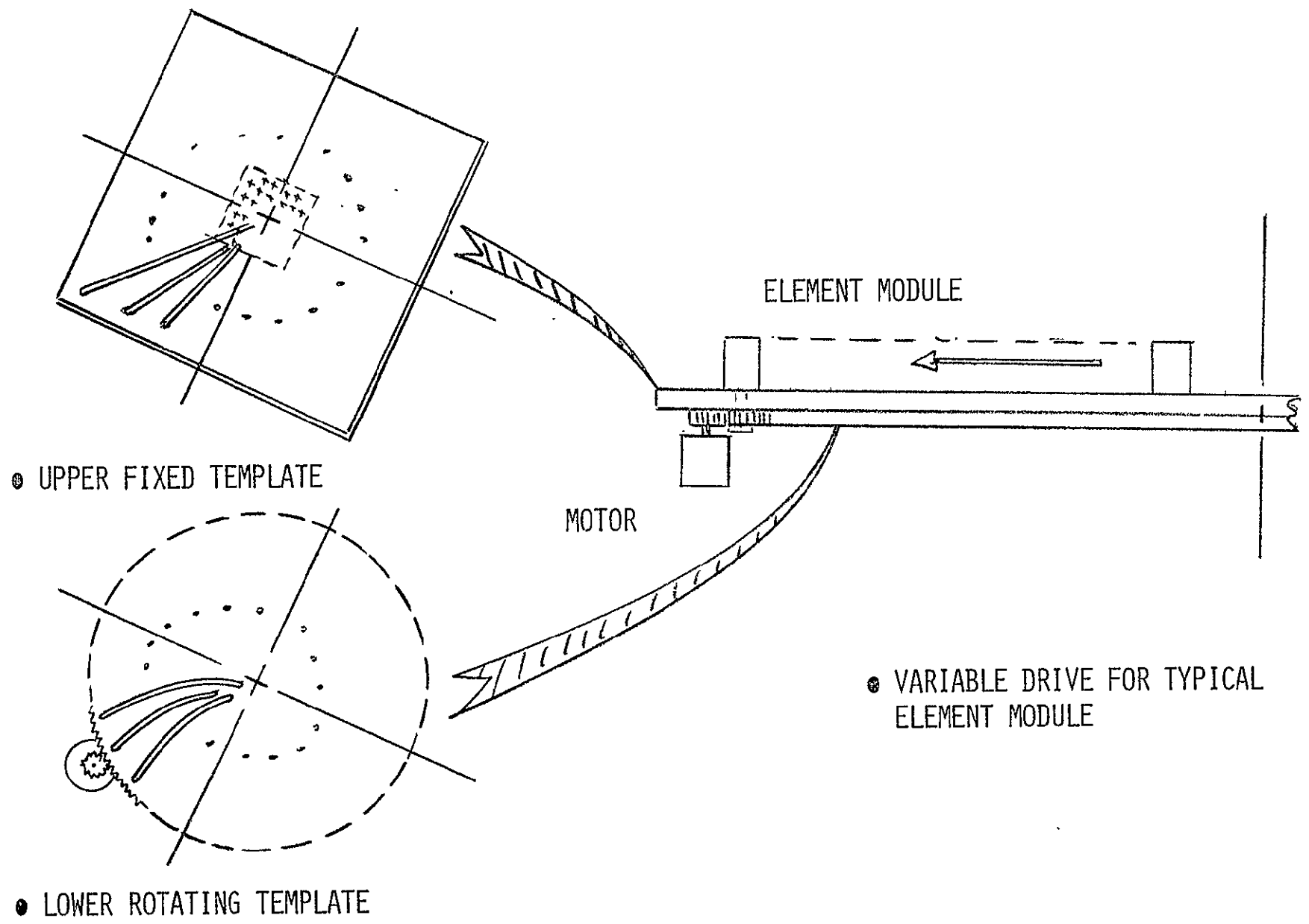
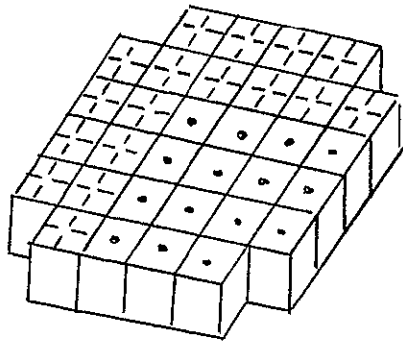
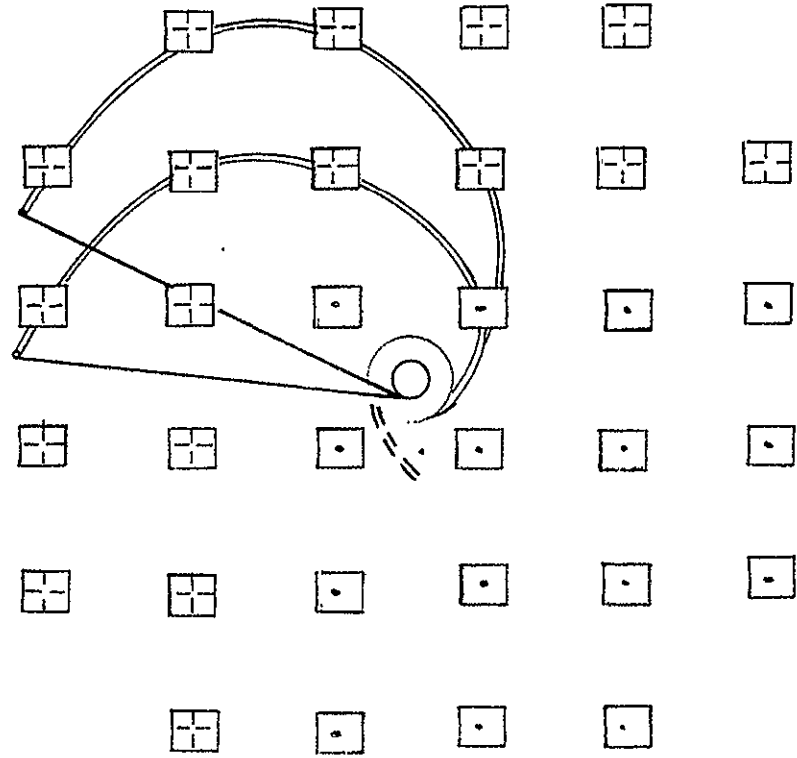


FIGURE 4.2-10. VARIABLE APERTURE : VARIABLE IRIS CONCEPT



● FILLED ARRAY



● THINNED ARRAY

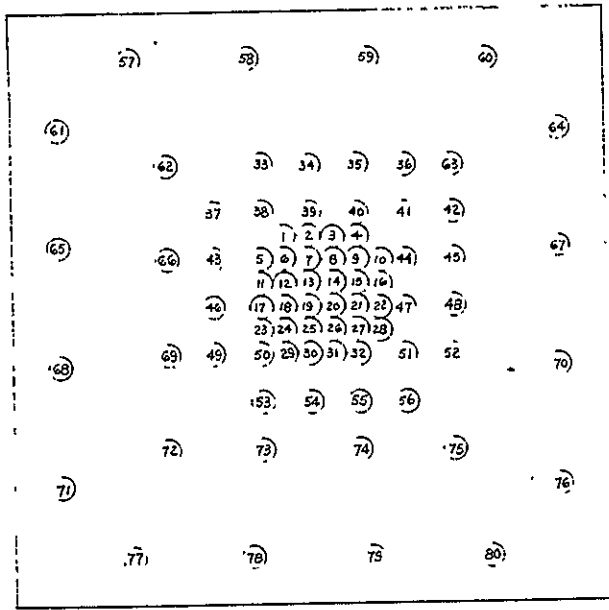
FIGURE 4.2-11. VARIABLE APERTURE : FLEX RIB CONCEPT

The electronically switched aperture phased array (SWAPA) configuration uses 80 antenna elements unsymmetrically spread over the 2.24 meter by 2.24 meter aperture as shown in Figure 4.2-12. Thirty two (32) of the elements are selected by an array switching matrix to provide discrete aperture sizes (referred to herein as aperture size factor) of 1, 2, 3 and 4.23 times the aperture for a filled array. The outputs from the array switch matrix are then fed to the 32 transmit/receive modules.

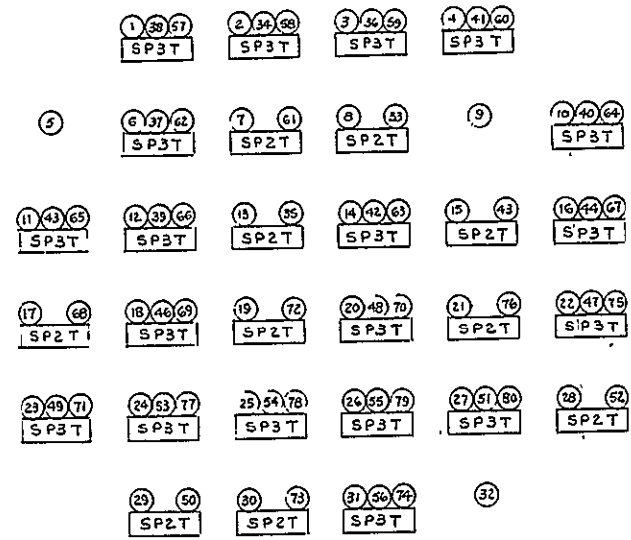
Although the electronically switched concept does not provide the continuously variable aperture sizes as the mechanical concept, it provides sufficient discrete levels to experimentally evaluate and establish the trend to determine:

- The achievable resolution of the array to spatially null interference signals that are closely spaced to the desired signal as a function of the aperture size factor.
- The achievable spatial dispersion of IM in a phased array as a function of the aperture size factor.
- The beam pointing requirements as a function of the aperture size factor.

Typical principal cardinal plane patterns as shown in Figures 4.2-13 through 4.2-16 were taken as the aperture size factors were increased from 1, 2, 3 and 4.23 (maximum allowable aperture size of 2.2 meter by 2.2 meter) and the HPBW and sidelobe characteristics summarized in Figure 4.2-17 as a function of the aperture size factor. These characteristics are identical for both the mechanically activated and electronically switched variable aperture phased arrays.



• ARRAY LAYOUT



• ARRAY SWITCH MATRIX

FIGURE 4.2-12. VARIABLE APERTURE PHASED ARRAY -- ELECTRICALLY SWITCHED

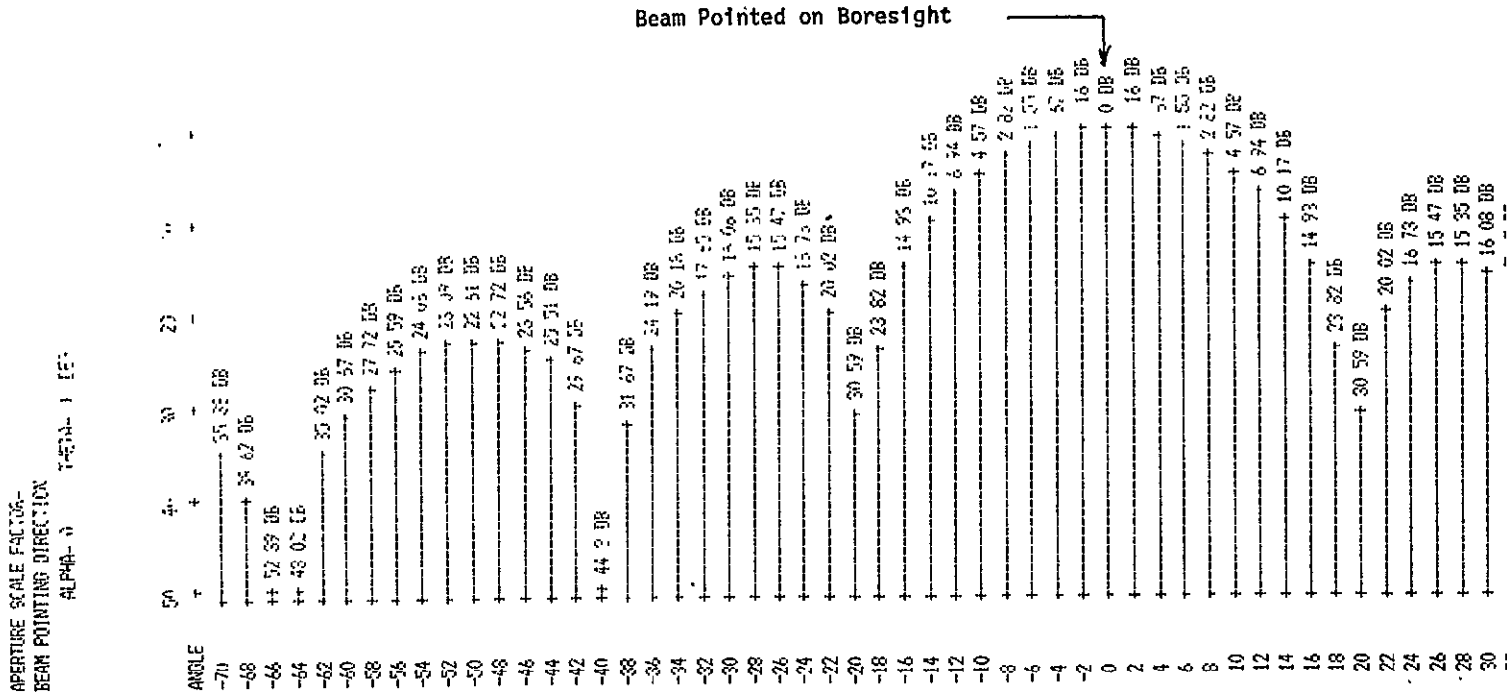


Figure 4.2-13. Principal Cardinal Plane Pattern - Variable Aperture Phased Array (Aperture Size Factor = 1.0)

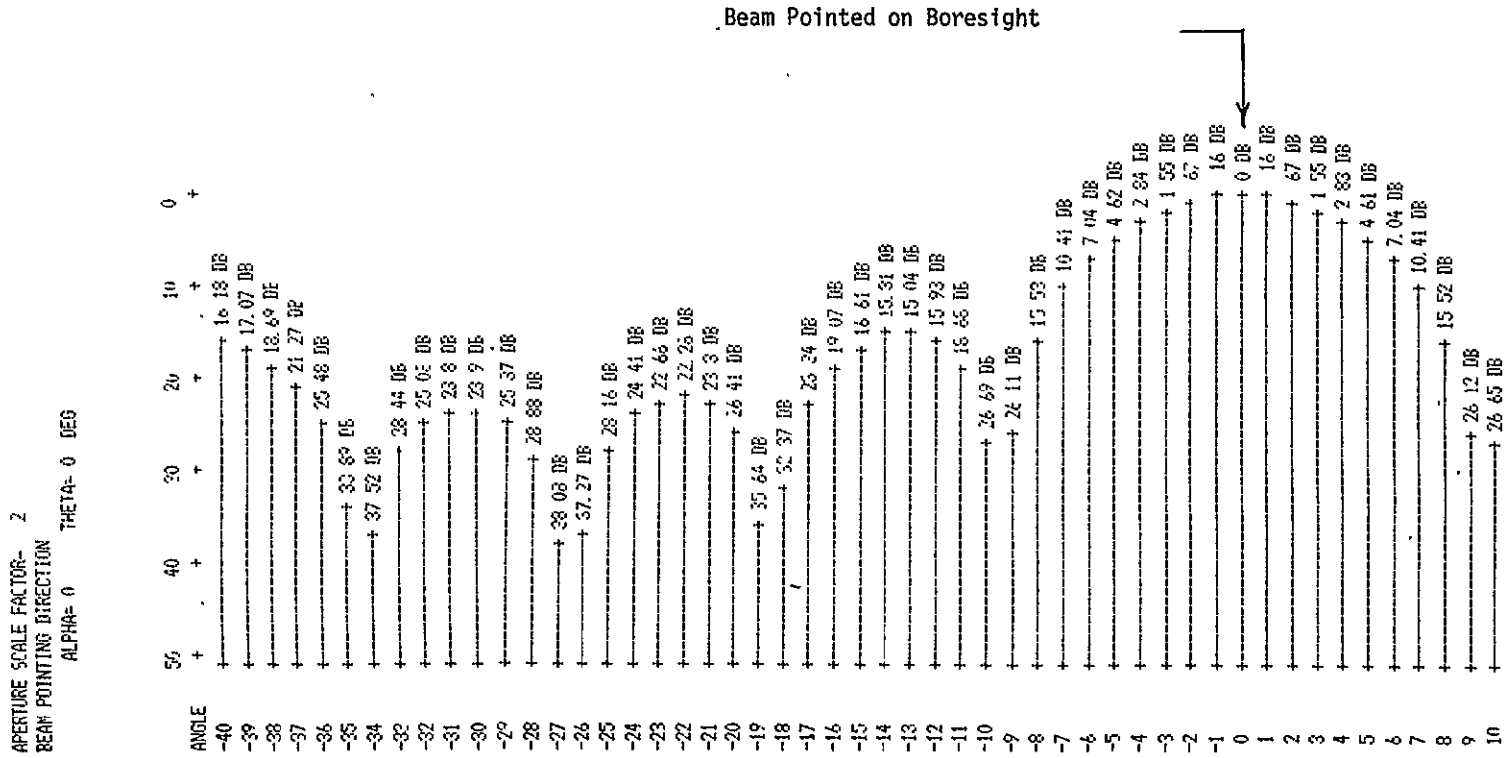


Figure 4.2-14, Principal Cardinal Plane Pattern - Variable Aperture Phased Array (Aperture Size Factor = 2.0)

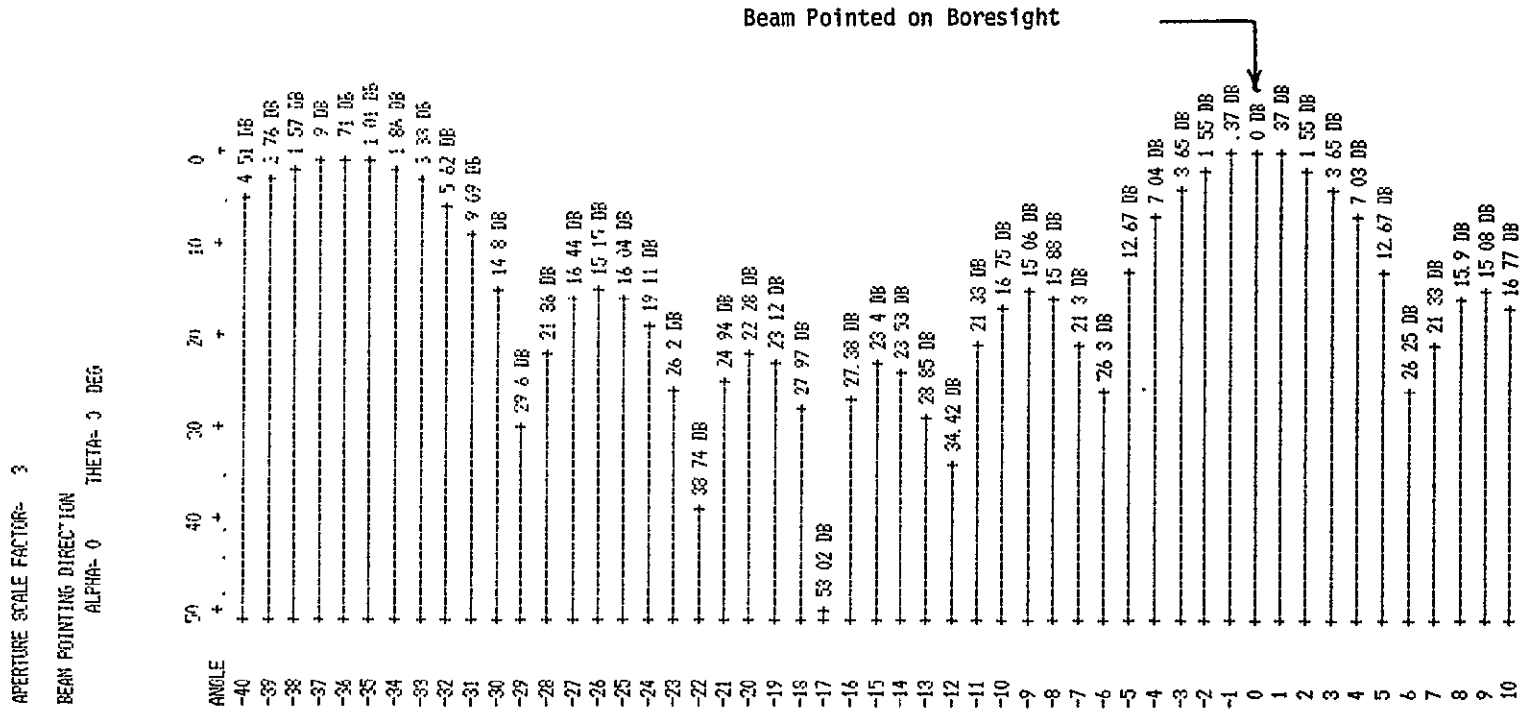


Figure 4.2-15. Principal Cardinal Plane Pattern - Variable Aperture Phased Array (Aperture Size Factor = 3.0)

APERTURE SCALE FACTOR= 4.23
 BEAM POINTING DIRECTION
 ALPHA= 0 THETA= 0 DEG

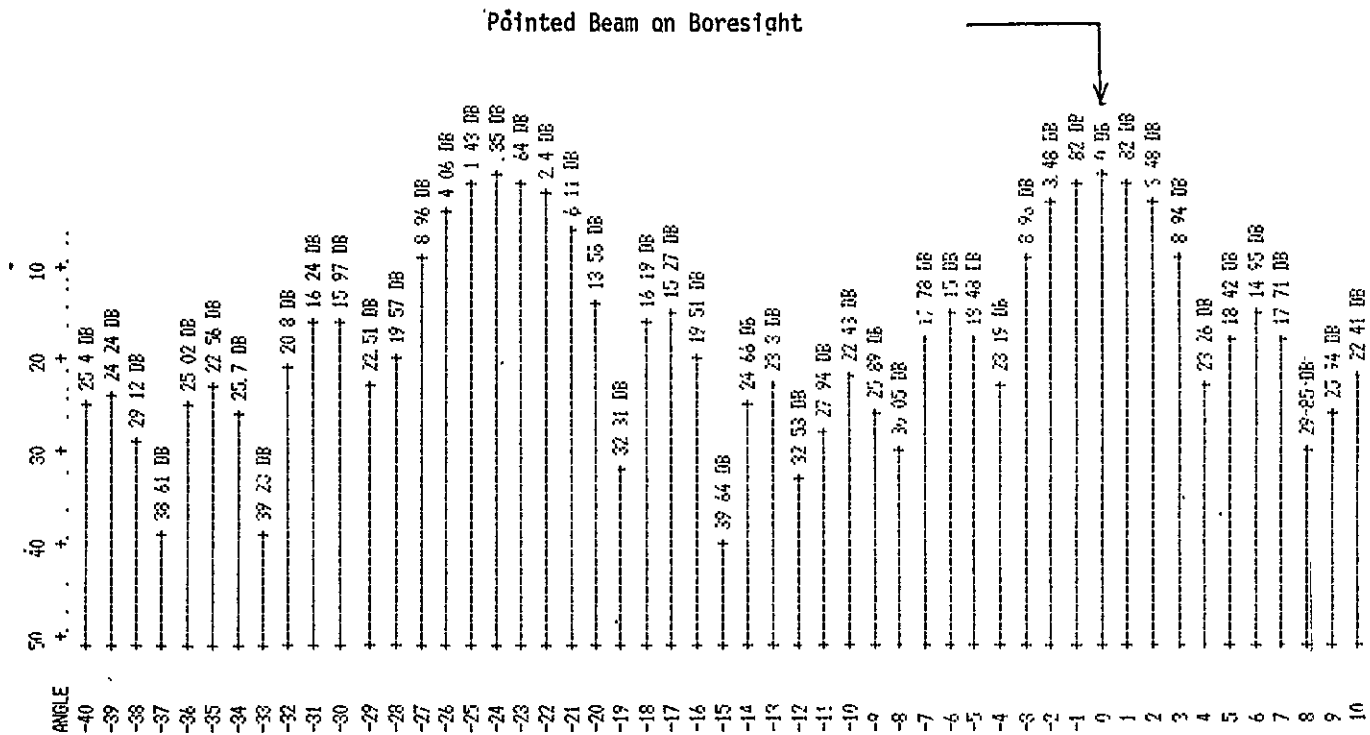


Figure 4.2-16. Principal Cardinal Plane Pattern - Variable Aperture Phased Array (Aperture Size Factor = 4.23)

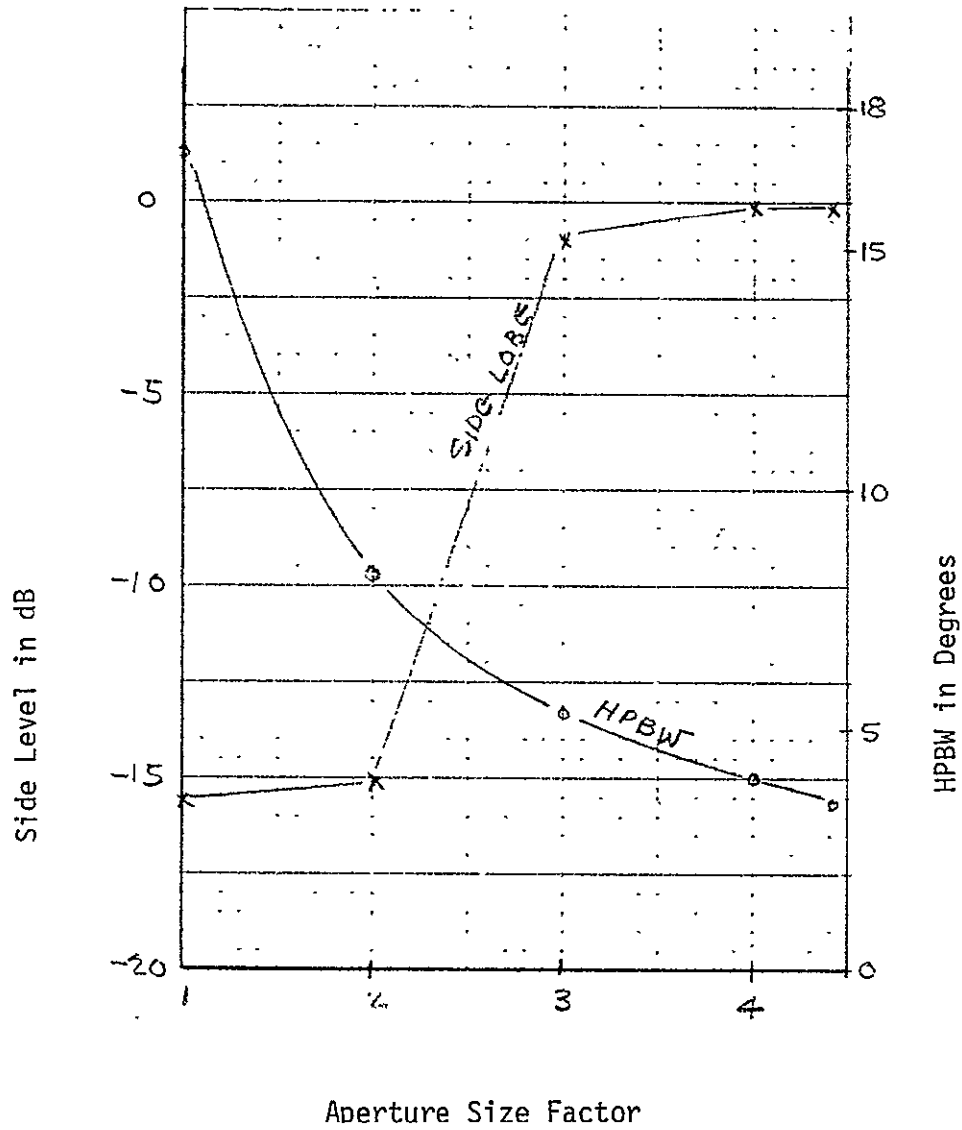


Figure 4.2-17. Array Performance Vs. Aperture Size Factor

4.2.2 Transmitter/Receiver Unit

4.2.2.1 General

The Transmitter/Receiver Unit includes the Transmitter/Receiver Assembly and a power monitor sampling switch. The Transmitter/Receiver Assembly includes 32 transmitter and 32 receiver modules.

4.2.2.2 Transmitter Module Design

4.2.2.2.1 Overall Description

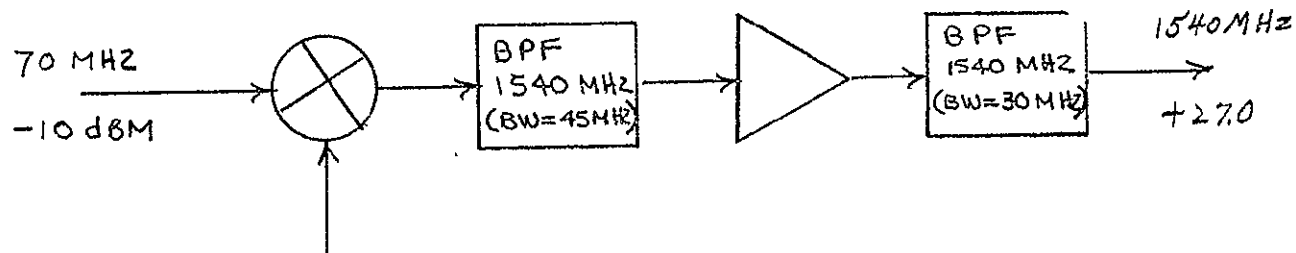
The transmitter module receives a signal from the transmitter beam processor unit and provides the required frequency translation, gain, output power and filtering to drive the transmit antenna array. There are 32 transmitter modules required, one for each element of the array.

Previous analysis of the forward link (AMPA-to-user) budget has indicated that for 32 elements, a radiated transmit power of 6.6 watts per beam is required for an operational system located in geostationary orbit. The AMPA Experiment transmitter will also be sized to radiate the same transmit power in order to design, develop and evaluate a design approach that may be suitable eventually for the operational system. For the AMPA experiment with two beams, the total radiated transmit power required is 13.2 watts. Allowing 1.5 dB for RF and diplexer losses results in an output power requirement of .582 watts or approximately +28 dBm for each of the 32 power amplifiers.

Prior to arriving at the final design, a number of tradeoffs were made which include:

- Type of output BPF
- IM rejection/amplifier design

The signal flow and gain/loss distribution within the transmitter module is shown in the block diagram of Figure 4.2-18 along with other essential performance parameters. Table 4.2-2 summarizes the performance requirements for the transmitter module. The input 70 MHz signal which contains the proper phase for beamforming is mixed with a 1470 MHz LO to produce the specified 1540 MHz transmit frequency. This signal is filtered and power amplified by 50 dB to provide an amplifier output level of +28 dBm. The bandpass filter following the amplifier serves to



4-61

		<u>MIXER</u>	<u>REJECTION (DB)</u>		<u>BPF</u>	<u>TOTAL</u>	<u>POWER LEVEL AT OUTPUT (DBM)</u>
			<u>BPF</u>	<u>AMPL.</u>			
LO	(1470 MHz)	30	30	--	30	90	-90
LOWER SIDEBAND	(1400 MHz)	--	50	--	50	100	-73
SECOND HARMONIC	(3080 MHz)	--	--	15	80	95	-68
RECEIVER FREQ.	(1640 MHz)	--	--	--	50	50	-104 dBm/MHz (Noise Power Density)
THIRD ORDER IM		35	--	14	--	14	+13

FIGURE 4.2-18. TRANSMITTER MODULE BLOCK DIAGRAM

TABLE 4.2-2 TRANSMITTER MODULE
PERFORMANCE CHARACTERISTICS

FREQUENCY	:	1540 MHZ
BANDWIDTH	:	>2.5 MHZ
GAIN	:	37.0 DB
P _{OUT} (3 DB FROM SAT.)	:	+27.0 DBM
LO RADIATION	:	-90 DBM
SECOND HARMONIC LEVEL	:	-68 DBM
LOWER SIDEBAND LEVEL	:	-73 DBM
NOISE POWER DENSITY AT 1640 MHZ	:	-104 DBM/MHZ
THIRD ORDER IM REJECTION	:	14 DB
AMPLITUDE LINEARITY	:	+0.2 DB
PHASE LINEARITY	:	+2°
DC POWER	:	24V AT 50 MA, 15V @ 80 MA

suppress radiation of the LO and provides rejection to protect the receiver module from wideband noise generated by the power amplifier.

4.2.2.2.2 Tradeoff Analysis

o Type of Bandpass Filter

The output bandpass centered at 1540 MHz must provide rejection to the LO (1470 MHz) and to wideband noise at the receiver frequency (1640 MHz). At the same time, it must be broadband to keep the phase characteristics linear over the 2.5 MHz information bandwidth and low loss so as not to impact the power requirement of the amplifier output stage. The choice of the filter type to best serve this application is similar to the tradeoff study conducted for the choice of preselector used in the receiver module (Section 4.2.2.3). After considering various filter types and studying all related factors, a similar 4-pole combline filter has been selected. This filter has less than 1 dB insertion loss and provides 50 dB of rejection at the receiver frequency.

o IM Rejection/Amplifier Design

The IF bandwidth required for passing a significant number of sidebands for recovery of a transmitted FM carrier is given by:

$$BW = 2 f_m (1 + \beta)$$

where $\beta = \text{modulation index} = \frac{\Delta f}{f_m}$

$\Delta f = \text{peak frequency deviation}$

$f_m = \text{baseband frequency}$

For a conventional baseband frequency of 3.5 kHz and assuming a reasonable modulation index of 1.86, the BW required for FM reception is approximately 20 kHz. With the operational system requirement to support Maritime users of high quality voice ($C/N_0 = +53 \text{ dB} - \text{Hz}$) and with the user receiver bandwidth determined to be 20 kHz, the resulting carrier-to-noise ratio (CNR) required at the users is 7 dB, including a 3 dB system margin.

Any intermodulation products generated by the transmitter power amplifier will degrade the CNR at the user receiver. For example, if a spurious signal with a carrier-to-spurious ratio equal to the CNR is present, the resulting CNR is reduced by 3 dB from its original value. From this an expression can be developed relating the degradation of CNR (ΔQ) at the user receiver as a function of transmitter intermodulation rejection. Thus,

$$\Delta Q = 10 \log [1 + 10 \text{ Exp. } ((-S/I + \text{CNR})/10)]$$

where ΔQ = degradation to CNR in dB

S/I = intermodulation rejection relative to signal in dB

Allowing an acceptable degradation of 1 dB for a channel with a CNR of 8 dB results in an intermodulation rejection requirement of 13.8 dB.

Therefore, for the user receiver to maintain a CNR of 7 dB for Maritime services, the input S/I ratio must be a minimum of 14 dB. This intermodulation rejection is equal to the IM rejection present at the transmitter power amplifier and will be further enhanced by spatial dispersion of IM products achieved with phased array.* Subsequent computer simulations will show that reductions of up to 14 dB in receiver intermodulation levels are achievable due to spatial dispersion by the use of phased arrays (Section 4.3.3). This improvement is due to the different phases between the desired signal and undesired signal causing the undesired signal to be dispersed in a different direction from the user being serviced. The amount of reduction of IM products by the technique of spatial dispersion is a function of user location separation and optimization of channel assignments. For the AMPA experiment, the transmitter power amplifier will be designed to provide the entire IM rejection requirement of 14 dB.

As part of the AMPA experiment, an intermodulation simulator is included to inject additional signals into each transmitter module to simulate more than two transmit beams. This will be used to evaluate the effectiveness of spatial dispersion for reducing the impact of IM generation.

*J. S. Prichard, Spatial Dispersion of Intermodulation Products by Phased Arrays, IEEE Canadian Communications and Power Conference, Montreal, Canada, 7-8 November 1974

It is possible to achieve the required IM rejection by designing a linear Class A power amplifier where the drive is "backed off". This would be undesirable since it would greatly reduce the efficiency of the amplifier which is low to begin with by virtue of the Class A operation.

A more efficient method to provide improved IM rejection without a subsequent increase in DC power is to use a technique employing a feedforward network*. The feedforward network compares samples taken before and after the distorting amplifier to obtain an error signal. The error signal is processed and combined beyond the amplifier output to provide an undistorted signal through cancellation of the common error terms. Application of the feedforward network to the amplifier results in a higher intercept point. The efficiency obtained with a feedforward network is higher than that obtained by "backing off" the amplifier to a point which yields the same IM rejection.

In general, a Class C amplifier generates least intermodulation products at 50% of saturated output. This 3 dB of "back off" is optimum since for a lower level signal the angle of flow is small and the resulting narrow pulses cause large intermodulation products. As the signal increases, the angle of flow will also increase and act to decrease the intermodulation generation. This will continue until saturation effects act to increase the non-linearity and thus increase the intermodulation products. After considering different types of operation for the power amplifier, a Class C configuration will be designed to operate nominally with 3 dB "back off". This design provides the highest efficiency and meets the intermodulation rejection requirement of 14 dB. However, in order to evaluate the impact of IM suppression with "back off" in the Class C amplifier as compared to the achievable spatial dispersion of IM products with a phased array, the signal input levels into the amplifiers will be variable so that the operating point can be changed. If the operating "back off" point can be reduced to 2 dB, this will have a large impact on the prime power requirement for an operational system.

*Linearizing Amplifiers for Multi-Signal Use, Microwaves April 1974

4.2.2.2.3 Detailed Design

• Mixer

The L-band mixer provides a constant low conversion loss over the required 2.5 MHz bandwidth with high LO to RF isolation. The mixer is a double-balanced type to reduce its susceptibility to even order spurious responses. The mixer is a MIC double balanced design which has been developed at AIL. A Schottky barrier diode quad mounted on an alumina substrate is used. This diode quad allows the use of 0 dBm local oscillator drive.

The required frequency translation is provided by mixing the 70 MHz input signal with a 1470 MHz local oscillator. The upper sideband of the conversion process is selected by a bandpass filter centered at 1540 MHz. The mixer provides an LO to RF isolation of 30 dB with a conversion loss of 7 dB. The third order intermodulation suppression is greater than 35 dB with input levels at -10 dBm.

• Bandpass Filter #1

The bandpass filter following the L-band upconversion must provide rejection to the lower sideband and LO frequencies in a lightweight and small size. A cavity filter which would provide low loss is unfortunately heavy and large. Additional loss can be tolerated since it can be made up by low level gain from the L-band amplifier without an extreme weight or power penalty. Therefore, a connectorless tubular filter providing large rejection in a light package has been selected. The filter is a 4-pole design of 1/4 inch diameter centered at 1540 MHz with a 45 MHz bandwidth. The insertion loss is 5.0 dB and the rejection to the 1470 MHz LO is 30 dB. The filter rejection to the lower sideband at 1400 MHz is 50 dB.

• Amplifier

The power amplifier is required to provide a minimum gain of 50 dB and have an output power capability of +28 dBm. This output is consistent with the transmission requirement of 13.2 watts for two beams of operation. The amplifier consists of four stages and utilizes thin-film microstrip techniques. The input section consists of three low level Class A stages

providing 40 dB of gain at an output power level of +18 dBm. The transistors used are linear power transistors MSC 8000 series. The output stage utilizes a MSC 3001 power transistor having 10 dB of gain and providing an output of +28 dBm. The output stage is operated at 3 dB down from saturated power output and maintains a collector efficiency of 50%. The transistors used are of the "MIC-PAC" configuration so as to mate with the microstrip packaging.

The amplifier generated second harmonic is 15 dB down from the fundamental and the third order intermodulation rejection is 14 dB. The amplifier has a noise figure of 10 dB and the deviation from linear phase over the 2.5 MHz information bandwidth is less than ± 1 degree.

• Bandpass Filter #2

The "transmit" bandpass filter following the power amplifier forms part of the diplexer which allows sharing of the antenna for receive and transmit signals. This filter must prevent the power amplifier noise from degrading the receiver sensitivity by keeping the transmitter noise well below the receiver noise. The filter is centered at 1540 MHz and provides 50 dB of rejection at the receiver frequency of 1640 MHz. The power amplifier with a gain of 50 dB and a noise figure of 10 dB has an output power noise density of $-114 + 10 + 50 = -54$ dBm/MHz. The noise power density of the receiver assuming a 2 dB noise figure is -112 dBm/MHz. With the antenna isolation (quadrature hybrid) of 20 dB and the filter rejection of 50 dB the noise power density entering the receiver from the transmitter is 12 dB below the system noise power density of the receiver. In addition to the transmitter noise rejection the filter provides 30 dB of rejection at the L0 frequency.

The insertion loss of the filter must be kept to less than 1 dB to minimize dissipative losses for the transmitter output. The filter type selected is a 4-pole combline design in order to meet the rejection and low insertion loss requirements. The bandwidth is 30 MHz which allows margin for temperature variations while maintaining a flat amplitude and linear phase characteristic over the required 2.5 MHz passband of operation.

• Power Monitor

An integrated strip line directional coupler with an insertion loss of less than 0.1 dB and a coupling factor of 20 dB will be included after the L-band amplifier in order to provide a means of remotely monitoring its performance. A crystal video detector is used to detect its output which is subsequently sampled by a power monitor sampling switch.

4.2.2.3 Receiver Module Design

4.2.2.3.1 Overall Description

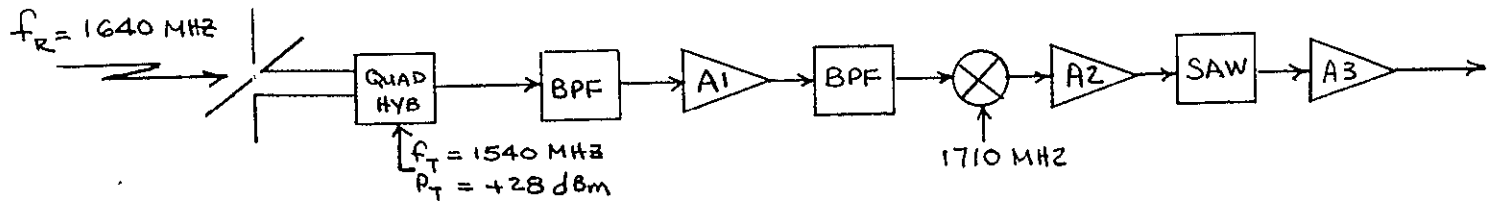
The receiver module receives a signal from the antenna element which is filtered, amplified, downconverted and then fed to the receiver beam processor unit. There are a total of 32 receiver modules, one for each of the antenna elements. The input signal into each element may be as small as -141.1 dBm and as large as -106 dBm, representing an input receiver dynamic range of 35 dB. The tradeoffs considered in the design of the receiver module include:

- Type of preselector
- Preselector rejection/amplifier design
- Type of IF filter

The receiver front end has also been designed with a goal of achieving a receiver noise figure of 2 dB by using a low noise bipolar transistor front end, and minimizing line and component losses ahead of the low noise amplifier.

Particular emphasis has also been given in the receiver module design to insure compatibility for use at geostationary orbit, in case a decision is made to conduct the AMPA experiment at geostationary orbit.

A functional block diagram for a typical receive channel is shown in Figure 4.2-19 along with essential performance requirements. User signals are received at a frequency of 1640 ± 1.25 MHz. All 32 channels are down-converted to 70 MHz IF with a 2.5 MHz bandwidth.



Parameter	BPF	A1	BPF	Mixer	A2	BPF	A3
Frequency (MHz)	1640	1640	1640	70	70	70	70
BW (MHz)	30		45			2.5	
Gain (dB)	-1	32	-5	-7	40	-20	40
NF (dB)	--	2			2		2
1 dB Comp. Power (dBm)	--	0			-5		+5
P_{Noise} (dBm) (2.5 MHz BW)	-108	-78	-83	-90	-50	-70	-30
Power at 1540 MHz (dBm) (+7)	-43	-13	-63	-70	-50	-120	
Min. P_{Signal} (dBm (-141))	-142	-110	-115	-122	-82	-102	-62
Out-of-Band Signal Producing In-Band IM	-106	-120	-125	-132	-92	-112	-72
Rejection at (dB) 1540 MHz (Xmitter)	50		50				
1780 MHz (Image)	60		60				
DC Power (mW)	--	275			225		300

FIGURE 4.2-19. RECEIVER MODULE BLOCK DIAGRAM

The input preselector provides rejection to the transmitter leakage and to the image signal. These signals, if not rejected, can cause intermodulation or receiver compression. The transmitter signal at nominally 1540 MHz is at approximately +7 dBm into the receiver module. (Transmitter module output +27 dBm less 20 dB for antenna isolation.) The preselector design is a combline filter so that low loss is achieved thereby preserving the receiver module noise. The L-band amplifier following the preselector establishes the receiver sensitivity by providing a low noise figure. The bandpass filter following the amplifier is used to provide additional rejection to the image and transmitter signals. The output from the bandpass is downconverted with a 1710 MHz LO by a mixer to produce a 70 MHz signal. This LO was chosen to operate above the signal rather than below so that the IF filter provides greater attenuation to the resulting transmitter difference signal (170 MHz vs. 30 MHz). The 70 MHz preamplifier is used to compensate for the lossy IF filter that follows. This is required so as not to contribute to the front end noise figure. The IF filter used is a surface acoustic wave (SAW) design to take advantage of the reduced size and weight as compared to the equivalent 5-pole filter required. The 2.5 MHz channel bandwidth is set by the SAW filter. The basic amplitude and phase response of the channel is also established by the SAW filter since all other components are wideband so as to be negligible in their contribution of amplitude and phase distortion. The 70 MHz postamplifier is used to increase the signal level before interfacing with the receiver beam processor unit.

The gain and loss allocations are budgeted throughout the module to provide sufficient net gains from a noise figure standpoint and tolerable levels from a spurious rejection standpoint.

The receiver module performance characteristics are listed in Table 4.2-3. It should be noted here that the receiver module has been designed for its ultimate application in geostationary orbit where the 32 channels are multiplexed together and fed to a common power amplifier for transmission to the ground for beam processing. Thus, this establishes the channel bandwidth requirement of 2.5 MHz in order to limit the operational system downlink to approximately 100 MHz. In addition, this imposes an amplitude and phase tracking requirement between modules to reduce distortion. The adjacent channel noise degradation shown assumes a channel spacing of 3 MHz.

TABLE 4.2-3 RECEIVER MODULE
PERFORMANCE CHARACTERISTICS

A. MODULE CHARACTERISTICS

INPUT FREQUENCY	:	1640 MHz
OUTPUT FREQUENCY	:	70 MHz
BANDWIDTH	:	2.5 MHz
GAIN	:	77 dB
NOISE FIGURE	:	3.06 dB
DYNAMIC RANGE (1 DB COMPRESSION)	:	64 dB
TRANSMITTER REJECTION	:	>137 dB
LO RADIATION	:	<120 dBm
PHASE DEVIATION	:	+4 degrees RMS
IMAGE REJECTION	:	120 dB
AMPLITUDE RIPPLE	:	+0.2 dB
NOMINAL IMPEDANCE	:	50 ohm
POWER CONSUMPTION	:	800 mw

B. INTERCHANNEL CHARACTERISTICS

PHASE TRACKING	:	+5 degrees RMS
AMPLITUDE TRACKING	:	+ .2 dB
CHANNEL ISOLATION (THRU MIXERS AND LO DISTRIBUTION)	:	50 dB
ADJACENT CHANNEL NOISE DEGRADATION FOR 3 MHZ SPACING	:	< .1 dB

The receiver module noise figure is 3.06 dB. The L-band amplifier noise figure is 2 dB with .06 being contributed from the back-end and 1 dB is included for the preselector loss. The required dynamic range of the channel is 35 dB with the 70 MHz postamplifier being the limiting item. The transmitter signal is attenuated by more than 137 dB which results in a transmitter signal 50 dB under the noise figure at the receiver module output. The receiver module image rejection is 120 dB.

4.2.2.3.2 Tradeoff Analysis

• Type of Preselector

The preselector must provide rejection to the transmitter signal (1540 MHz) and to the image frequency (1780 MHz). At the same time, it must be broadband to keep the phase characteristics linear and low loss as not to degrade the noise figure significantly. These requirements are contradictory when the size and weight are also constrained and therefore a compromise is required. The type of filters considered were:

- Compline
- Tubular
- Cavity
- Microstrip

After studying all related factors, the choice made was to use a 4-pole combline filter. This filter has less than 1 dB loss in a small size is lightweight and provides 50 dB of rejection at the transmitter frequency. The balance of transmitter rejection required is made up by a filter following the low noise amplifier.

• Preselector Rejection/Amplifier Design

For the amplifier to provide a low receiver module noise figure, the gain should be high so as not to allow circuitry after the amplifier to contribute to the overall noise figure. However, a large gain requires a higher preselector rejection or a greater 1 dB compression point for the amplifier to prevent the transmitter signal from producing distortion. Greater rejection results in a larger insertion loss. A larger compression point for the amplifier means greater power consumption. It has been concluded that a

gain of 30 dB is adequate since the remaining noise figure contribution is quite small. With this gain, the preselector rejection at the transmitter frequency is required to be 50 dB which results in a transmitter leakage level at the output of the amplifier of -13 dBm. Thus, an amplifier compression point of 0 dBm is selected which accomplishes the following:

- No transmitter distortion
- Low amplifier power consumption
- Good operating point for best noise figure

Assuming the amplifier has an intercept point of +10 dBm, an interfering signal at the same level of the transmitter leakage (-13 dBm) could generate an in-band IM signal at a resulting power level of -59 dBm. The minimum received signal at the output of the amplifier is -110 dBm. Thus, to ensure any IM generated signals to be 10 dB less than the minimum received signal requires the interfering signal be limited to -74 dBm $[-13 - (110 + 10 - 59)]$ at the amplifier output. With the amplifier gain of 30 dB and assuming 30 dB of preselector rejection the resulting received interfering signal at the antenna is -74 dBm. This would require an interfering transmitter having an ERP of +44.9 dBm which is highly unlikely and thus any generated IM signals are expected to be well below receiver noise.

• Type of IF Filter

The IF filter is a critical item. The filter must have low amplitude ripple and good phase linearity over the passband to minimize distortion effects. In addition, the skirt selectivity is important in order to keep the adjacent channel noise degradation to a minimum. Among the filter types considered for this application were the following:

- Cavity
- Discrete Component
- Active
- SAW

Although cavity filters offer the best performance electrically, a large penalty in size and weight is incurred. For this reason, a SAW filter was selected which is adequate electrically and one-fifth the size and one-tenth the weight of the equivalent cavity filter. In addition, the SAW filter has a greater stability and reproducibility as compared to the cavity filter. The additional insertion loss of the SAW filter is made up by a preamplifier at the expense of a small increase in power consumption.

4.2.2.3.3 Detailed Design

- Preselector

The preselector used is a 4-pole combline filter centered at 1640 MHz having 50 dB of rejection at the transmit frequency of 1540 MHz. The filter also provides 60 dB of rejection at the image frequency 1780 MHz thus solving the problem of intermodulation distortion in the RF amplifier with less than 1.0 dB filter insertion loss.

The combline filter consists of four finger-like structures that are foreshortened one-eighth wavelength resonators. These are fine tuned by screws projecting into the cavity towards the "finger" ends (capacitive end-loading). The input and output of the filter contains a shorted line that acts as a transformer section. The desired transformation is obtained by adjusting its position relative to the adjacent resonator. The loss of the filter is determined by the bandwidth and Q of the filter. The Q is determined by the ground plane spacing so that by moving the top and bottom further apart the loss can be reduced at a sacrifice in size and weight.

- 1640 MHz Amplifier

The 1640 MHz amplifier is a 3-stage transistorized design. The first stage is an HXTR-6101 NPN bi-polar transistor designed for minimum noise. The transistor utilizes 10N implantation techniques with sub-micron emitter widths. The chip is mounted in an HPAC-70GT which is a rugged metal/ceramic hermetic package. The transistor has a typical noise figure of 1.5 dB and a typical gain of 15 dB at 1540 MHz with 4 ma of collector current. The second and third stages utilize an HP35821E transistor which has a noise figure of less than 4 dB at 1640 MHz with a typical gain of 8 dB at 5 ma of collector current.

The overall amplifier noise figure is less than 2 dB and provides a gain of 30 dB. The amplifier is a microstrip circuit built on an alumina substrate. The circuitry is a combination of printed and chip components.

• Bandpass Filter

The remaining rejection required for the image and transmitter frequencies is obtained by a 1640 MHz bandpass filter following the RF amplifier. The filter selected for this application is a tubular type since it is small and lightweight. The filter is a 4-pole design and has an insertion loss of 5 dB. The high insertion loss is not objectionable since it is preceded by 30 dB of gain thus introducing a negligible contribution to the receiver noise figure. The filter is of 1/4" diameter and provides 50 dB rejection at the transmitter frequency and 60 dB rejection at the image frequency.

• Mixer

The mixer provides a low conversion loss over the 2.5 MHz bandwidth of interest with good RF-to-LO isolation for high cross channel isolation. A double balanced mixer is employed to reduce its susceptibility to even order spurious responses. The mixer has been developed at AIL and consists of a combination of a slotline on microstrip with a transmission line consisting of a wire near a ground plane. A Schottky barrier diode quad and chip capacitor are mounted on the etched circuitry and alumina substrate. The diode and quad allows the use of 0 dBm local oscillator drive thus reducing the frequency source power requirements for supplying the 32 LO's.

The mixer downconverts the 1640 MHz input to 70 MHz with a conversion loss of less than 7 dB. The RF-to-LO isolation is greater than 25 dB.

• 70 MHz Preamplifier

The preamplifier is sufficiently broadband such that its contribution to amplitude ripple and deviation from linear phase is negligible. The amplifier is designed with feedback employing transistors that provide adequate gain with low bias currents. The amplifier provides 40 dB of gain which is sufficient to compensate for the loss of the SAW filter. The anticipated output noise level is -50 dBm and the amplifier output 1 dB compression point is -5 dBm.

● Surface Acoustic Wave Filter

The 70 MHz SAW filter establishes the 2.5 MHz channel bandwidth. Most of the channel amplitude ripple and deviation from linear phase is taken up by the SAW filter. Within the passband, the ripple is ± 2 dB and phase deviation is ± 4 degree RMS. The filter has an insertion loss of 20 dB and an ultimate attenuation of 70 dB. The SAW filter rejects the transmitter leakage difference signal to a level under the noise floor of the 70 MHz postamplifier.

The SAW filter consists of a quartz crystal substrate (ST-cut) with two aluminum interdigital transducers. The ST-cut quartz is temperature insensitive and aluminum produces minimal dispersive loading. One transducer will be of the uniform broadband type, while the other will be an apodized frequency selective transducer. In addition to the standard $\sin x/x$ apodization, weighting factors will be included to limit frequency sidelobes and passband ripple. Weighting factors will also be included to compensate for the rounding effect of the broadband transducer and acoustic diffraction from fingers with small overlaps. A number of design elements will be included to minimize other second order effects. In particular, the following techniques will be used:

- split fingers to prevent phase front distortions of the acoustic beam
- grooves cut in the back of the substrate to suppress bulk waves
- pattern following buss bars to reduce defects and increase yield
- acoustic absorbent films to prevent end reflections and resultant passband ripple
- transducer spacing and layout to minimize direct electrical feedthrough

All of these techniques have been used and proven successful in our laboratory.

● 70 MHz Postamplifier

The postamplifier is used to bring the signal level up to a level which is compatible with the receiver beam processor unit. The postamplifier provides 40 dB of gain and is similar in design to the preamplifier. The post-amplifier is biased with more current to obtain a higher 1 dB compression point to guarantee linear operation for the higher level input signal.

4.2.2.4 Power Monitor Sampling Switch

The Power Monitor Sampling Switch is a single-pole 32 throw (SP32T) pin diode switch that allows the output power of each of the transmitter module to be monitored. This will allow acknowledgement of degradation or failure of an L-band transmitter module to be assessed during the flight.

4.2.2.5 Layout

The transmitter and receiver modules are laid out as shown in Figure 4.2-20 in back-to-back hogged out chassis. The two modules were laid out on a common chassis to provide the flexibility to be used in any one of the variable aperture array configurations described in Section 4.2.1.

In the mechanically actuated variable aperture configuration, the antenna element will also be packaged together with the transmitter and receiver modules. In the electrically switched aperture phased array configuration, the elements will be fixed on the array structure, and the 32 transmitter/receiver modules will be packaged as one Transmitter/Receiver Assembly.

SIZE: 101.6 MM X 101.6 MM X 177.8 MM
(4 IN) (4 IN) (7 IN)
WEIGHT: 0.909 KG
2.0 LBS
WATTS: 3.4 WATTS

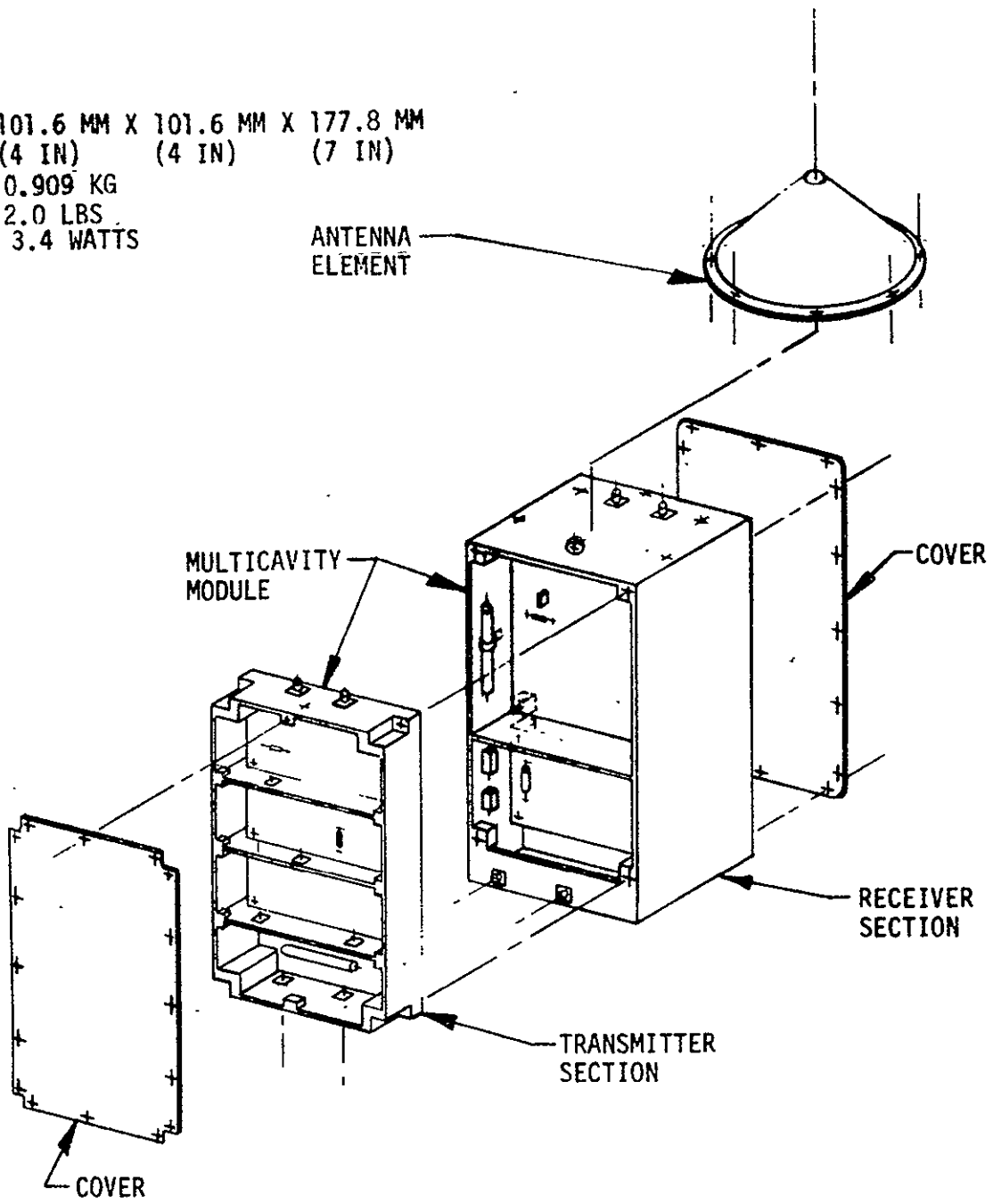


FIGURE 4.2-20 ANTENNA ELEMENT AND TRANSMITTER/RECEIVER MODULE

4.2.3 Frequency Source

4.2.3.1 General

The pallet frequency source generates the LO frequencies required for use by the element module. The frequencies generated are coherent to the reference standard housed in the Spacelab Module frequency source. Phase locked sources are employed to generate the required frequencies.

Two reference frequencies at 147 MHz and 171 MHz are received from the Spacelab Module frequency source. From these references, 1470 MHz and 1710 MHz are produced in the Pallet Frequency source. Each of these signals is fed to an LO distribution network which provides 32 output lines for each frequency. The 1470 MHz is used as an LO for the 32 transmitter modules and 1710 MHz is used as an LO for each receiver module.

4.2.3.2 Tradeoff Analysis - Phased Locked Loop Vs. Multiplier

Two approaches were considered for the generation of the L-band LO's. One approach was a multiplier design whereby a reference is multiplied and filtered to achieve the desired harmonic. The filtered output is then fed to a power amplifier to provide the required output power level. The other technique is to generate a low level reference and then phase lock it to a voltage controlled oscillator (VCO). The VCO output provides the required frequency and power level.

The method selected for the frequency generation is the phase locked loop (PLL) technique. The PLL approach is superior in terms of spectral purity and spurious rejection. In addition, the PLL weighs less and is more efficient than the multiplier method. The efficiency of the PLL method is higher since oscillator efficiencies are better than Class A power amplifier efficiencies for identical output power and spurious requirements. The multiplier method tends to be heavier than the PLL approach due to the additional requirement of a large multipole L-band filter which has to provide the spurious rejection requirements. In the PLL approach, an L-band filter is not required since the loop effectively acts as a narrowband filter.

As previously mentioned, the prime reason for the selection of the PLL method is its superiority in terms of spectral purity. In the design of a PLL, the loop bandwidth is set so that the loop acts as a narrowband filter so as to optimize the noise characteristic. While the noise inside the loop bandwidth is a function of the input reference, the loop rejects the noise of the reference outside the loop bandwidth. The result is a composite noise density that optimizes the close-in noise characteristics of the reference, and the superior far-out noise characteristics of the VCO.

The phase locked loop method is implemented in order to achieve the required system spurious response rejection. The receiver module spurious response characteristics depend on the spectral purity of the 1710 MHz LO. If the far-out noise characteristic of the LO is not kept low, the receiver module will be desensitized in the presence of a large out-of-band signal.

The 1710 MHz LO derived from the PLL will have a phase noise spectral density at 1 MHz removed from the carrier of -145 dBm/Hz. With a multiplier design, the phase noise spectral density at 1 MHz from the carrier would be approximately -110 dBm/Hz which is 38.6 dB greater than the 20 MHz TCXO noise floor due to the frequency multiplication factor of 85.5 (1710/20). The PLL method thus results in a 35 dB improvement in phase noise 1 MHz from the carrier. For frequencies greater than 1 MHz out from the carrier, the improvement is even larger since the multiplier noise is flat while the PLL noise is decreasing due to the VCO noise characteristic. Therefore, with the LO derived from an PLL an interfering signal 1 MHz from the desired channel would have to be 35 dB greater to result in the same desensitization for a receiver using an LO derived by multiplication.

The PLL's employed in the pallet frequency source operate in the following manner. The reference signal received from the Spacelab frequency source is amplified to a level sufficient to drive a comb generator which generates harmonics of the reference signal. The output from the comb generator and a low level sample from the loop VCO are fed to a phase detector. If the appropriate harmonic of the reference signal is at exactly the same frequency as the VCO, the phase detector's output will be a DC voltage, the amplitude and polarity of which will be a function of the phase difference between the two signals.

If the two signals are not at the same frequency, the phase detector's output will be a signal at the difference frequency. When a phase or frequency error occurs between the two signals, the error signal from the phase detector is amplified and fed to the tuning input of the VCO so as to correct its phase or frequency until the phase error is essentially reduced to zero. By this method, the VCO is phase locked, cycle to cycle, to the appropriate harmonic of the reference signal.

4.2.3.3 Design

A functional block diagram of the pallet frequency source is illustrated in Figure 4.2-21. The frequency source consists of two phase locked sources whose outputs are fed to the LO distribution network. The input references are received from the Spacelab frequency source. The LO distribution network provides 32 outputs to the receiver module and 32 outputs to the transmitter module.

The performance characteristics of the frequency source are indicated in Table 4.2-4 . The close-in phase noise is based on the TCXO standard used in the Spacelab frequency source.

The L-band LO's are generated by initially amplifying the input reference signal to a suitable level for driving a step recovery diode multiplier. A phase comparison is made with the tenth harmonic of the input reference and a sample of the VCO in a phase detector. When the signals are out of phase, the phase detector provides an output voltage proportional to the phase difference. This voltage is applied to the loop amplifier which feeds the tuning port of the VCO. This frequency control closes the loop by phase locking the oscillator to the input reference.

The VCO employed is a fundamental cavity oscillator with the cavity structure maintaining a high leaded Q to provide the low noise performance. When the unit is turned on or lock has broken due to any voltage or noise transient, the reference and VCO frequency separation can be greater than the narrowband loop can accommodate to acquire lock. To overcome this problem, a low frequency search oscillator is incorporated within the phase locked loop. The effect of the search oscillator is to superimpose an AC sweep voltage onto

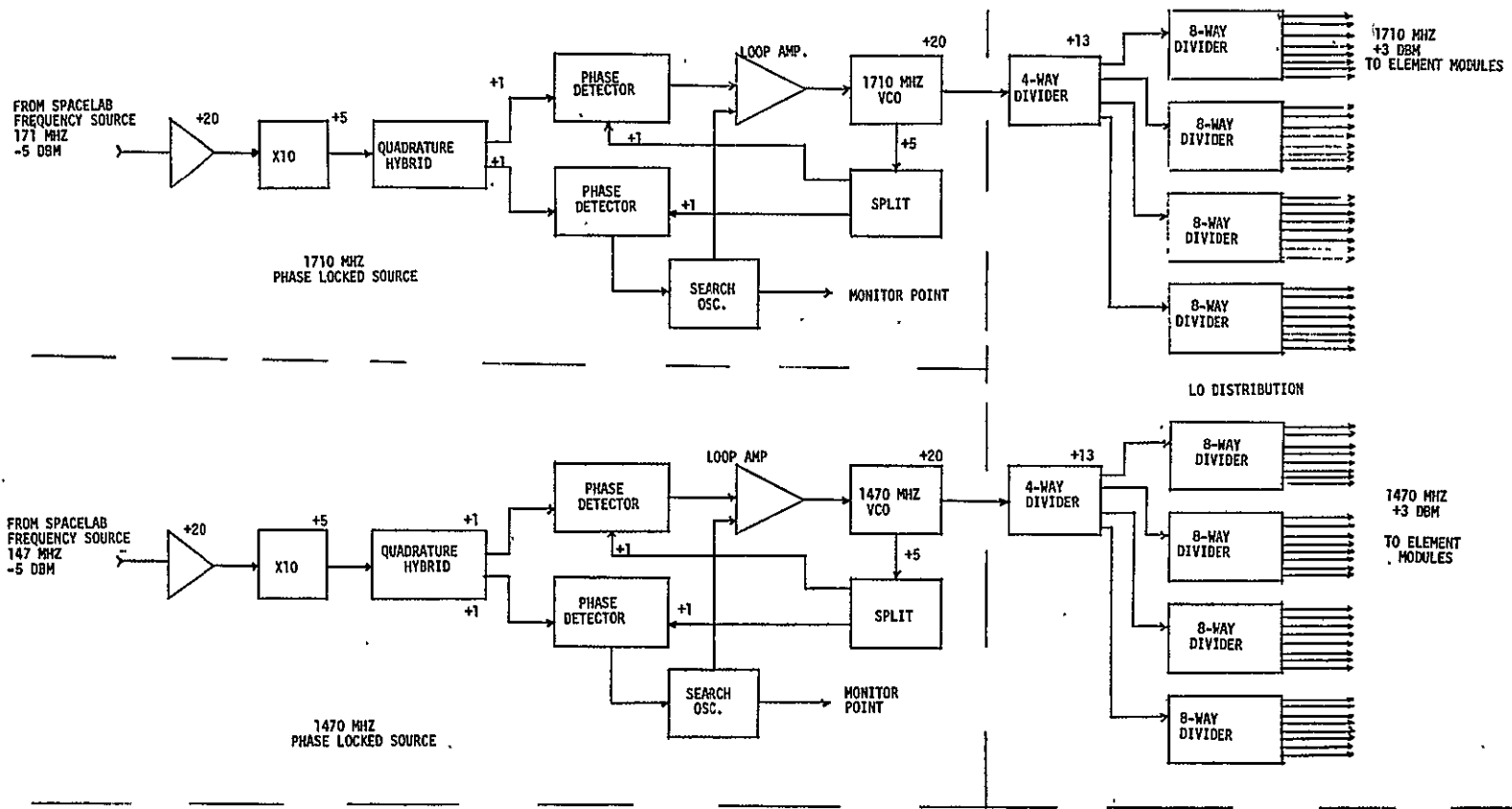


FIGURE 4.2-21. PALLET FREQUENCY SOURCE BLOCK DIAGRAM

TABLE 4.2-4. FREQUENCY SOURCE PERFORMANCE CHARACTERISTICS

OUTPUT FREQUENCY	:	1710 MHZ, 1470 MHZ
OUTPUT POWER	:	+20 DBM (PHASE LOCKED SOURCE) +3 DBM (LO DISTRIBUTION)
POWER STABILITY	:	± 1 DB
SPURIOUS	:	-70 DBC
HARMONICS	:	-30 DBC
LOOP BANDWIDTH	:	100 KHZ
PHASE NOISE (10 HZ-1 KHZ) (AT 1 MHZ)	:	3 DEGREES -145 DBC/HZ
VSWR	:	1.5
ISOLATION	:	20 DB (LO DISTRIBUTION)
INPUT FREQUENCY	:	171 MHZ, 147 MHZ
INPUT POWER	:	-5 DBM
DC POWER	:	9 WATTS
WEIGHT	:	8 LBS

the tuning port of the VCO. This voltage tunes the VCO about its center frequency. When the VCO matches the appropriate harmonic of the reference, lock is achieved. The search oscillator is then automatically disabled.

The acquisition is implemented by having a VCO sample compared in a secondary phase detector with the input reference after a 90° phase shift. The phase shift is obtained by the use of a quadrature hybrid. When the loop is unlocked, the phase detector output triggers the search oscillator which generates the sweep voltage. A monitor point is provided from each loop to indicate the lock status.

The phase locked output signal is fed to a distribution network which provides a 32-way power division. The 32-way divider consists of one 4-way divider which feeds four 8-way dividers. Two 32-way dividers are incorporated to provide 32 outputs at 1470 MHz and 32 outputs at 1710 MHz to be used as LO's for the element modules.

4.2.4 Power Conditioner

4.2.4.1 General

The Pallet Power Conditioner accepts the 28 VDC input and derives the regulated DC voltages required for the element modules and frequency source.

The design and major tradeoffs made are identical to that of the Space-lab Power Conditioner, discussed in greater detail in Section 4.3.7.

The Power Conditioner provides the following output characteristics:

+15V	+15V \pm 1V @ 4.6 amps with a resistive load and other outputs loaded
+24V	+24V \pm 1V @ 1.6 amps with a resistive load and other outputs loaded.
-5V	-5V \pm 0.2V @ 1.3 amps with a resistive load and other outputs loaded.

Total internal dissipation : 45 watts

Ripple on all outputs : 1 millivolt peak to peak

4.2.5 Pallet Mounted Subsystem Layout

4.2.5.1 Recommended Hard Mounted Configuration

The electrically actuated switched aperture phased array has been shown to provide the best compromise to provide a variable aperture phased array with minimal implementation and cost impacts. Figure 4.2-22 illustrates how the Pallet Subsystem can be mounted on the pallet structure. The array support structure is a 2.8 meter by 2.8 meter (plate) of one inch sandwich construction with 0.020 aluminum skins. The 80 modified flared-cone turnstile antenna elements are mounted to the structure as well as the array switch matrix which is used to select the desired 32 elements. The array support structure plus the switch matrix and interconnecting cables (RG-141 type) weigh a total of 44.57 kg.

The Transmitter/Receiver Unit containing the 32 transmitter and receiver modules, Frequency Source and Power Conditioner are packaged in separate housings. The Transmitter/Receiver Unit and the Frequency Source are mounted on the array support structure to minimize interconnecting cable lengths, and the Power Conditioner is mounted on the floor of the pallet structure. The size, weight and power requirements for these units are shown in the previous Figure 4.2-22.

4.2.5.2 Alternate Hard Mounted Configuration

Figures 4.2-23 , 4.2-24 and 4.2-25 illustrate equipment layout on the pallet structure for alternate array configurations; viz: mechanically actuated variable aperture phased array, filled array and thinned array configurations, respectively.

The size, weight and power requirements are included on the figures.

4.2.5.3 Optional Erectable Configuration

Previous discussions have shown that an erectable array can provide an unobstructed field-of-view that allows experiments to be performed out to the horizon (+70 degrees), thereby greatly enhancing the allowable dwell time on a desired signal. Figure 4.2-26 illustrates a conceptual layout showing how any one of 4 array configurations considered herein could be stowed on the pallet structure and extended out of the Orbiter's payload bay to clear all

REPRODUCIBILITY OF THE ORIGINAL DRAWING IS POOR

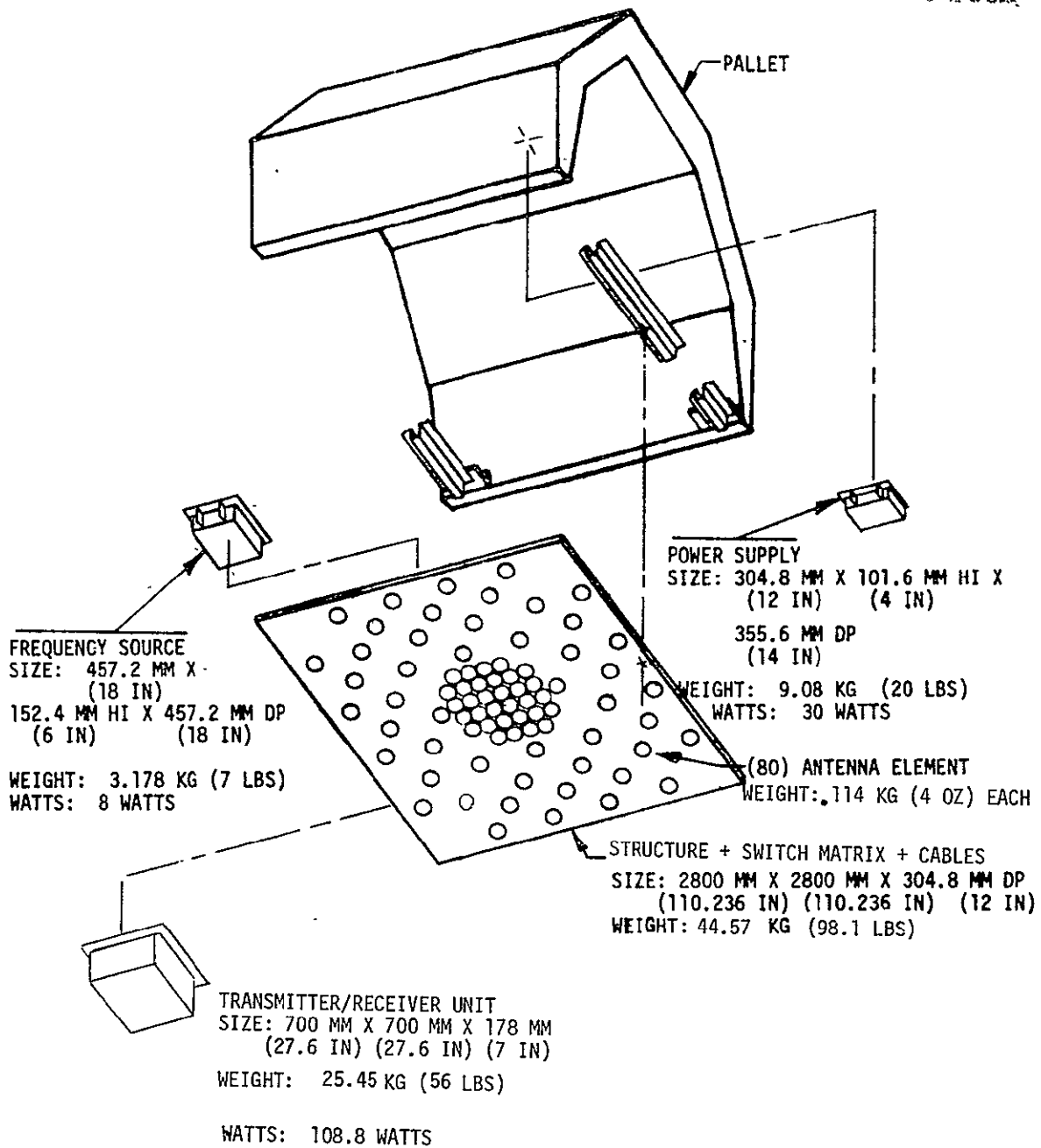


FIGURE 4.2-22 PALLET EQUIPMENT - SWITCHED APERTURE PHASED ARRAY

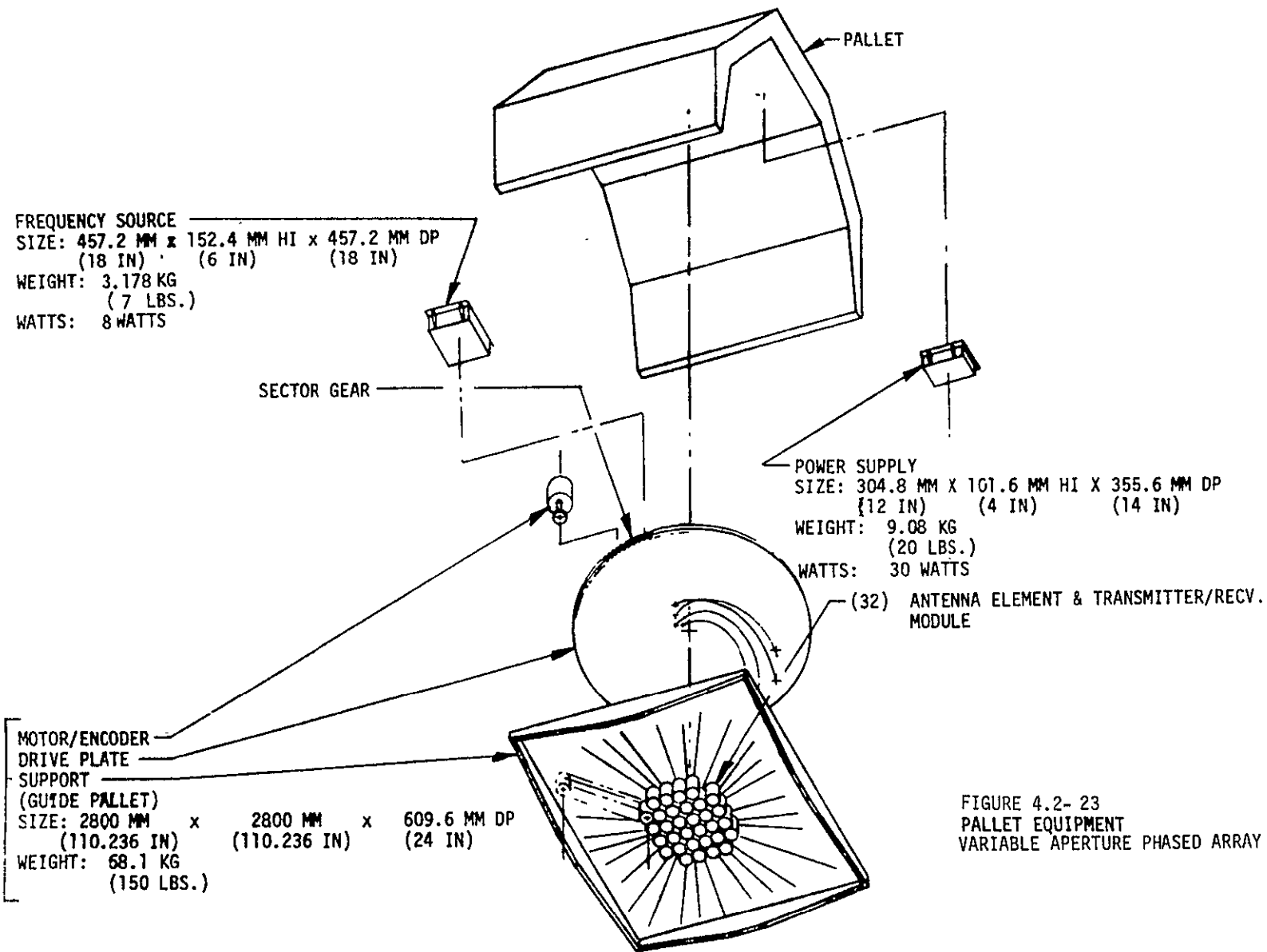


FIGURE 4.2- 23
 PALLET EQUIPMENT
 VARIABLE APERTURE PHASED ARRAY

FREQUENCY SOURCE
 SIZE: 457.2 MM X 152.4 MM HI X 457.2 MM DP
 (18 IN) (6 IN) (18 IN)
 WEIGHT: 3.178 KG (7 LBS)
 WATTS: 8 WATTS

POWER SUPPLY
 SIZE: 304.8 MM X 101.6 MM HI X
 (12 IN) (4 IN)
 355.6 MM DP
 (14 IN)
 WEIGHT: 9.08 KG (20 LBS)
 WATTS: 30 WATTS

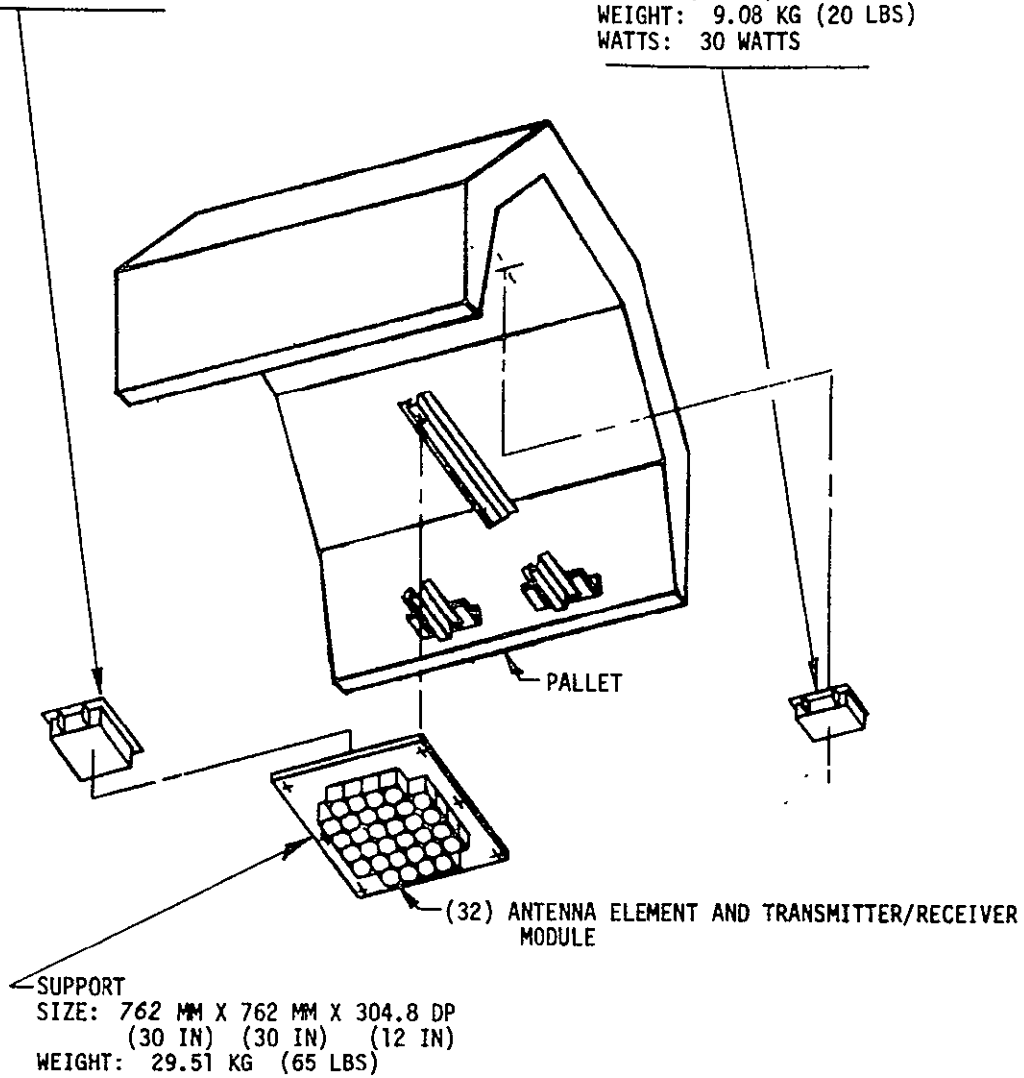


FIGURE 4.2-24 PALLET EQUIPMENT-FILLED
 ARRAY CONFIGURATION

REPRODUCIBILITY OF THE ORIGINAL PAGE IS POOR

FREQUENCY SOURCE
SIZE: 457.2 MM X 152.4 MM X 457.2 MM DP
(18 IN) (6 IN) (18 IN)
WEIGHT: 3.178 KG (7 LBS)
WATTS: 8 WATTS

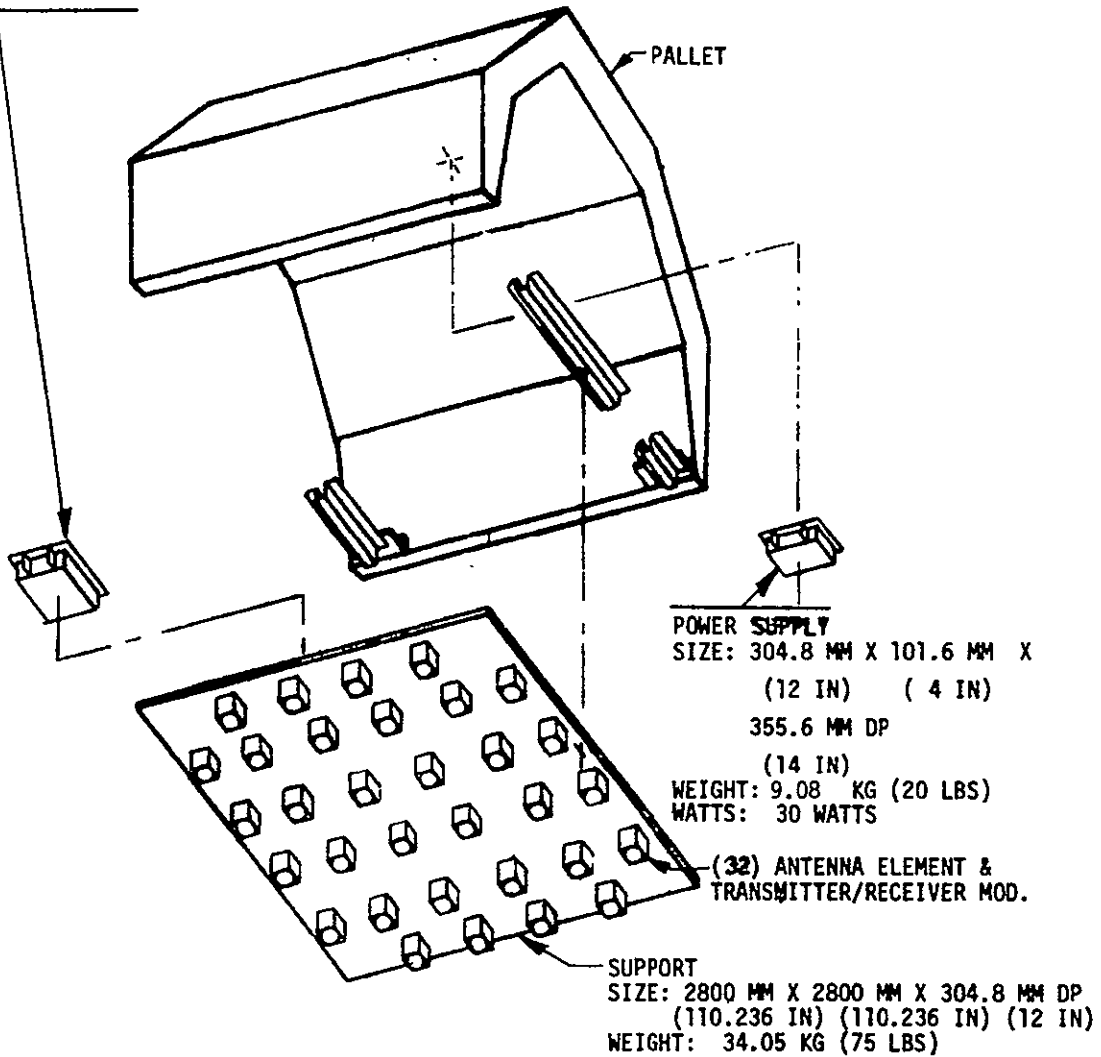


FIGURE 4.2-25 PALLET EQUIPMENT - THINNED ARRAY CONFIGURATION

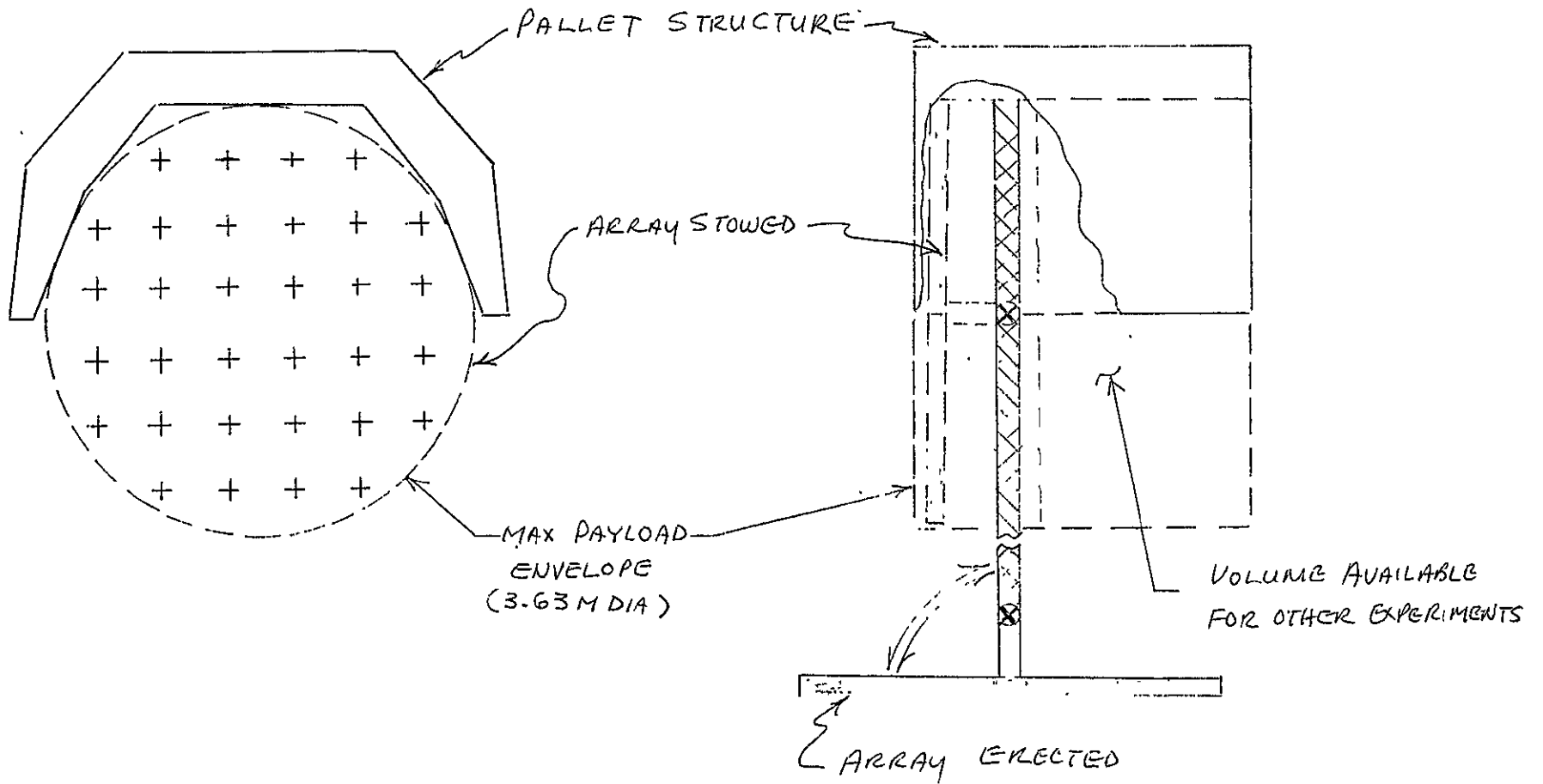


FIGURE 4.2-26. OPTIONAL ERECTABLE AMPA ARRAY CONFIGURATION

structural obstructions.

For stowage, the array structure is rotated 90 degrees. This conserves volume on the pallet structure so that other experiments can share the same pallet. In addition, the maximum allowable payload envelope of 3.63 meter diameter-allows the maximum aperture size for the arrays (in its thinned array configuration) to be increased to approximately 3 meter by 3 meter. This increased aperture size provides improved resolution which enhances operation near RFI's by reducing the array HPBW from approximately 4 degrees to 3 degrees. In addition, the increased aperture size factor from 4.23 to 5.77 will enhance the spatial dispersion of IM products even more, allowing the L-band transmitter power amplifiers to be operated with less back-off for greater RF-to-DC power conversion efficiency.

A summary comparison of the total AMPA Experiment System implementation for the four hard mounted array configurations has been made as shown below, excluding the Digital Processor Network. The summary includes the weight and power for both the Pallet and Spacelab Module Subsystems.

<u>ARRAY APPROACH</u>	<u>WEIGHT-KG*</u>	<u>POWER-WATTS</u>	<u>Δ COST \$*</u>
1. Filled Array	235	383	---
2. Thinned Array (Maximally Thinned)	235	383	36K
3. Variable Aperture Phased Array (Mechanically Actuated, Continuous Variation)	274	383	+521K
4. Switched Aperture Phased Array (Electrically Switched, Three Discrete Variations)	250	383	75K

*Does not include Digital Processor Network

The summary shows that the features to be gained with a variable aperture can be gained with minimal implementation and cost impacts with the switched aperture approach.

4.3 SPACELAB MODULE MOUNTED SUBSYSTEM

Components of the Spacelab Module Subsystem are shown in Figure 4.3-1 and include a 32 X 2 way divider matrix, 2 adaptive receiver processors, 2 transmitter beam processors, a summer/amplifier matrix, digital processor network, frequency source, power conditioner and AMPA control unit. The Spacelab Module Subsystem is interconnected with the Pallet Subsystem by hardwire.

4.3.1 Receiver Processor Unit

4.3.1.1 General

As shown previously in the AMPA Experiment System block diagram (Figure 4.1-11), the Receiver Processor unit includes two Adaptive Processor assemblies, and an Array Divider Matrix that divides the 32 input signals from the array to the two processors. Each Adaptive Processor is then further subdivided into a Beam Forming Network, Correlator Processor subassembly, Channel Downconverter subassemblies, sampling switch, and a Signal Processor subassembly. The Signal Processor includes the Doppler Processor, Modem and Data Conditioner.

The Adaptive Processor is a beam forming network which uses a hybrid correlation loop to optimize the signal-to-interference plus noise ratio $[S/(I+N)]$. The Adaptive Processors can operate in the pointed, directed-adaptation or fully adaptive modes with the aid of a common Digital Processor Network.

The signal processing requirements for the AMPA Experimental System are made more difficult by the dynamically changing signal environment caused by Spacelab movement as described previously in Section 4.1.3. Signal acquisition times are longer and signal tracking is more difficult for these high angular tracking rates. The angular rate of change is approximately 1.1 degree per second for direct overpass of an emitter. Because of this, processing speed is very critical.

Figure 4.3-2 shows the essentials of the Adaptive Processor that perform the $S/(I+N)$ maximization. The Adaptive Processor initially separates the desired signal and interference signals in the individual channels as well as from the array sum output, and their correlated outputs provide the information required to compute the changes to be made to the weighting factors (amplitude and phase) to optimize the $S/(I+N)$. Since the adjustments in the weighting factors in the individual channels are interdependent, an iterative rapid convergence technique has been developed using a digital processor to calculate the magnitude and direction of successive steps. Signal and interference

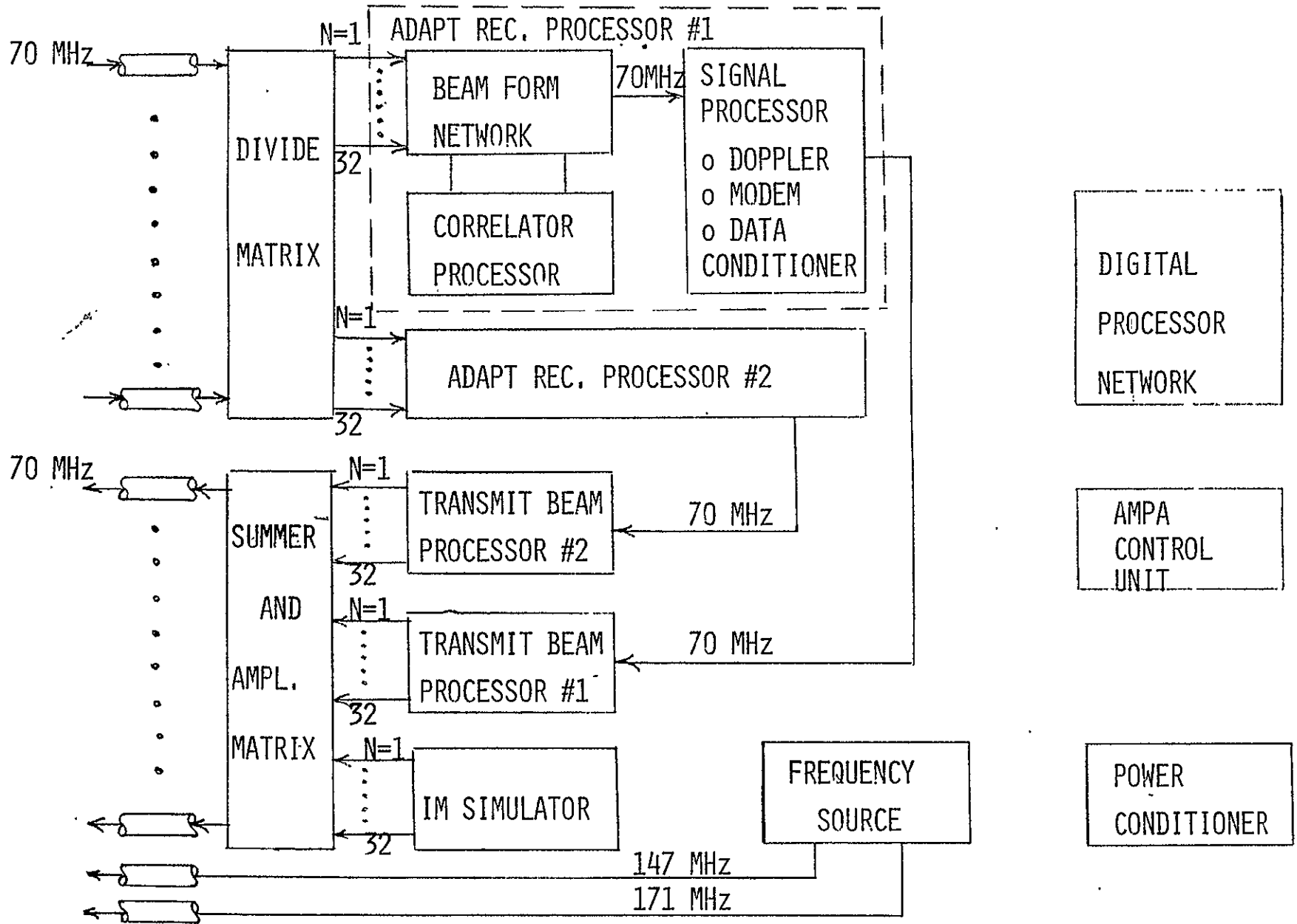


FIGURE 4.3-1 COMPONENTS OF SPACELAB MODULE SUBSYSTEM

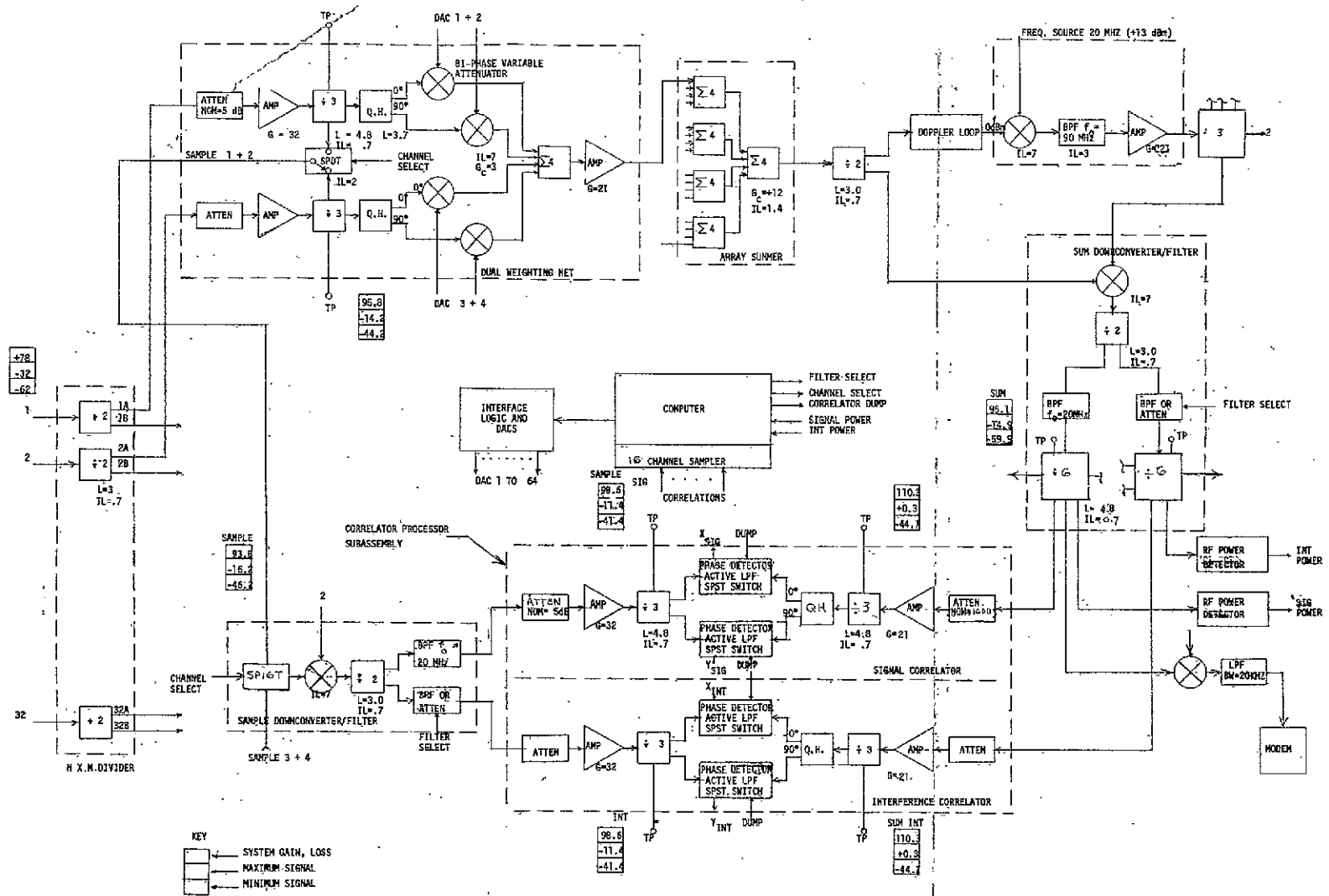


Figure 4: 3-2 AMPA Adaptive Receiver Processor

correlator outputs are sampled from each channel. They are sequentially read in and stored in the Digital Processor Network. After reading in all the channel outputs, the digital processor determines and commands the appropriate adjustments to be made to each weighting network. The routine is continued until the resultant $S/(I+N)$ converges to maximum. The entire $S/(I+N)$ optimization process takes only a few tens of milliseconds for initial acquisition, and considerably less for tracking.

For automatic acquisition and track, the filters for Adaptive Processor uses a narrowband filter (7.5 kHz) to pass or reject a CW pilot tone that provides the unique user signature required by the adaptive algorithm.

4.3.1.2 Tradeoffs



Due to the relatively rapid angular motion (maximum of 1.1 degrees per second for the case when the Spacelab passes directly over a signal) between the Spacelab and the signal environment, the key tradeoff in the Adaptive Processor and the Digital Processor Network is the overall processing time required to measure, compute and make the iterative changes to the weighting network, so that high array gain can be maintained on the desired signal while spatial nulls are simultaneously placed on interference emitters.


The total processing time (T_0) is the sum of the correlator processor integration time (T_{CP}) to sample each of 32 array channels and the digital processor computation time (T_{dp}) required to process the $S/(I+N)$ algorithm. The correlator integration time for the minimum detectable signal for one correlator processor is approximately one millisecond. If we assume a digital processor computation time of 40 milliseconds, and sequential sampling of 32 array channels with one correlator processor, the total processing time is 72 milliseconds, or $T_0 = T_{dp} + \frac{32T_{CP}}{N}$ where N is the number of correlator processors. On the other hand, with 32 parallel correlator processors, the total process time can be reduced to 41 milliseconds. For other numbers of parallel correlator processors, such as 16, 8, 4 and 2, the total process time will increase to 42, 44, 48 and 56 milliseconds, respectively. In all cases, it is evident that the digital computation time is the major component of the overall process time.

In order to evaluate the impact of the dynamic signal environment on the total processing time, the AMPA array was synthesized by means of computer simulation:

- With only a desired signal located on the flight path, representing the highest dynamic rate, and
- 3 RFI emitters added to the above desired signal environment.

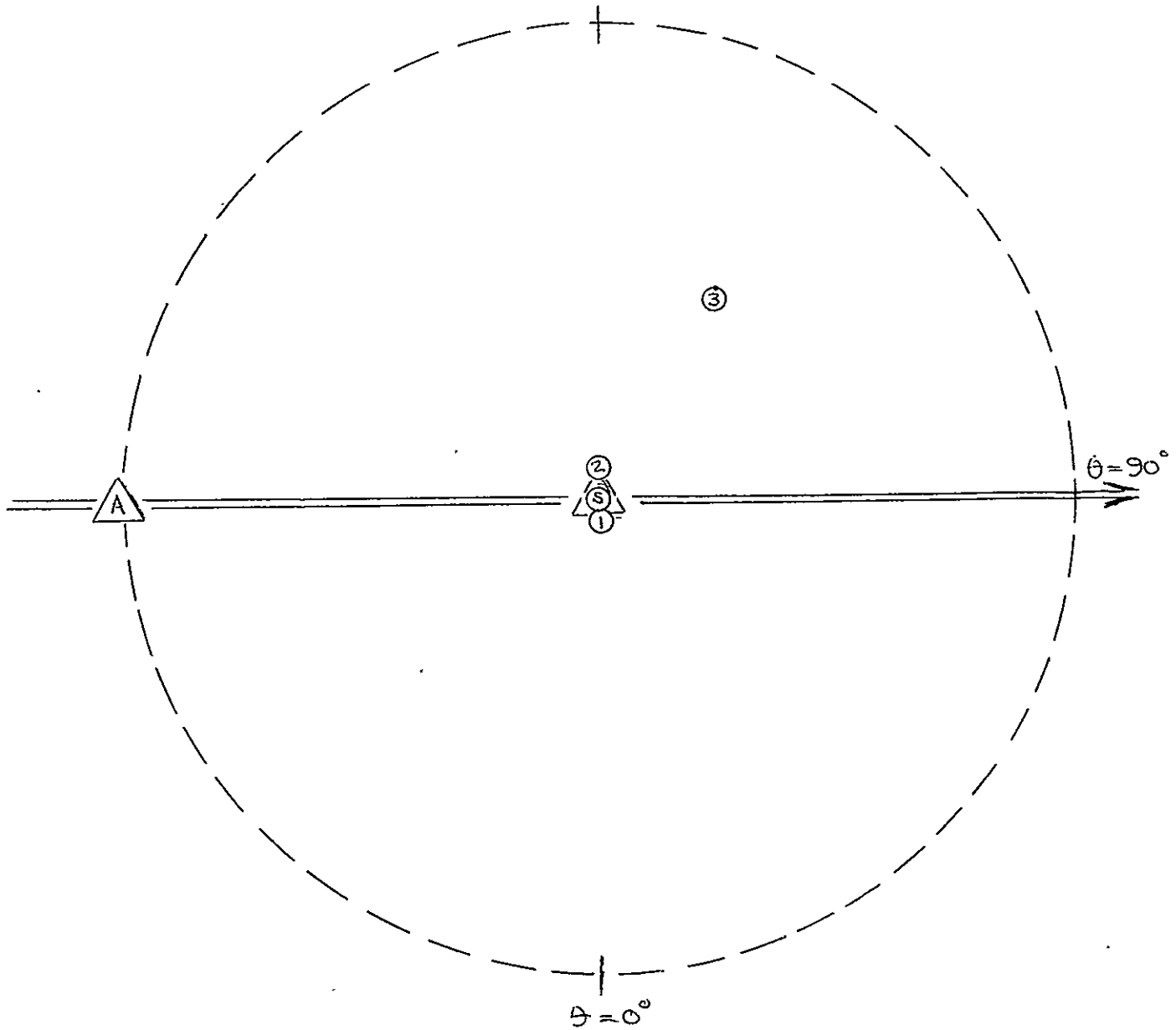
The signal scenario is shown in Figure 4.3-3, showing the signal location relative to the Spacelab positions:

-  When the Spacelab first sees the desired signal on the horizon
-  When the Spacelab is directly over the desired signal

The angle θ represents the azimuthal angle to the signals (flight path = 90 degrees) and α is the elevation angle to the signals measured from the Spacelab nadir. The signal scenario represents a very difficult environment when the Spacelab initially comes over the horizon (Position  in Figure 4.3-3). At this time, RFI #1 and #2 are 1.39 and 2.78 degrees, respectively, in azimuth from the desired signal, considerably less than the HPBW of the array (≈ 4 degrees). However, as the Spacelab moves toward the desired signal, the angular separation to RFI #1 and #2 increases to 7.91 and 15.52 degrees, respectively.

All of the 4 signal sources are of equal power, designed to provide a CNR of +7 dB at scan limits (± 70 degrees) in the absence of interferers. When the Spacelab is directly overhead of the desired signal, its maximum achievable CNR increases to 24.4 dB (due to the reduced space path loss of 15.2 dB and array scan loss of 2.2 dB).

Computer simulations were conducted for these signal scenarios as a function of adaptive process times, representing different combinations of digital process speeds, number of parallel correlator processors, and number of users being supported simultaneously. Subsequent tradeoff analyses in Section 4.3.3 summarize the pertinent performance characteristics of candidate digital processors that have been qualified for military or space applications and have computation speeds that are consistent with the AMPA requirements.



SIGNAL	SIGNAL - RECEIVER TO SPACELAB			
	POS A		POS B	
	α°	θ°	α°	θ°
DESIRED	70.21	90	0	0
RFI #1	70.21	88.61	7.91	0
RFI #2	70.21	92.78	15.52	180
RFI #3	*	98.71	52.63	240

*Below Horizon

FIGURE 4.3-3 SIGNAL SCENARIO FOR DYNAMIC ENVIRONMENT SIMULATION

In general, the computation speeds of the candidate digital processors to process AMPA's adaptive algorithms fall into two categories, viz, 20 and 40 milliseconds per received beam, or 40 and 80 milliseconds for two simultaneous received beams per iterations. Computer simulations have been conducted for the following cases:

CASE	# BEAMS	# CORRELATOR PROCESSORS	CORRELATOR INTEGRATION TIME-MILLISEC	DIGITAL PROC. TIME MILLISEC	TOTAL PROC. TIME MILLISEC
1	2	1	32	80	112
2	2	32	1	80	81
3	2	1	32	40	72
4	2	32	1	40	41

Computer simulations were initially conducted for the case with no RFI's to insure adequate processing speeds and the results are summarized in Figure 4.3-4. Figure 4.3-4 indicates that the sequential sampling with one correlator processor with the slower digital processor speed of 80 milliseconds for the two beams is adequate to track the desired signal throughout the flight path. Shown also in Figure 4.3-4 is the omniscient solution (maximum achievable theoretical solution) if the total process time was infinitely fast; or in other words, if the Spacelab was stationary. The deviation from the omniscient solution is due to the moving scenario, to the finite processing time, and to the iterative adaptive convergence process. The results indicate, however, that even with the slower processing time of 112 milliseconds the desired signal can be tracked and the performance maintained above the CNR threshold of +7 dB throughout the flight path.

Figure 4.3-5 summarizes the cases 1 through 4 in the presence of the 3 RFI's. Even for these cases, it is seen that the required CNR threshold is maintained throughout the flight path, although the deviation is slightly greater than for the no RFI cases. Note that Case 1 represents the least complex implementation impact since a single correlator processor is used to sequentially sample all 32 channels, and since a relatively slow digital processor (40 milliseconds per beam) is used.

4-100

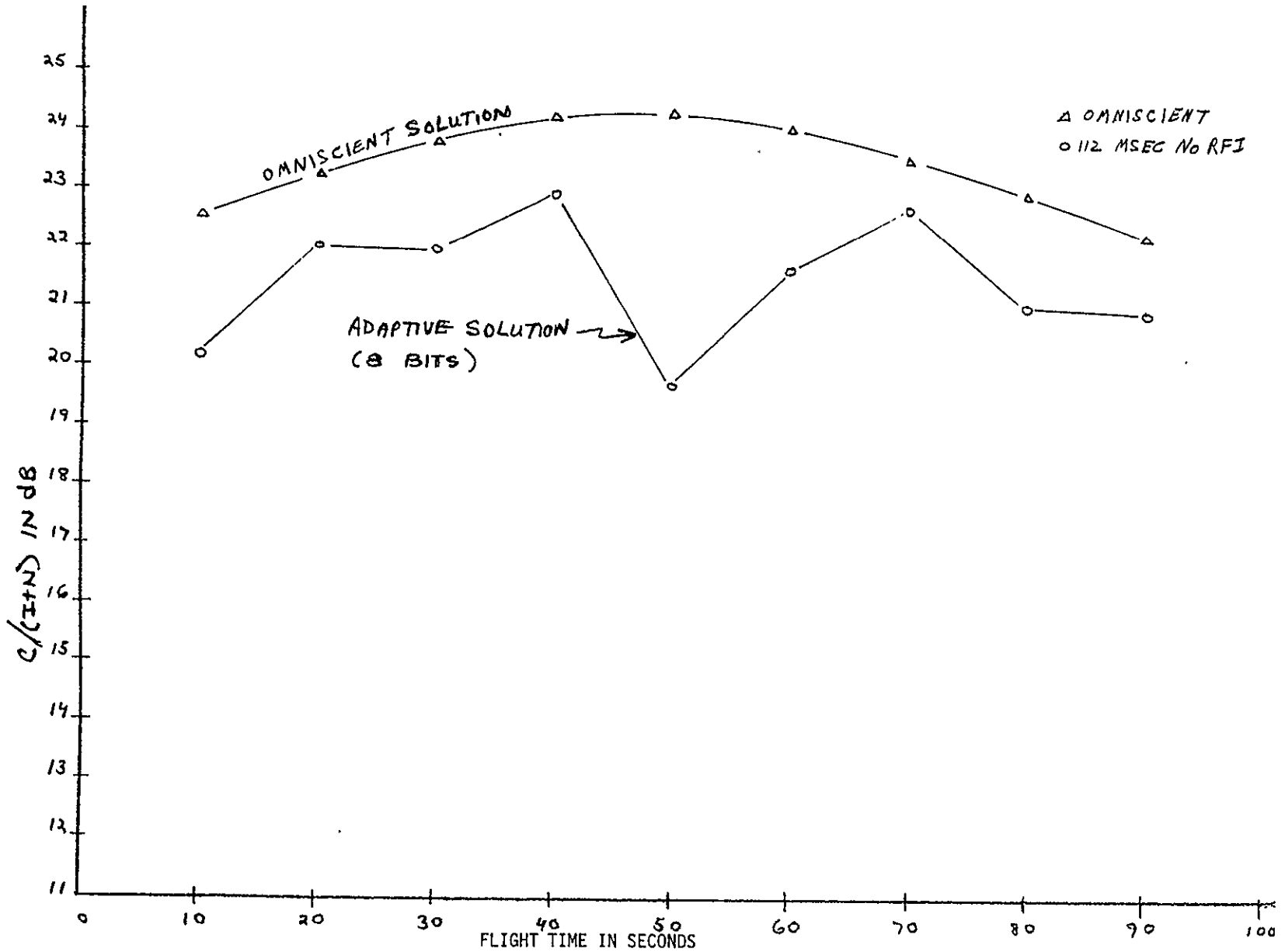


FIGURE 4.3-4 ADAPTIVE PERFORMANCE VS. PROCESS SPEEDS - NO RFI

4-101

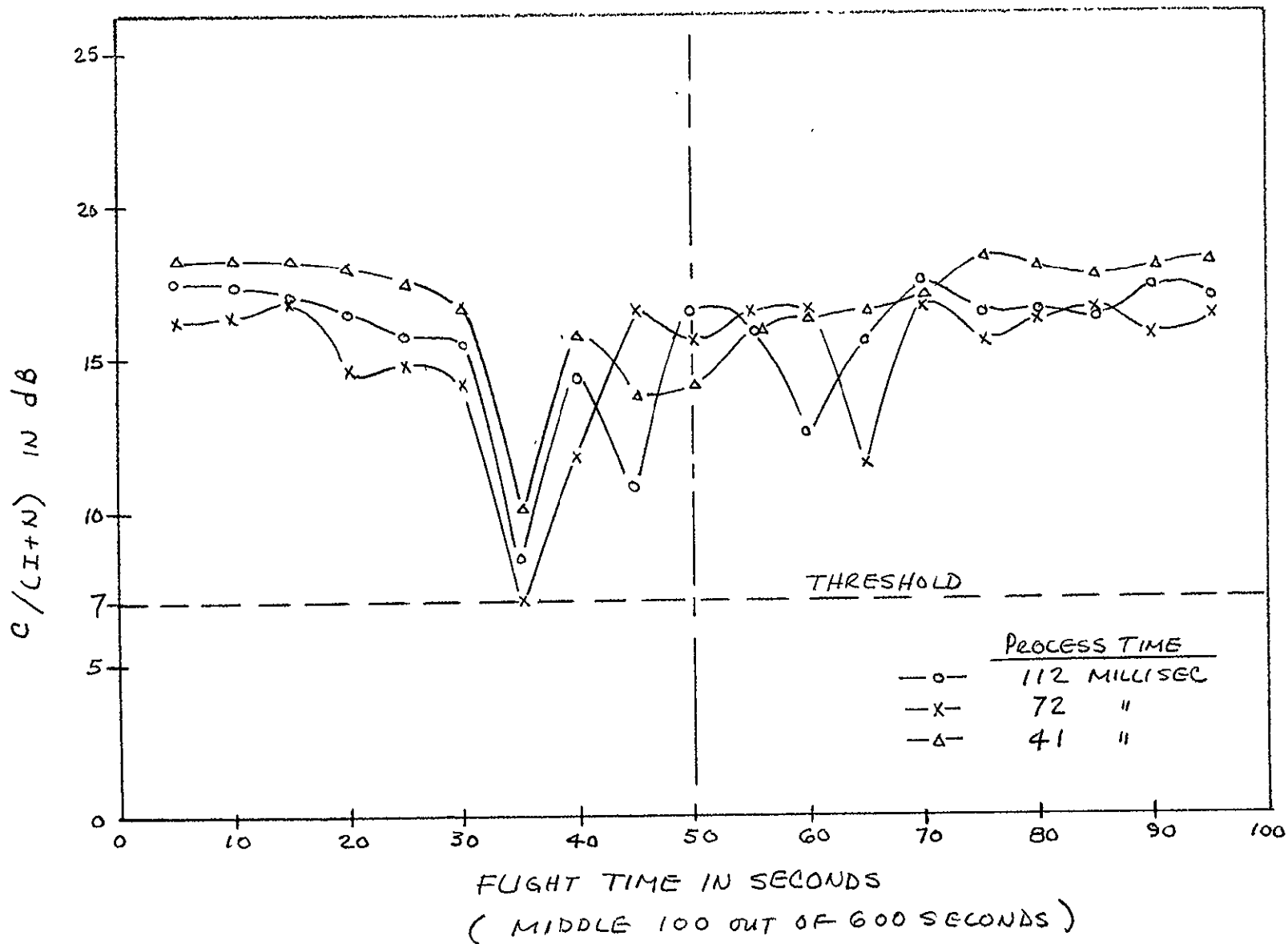


FIGURE 4.3-5 ADAPTIVE PERFORMANCE VS PROCESS SPEEDS WITH THREE RFI'S

As a result, it is recommended that a single correlator processor and a digital processor of 40 milliseconds per beam be used in the AMPA Experiment System.

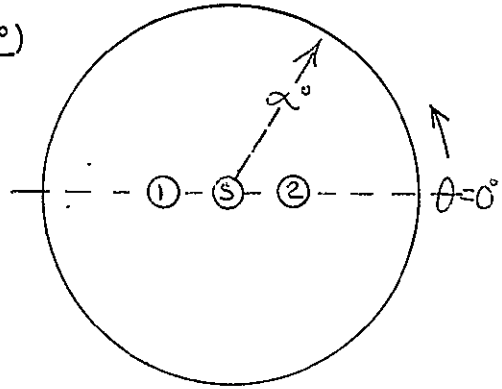
Computer simulations have been conducted to determine the resolution required to adjust the weighting network as well as the resolution to read out the data from the correlator processors; initially, in a static environment and subsequently under the dynamic environment with a moving Spacelab. The static simulations were conducted with 2 RFI's with 4, 6, 8 and 16 bits and as the interference to desired signal power ratios (RFI/S) were varied from 0 to 30 dB. Table 4.3-1 presents the adapted performance vs. resolution tradeoff for a scenario with two closely located RFI's. It can be seen that eight bits are indeed adequate for this moderately difficult scenario. With two 30 dB RFI's, the degradation is on the order of only 0.2 dB. Round off to six bits causes a 6 dB degradation for the same scenario. The static environment simulation indicates that 8 bit resolution is adequate.

Computer simulations were also conducted under dynamic environment to evaluate the choice of 8 bit resolution, using the same 3 RFI signal environment (Figure 4.3-3) used previously. The results with 8 bit and 12 bit resolution are shown in Figure 4.3-6, and confirms that 8 bit resolution is adequate for the dynamic environment. Thus, 8 bit resolution is chosen.

TABLE 4.3-1. PERFORMANCE VS WEIGHTING NETWORK RESOLUTION FOR THE STATIC ENVIRONMENT

Element Spacing = 2.39λ

<u>Signal</u>	<u>Ele. Ang. (α°)</u>	<u>Rot. Ang. (θ°)</u>
Desired	0	0
RFI	6	180
RFI	2	0



Input S/N-dB*	Input RFI/N-dB*	S/(I+N) - dB			
		16 Bits	8 Bits	6 Bits	4 Bits
0	0	12.19	12.19	12.19	12.17
0	10	12.08	12.07	11.94	11.19
0	20	12.07	12.06	10.84	6.36
0	30	12.07	11.89	5.71	---
0	40	12.07	10.05	---	---

* Input signal and RFI power levels relative to noise into each array element

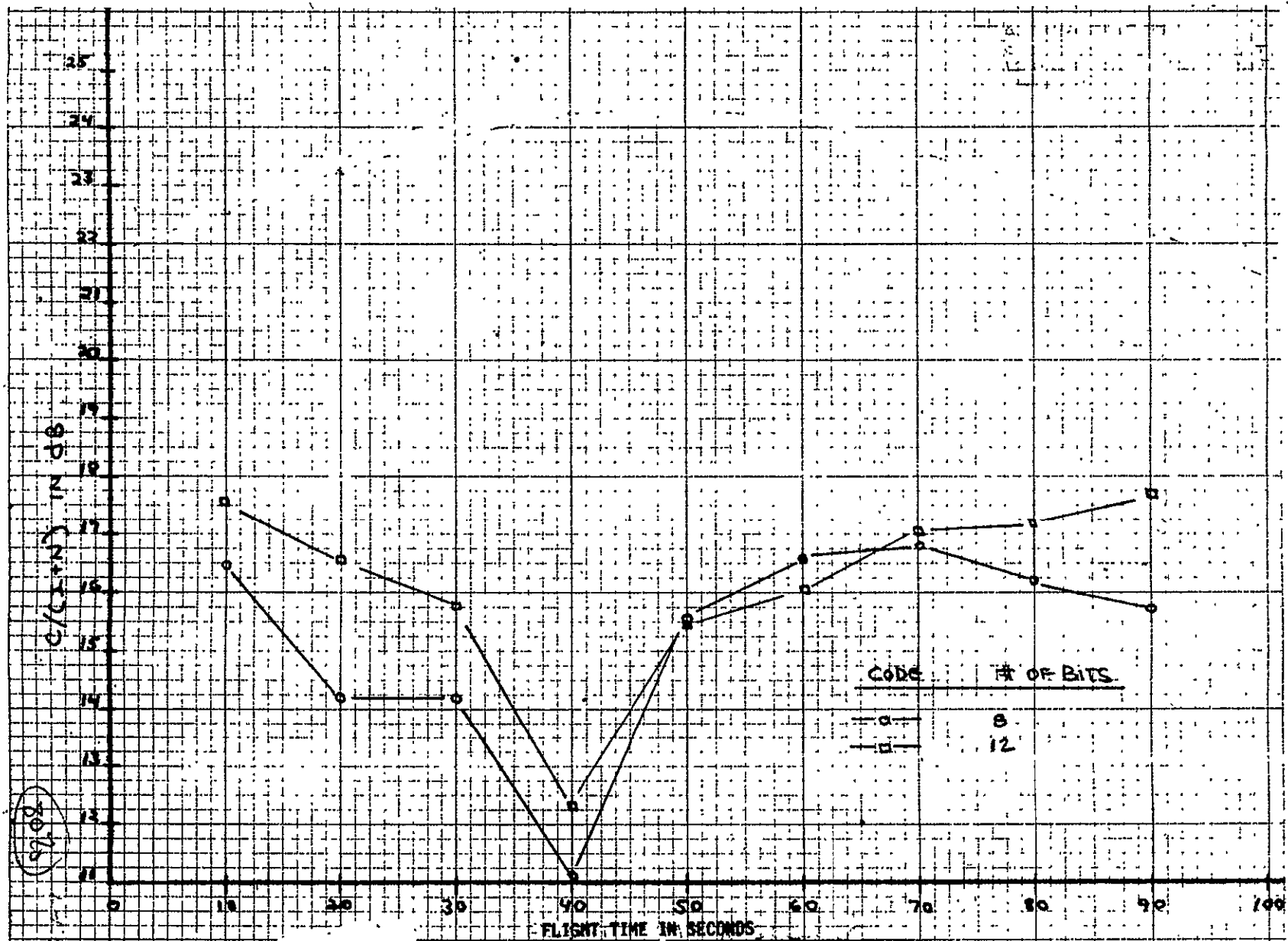


FIGURE 4-3-5. ADAPTIVE PERFORMANCE VS. NUMBER OF BITS WITH THREE RFIS FOR THE DYNAMIC ENVIRONMENT

4.3.1.3 Design of the Beam Forming Network Subassembly

The Beam Forming Network includes 32 weighting networks. The function of the weighting network is to provide the proper phase and amplitude weighting of the element signals, prior to summing. Complex weighting is employed by splitting the signal into in-phase (0°) and quadrature (90°) components. Two biphase variable attenuators controlled by the computer via digital to analog converters (DACs) give a 0° to 360° phase shift capability and a 20 dB attenuation range. From computer simulations, it has been determined that an 8 bit DAC has sufficient resolution for the system to adequately null maximum power interferers (RFIs). Two weighting networks are packaged in a dual unit (Figure 4.3-7).

Component characteristics for the biphase variable attenuators are given in Table 4.3-2. The important parameters are attenuation linearity and constant phase shift. This is the only non-standard part in the weighting network. In an in-house R&D program, biphase variable attenuators using quadrature hybrids have been developed which meet the listed electrical specifications. Since identical biphase variable attenuators are used in two receive and two transmit beam forming networks for a total of 128 units these units will be printed as a hybrid unit in order to minimize its size and weight.

4.3.1.4 Design of the Channel Downconverter Subassemblies and the Sampling Switch

Sampled Channel Downconverter and Sum Channel Downconverter subassemblies are used, both identical except for their output format. Both subassemblies operate on a 70 MHz input signal, downconvert the signal to 20 MHz and separate the desired and interference signals with a bandpass and bandreject filters. The narrow bandpass filter passes only the unique CW tone associated with the desired signal; and the band reject filter simply rejects the same CW tone from the interference signal channel. In both subassemblies, the local oscillator reference is a doppler corrected signal from the Doppler Processor Subassembly.

TABLE 4.3-2. CHARACTERISTICS FOR BI-PHASE ATTENUATOR
FOR WEIGHTING NETWORKS

CENTER FREQUENCY	:	70 MHz
BANDWIDTH	:	2.5 MHz
ATTENUATION RANGE	:	20 DB (MINIMUM)
ATTENUATION LINEARITY	:	+4% OVER ATTENUATION RANGE AND BANDWIDTH
BI-PHASE	:	0°, 180° POSITIVE, NEGATIVE
MAXIMUM POWER	:	-10 DBM INTO DEVICE
IMPEDANCE	:	50 OHMS (INPUT AND OUTPUT)
DC POWER CONSUMPTION	:	20 MW (MAXIMUM)
PHASE LINEARITY	:	+4° OVER SPECIFIED ATTENUATION AND BANDWIDTH

The Sampled Channel Downconverter sequentially samples the inputs from all 32 channels by way of the SP16T channel sampling switch and the SP2T switch in the dual weighting network module. Both switches are pin diode devices.

The performance characteristics of the bandpass and bandreject filters and the sampling switch are shown in Tables 4.3-3 and 4.3-4.

4.3.1.5 Design of the Correlator Processor Subassembly

The Correlator Processor Subassembly includes a signal and interference correlator that correlates the sampled channel signal or interference with the sum channel signal or interference. The 20 MHz inputs to the Correlator Processor come from the Sampled Channel and Sum Channel Downconverter sub-assemblies, as shown in Figure 4.3-8.

The correlators are analog phase detectors. The in-phase and quadrature (x, y) outputs are a measure of the correlation of the sample and summed signal. These phase detectors must be able to work over a 35 dB input power range. The RF power detector input to the digital processor can be used to vary the correlator integration time. For small amplitude signals (with a low S/N) the integration time should be longer than for large amplitude signals (with a higher S/N). The correlators are sampled and then dumped to zero. The sample inputs are switched to the next set of channels until all channels have been read.

Component characteristics for the correlator are shown in Table 4.3-5.

TABLE 4.3-3 CHARACTERISTICS FOR BANDPASS AND BANDREJECT FILTERS

1. FILTER, BANDPASS

Center Frequency	20.035 MHz \pm 500 Hz
3 d B Bandwidth	7.5 \pm 2 kHz
Source Impedance	50 ohms
Load Impedance	50 ohms
Ultimate Rejection	40 dB minimum
Spurious Rejection	30 dB minimum
Shape Factor 6:1	40/3
Insertion Loss	4 dB Maximum
Phase Tracking	Constant to within $\pm 5^\circ$ maximum over 3 dB bandwidths
VSWR	1.5:1 maximum input and output

2. FILTER, BANDREJECT

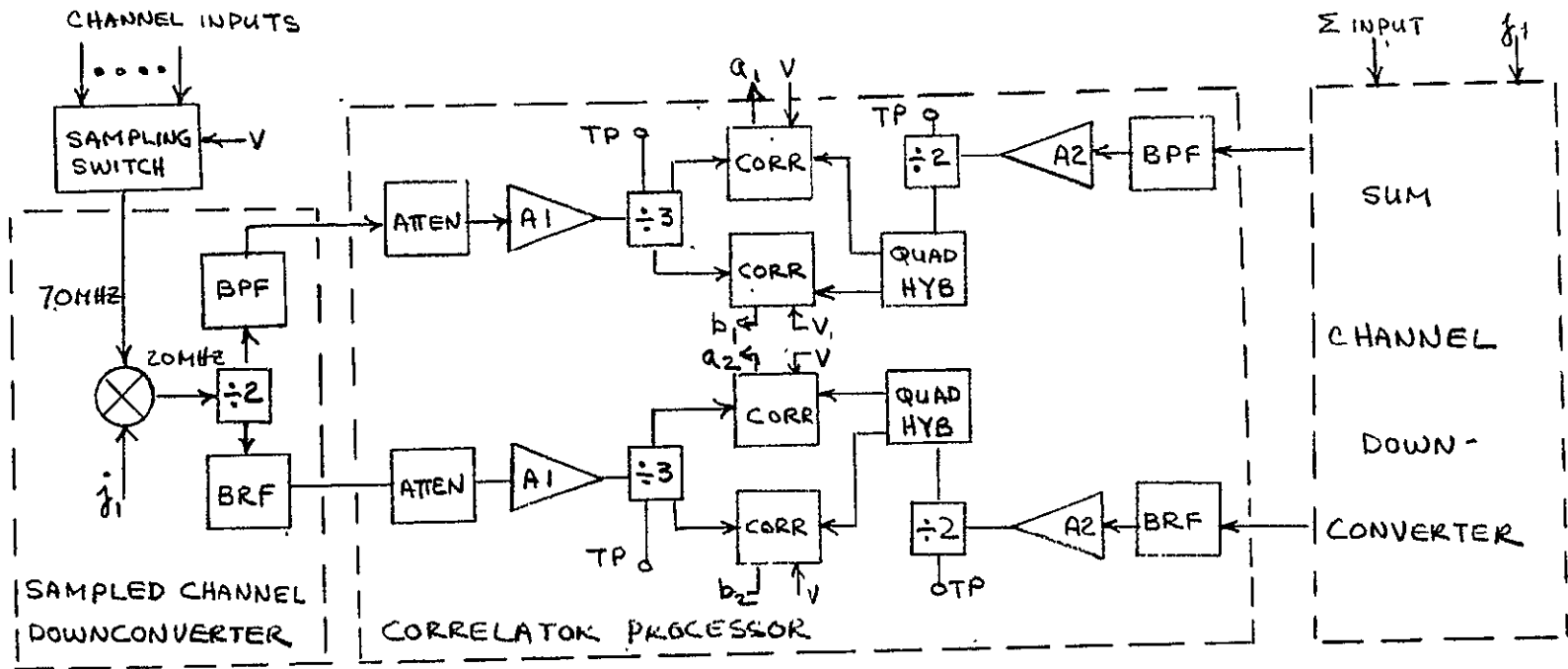
Center Frequency	20.023 MHz \pm 500 Hz
3 dB Bandwidth	7.5 \pm 2 kHz
Source Impedance	50 ohms
Load Impedance	50 ohms
Ultimate Rejection	40 dB Minimum
Spurious Rejection	4 dB Minimum (in passband)
Shape Factor 6:1	40/3
Insertion Loss	4 dB Maximum
Phase Tracking	Constant to within $\pm 5^\circ$ maximum over 3 dB passband widths
Passband Width	± 2 MHz at 3 dB maximum attenuation
VSWR	1.5:1 maximum input and output

TABLE 4.3-4. CHARACTERISTICS FOR THE
CHANNEL SAMPLING SWITCH

1. RF TYPE SAMPLING SWITCH

FREQUENCY RANGE	:	18 MHZ TO 22 MHZ
INSERTION LOSS (MAX)	:	2 DB
SIGNAL ISOLATION (MIN)	:	50 DB
VSWR (MAX)	:	1.3:1
SWITCHING TIME (MAX)	:	5 NS
INTERMODULATION DISTORTION (MIN)	:	2ND ORDER -50 DB (2 TONES TO +10 DBM, 19 MHZ & 21 MHZ) 3RD ORDER -40 DB
DRIVE VOLTAGE LEVEL	:	TTL COMPATIBLE
POWER DISSIPATION (MAX)	:	50 MW
WEIGHT (MAX)	:	0.25 OZ
CONNECTORS	:	PC MOUNTING

4-111



$f_1 = \text{DOPPLER CORRECTED LO}$

$a_n = \left. \begin{array}{l} \\ \end{array} \right\} \text{CORRELATOR OUTPUT TO DIGITAL PROCESSOR}$
 $b_n = \left. \begin{array}{l} \\ \end{array} \right\}$
 $V = \text{CONTROL}$

FIGURE 4.3-8 CORRELATOR PROCESSOR & DOWNCONVERTER SUBASSEMBLIES

TABLE 4.3-5. CHARACTERISTICS OF CORRELATOR

Frequency Range	: 18 MHz to 22 MHz
Input Impedance	: 50 ohms
VSWR (Max.)	: 1.5:1
Phase Linearity	: Less than $\pm 6^\circ$ over frequency range
Amplitude Flatness	: Less than ± 1 dB to maintain a fixed video output voltage across the frequency band
Tangential Sensitivity (Min.)	: -43 dBm in 1 MHz video bandwidth resulting in a signal-to-noise ratio of 6 dB minimum
Dynamic Range	: Minimum of 40 dB as measured between the lower limit defined by the tangential sensitivity and the upper limit defined by the transition between square law and linear detection
Voltage/Power Sensitivity (Min.)	: 100 MV/MW into 1000 ohms for RF power levels of 0 dBm at each input port and with the phase difference between the inputs adjusted to maximize the output
Connectors	: Input SMA; Output solder lugs

4.3.1.6 Design of the Array Divider and Array Summer Matrices

The Array Divider Matrix inputs the signal from the 32 Receiver Modules and divides their signal into the two Adaptive Processors.

The Array Summer Matrix receives its 32 input signals from the weighting network and combines or sums their signal.

Both matrices are assemblies of two-way power dividers having the following characteristics:

• Frequency Range	68 MHz to 72 MHz
• Insertion Loss above 3 dB Split (Max)	0.5 dB
• Signal Isolation (Min)	40 dB
• VSWR (Max)	1.3:1 All ports
• Impedance, All ports	50 ohms
• Amplitude unbalance (Max)	1 dB
• Phase Unbalance	1 degree
• Weight (Max)	0.5 az.
• Connectors	PC mounting

4.3.1.7 Design of the Doppler Processor Subassembly

The motion of a receiver with respect to a transmitter causes a frequency shift of the received signal known as the doppler shift. This phenomenon is useful for some applications, for example, tracking radars where the source's velocity component normal to the receiver can be calculated from the doppler frequency. For communications systems, however, the doppler frequency shift creates a problem since the received signal will be at a constantly changing frequency. This is especially important in narrowband systems where the doppler shift causes signal spillover into adjacent channels. In the AMPA receiver processor, a doppler tracking loop is used to provide the necessary frequency correction.

Since a positive signal-to-noise ratio (SNR) is required for acquisition, the doppler loop must be placed after the array summer, if no processing gain is available for the desired signal. Acquisition will depend on the ability of the spatial filter to enhance the input SNR into the loop. An open loop spatial search must be performed by the receiver processor to bring the SNR above the loop's capture range. Once a stable lock has been achieved, the receiver processor will be operated closed loop, fully adaptive. The LO's for the sum and sample channel downconverters, which are derived from the doppler loop output, provide the required doppler correction at a 20 MHz IF.

The design of the doppler tracking loop differs for the BPSK digital data and for NBFM voice. A ground command selects the desired tracking loop as shown in Figure 4.3-9, depending upon the type of signal that is being received. For digital data, the doppler tracking loop is a simple squaring loop. The input is assumed to be a modulated binary phase-shift keyed signal (BPSK) at 4800 bps, with a nominal 70 MHz center frequency. The center frequency can vary +38 kHz depending on the amount of uncorrected doppler.

The tracking loop for the BPSK data, as shown in Figure 4.3-10, works as follows: the modulated BPSK signal is bandpassed filtered and then passes through a frequency doubler (a square-law device) to eliminate the phase reversals due to the data transitions. If the input signal to the square-law device (disregarding noise) is written as:

$$V(t) = \pm A \sin (\omega_0 t)$$

4-115

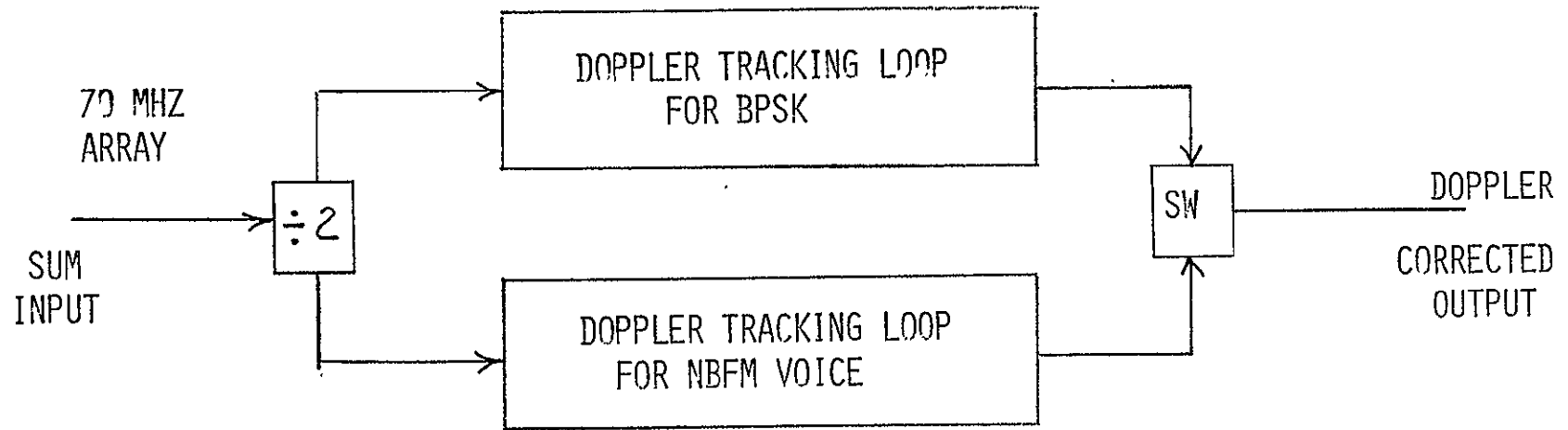


FIGURE 4.3-9 DOPPLER PROCESSOR SUBASSEMBLY

the output becomes:

$$V^2(t) = A^2 \sin^2 (\omega_0 t) = \frac{A^2}{2} [1 - \cos (2\omega_0 t)]$$

The DC component is eliminated by a bandpass filter centered at $2\omega_0$. This is followed by a conventional phase-locked loop (PLL) to track the reinserted carrier term. The signal level into the loop is held constant (within 1 dB) by an AGC amplifier. The PLL output is frequency divided by two providing the coherent reference signal necessary for the doppler correction downconverters and data demodulation.

Figure 4.3-10 also shows the data demodulator which consists of a balanced mixer, an integrate, sample, and dump (ISD) matched filter, a threshold device and a differential decoder. The timing extractor loop is a phase-locked loop which derives the received clock from the data transitions and provides the delayed dump pulse to the ISD. The ISD output is compared to a zero-volt reference to determine if a logic ONE or ZERO was received. The received bit and the most recent bit are modulo-2 added in the differential decoder. Finally, the decoded data stream is sent to the Modem subassembly for processing.

A block diagram of the doppler tracking loop for NBFM operation is illustrated in Figure 4.3-11. The input 70 MHz signal with the maximum doppler shift of ± 38 kHz is downconverted with a nominal 50 MHz voltage controlled oscillator (VCO) to result in 20 MHz. This 20 MHz signal is fed to a limiter to remove amplitude variations. The limiter output interfaces with a discriminator whose output DC voltage characteristic is linearly related to the ± 38 kHz input frequency variation from the 20 MHz center frequency. The discriminator output voltage after filtering and amplification is fed to the tuning port of the VCO. This DC voltage effectively acts as a frequency control for the loop by adjusting the VCO frequency until it tracks the input doppler shifted signal. Thus, the VCO frequency is continuously tracking any doppler shift present, with the tuning voltage being a measure of the amount of doppler shift.

The tuning voltage is digitized by an A/D converter to provide a doppler word indication.

The VCO output is upconverted with the 20 MHz LO to produce the required 70 MHz signal which interfaces with the downconverters.

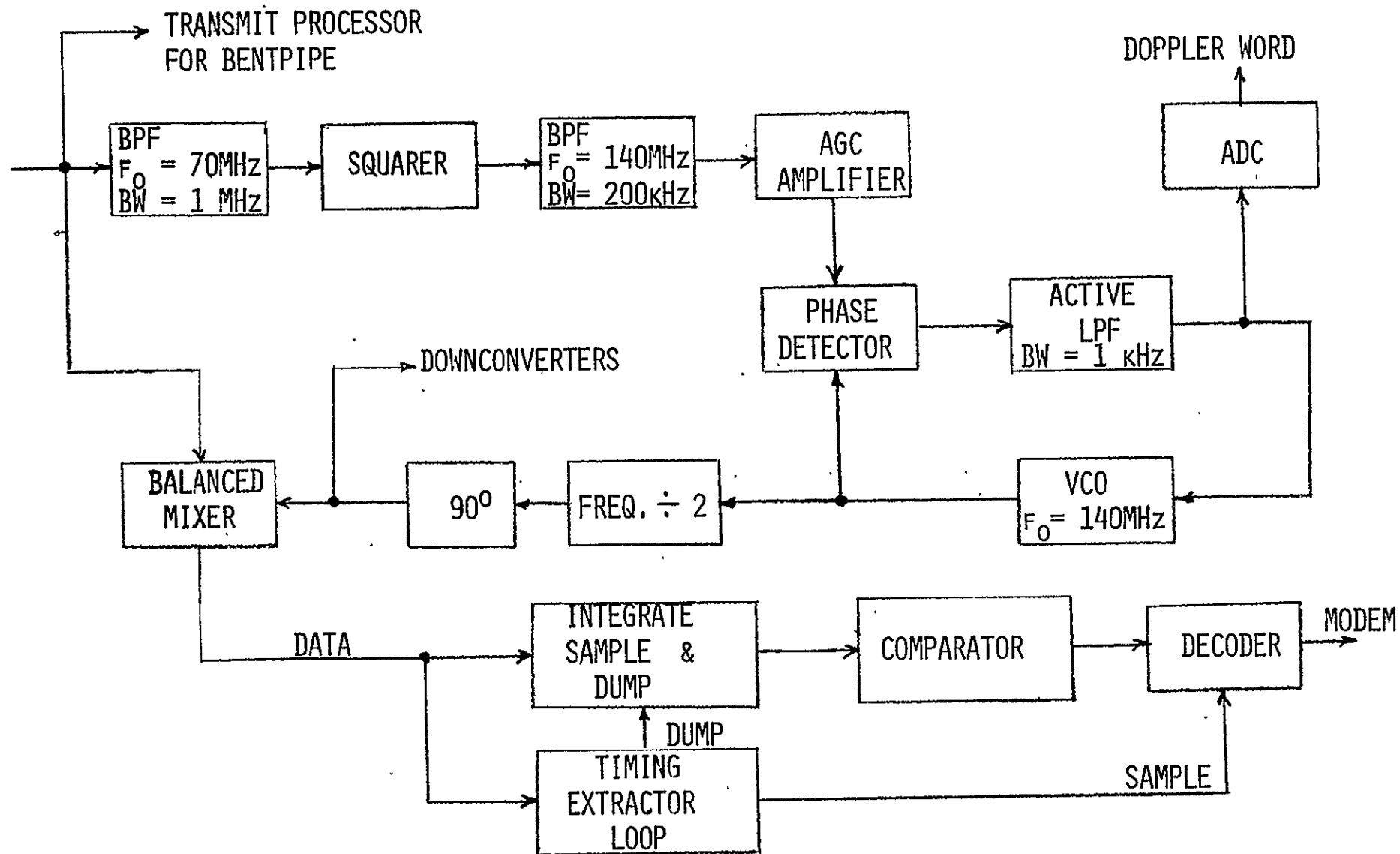


FIGURE 4.3-10 DOPPLER TRACKING LOOP AND DATA DEMODULATOR FOR BPSK

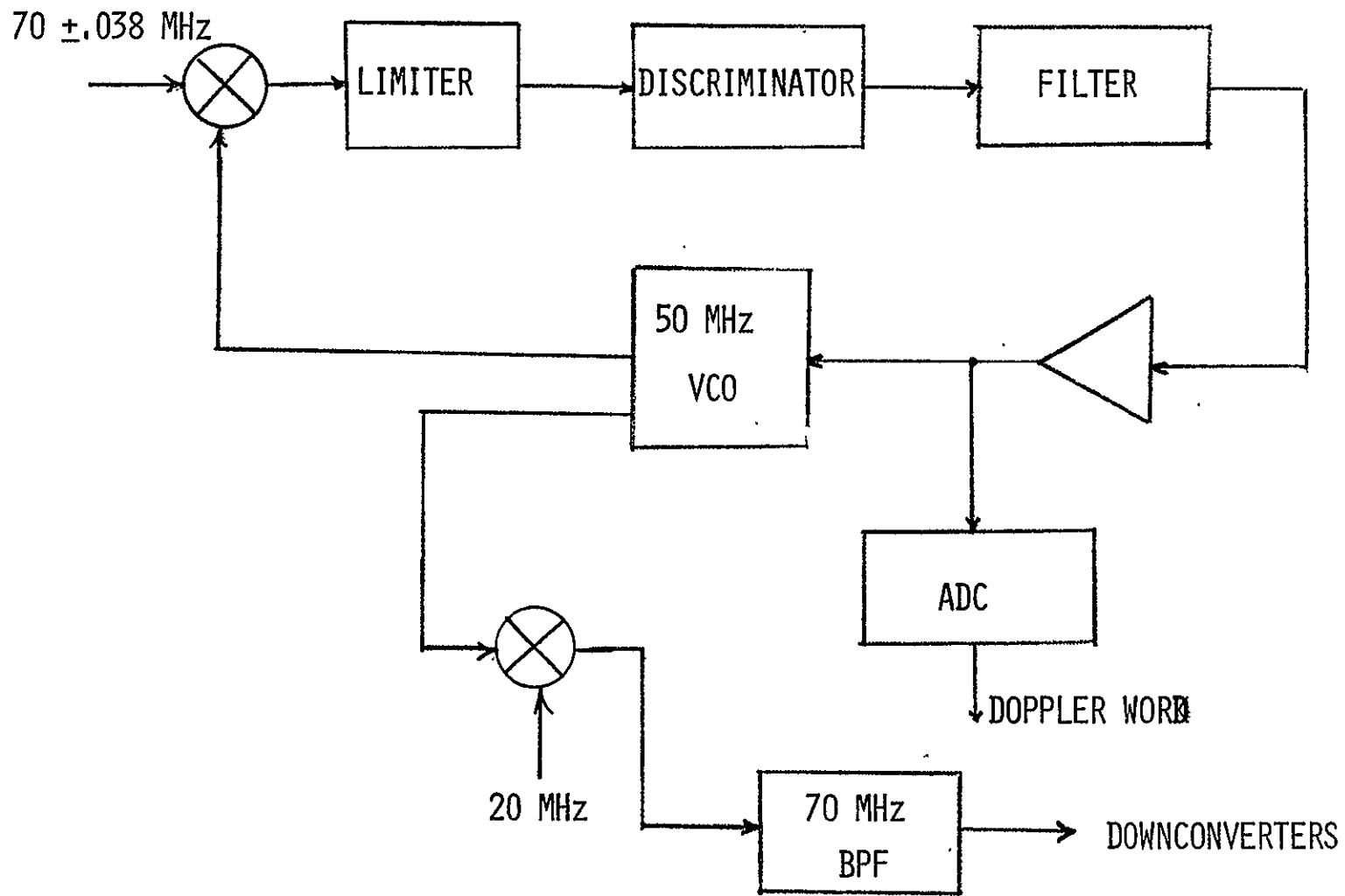


FIGURE 4.3-11 DOPPLER TRACKING LOOP FOR NBFM VOICE

4.3.1.8 Modem Subassembly

The Modem Subassembly handles all information signal processing for both the forward and return links. There are three requirements for the Modem.

These are:

- o Demodulate NBFM or BPSK for:
 - o On-board recording and/or
 - o Relay to ground via TDRSS link
- o Modulate baseband AM voice or PCM data from ground for relay to user
- o Provide IF turnaround for bentpipe mode

Looking at the first requirement, if the information signal is already in digital form (BPSK), the modem unit will simply switch the data detector output from the doppler processor into the HRM. If, however, it is an analog signal (NBFM voice), the analog information signal is first recovered by a balanced discriminator. The recovered signal is then digitized by the forward link data conditioner. Finally, the digitized data (PCM) is sent to the HRM.

To accomplish the second requirement, PCM BPSK data either modulates the carrier directly or the digitized NBFM voice data is converted to analog form via the return link data conditioner. The analog signal then frequency modulates the 70 MHz carrier (TCXO).

For the bentpipe mode, the Modem subassembly simply switches the received 70 MHz array output to the transmitter beam processor for re-transmission to the ultimate user.

Figure 4.3-12 shows the representative block diagram for the Modem Subassembly. The dashed blocks signify units which are not part of the modem assembly but interface with it. The CMOS analog switches are controlled by a multiplexer (not shown) whose outputs will depend on the type of modulation being used and the mode of operation.

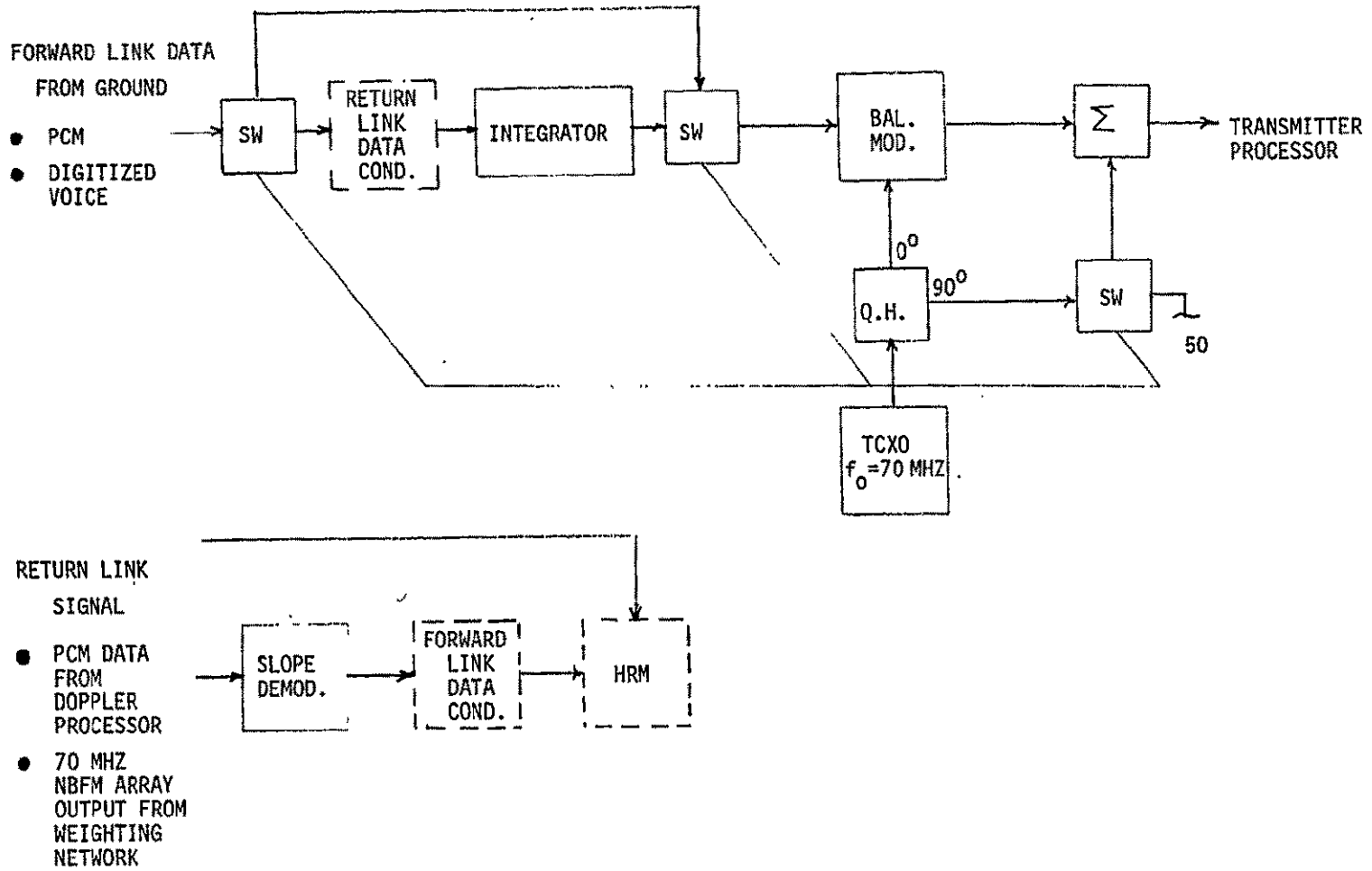


FIGURE 4.3-12 MODEM SUBASSEMBLY

4.3.1.9 Data Conditioner

The Data Conditioner interfaces with the on-board High Rate Multiplexer (HRM) as shown in Figure 4.3-13 to convert analog signal to digital format or vice versa. For incoming digital data, the Data Conditioner provides switching and multiplexing/demultiplexing functions also.

On the AMPA Experiment System, the analog signals to be digitized include the baseband analog voice signals from the Modem subassembly, analog monitor signal from the test points, and a clock reference that provides a time reference to calibrate AMPA experiment event times, such as acquisition and lock-on times. If a time reference is already available from the Spacelab for other experiments, this reference will not be needed. The digitized signals will then be multiplexed in the HRM with other Spacelab or experiment data for subsequent recording on the Payload Recorder, or for retransmission to the ground by way of the Orbiter's TDRS multiple access transceivers.

For digitized voice signals that are received from the ground station, the Data Conditioner converts the digital signal to analog for retransmission to the user by way of the appropriate Modem subassembly. Digital data from the ground that is to be sent to a user will be directly switched by the appropriate Modem subassembly. Command data from the ground to change the modes of operation or monitor test functions will be demultiplexed in the Data Conditioner for subsequent routing to the appropriate units.

The key tradeoff in the Data Conditioner is to provide a means to quantitatively measure the performance of the receiver adaptive processor. Since one of the objectives of the experiment is to demonstrate the signal quality (i.e., intelligibility for NBFM voice or bit error rate for BPSK), it is important that the received signal be converted as faithfully as possible. The Data Conditioner, therefore, must not be allowed to introduce excessive amounts of noise or to distort the voice signal.

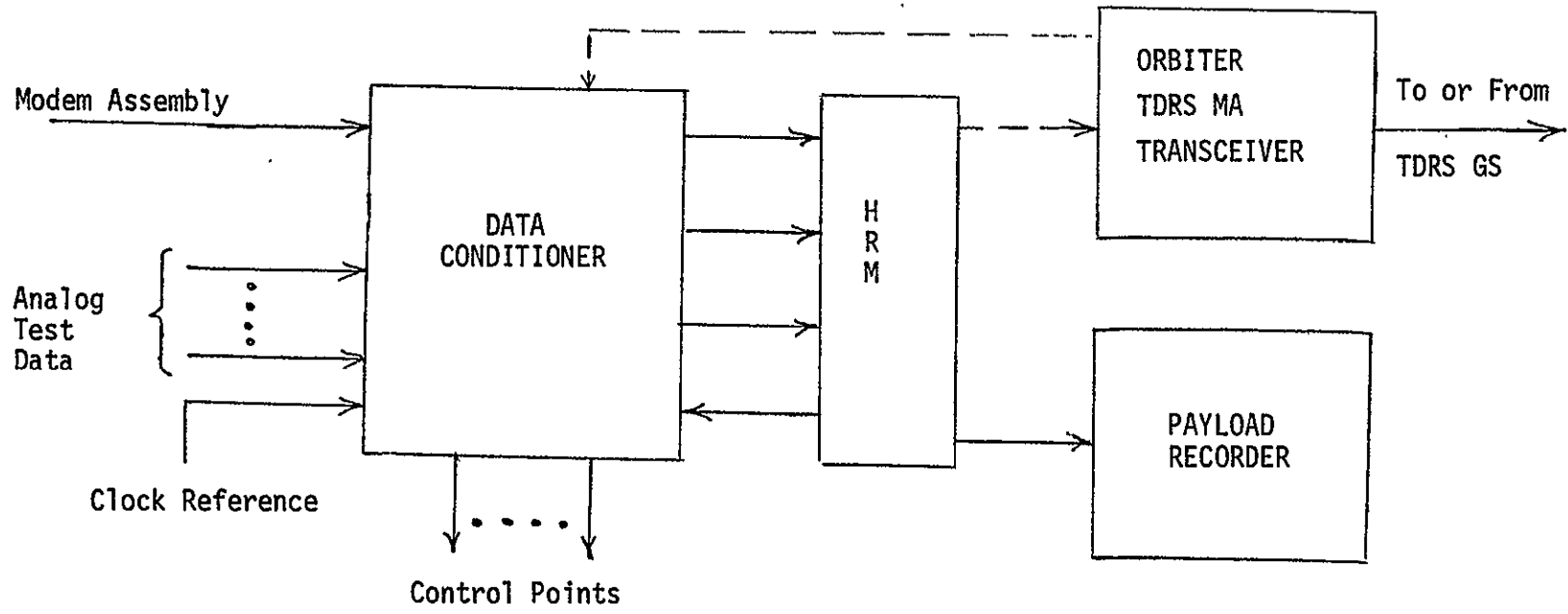


FIGURE 4.3-13 DATA CONDITIONER INTERFACES

It would be desirable, therefore, to employ strictly linear sampling of the analog signal. However, the transmission rate must be less than 50 kbps in order to relay the data to ground by way of the Orbiter's TDRS MA transceiver.

An analysis was conducted to determine the minimum number of quantum levels needed for acceptable signal reconstruction. An analytical expression was derived for determining the signal to quantization noise (S/N_q) as a function of the number of binary bits, assuming ideal sampling, as shown below.

$$S/N_q = 10 \log (1.5 * 2^{2N}) \text{ dB}$$

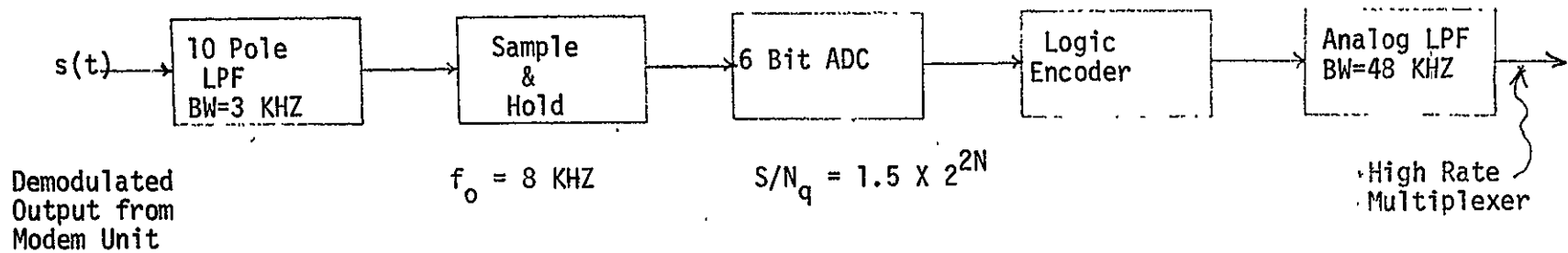
where N is the number of bits

This analysis shows that a 6 bit analog-to-digital converter (ADC) will theoretically result in a S/N_q of 37 dB. By narrowband filtering to the message bandwidth (37 kHz) and using an 8 kHz sampling rate, the effective S/N_q is approximately 44 dB. The aperture uncertainty of the Sample and Hold must be less than 1 us to prevent signal distortion. This is well within the capability of almost any Sample and Hold.

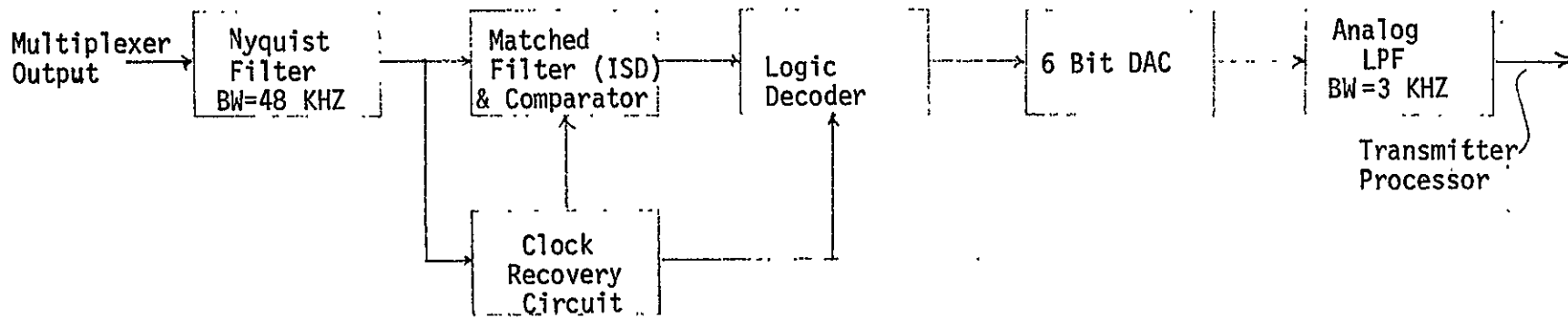
Figure 4.3-14 shows the forward link (AMPA-to-ground) and return link (ground-to-AMPA) sections of the data conditioner assembly. The forward section accepts as input the analog output from the FM demodulator located in the modem assembly. This is filtered by a 10 pole lowpass filter with 3 kHz cut-off frequency and is sampled at 8 kHz. This causes the aliasing error to be approximately -40 dB. The sampled analog voltages are then digitized, encoded, and passed through an LPF designed to minimize intersymbol interference. The return section consists of a Nyquist filter, and integrate sample and dump matched filter, a comparator, and logic decoder. A synchronization word added at the forward sections logic encoder is used to periodically realign the data frames should sync loss occur. This is followed by the DAC and the reconstruction low pass filter.

The data conditioner is also responsible for monitoring all system test points. This requires an 8 channel analog multiplexer, a sample and hold and an 8 bit ADC.

The Spacelab portion of the Data Conditioner is packaged in the Transmitter Processor/IM Simulator drawer.



FORWARD LINK DATA CONDITIONER



RETURN LINK DATA CONDITIONER

FIGURE 4.3-14 AMPA DATA CONDITIONER

4.3.1.10 Adaptive Processor Layout

Both adaptive processors have been laid out to fit into standard rack drawers for mounting within the available Spacelab racks. All of the components of the adaptive processors have been laid out in modules or subassemblies which can be conveniently laid out in the rack drawers as illustrated in Figure 4.3-15 for ease in assembly, maintenance and testing during development as well as during the integration phases.

The total adaptive processor weight and prime power requirements are 21.1 kg and 33 watts, respectively.

SIZE: 482.6 MM RACK MOUNTABLE X 304.8 MM HI X 609.6 DP
 (19 IN) (12 IN) (24 IN)
 WEIGHT: 22.0 KG
 (48.4 LBS.)
 WATTS: 28 WATTS

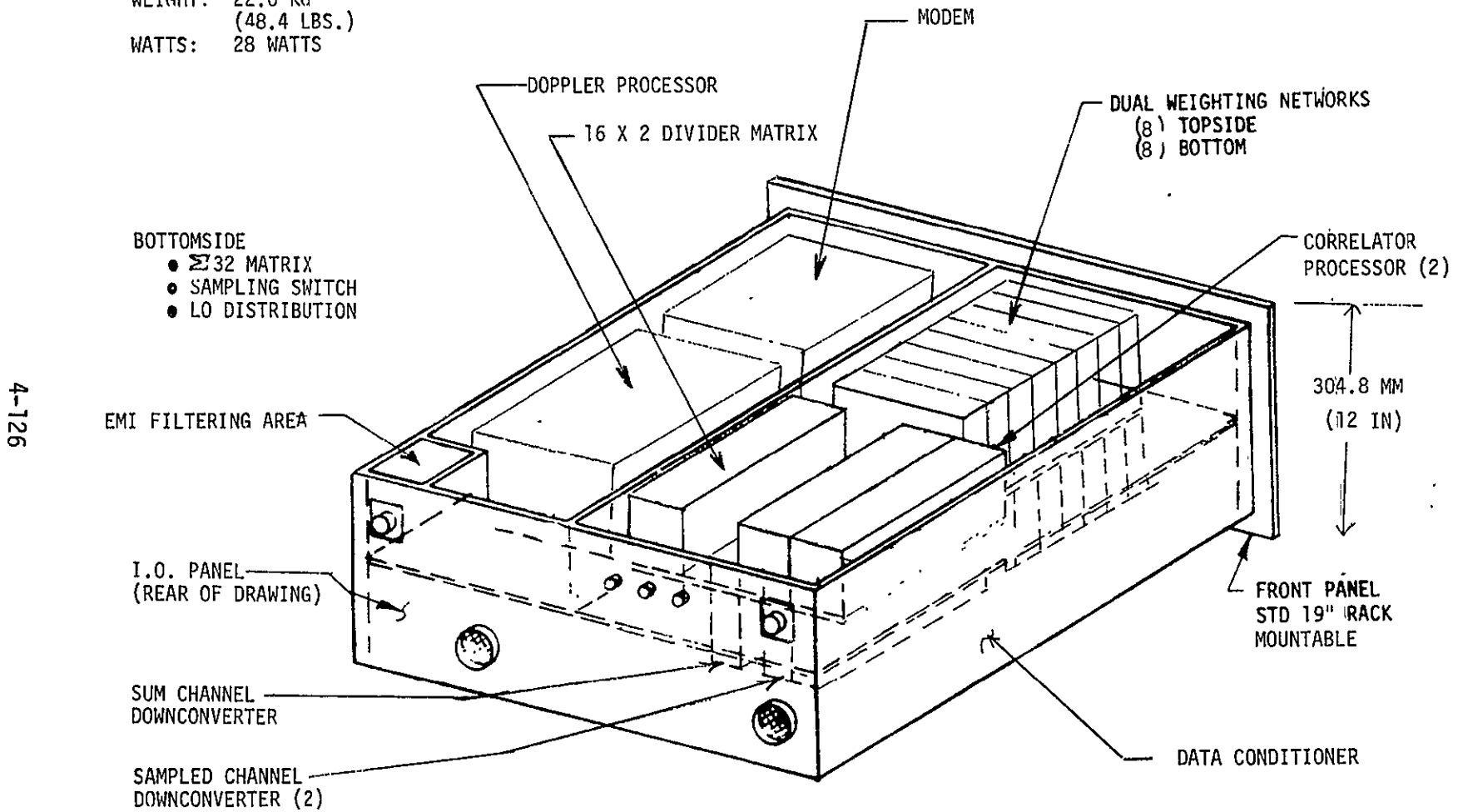


FIGURE 4.3-15. ADAPTIVE PROCESSOR (TWO DRAWERS)

4.3.2 Transmitter Beam Processor Assembly

4.3.2.1 Overall Description

The Transmitter Beam Processor Assembly includes two transmitter beam processors, an IM simulator and a Summer/Amplifier Matrix. Each of the two Transmitter Beam Processors provide an independently steerable transmit beam that are formed at IF frequencies.

4.3.2.2 Transmitter Beam Processor

4.3.2.2.1 General

Each Transmitter Beam Processor receives a signal from a receiver adaptive processor which are each split 32 ways, weighted (amplitude and phase adjusted), combined and fed to the 32 transmitter modules to form two independently steerable transmit beams. The transmit module uses L-band power amplifiers operated in the Class C state with approximately 3 dB backoff to minimize generation of intermodulation (IM) products. In addition, signals from the IM simulator unit are injected and combined to simulate an additional 8 transmit beams. This simulation will be used to evaluate the effectiveness of spatial dispersion of IM products achieved with the use of a phased array.

Particular emphasis was given in the tradeoff consideration for the choice of the type of weighting network to be employed. Since 64 weighting networks are required, the selection of the type of weighting network used is critical in its impact on system weight and power.

A functional block diagram of the transmitter beam processor is shown in Figure 4.3-16 along with associated power levels. Table 4.3-6 summarized the performance characteristics for the transmitter beam processor. The input signal from the receiver adaptive processor is fed to a voltage controlled attenuator that allows the L-band power amplifier to be operated at saturation or with backoff. For normal operation with two beams, this attenuator will be set to provide approximately 3 dB backoff in order to minimize generation of IM in the power amplifier. However, when the 8 additional signals are injected from the IM simulator to simulate an operational system with many beams, the

4-128

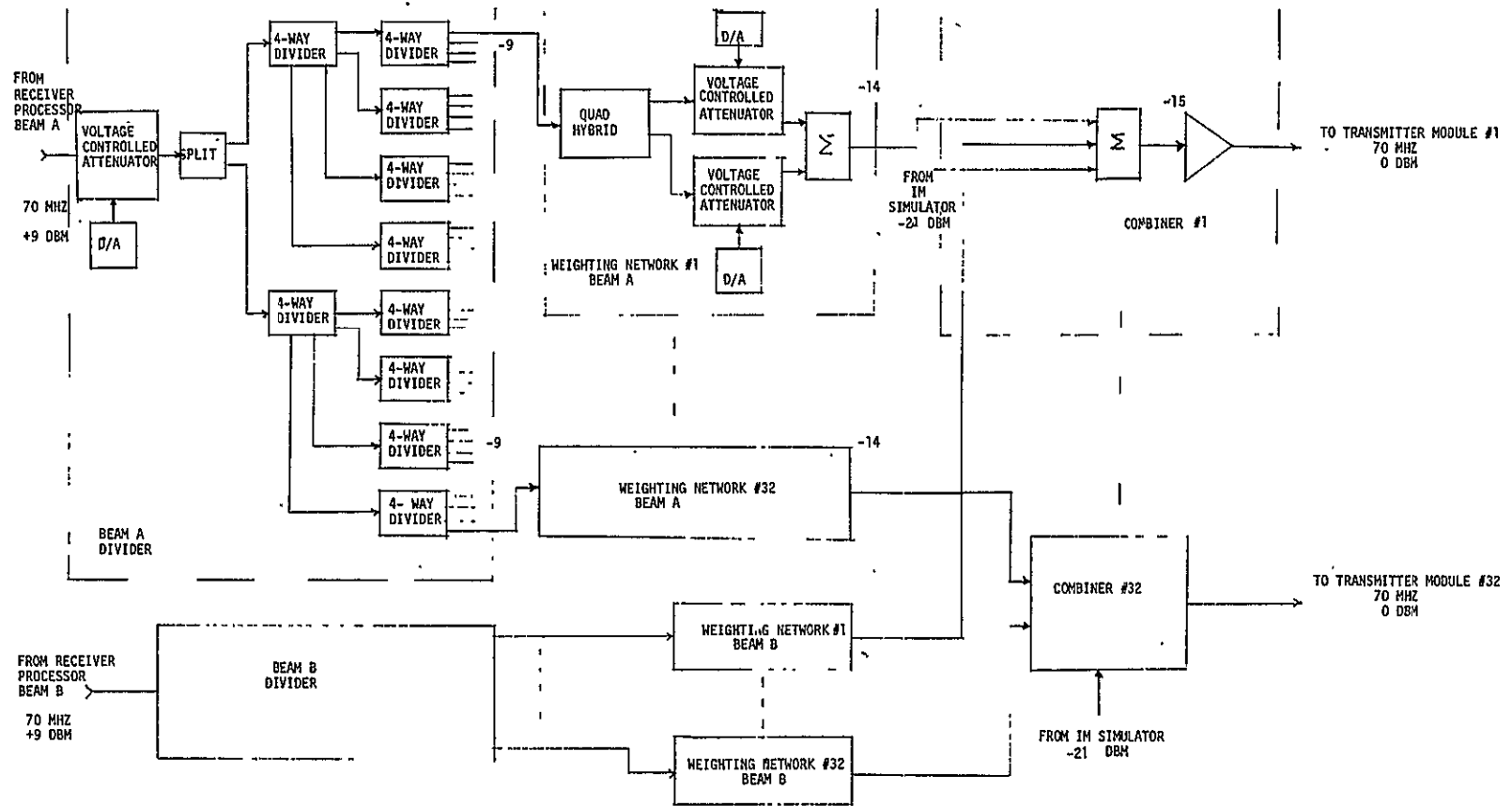


FIGURE 4.3-16. TRANSMITTER BEAM PROCESSOR

TABLE 4.3-6. TRANSMITTER BEAM PROCESSOR
PERFORMANCE CHARACTERISTICS

Frequency	70 MHz
Bandwidth	2.5 MHz
Receiver Processor Input Power (2 lines)	+9 dBm
IM Simulator Input Power	-21 dBm
Output Power (32 lines)	0 dBm
Third Order Rejection	35 dB
VSWR	1.5
Nominal Impedance	50 ohms
Phase Shift Range	360 ^o
Phase Error	4 ^o RMS
Amplitude Range	20 dB
Amplitude Error	±0.5 dB
Processing Time	25 usec
DC Power Requirements	
+15V @ 1000 ma	
-15V @ 200 ma	

variable attenuator is increased an additional 7 dB. This reduces the input signals from the receiver adaptive processor so that the power amplifier will operate with the same backoff as for the case with only two beams. The variable attenuator can be operated with less than 3 dB backoff up to full saturation, for experimental evaluation purposes. This will allow better assessment of the spatial dispersion of the IM products in a phased array; and more significantly, determine if adequate IM suppression can be obtained with the phased array alone and permit operation of the power amplifier at full saturation for better amplifier efficiency.

Both of the input signals from the receiver processor are split 32 ways with each output leg fed to a weighting network. The amplitude and phase adjustments weighting networks are each set by a 8 bit word* from the computer interface unit. All adjustments are done simultaneously with a maximum setting time 25 usec.

Each of the 32 combiners sum two weighting network outputs for the two steerable beams along with 8 simulated beams from the IM simulator. The resulting output lines containing amplitude and phase information for 10 signals is amplified and fed to the transmitter module where it is upconverted and power amplified for transmission to the user.

4.3.2.2.2 Tradeoff Analysis

Type of Weighting Network

The weighting network function has been chosen to be performed at IF rather than at L-band. Weighting networks have higher insertion loss at L-band as compared to those operating at IF. This would be particularly true for L-band switch losses which would be used in a weighting network designed for switching in different line lengths. With the phase function at L-band the insertion loss would have to be made up by less efficient L-band amplification as compared to IF amplification. The weighting network function at IF has the further advantage of removing hardware and control lines from the array thus simplifying array/Spacelab interface connections.

* Simulation results described in Section 4.3.1 has shown that 8 bit level is required.

A common type of phase shifter consists of precisely dimensioned segments of transmission line which correspond to the required phase shift. These line segments are open or shorted by a pin diode switch; thereby inserting each time a different phase shift. At L-band, this type of phase shifter would be utilized; however, at IF it is not practical due to the size of the line segments required.

Methods for obtaining phase shift at IF consist of changing the reactance of a diode through the application of a varying DC bias voltage or changing the impedance match at the isolated port of a hybrid. For these methods, many sections of phase shift would be required to provide the capability for varying the phase of the signals fed to the array over a 360 degree range. In addition, if amplitude control requirements are included, these units would not be small.

The smallest and lightest type of device to provide the required range of phase shift and amplitude variation is a vector generator similar to that used for the weighting networks in the receiver adaptive processor unit. This device consists of a quadrature hybrid, two voltage controlled attenuators and a summer which are all of a flatpack configuration and mounted on a printed circuit board providing a small and lightweight package.

The phase and amplitude variation is obtained by splitting the 70 MHz input in quadrature, with each output being independently attenuated. By controlling both attenuator voltages any phase from 0-90° along with an amplitude variation can be obtained after summing both signals. Furthermore, if each attenuator is capable of reversing phase by 180° then a phase in any quadrant is achievable. Thus, this technique is used to provide 360° phase shift range and 20 dB amplitude variation required for forming the antenna pattern for the array on transmission.

4.3.2.2.3 Detailed Design

Divider Matrix

The divider accepts the input from the receiver adaptive processor and distributes it to 32 weighting networks. A voltage controlled attenuator

is added prior to the divider to provide a power level variation of 9 dB. A D/A converter controls the variable attenuator which utilizes a pin diode to provide the required attenuation. The 32-way split is obtained by an initial two-way split with each output fed to a 4-way divider resulting in eight outputs. Each of the eight outputs are then fed to 4-way dividers to produce the required 32 outputs. The division is done in this manner to take advantage of the use of flatpack parts which are mounted on a single PC board to provide a small non-connectorized 32-way divider.

The divider has an output amplitude balance of ± 0.2 dB and a phase balance of $\pm 2^\circ$ with an insertion loss of 18 dB and the isolation between any two outputs is a minimum of 20 dB.

Weighting Network

The phase shift and amplitude variation is obtained by utilizing a vector generator type design as described in the tradeoff analysis section. There are a total of 64 vector generators required to provide the two independently steerable transmit beams.

The quadrature hybrid is Anzac model JH115 and the summer is Anzac model DS109, both of flatpack construction. Variable attenuation is achieved by controlling the current flowing through the IF port of a balanced mixer.

The D/A converter employed is Datel model DAC-CM8B which provides a bipolar output voltage. This unit has a maximum output setting time of 25 usec and supplies 2 ma of current at an extremely low total power consumption of only 40 milliwatts.

Each of the 64 weighting networks required employ two voltage controlled attenuators and two D/A converters. Thus, each network has a power consumption of 80 milliwatts. An 8-bit data word provides phase settings over a 360° range and amplitude variation over a 20 dB range. The phase shifter insertion loss is 5 dB.

4.3.2.3 IM Simulator

4.3.2.3.1 General

When two or more frequencies are combined in a non-linear device such as the transmitter amplifier output stage, products at other than the original frequencies are generated. These are called intermodulation (IM) products and they cause interference within other assigned channels and thus degrade channel performance capability. The power of the generated signal is a function of the product order number and the characteristics of the amplifier. In order to limit the power level of the intermodulation product the input signals to the amplifier are usually "backed off" to a level below that which would produce saturated output. This has the undesirable consequence of reducing output power and amplifier efficiency. However, with the use of a phased array, the intermodulation products are spatially dispersed and the IM power as received by a user is reduced from that which is generated at the transmitting amplifiers. The IM level reduction is due to the different phases between the desired signal and the IM product at the array which causes the IM product to be dispersed in a different direction from where the beam is pointed.

Interference is not experienced from even order products due to the large frequency separation from the desired signal where it can be easily filtered out. Odd order products have sum difference products formed which are close to those frequencies which generated them. The most general form of third order interference occurs when three frequencies A, B and C intermodulate to product interference on a channel at frequency D; such that $A+B=C+D$. Another form of third order interference occurs when the second harmonic of A intermodulates with B to produce interference on a channel at frequency C; such that $2A-B=C$. The phase shift imparted to the product at frequency C for the above case is two times the channel A phase shift minus the channel B phase shift, that is $\phi_C = 2\phi_A - \phi_B$.

Since θ_A and θ_B are different for each element of the array when the contributions of each element of the array are summed, the intermodulation product at C cannot be pointed in the same direction as beam A or beam B. Therefore, the power received at the user corresponding to frequency C which is due to the 2A-B IM product is reduced by the array factor.

As part of the AMPA experiment, the reduction in intermodulation products due to spatial dispersion will be measured. The IM simulator will inject signals into the transmitter beam processor which will be combined with the two beam formed transmit signals, causing a large spectrum of IM products to be generated. The frequencies and power levels of the IM products generated at the transmitter power amplifiers will be recorded. Since the direction of the beam maximum of each IM product differs from that of the desired transmitted user signal, the received IM power at the user is reduced. The reduced IM power levels are recorded at the user to provide a measure of the enhancement achieved through spatial dispersion.

Factors which affect the reduction in received IM levels are:

- Antenna aperture
- Beamwidth
- User separation
- Channel assignments

A large aperture reduces the beamwidth and provides improved resolution to discriminate users for the fundamental frequencies as well as for the IM products, resulting in better spatial dispersion and reduced probability of the IM products falling on existing user. Channel assignments also affect the received intermodulation power levels. With an orderly, and contiguously spaced (in the space domain) assignment of channel numbers for a given bandwidth, the dispersion of IM products is best at the end channels and much less at the center assigned channels. Random spatial assignment of channels provides greater dispersion of IM products.

It is possible to achieve improved IM performance by assigning channels in the frequency domain for optimum performance. The operating channels can be selected in such a fashion that the IM products all fall on non-operating channels. This is readily accomplished for third order products as shown by Babcock* by selecting operating channels such that the frequency difference between any pair of channels is unlike that between any other pair of channels. To provide 10 channels which avoid third order interference would require an availability of 62 consecutive channels; and to provide 10 channels which avoid both third order and fifth order interference would require 300 consecutive channels. In both cases, the channel utilization is very inefficient.

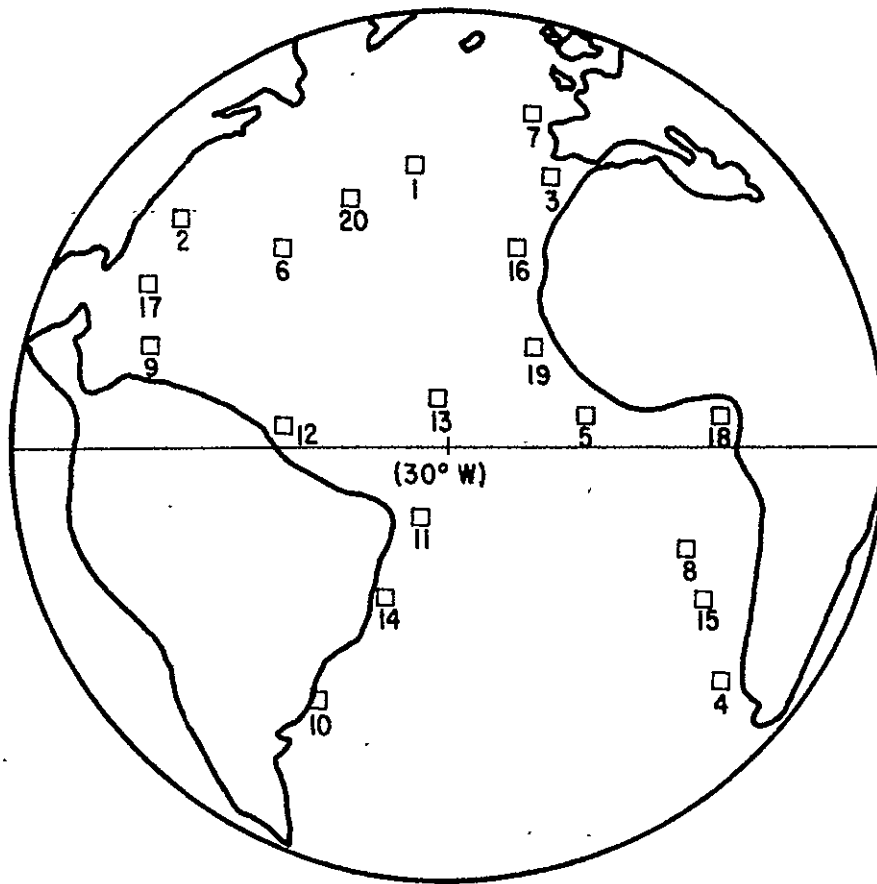
For the AMPA experiment with 2.5 MHz bandwidth there are only 50 consecutive 50 kHz channels. For 50 available channels there can only be nine operating channels for elimination of third order interference or six operating channels for elimination of both third and fifth order interference using Babcock channel selection criteria, severely limiting spectrum utilization.

To determine the expected spatial dispersion of IM products for the AMPA array, the Maritime scenario (Figure 4.3-17) Pritchard* with 10 and 20 signals were synthesized as a function of array size factor (ASF). Scenario #1 shows the location of the signals as nominally seen from Spacelab altitude, and Scenario #2 represents the case with all signals located an order of magnitude closer. The 10 signal scenario (first 10 signal sources in Figure 4.3-17) represents the selected AMPA experiment system with two variable beams and eight fixed beams for IM simulation experiment; and the 20 signals have been synthesized to determine the impact of more signals. It has been assumed that consecutive channels are used and that all IM product power levels are the same as the desired signal, representing the most severe case. The latter assumes that the L-band transmit amplifier is operating at full saturation.

The results of the computer simulation runs are summarized in Figure 4.3-18 for the 10 signal case which shows that the average IM level to the 10 users has been suppressed by at least 14 dB. This represents an output CNR degradation

*Babcock - Intermodulation interference in Radio Systems Bell System Technical Journal, January 1953.

*Pritchard, J.S., Spatial Dispersion of Intermodulation Products by Phased Arrays, IEEE Canadian Communications and Power Conference, Montreal, Canada 7-8 November 1974



SCENARIO #1				SCENARIO #2			
SIGNAL #	LONG.	LAT.	DEGREES	SIGNAL #	LONG.	LAT.	DEGREES
1	-6.6	56		1	-.66	5.6	
2	-52.7	46.1		2	-5.27	4.61	
3	19.8	52.7		3	1.98	5.27	
4	52.7	-46.1		4	5.27	-4.61	
5	26.4	6.6		5	2.64	.66	
6	-32.9	39.5		6	-3.29	3.95	
7	16.5	65.9		7	1.65	6.59	
8	46.1	-19.8		8	4.61	-1.98	
9	-58.3	19.8		9	-5.83	1.98	
10	-26.4	-49.4		10	-2.64	-4.94	
11	-6.6	-13.2		11	-.66	-1.32	
12	-32.9	3.3		12	-3.29	.33	
13	-3.3	9.9		13	-.33	.99	
14	-13.2	-29.7		14	-1.32	-2.97	
15	49.4	-29.7		15	4.94	-2.97	
16	13.2	39.5		16	1.32	3.95	
17	-59.3	32.9		17	-5.93	3.29	
18	52.7	6.6		18	5.27	.66	
19	16.5	19.8		19	1.65	1.98	
20	-19.8	49.4		20	-1.98	4.94	

FIGURE 4.3-17 SIGNAL SCENARIO FOR INTERMODULATION ANALYSIS

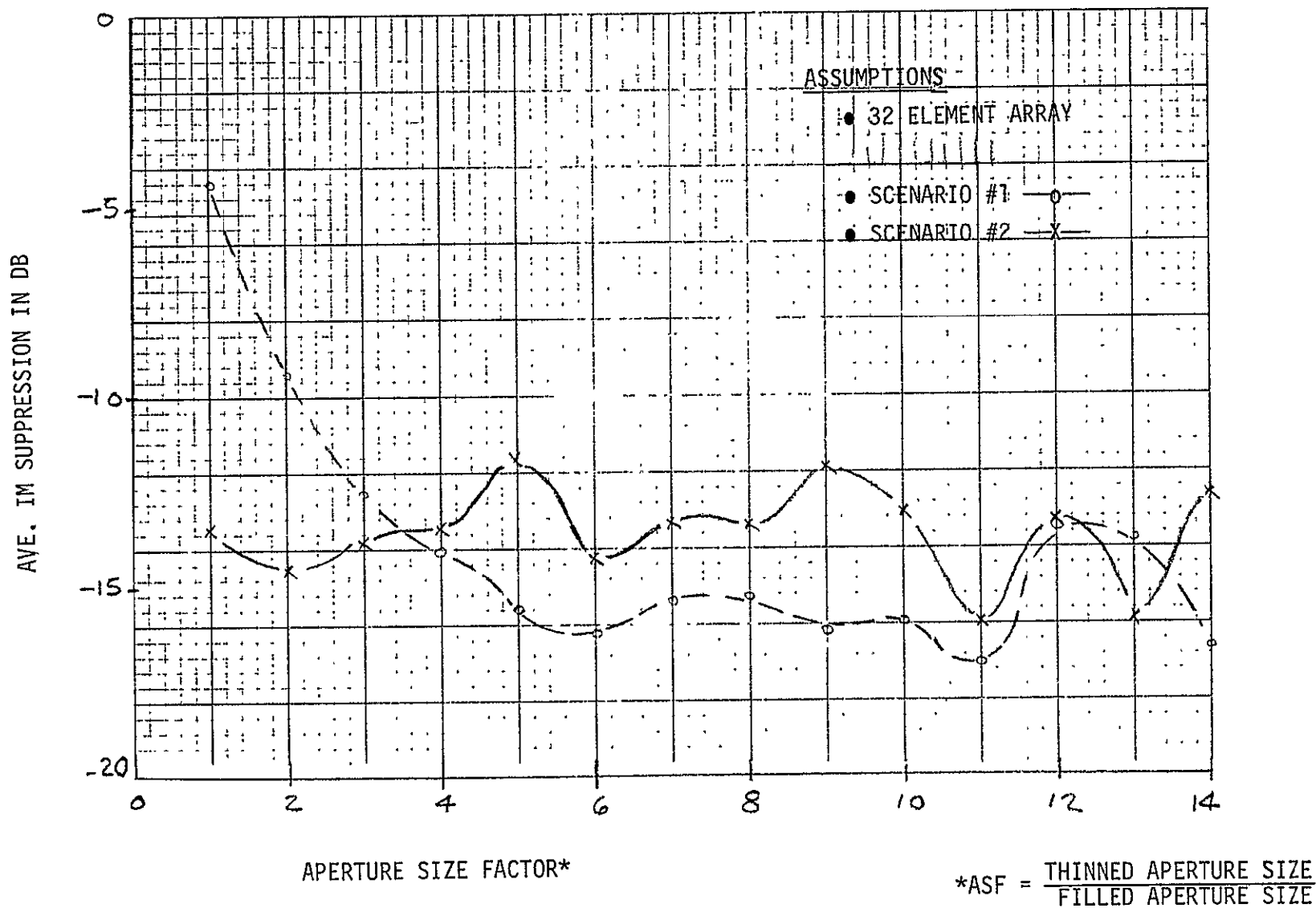


FIGURE 4.3-18. SPATIAL DISPERSION OF IM PRODUCTS - 10 SIGNAL CASE

(ΔQ) due to IM of:

$$\Delta Q = C/(IM+N) \div CNR \cong \left[\frac{IM}{N} + 1 \right]^{-1}$$

For a required output CNR of +7 dB, this represents a negligible ΔQ of 0.8 dB. This indicates that for this scenario adequate suppression of IM is achievable with the phased array so that the L-band power amplifier can be effectively operated in the efficient saturated state.

For a more severe case, the signals were assumed to be order of magnitude closer (Scenario #2 of Figure 4.3-17) and a similar IM suppression vs. aperture size factor was synthesized as summarized also in Figure 4.3-18. Even for this severe case with the angular separation to the signals reduced by an order of magnitude, the IM suppression is seen to be excellent, degraded on the average less than 1 dB from the previous case (Scenario #1). This indicates that reasonable spatial dispersion of IM products with a phased array appears to be achievable.

In the 20 signal case, the spatial dispersion is seen to be approximately the same for both scenarios, showing that spatial dispersion increases with the number of signals as long as the signals are more-or-less randomly distributed (Prichard's paper shows that if all signals are symmetrically displaced along a common radial axis with a sequential assignment of channels the IM products would add up and fall into one of the assigned channels, representing a very poor selection of operating channel). See Figure 4.3-19.

4.3.2.3.2 Tradeoffs

Channel Assignment

For the AMPA experiment, consecutive channels will be selected for the operating and simulated beam channels. This choice is made to demonstrate that communications can be maintained with known IM products intentionally made to fall on the operating channels. Adequate communications will be achieved due to the enhancement of IM rejection from spatial dispersion.

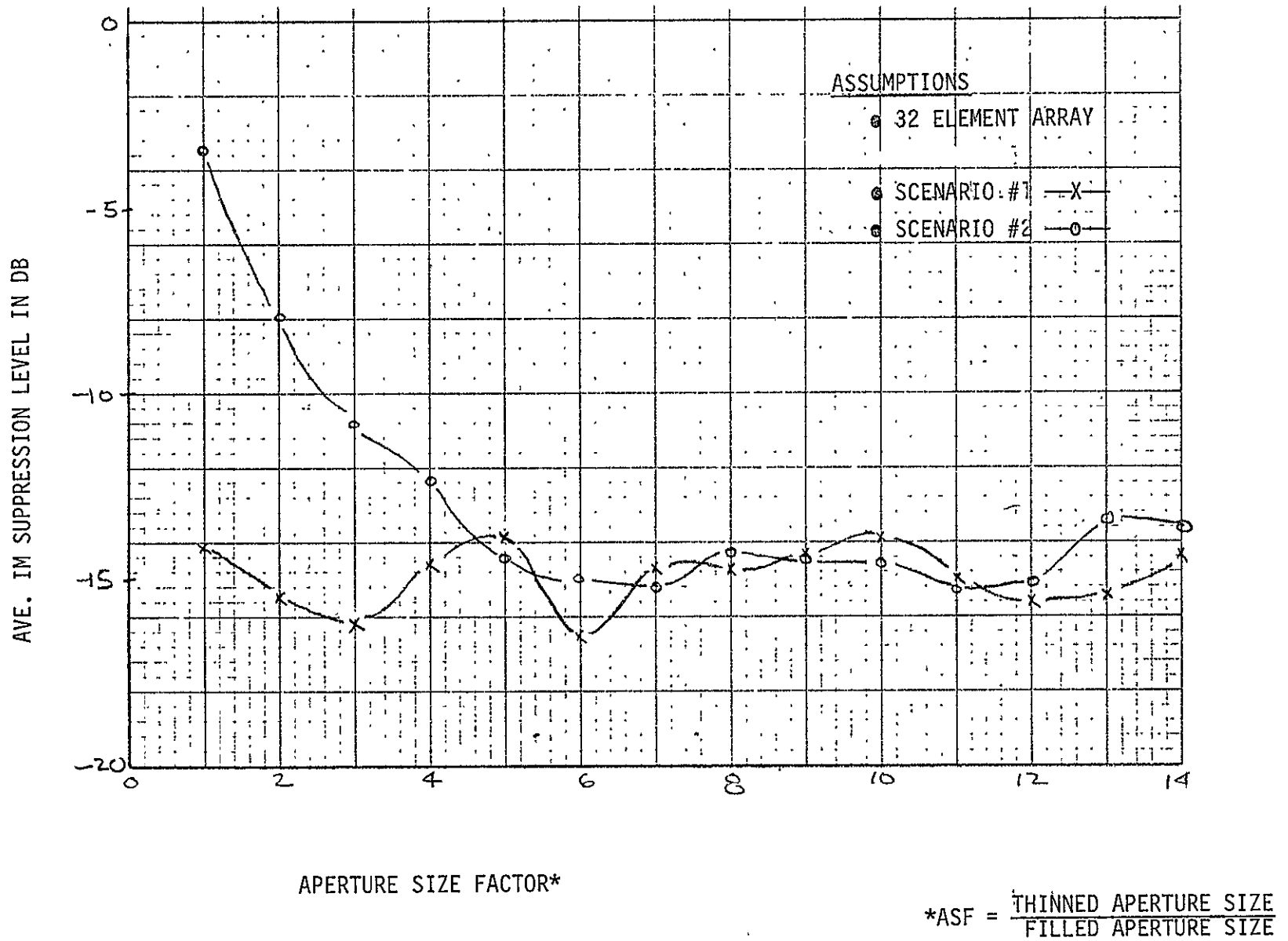


FIGURE 4.3-19. SPATIAL DISPERSION OF IM PRODUCTS - 20 SIGNAL CASE

• Number of Simulated Signals

The greater the number of simulated beams, the larger the number of IM products generated with a corresponding increase in the dispersion of these products. For the AMPA experiment, the choice made is to simulate eight beams. This number is adequate to demonstrate the effects of spatial dispersion, with little to be gained that would justify the increased cost of simulating more beams.

4.3.2.3.3 Design of the IM Simulator

A functional block diagram of the IM simulator is shown in Figure 4.3-20. The eight simulated signals are obtained by utilizing eight crystal oscillators which are separated by 50 kHz intervals starting from 69.8 MHz and extending to 70.25 MHz. The 70 MHz and 70.05 MHz frequencies are not used since they are reserved for the two steerable beam channels. By having the two steerable beam channels in the center of the transmit spectrum with four simulated beam channels on each side, the largest number of IM products falling on the two operating channels are obtained with the least amount of dispersion of these products. Thus, under this worst case condition of channel assignment, the effectiveness of spatial dispersion of IM products will be evaluated.

The eight fixed frequency oscillators utilized are Greenray Industries Model number Y-367. These crystal oscillators have a frequency stability over a -40°C to +70°C temperature range of $\pm 0.005\%$. Each oscillator provides +10 dBm output power with 20 dB minimum harmonic rejection.

Each oscillator is fed to a 32-way divider. The divider outputs are in turn fed to phase shift networks which provide a fixed phase shift. The 32 fixed phase shifts associated with each beam are different for each simulated signal in order to provide eight simulated beams which are spatially focused in eight different directions. With the simulated beams pointing in different directions the dispersion of each IM product will not be identical but will be a function of the location of each particular simulated beam center relative to the steerable beam center.

4-141

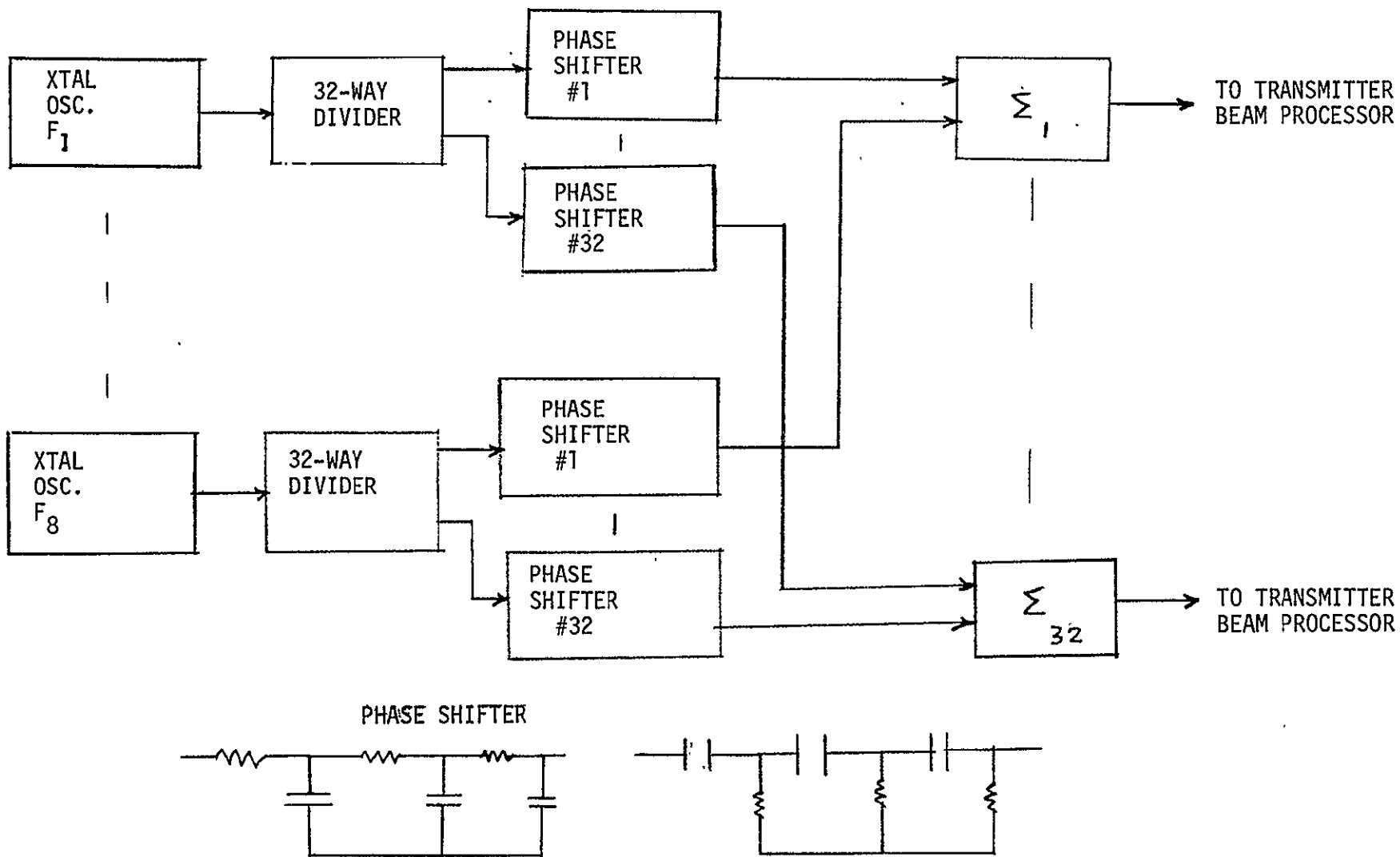


FIGURE 4.3-20. IM SIMULATOR BLOCK DIAGRAM

The 32-way divider consists of a 4-way divider which feeds four 8-way dividers. The dividers are PC mounted and are Mini-Circuits Lab models PSC-4-3 and PSC-8-1. The phase shift networks consist of resistor and capacitor ladder sections connected in series. By selecting the appropriate values of resistors and capacitors any fixed phase shift in the range of 0-360 degrees can be achieved.

The phase shifted signals are combined in 32 8-way summers. The summer outputs are fed to the transmitter beam processor where further combining takes place with the steerable beam signals. The summers used are Mini-Circuits Lab model PSC-8-1.

4.3.2.4 Summer/Amplifier Matrix

There are a total of 32 three-way combiners. Each combiner sums two signals for the steerable beams and eight signals from the IM simulator. The eight simulated signals are combined on a single line at the IM simulator. The summed output is fed to an amplifier (Aydin vector model MHT-252). This amplifier is housed in a T0-8 package and provides 15 dB of gain. The amplifier outputs from each combiner interface with the transmitter modules for subsequent transmission to the user.

4.3.2.5 Layout

The two Transmitter Beam Processors have been laid out in two identical drawers as shown in Figures 4.3-21 and 4.3-22 for mounting in a Spacelab Module rack. However, the IM Simulator is included in one of the drawers, and the Frequency Source in the other. The total size, weight and power requirements of the two drawers are shown also on the figures.

SIZE: 482.6 MM RACK MOUNTABLE X 222.5 MM HI X 508 MM DP.
(19 IN) (8 3/4 IN) (.20 IN)
WEIGHT: 14.98 KG
(36 LBS.)
WATTS: 17.6 WATTS

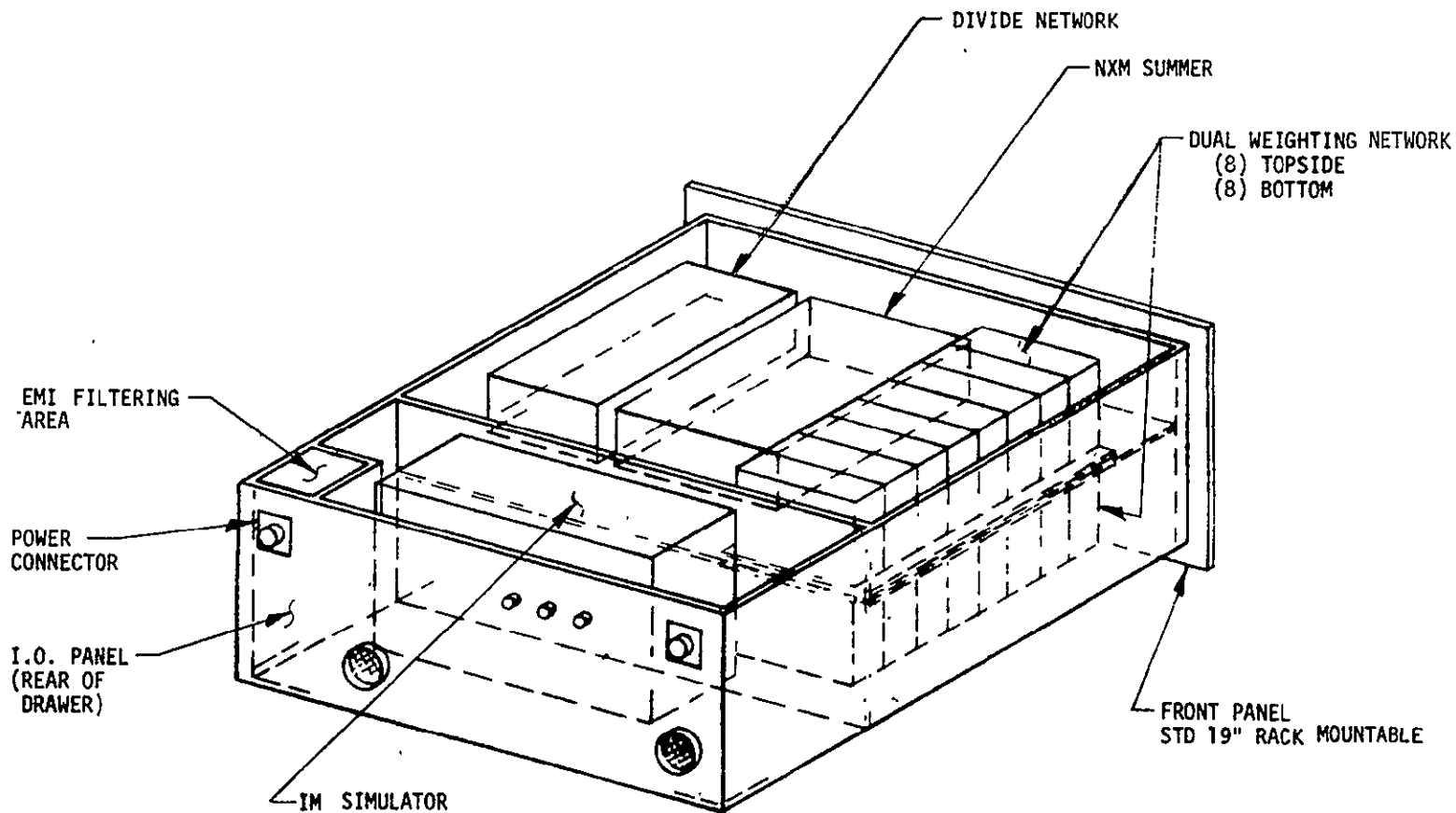


FIGURE 4.3-21 TRANSMITTER PROCESSOR/IM SIMULATOR

4-1143

SIZE: 482.6 MM RACK MOUNTABLE X 222.5 MM HI X 508 MM DP.
 (19 IN) (8-3/4 IN) (20 IN)
 WEIGHT: 14.982 KG
 (33 LBS.)
 WATTS: 15.6 WATTS

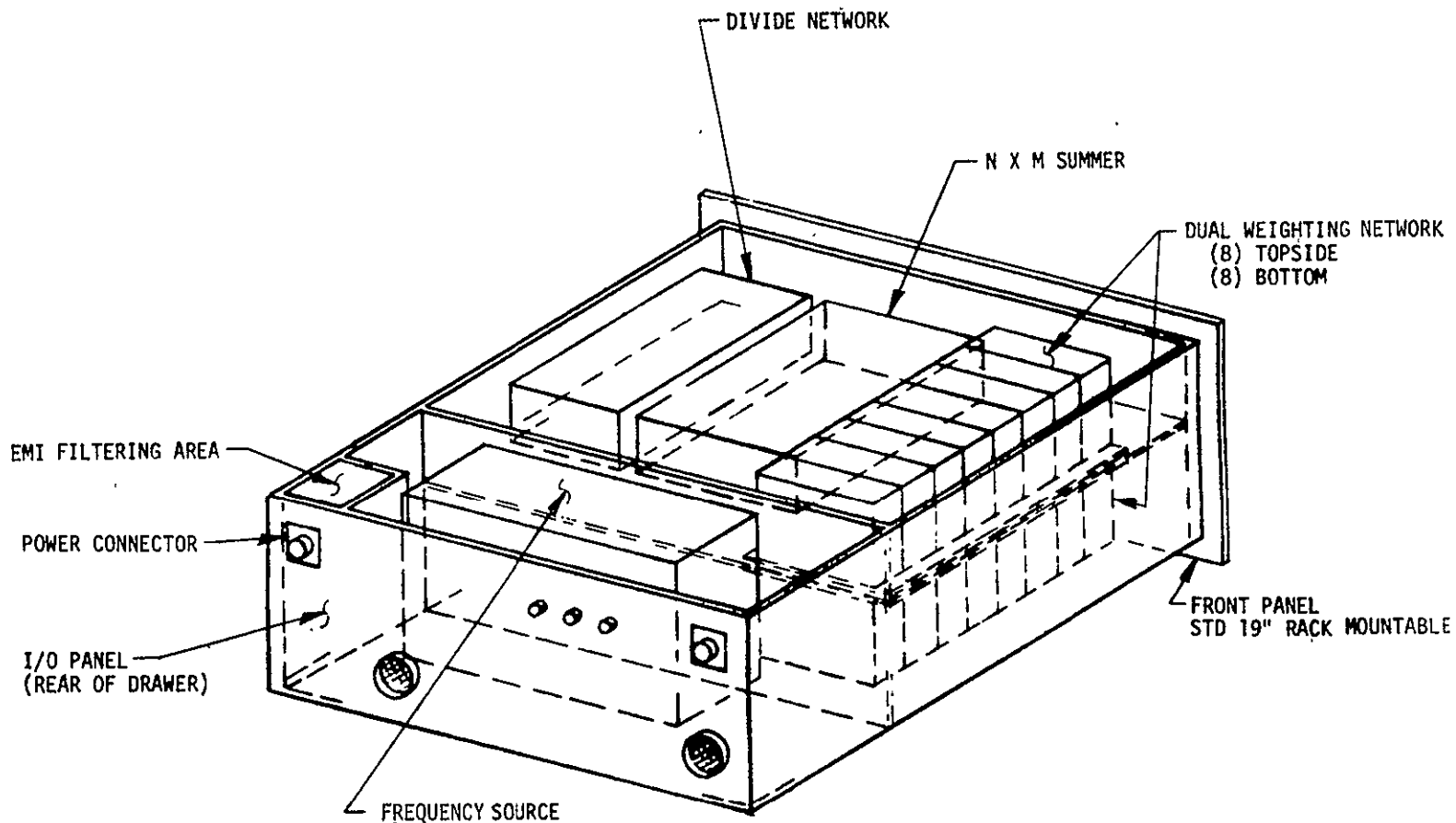


FIGURE 4.3-22 TRANSMITTER PROCESSOR AND FREQUENCY SOURCE

4.3.3 Digital Processor Network

4.3.3.1 General

The AMPA Digital Processor Network must be able to satisfy the real-time processing requirements of the two adaptive receiver processors and the two transmitter processors, as well as the control and monitor functions of the AMPA Experiment System. A functional block diagram of the Digital Processor Network is shown in Figure 4.3-23. A digital processor operates on the selected algorithms and interfaces with the analog devices in the receiver and transmitter beam processors by digital-to-analog converters (DAC's). The multiplexed sampler is a 16 channel multiplexed 8 bit analog to digital converter (ADC), which digitizes the analog outputs from the correlators. The weights for both the receiver and transmitter weighting networks are output to the appropriate network via the Interface Logic assembly and 8 bit DAC's.

As far as the receiver processor is concerned, the Digital Processor will be programmed to perform the $S/(I+N)$ maximization fully adaptive, directed-adaptation, and pointed beam algorithms (see Sec. 3.3.2 for a description of these algorithms). Because time delay weighting is not being used in the receiver processor to measure true phase delay to each element, a fully adaptive retrodirective transmit mode has not been included on transmit. However, a pointed beam (phase only steering) and open loop beam and null forming (pseudo-adaptive) algorithms that places the main beam on the desired user and spatial nulls on RFI's has been included. Both of these modes depend on knowledge of signal locations, and array locations. A routine to calculate signal pointing directions from the Spacelab Navigation System is part of the digital processor program package.

The digital processor is also used to initiate control and monitor functions, including the variable aperture and IM Simulator controls, as well as all system status checks (see Section 4.3.7 for a more detailed discussion of this function). All of the system software is activated by ground commands relayed to the Spacelab by way of the Orbiter's TDRS multiple access transceiver. An executive program accepts all commands and starts the requested routine. Control is passed back to the executive when the function has been completed or when it is terminated by another command. The executive will have the capability to stack single commands to provide an automatic task sequencer.

4-146

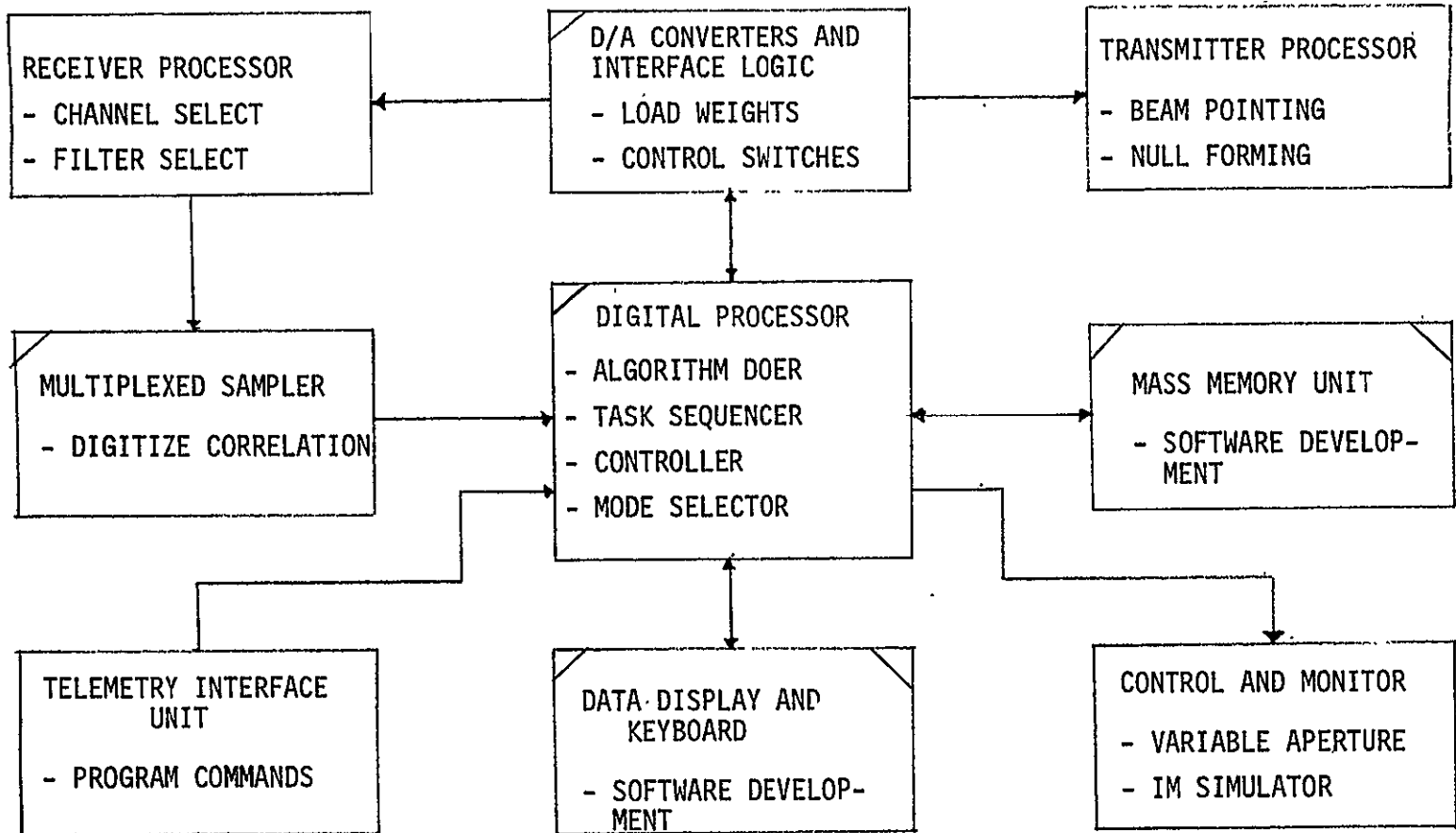


FIGURE 4.3-23 DIGITAL PROCESSOR NETWORK FUNCTIONAL BLOCK DIAGRAM

4.3.3.2 Tradeoffs

Because of the dynamically changing signal environment caused by Spacelab motion, the signal processing requirements of the AMPA Experiment System cannot be satisfied by the on-board Spacelab Experiment Computer Network without including a special add-on processor to increase processing speed. In addition, we have assumed that the on-board experiment computer would have the baseline performance capabilities as described in the Spacelab Payload Accommodation Handbook*, and the AMPA experiment would have exclusive use of the computer during the ten minute experiment passes. However, since neither of these assumptions have been confirmed, and we have in fact been told that it is unlikely that the experiment computer will be as baselined, a separate dedicated digital processor must be considered for this experiment. This decision is made with some reluctance since an experiment dedicated digital processor will increase the cost of the experiment. Besides the obvious expense of the digital processor itself, software development and checkout costs, and hardware interface costs will be greater than would be incurred by using the existing Spacelab experiment computer. Also, the power and weight requirements of the experiment system are affected. However, there is really no alternative but to use a separate dedicated digital processor if we wish to prevent the experiment from being comprised by relying on an inadequate processing capability.

The search for an acceptable digital processor which meets the experiment requirements (Sec. 4.3.2.5) has produced several candidate systems. A partial summary of six digital processors which are or have been considered for AMPA, has been prepared (Table 4.3-7). The selection process can be simplified by elimination based on the given performance specifications. It can be seen that only the ROLM and IBM machines meet the baseline requirements as stand-alone systems. Comparing the two, the ROLM is the less expensive (\$75K vs. \$125K) and uses the Data General Corporation assembly language. This is important from AIL's standpoint, since there are presently two DGC systems in-house with a third soon to be purchased. This can significantly reduce expenditures for software development. Furthermore, the ROLM machine can be microprogrammed to increase programming efficiency. This feature

* ESA Ref. No. SLP/2104 dated May 1976

TABLE 4.3-7. CANDIDATE DIGITAL PROCESSORS FOR AMPA

NAME	CORE SIZE (WORDS) WORD LENGTH (8 BITS)	THROUGHPUT (KBPS)	REGISTER ARCHITECTURE	INTERRUPT CAPABILITY	INPUT/OUTPUT	WEIGHT (LBS) POWER (WATTS) HARDWARE COSTS	MICRO-PROGRAMMABLE	FLOATING POINT	LANGUAGES	ENVIRONMENTAL SPECS MIL-5400	COMMENTS
CII MITRA 125	64K 16	350 GIBSON MIX	256 GENERAL 32 BASE 32 SIZE	32 VECTORED	DMA PARALLEL I/O	N/A N/A --	CONTROLLER ONLY	HARDWARE	ASSEMBLER PL LP-15 FORTRAN ALGOL	YES	TOO SLOW AS STAND ALONE EXCELLENT ARCHITECTURE AND SOFTWARE OVERALL: UNACCEPTABLE
ROLM 16/64	32K 16	450	16 GENERAL	16 HARDWARE	DMA PARALLEL I/O	75 250 75K	YES	HARDWARE	ASSEMBLER (DGC) FORTRAN	YES	GOOD THROUGHPUT FLEXIBLE MICROS NOVA COMPATIBLE SOFTWARE OVERALL: ACCEPTABLE
IBM AP-101	32K 32	550	16 FIXED POINT 8 FLOATING POINT	ONE INTERRUPT LINE	DMA (500 KW) PARALLEL I/O	56 500 \$125K	CONTROLLER ONLY	HARDWARE	ASSEMBLER FORTRAN	YES	HIGH THROUGHPUT HIGH COST OVERALL: ACCEPTABLE
SANDERS MIP-16	32K 16	500	16 GENERAL	48 HARDWARE 6 VECTORED	DMA PARALLEL I/O SERIAL I/O	40 200 \$75K	YES	NONE	ASSEMBLER (DEC)	YES	HIGH THROUGHPUT NO FLOATING POINT NO PROGRAMMING LANGUAGE OVERALL: UNACCEPTABLE
NASA SPACE-CRAFT COMPUTER #1	32K 16	200	SINGLE REGISTER	16 LEVEL PRIORITY	PARALLEL I/O CYCLE STEALING	49 25 --	NO	SOFTWARE	ASSEMBLER	YES	TOO SLOW NO FLOATING POINT HARDWARE NO PROGRAMMING LANGUAGE OVERALL: UNACCEPTABLE
NASA SPACE-CRAFT COMPUTER #2	32K 32	450	16 GENERAL	16 DEVICES	DMA PARALLEL I/O	90 230 --	YES	HARDWARE	IBM INSTRU- CTION SET	YES	OVERALL: ACCEPTABLE

4-148

can be used to great advantage to lower the total digital processing time for the adaptive processors. A detailed analysis has not been attempted, but from preliminary indications, this could result in a 50 to 100 percent increase in processor efficiency.

Another possibility which has been discussed is to use the same Mitra (as baselined in the Spacelab Payload Accommodations Handbook) but dedicated for the AMPA Experiment and to add a special hardware processor (at experiment expense) to increase system throughput. This would lower total expenditures for the digital processor network and maintain software compatibility with the development facilities provided for the experiments. This naturally assumes that a spare Mitra would be available or an equivalent one be purchased for the AMPA experiment.

A third alternative is to develop a dedicated high speed processor. This approach would not be economically feasible if the AMPA experiment were required to bear the entire development costs.

4.3.3.3 Design

The major subassemblies in the AMPA Digital Processor network other than the digital processor itself are the Interface Logic Assembly and the Multiplexed Sampler. The Interface Logic Assembly is described in the subsequent section 4.3.4.

The Multiplexed Sampler Unit digitizes the analog outputs of the correlators into an 8 bit digital word to be input to the digital processor. This will be a purchased item and will be housed within the digital processor. There are many industrial organizations which market suitable data conversion units for this purpose.

The AMPA Experiment Digital Processor Network shall meet the following baseline requirements:

- Word size - 16 bits (minimum)
- Core capacity - 32K words (minimum)
- Mass memory - 10 megabytes (minimum)
- Throughput - Equivalent to NOVA 800 series
- Direct memory access
- Interrupt processing
- Fast arithmetic processor (complex arithmetic)
- Fortran compiler
- Mux Sampler (16 channel muxed ADC)
- Scientific program library

The fast arithmetic processor is essential for successful operation of the AMPA experiment. It should be capable of performing a complex multiplication in 1 usec or less. This includes access time and other overhead.

The analog data conversion unit is capable of supporting 16 full differential analog inputs and has a resolution of 8 binary bits, nonlinearity $\pm 1/2$ LSB maximum, and total acquisition and conversion times of 10 microseconds maximum.

The Mass Memory Unit is a tape recorder used during software development and testing only. This unit is not required to be flyable.

4.3.3.4 Layout

The Digital Processor will be located in drawers that are compatible for mounting in the Spacelab Module AMPA Experiment System rack as shown in Figure 4.3-31 of section 4.3.8.

4.3.4 Interface Logic Assembly

4.3.4.1 General

The interface unit houses the Input/Output (I/O) gating logic and computer data bus terminations, and the interface logic and DAC's for both the receiver and transmitter beam processors. All I/O with the computer is handled by the Interface Logic Assembly with the exception of the Multiplexed Sampler.

4.3.4.2 Tradeoffs

An important objective in the design of the interface unit is to keep the number of harness wires to a minimum. Since there are a total of 256-8 bit DAC's, it is impractical to house the logic in the I/O unit and the DAC's within the weighting networks. This would require over 2,000 harness wires and TTL line driver/receiver pairs.

A second alternative would be to place both the logic and DAC's in with the receiver and transmitter processors. A total of 4 harness wires and driver/receivers would be required by each processor. However, this would be impractical because of the large number of parts involved and the resultant increase in size and weight.

All conversions are therefore made in the I/O units, and the analog voltages are then sent to the biphas attenuators in the weighting networks. A total of 256 wires are thus required.

4.3.4.3 Design

The minimal logic diagram for the weighting network interface is shown in Figure 4.3-24. In order to minimize the number of printed circuit lines, the data is first parallel-loaded from the digital processor into a storage register, and then serial-loaded into a serial/parallel shift register. The TTL clock to clock-in the data is present at only one of the channel shift registers. After load-in, the multiplexer is advanced to the next channel, until all weights have been read out. A command is then sent to the latches to change all the weights simultaneously and to reset the multiplexer to channel one. This is done to minimize signal distortion during the weight change period (less than 10 usec for this particular DAC).

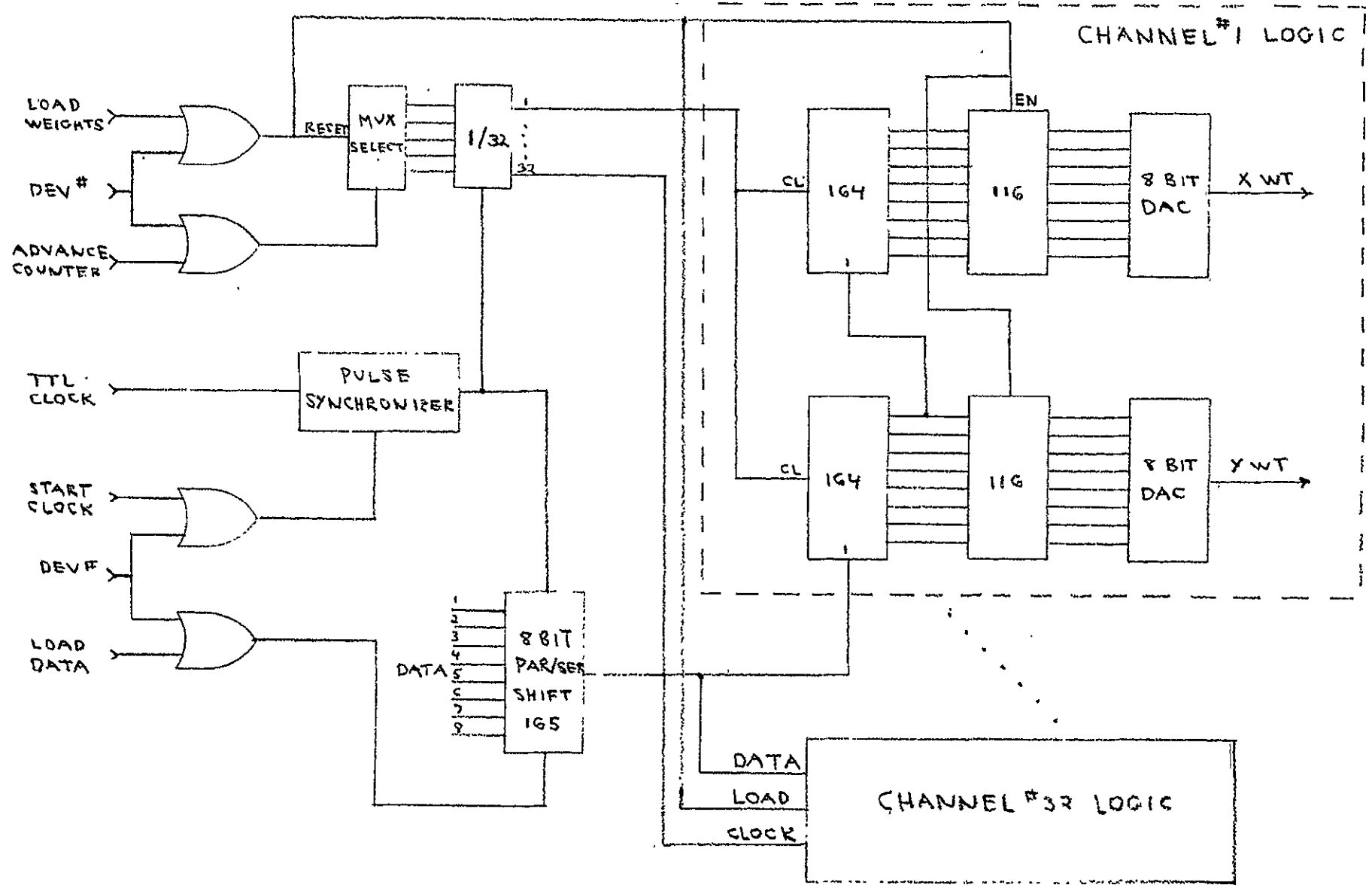


FIGURE 4.3-24. MINIMAL LOGIC WEIGHTING NETWORK INTERFACE

All logic is standard 5400 TTL. The DAC's are low power CMOS which is also TTL compatible (Datel DAC-CM8B or Hybrid System's DAC385I-8). These units are commercial parts. An equivalent high rel version will be used for the experiment system.

4.3.4.4 Layout

The interface logic is placed on one-sixteenth glass epoxy printed circuit boards. The logic and DAC's needed for one dual weighting network are arranged on a single modular board.

The Interface Logic Assembly has been laid out in a drawer as shown in Figure 4.3-25 for mounting in the Spacelab Module rack. The weight of the assembly is 23.59 kg and requires 41 watts of prime power.

SIZE: 482.6 MM RACK MOUNTABLE X 177.8 MM HI X 400.05 MM DP.
(19 IN) (7 IN) (15-3/4 IN)
WEIGHT: 23.59 KG
(51.9 LBS.)
WATTS: 47 WATTS

4-154

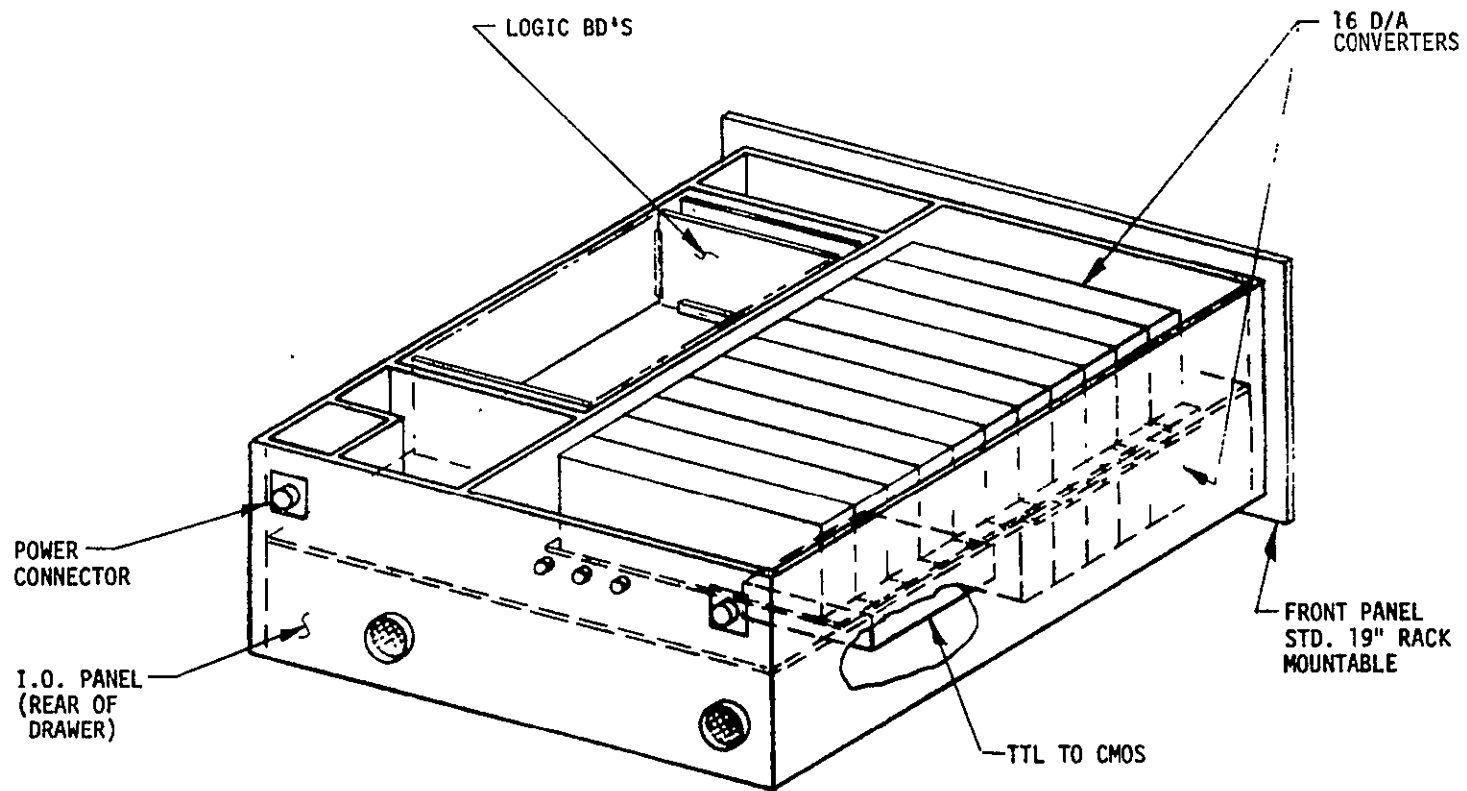


FIGURE 4.3-25 INTERFACE LOGIC

4.3.5 Frequency Source

4.3.5.1 General

The Spacelab module frequency source derives three low noise reference frequencies required for system operation. The frequencies generated are coherent to a basic reference standard which is a stable spectrally pure temperature compensated crystal oscillator (TCXO). Frequencies are generated by division, multiplication and mixing operations.

The three frequencies generated are 20 MHz, 147 MHz and 171 MHz. The 20 MHz signal interfaces with the receiver adaptive processor where after distribution is used as the LO for the downconverters. The 147 MHz and 171 MHz signals are fed to the pallet frequency source. These signals are used as references for the L-band phase locked sources which provide the LO's for the receiver and transmitter modules.

The frequency sources basic reference is a 20 MHz TCXO having a stability over a 0°C - 50°C temperature range of ± 1 part per million. The performance characteristics of the frequency source are indicated in Table 4.3-8.

4.3.5.2 Frequency Generation - Tradeoff Analysis

The choice of the frequency of the standard to be employed and the manner in which to generate the additional references required represent a large number of designs which would give satisfactory performance. With the requirement to provide a 20 MHz signal, it is logical to select 20 MHz as the frequency of the standard. With this choice, additional conversions and filtering are eliminated. In addition, 20 MHz high stability TCXO's are available with good spectral purity.

The generation of the additional two references required have been accomplished with two upconversions and represents a design requiring a minimum number of filters and amplifiers.

TABLE 4.3-8 FREQUENCY SOURCE PERFORMANCE CHARACTERISTICS

<u>FREQUENCY</u>	<u>OUTPUT POWER</u>	<u>SPURIOUS</u>
20 MHZ	+21 DBM	-70 DBC
147 MHZ	+ 5 DBM	-40 DBC
171 MHZ	+ 5 DBM	-40 DBC

POWER STABILITY	<u>+1</u> DB
HARMONICS	-40 DBC
VSWR	1.5
PHASE NOISE (10 HZ-1 KHZ)	0.3 DEGREES
DC POWER	8.0 WATTS
WEIGHT	7.0 LBS.

C-3

The L-band frequency generation is not done at the Spacelab frequency source module. This is due to the large losses which would result in the interconnecting cables carrying L-band frequencies from Spacelab to pallet. The L-band frequency generation is accomplished at the pallet frequency source which thus results in improved system efficiency. Two VHF references at low power levels are fed from the Spacelab frequency source to the pallet frequency source. These references lock up two L-band phase locked sources which provide the LO's for the element modules.

4.3.5.3 Design

A functional block diagram of the Spacelab frequency source is illustrated in Figure 4.3-26. A 20 MHz TCXO is used as the frequency standard to provide coherency and establish the high stability for all generated frequencies. The TCXO employs a precision "AT" cut crystal as its frequency determining element. An AGC circuit maintains crystal current at a level which represents the best compromise between the low current desired for long term stability, and the high current desired for good short term (phase) stability. Temperature compensation is achieved with a thermistor network which exhibits an effect on frequency which is opposite to that of the crystal as the temperature changes. Buffer amplifiers isolate the oscillator from external load variation, while a zener diode regulator minimizes the effect of power supply fluctuations.

The TCXO output is fed to a 3-way divider. One output of the divider is amplified to provide the 20 MHz output signal at +21 dBm which interfaces with the receiver adaptive processors. The other divider outputs feed a multiply by eight and a divide by twenty network.

The multiply by eight network is a transistorized multiplier which receives the 20 MHz input and produces a 160 MHz output. This output feeds a 160 MHz bandpass filter which rejects the 140 MHz and 180 MHz sidebands. The filtered output is split two ways with each output fed to a balanced mixer.

4-158

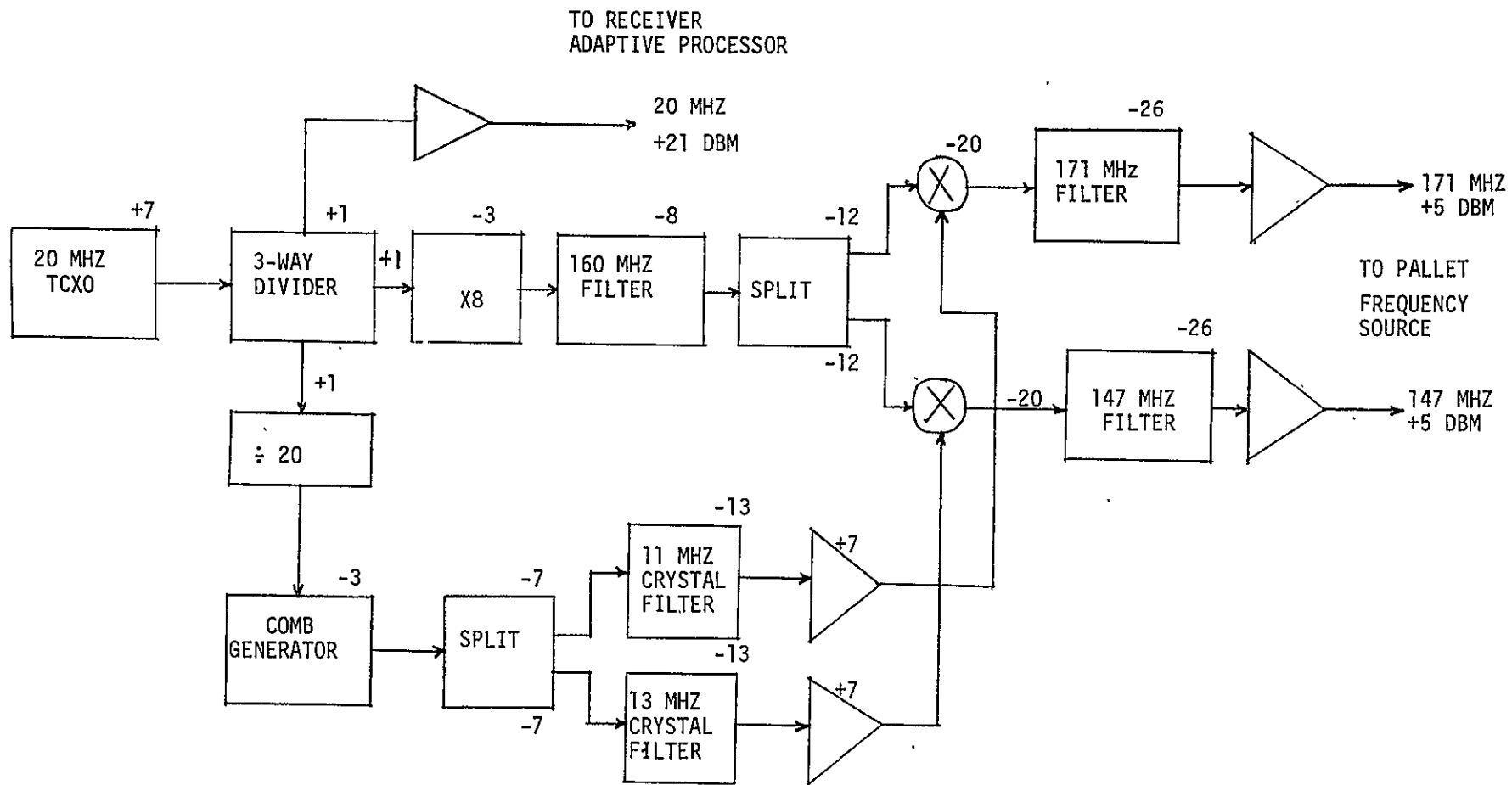


FIGURE 4.3-26. SPACELAB FREQUENCY SOURCE BLOCK DIAGRAM

The divide by twenty network counts down the 20 MHz input to result in 1 MHz. This 1 MHz signal is fed to a comb generator which produces a spectrum of signals which are spaced at 1 MHz intervals. The output spectrum is fed to a splitter whose outputs are passed through 11 MHz and 13 MHz crystal filters. The filters reject the 1 MHz sidebands of the comb resulting in spurious free 11 MHz and 13 MHz signals. Each of these signals are amplified so as to serve as an LO for the two balanced mixers.

The 160 MHz signal is upconverted with the 11 MHz signal to produce 171 MHz. The 171 MHz signal is filtered and amplified to a level of +5 dBm. This output interfaces with the pallet frequency source to derive the 1710 MHz signal user for the receiver module LO.

The 160 MHz signal is also mixed with the 13 MHz signal to result in 147 MHz. The 147 MHz signal after filtering and amplification interfaces with the pallet frequency source which generated the 1470 MHz LO used for the transmitter module.

4.3.5.4 Layout

The Frequency Source has been laid out in the same rack drawer as the Transmitter Beam Processor (Figure 4.3-22).

4.3.6 AMPA Control Unit

4.3.6.1 General

The purpose of the Control Unit is to provide a means to quickly determine the status and performance of key system parameters. An efficiently designed Control Unit is necessary for facilitation, development, test and demonstration of the Experiment System during the contractor ground based development phase as well as during the subsequent system integration at NASA and during the in-flight experiment phases.

4.3.6.2 Tradeoffs

In order to keep the weight and power requirements to a minimum for the flyable system, the AMPA Control Unit has been split into two units; one for space application and a second for ground testing. The spaceborne unit, which is less complex than the ground unit, has been designed to perform only those functions which are necessary for flight safety or to insure operation of the system.

4.3.6.3 Design

4.3.6.3.1 Ground-Based Unit

There are three general functions performed by the control unit; namely, control, test and monitor. The ground based unit is physically separated from the experiment rack. All DC and AC power is supplied from the rack by a multi-wire cable. The test voltages to be monitored, as well as several RF signals, are supplied by a separate multi-wire cable. A second box is used to generate scenario test signals for testing the two adaptive receive processors. This is also DC powered by the rack.

There are a total of five identical L-band sources (VCO's) in the scenario generator assembly (Figure 4.3-27), any four of which can be used as RFI's with the remaining one as a desired signal. The modulation format, frequency, and power of all sources are selected by front panel controls. There are two types of modulation available; narrowband FM (NBFM) and binary phase shift keyed (BPSK) data at 4800 bps. An audio tone generator (or recorded voice) which can be varied from 0.3 to 3 kHz is supplied for FM modulation. The

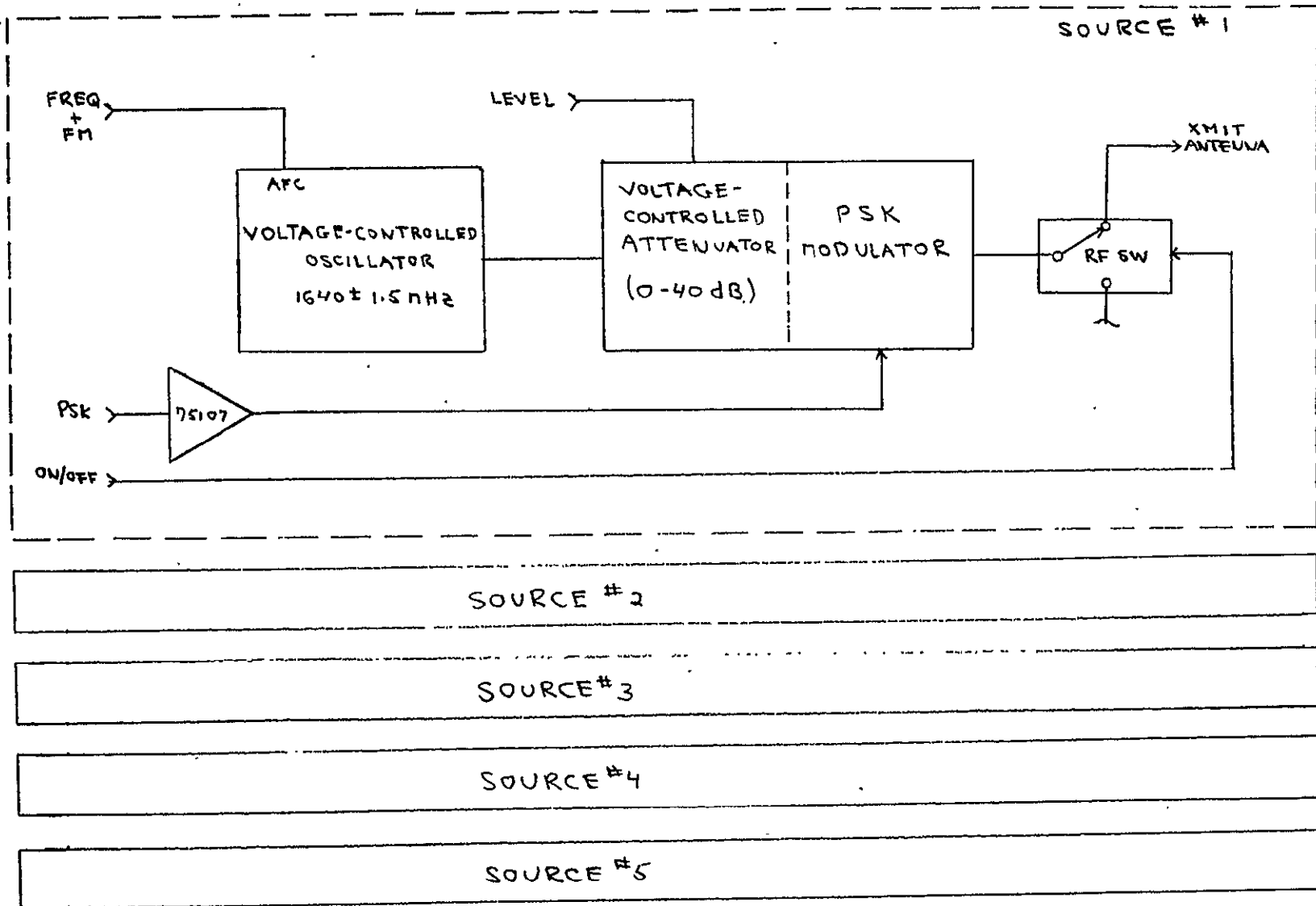


FIGURE 4.3-27. SCENARIO TEST SIGNAL GENERATORS

BPSK is generated by a shift register with the repetition rate variable from 2^6 to 2^{15} bits and a balanced mixer. The output power of all sources can be varied over a 40 dB range or eliminated completely by a coaxial switch.

All DC voltages tapped directly at the power conditioner as well as the weighting voltages for both receiver and transmitter processors are monitored by front panel meters.

A synchronous detector and a bit error rate tester (BERT) are used to measure the signal-to-interference plus noise ratio $[S/(I+N)]$ at the output of both receiver adaptive processors. Also, a chart recorder is available to plot the resultant antenna pattern.

There are three front panel indicators for the receiver processor modes; viz, pointed (P), directed-adaption (D-A) and fully adaptive (FA); and two for the transmitter; pointed (P) and open loop beam and null forming (NF). One of each set will be lit to indicate the adaptive algorithm currently being performed by each processor.

Besides power supply voltages and weights, the digital panel meters will display the DC outputs of the RF power detectors which monitors the L-band amplifiers in the transmitter channels. This will indicate if a total failure has occurred some place in the transmitter chain. The DC power to the transmitter channels can be shut off by toggle switches on the front panel. These provide a TTL level voltage to a relay in the transmitter amplifier assembly. Correlator voltages will also be displayed. This is useful during system calibration to align the correlators. The front panel layout is shown in Figure 4.3-28.

4.3.6.3.2 Spaceborne Unit

The space version control unit will be much simpler than the ground version. Included here are system power switches to de-energize the system in an emergency and a high speed paper tape reader. The paper tape reader has been included to reload the adaptive algorithm into core memory of the digital processor in the event that core memory is destroyed prior to operation in space. All other

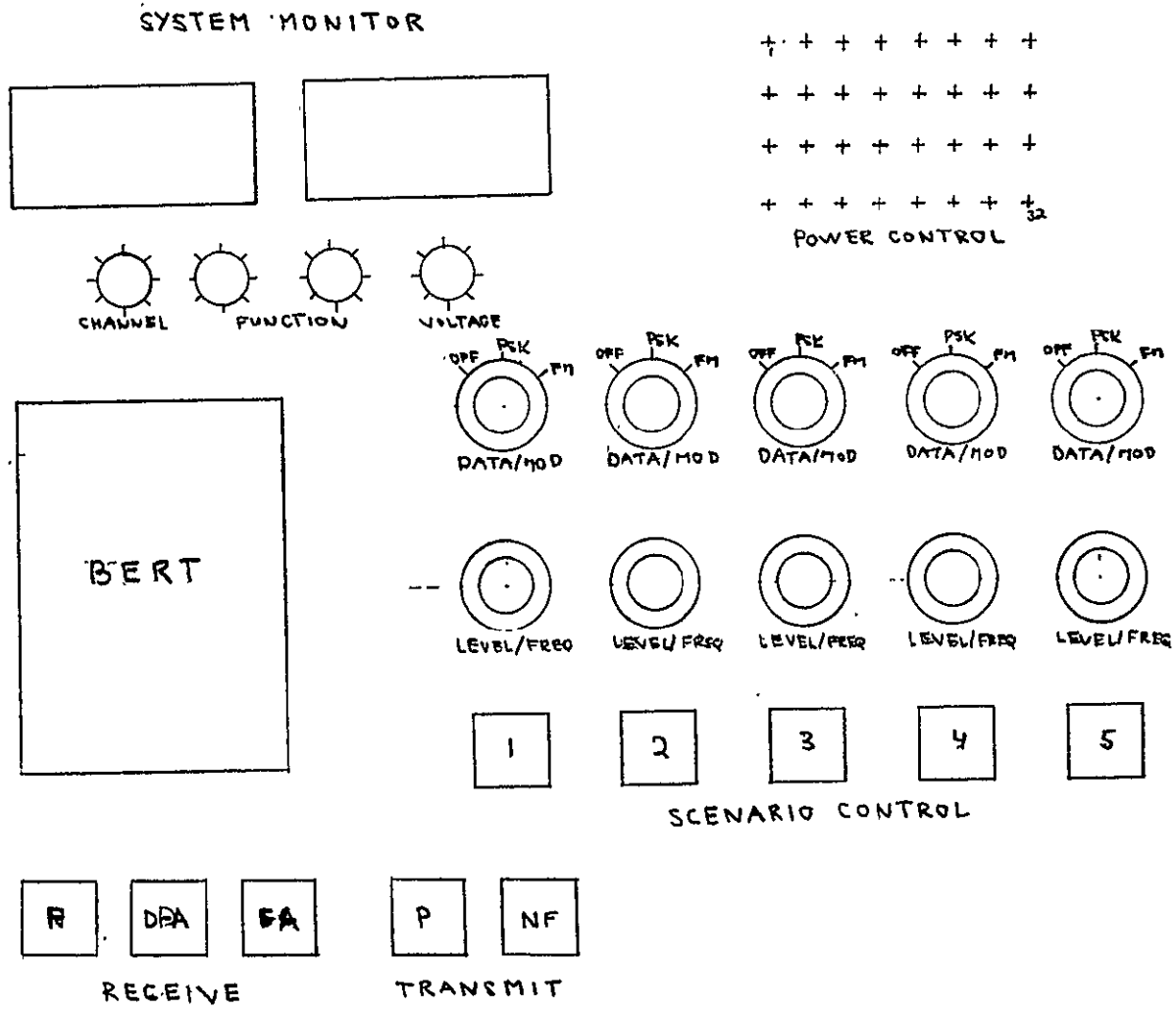


FIGURE A.3-28 FRONT PANEL GROUND-BASED CONTROL UNIT

space controls and/or changes in modes of operation will be initiated by ground commands and relayed to the AMPA system by way of the TDRSS link. The front panel layout is shown in Figure 4.3-29.

4.3.7 Power Conditioner

4.3.7.1 General

The Spacelab module power conditioner accepts the input 28 VDC shuttle bus. It is required to derive the conditioned regulated DC voltages needed for Spacelab module subsystem operation.

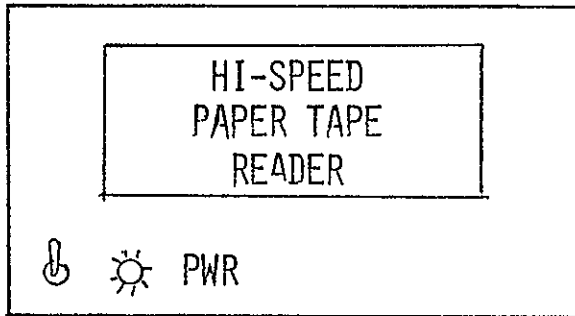
The unit will meet the performance criteria below, when driven from an input voltage having the indicated characteristics.

Input Characteristics

Voltage	28 VDC
Steady State Regulation	± 4 VDC

Output Characteristics

+15V	+15 \pm 1V @ 8 amps with a resistive load and other outputs loaded.
+5V	+5V \pm 0.2V @ 20 amps with a resistive load and other outputs loaded.
-15V	-15V \pm 1V @ .8 amps with a resistive load and other outputs loaded.
Total Internal Dissipation loaded	- 75 watts
Ripple on all outputs	- 5 milliwatts peak-to-peak (maximum)



- o POWER: ON-OFF SWITCH TO DE-ENERGIZE IN EMERGENCY
- o LOAD DIGITAL PROCESSOR CORE MEMORY IN EVENT MEMORY IS DESTROYED

FIGURE 4.3-29 SPACELAB HUMAN INTERFACE

The distribution of the above DC voltages is as shown below:

+15V	Adaptive Receiver Assembly (2100) Transmitter Beam Processor (2200) Frequency Source (2600) IM Simulator (2220) D/A Converter (2310) Control/Monitor (2500) Data Conditioner (2800)
-15V	Adaptive Receiver Assembly D/A Converter Control/Monitor Data Conditioner
+5V	Adaptive Receiver Processor Frequency Source Interface Logic (2300) Control/Monitor

4.3.7.2 Tradeoffs

The major tradeoffs made prior to the detailed design phase are listed below:

- Type of Power Supply
- Single or Dual outputs

4.3.7.2.1 Type of Power Supply

Based on the $28V \pm 4V$ input, regulation is required for maintaining steady state voltage. In addition with the ripple spectrum of the input not known, regulation is required to provide low frequency ripple rejection so as not to detract from overall system performance.

To design a discrete regulator capable of handling the entire load would require a costly design effort and result in a heavy package, requiring extensive heat sinking in the regulator area. A single preregulator at the input would serve to filter out the input ripple but is not practical due to high dissipative losses.

The approach taken was to use a multioutput DC-DC converter followed by regulators for each voltage required. This implementation provides a smaller package with a distributed thermal footprint.

The loads can be distributed to minimize crosstalk through the power lines. Additionally, since the outputs of each regulator are floating, both the hot side and the return can be filtered, prior to tying the returns to chassis ground.

Once the need for regulation was established and it was determined that it was more practical to provide a regulator, the basic question was to determine whether a dissipative or non-dissipative (switching) regulator was most compatible with our requirements. Table 4.3-9 compares the regulator types considered.

The series dissipative regulator was chosen primarily because of low output ripple and a low EMI susceptibility. The main disadvantage of a dissipative regulator is its relatively low efficiency. This is offset somewhat by the design chosen. It utilizes a multi-tapped transformer at the output of the inverter. This provides inputs to the regulator that are close to the desired output voltages. This improves the efficiency and also reduces the power dissipated in the series control element. The regulators used are IC types requiring a minimum of external components.

4.3.7.2.2 Single or Dual Outputs

The regulators chosen to supply the voltage outputs do not have the capacity to supply the entire space lab module load. With a single regulator device used in conjunction with an external pass transistor to supply the high current, the number of components are at a minimum. However, the transistor and resistors would be high power devices requiring heat sinking.

TABLE 4.3-9. COMPARISON OF DISSIPATIVE AND SWITCHING REGULATORS

<u>DISSIPATIVE</u>	<u>SWITCHING</u>
Low Noise (EMI)	High Noise (EMI) generator requires heavy output filters
Precision Regulation	Precise regulation
Lower Efficiency	High efficiency (varys with switching frequency)
Low Parts Count	Complex circuitry
High Thermal Dissipation	Lower thermal dissipation

The other approach considered and ultimately chosen is to use two separate regulators driven from a common input. The two regulator method enables the loads to be separated by function. For example, the +15V used for the adaptive receiver assembly is isolated from the +15V that supplies the transmitter beam processor. This eliminates crosstalk through the power lines for receive and transmit functions.

4.3.7.3 Design

The power conditioner block diagram is shown in Figure 4.3-30. The 28 volt input excites the oscillator/driver and the inverter. The oscillator is a 10 kHz square wave multivibrator utilizing a saturated transformer. The square wave output alternately drives the inverter from cutoff to saturation. The inverter provides the large AC swing into the non-saturating output transformer primary. The secondary of the transformer is multi-tapped to obtain the required inputs for the full wave rectifiers that follow.

Secondary no. 1 is a centertapped winding providing an output of $\pm 19V$ relative to the centertap. Full wave rectification and filtering follows. The resultant DC outputs of $\pm 18V$ are then fed to the regulators, to derive the +15 volt and -15 volt lines.

Secondary no. 2 provides +9V relating to the centertap. After rectification and filtering the resultant 8V feeds the regulator which derives the +5 volts.

The prime conditioner is laid out in a drawer for mounting in a Spacelab Module rack as shown in Figure 4.3-21, and requires:

- Size: 222.25 mm high and 400.05 mm deep drawer
(8 3/4 in.) (15 3/4 in.)
- Weight: 11.35 kg (25 lbs.)
- Power: 75 Watts

4-170

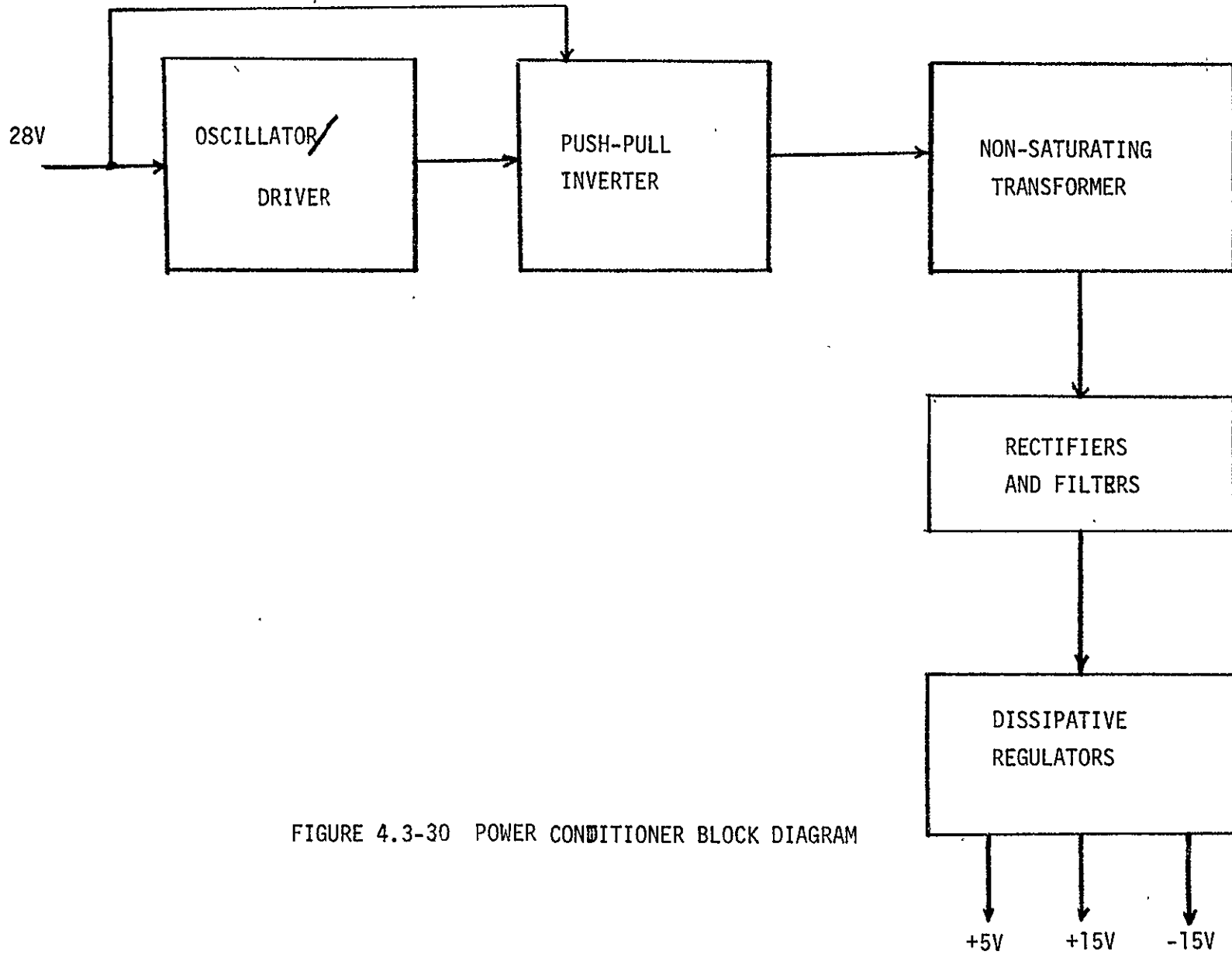


FIGURE 4.3-30 POWER CONDITIONER BLOCK DIAGRAM

4.3.8 Spacelab Module Mounted Subsystem Layout

All of the hardware located in the Spacelab Module has been conveniently laid-out in standard ATR drawers for mounting in one of the racks as shown in Figure 4.3-31. Rack mounting requires some additional weight and volume, but arranges the Module Subsystem hardware for ease in hardware development and test during the ground based phase as well as after the AMPA Experiment System has been integrated with the Spacelab Module during ground based system integration phases as well as in flight. A similar rack will be provided for the ground based development phase and the rack mounted equipment will simply be transferred to the Spacelab Module racks for system integration and flight phases.

At this time, the Spacelab Module Subsystem has been laid out in 9 drawers; two of the drawers being reserved for the digital processor and the mass memory device whose size, weight and power requirements are not firm at this point. Several candidate types have been evaluated, some requiring two drawers and others only one. Depending upon the ultimate choice in the Digital Processor Network, there may be an extra drawer available for other experiment functions.

A full drawer has also been allocated for the Control Unit which will be fully occupied for the ground development phase. However, for space flight, many of the control, monitor and test functions have been removed and will be activated remotely from the ground by way of the Orbiter's TDRS multiple access link. Consequently, this drawer will be approximately 50 percent occupied and is available for other experiment functions.

All thermal cooling is provided through the cooling and exhaust ducts already existing in the Spacelab Module rack.

The total weight and power requirements for the Spacelab Module Subsystem exclusive of the existing rack, are 122 kg and 236 watts, exclusive of the Digital Processor Network.

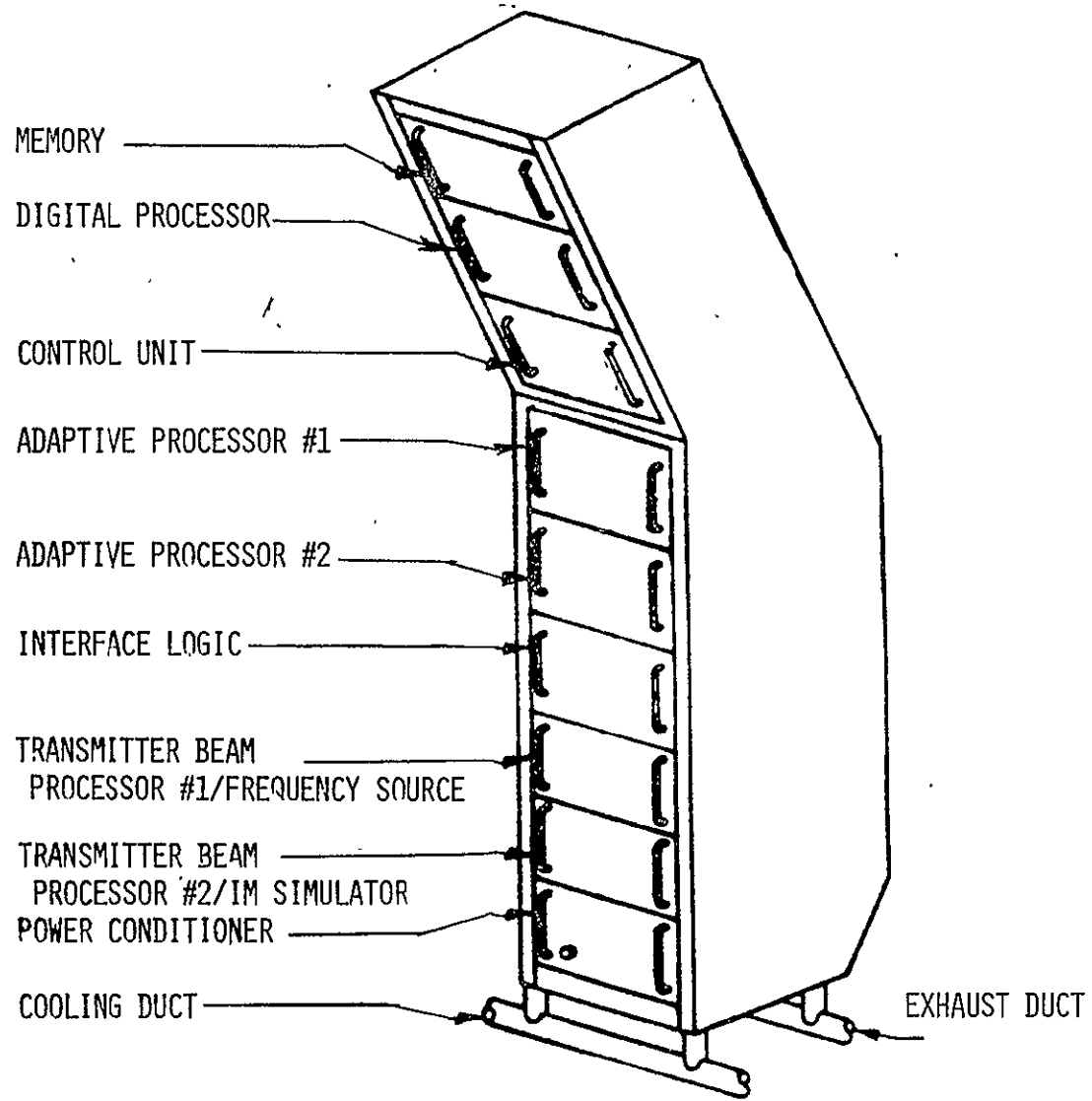


FIGURE 4.3-31 SPACELAB MODULE SUBSYSTEM LAYOUT

4.3.9 Thermal Analysis of the AMPA Experiment System

4.3.9.1 General

The thermal management for the AMPA Experiment System utilizes the following available spacecraft cooling systems.

- Heat generating equipment located on the experiment pallet is cold plate cooled (coolant, freon).
- Spacelab Module Subsystem is rack mounted and cooled with Avionics Air Loop.
- Phased Array Antenna Structure is passively controlled by use of thermal coatings and high performance insulation blankets.

4.3.9.2 Heat Generating Pallet Mounted Equipment

The power supply, frequency, source, and transmitter/receiver units dissipate a maximum of 147 watts and are mounted to the experiment pallet segment cold plates (approximately 750 mm x 500 mm). In addition, all exposed surfaces will be covered with multilayer insulation blankets to limit both the heat exchange between the surrounding pallet structure, and to minimize heat infiltration from external radiant fluxes. The equipment temperature, during all operational modes, will be limited to the temperature range 10°C to 50°C.

4.3.9.3 Passive Pallet Mounted Equipment

The Phased Array Antenna structure is thermally controlled by passive thermal coatings and high performance insulation blankets in order to minimize the temperature extremes resulting from external radiant fluxes and surrounding pallet structure.

Preliminary estimate for the resulting maximum/minimum antenna structure temperature is a range of +110°C to -125°C for the radiant flux extremes encountered in operation. Special thermal design consideration is given to the antenna in order to minimize the induced thermal stresses over the 2800mm x 2800 mm aluminum Honeycomb structure. These design features include the following:

1. Provide sufficient conductive coupling across the Honeycomb structure to minimize the temperature gradient of opposing Honeycomb face sheets.

2. Utilize appropriate thermal coatings on the interior side (opposing) of the Honeycomb face sheets in order to minimize the radiation coupling resistance.
3. Minimize the induced thermal/structural loading and deflections imposed by the antenna/spacecraft tie-down structure through the use of structurally determinate support structure and thermal isolation at the support points.

4.3.9.4 Spacelab Module Subsystem

The Spacelab Module Subsystem is rack cooled utilizing the Avionics Air Loop. The maximum system heat dissipation is 486 watts which includes a 250 watt allocation for the ROLM digital processor and mass memory units (see Table 4.3-7). The equipment temperature is limited to safe operating levels with a maximum supply air temperature of 22°C. The chassis will be the enclosed or open type designs as required to permit efficient utilization of the rack cooling air. A heat dissipation summary table for the Spacelab Module Subsystem is shown below.

SUMMARY TABLE

Chassis Nomenclature	Qty.	Maximum Heat Dissipation (Watts)
● Power Conditioner	1	75.0
● Transmitter Processor Frequency Source	1	15.6
● Transmitter Beam Processor, I.M. Simulator	1	22.6
● Adaptive Receiver Processor	2	66.0
● Interface Logic	1	47.0
● Control Unit	1	10.0
● Digital Processor/ mass memory	1	250.0
TOTAL DISSIPATION		486.2

5.0 EXPERIMENT PLAN

5.1 GENERAL

The primary purpose of the AMPA Experiment System is to conduct experiments to evaluate the achievable performance of an adaptive multibeam phased array to service and support Maritime and Aeronautical users transmitting NBFM voice or BPSK data at 4.8 kbps. In addition, in order to enhance communication time the users will be located within the Spacelab's instantaneous horizon limits of +70 degrees. It is recommended also that the user terminals be land based on CONUS or on U.S. territory that minimizes the cost impact for installation, maintenance and up-keep of the terminals, especially if the terminals can be located on existing NASA or other government owned facilities.

The user terminals can be very austere, especially those terminals that are planned primarily as interference emitters, and or other terminals that do not require extensive instrumentation to monitor performances. Consequently, it is recommended that many austere transmit and receive terminals be employed as illustrated in Figure 5-1 to increase available experiment time per orbital pass as well as from orbit-to-orbit; however, only few of these terminals need be instrumented for detailed experiment analysis. In addition, it is recommended that some user terminals be implemented in mobile vehicles so that the terminals can be more efficiently relocated and used from one orbital pass to another.

For all of the planned experiments, it is recommended that each "problem" be accurately synthesized by means of computer simulation in parallel with, or prior to, the conduct of the actual experiment in order to determine the expected performance. This will provide a means to correlate theoretical and empirical results that will provide an excellent reference or guideline for the design of future systems.

5.2 COMMUNICATION EXPERIMENTS

5.2.1 General

Communication experiments shall be conducted to evaluate the AMPA Experiment Systems capability to support NBFM voice or BPSK data at 4.8 kbps with a

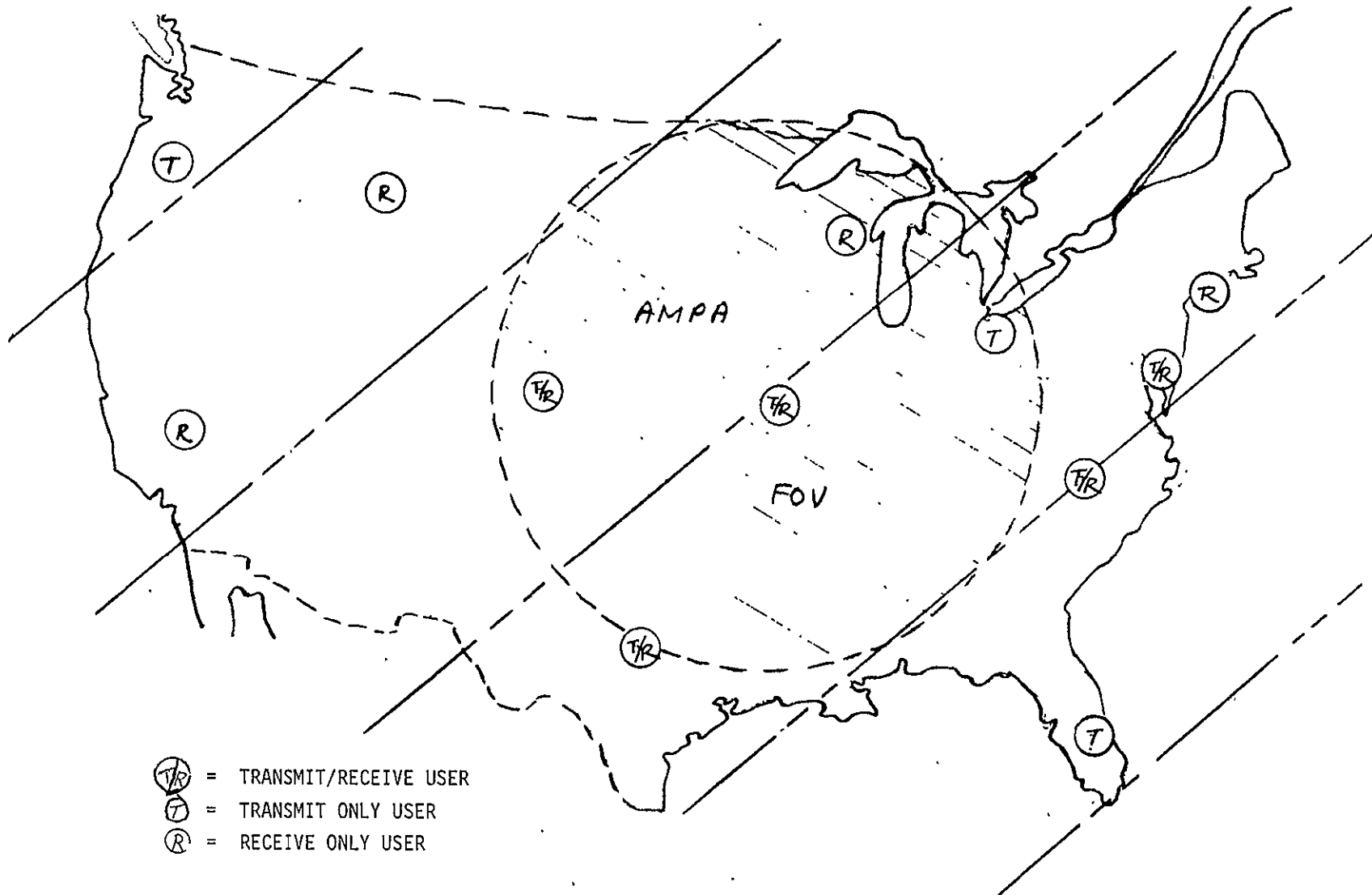


FIGURE 5.1. EXPERIMENT SCENARIO (EXAMPLE)

C/N₀ of +53 dB-Hz for Maritime service, and C/N₀ of +46 dB-Hz for Aeronautical service with users located anywhere within the SpaceLab's instantaneous horizon FOV. To meet these requirements, the user terminal must provide into the upper hemisphere an effective radiated power (ERP) of +8 dBw (typically a radiated transmit power of +10 dBw into a minus 2 dBi hemispherical coverage antenna element) and a receiver sensitivity (antenna gain-to-system noise temperature ratio = G/T_S) of minus 29.9 dB-⁰K.

The candidate communication experiments will be planned to evaluate all three modes of adaption, viz pointed, directed-adaption and fully adaptive on receive, and pointed and open loop beams and null forming on transmit. In addition, the experiments will be performed with and without interference emitters (intentional) that will illustrate the effectiveness of the adaptive process to null the RFI's as well as to track the desired signal.

Other communication experiments include a Frequency Reuse Experiment that evaluates the reuse of the same frequency, using spatial nulling of co-channel users to provide the required isolation. This approach is a much simpler approach than polarization isolation to provide spectrum reuse, and can potentially provide better isolation.

Another communication experiment evaluates the achievable spatial dispersion of IM products with a phased array. This is a most significant experiment since it sizes the back-off requirement for the L-band transmitter amplifier. Less back-off means that the amplifier can operate more efficiently, and ultimately provide the data base that will increase the number of beams that can be simultaneously supported in an advanced system operating in geostationary orbit.

The communication experiments will also be conducted as a function of different aperture size factor (ASF) from a filled array (ASF=1) to a thinned array with an ASF of 4.23 (maximum size that can be hard mounted on a pallet structure without folding the array). This will provide extremely valuable information for future application where high resolution is required and for the spatial dispersion of IM products where computer simulations have shown large improvement in IM suppression as a function of increasing aperture sizes.

5.2.2 Simplex and Full Duplex Modes

The AMPA Experiment System provides two independently steerable beams on receive as well as on transmit that allows simplex communication to be established to 4 independent user terminals, or full duplex communications to 2 independent user terminals. In this case, simplex (or one way) communication will be established to-or-from a user terminal to the Spacelab where the signal modulation and demodulation (Modem) functions are performed even though the ultimate signal terminous may be relayed to-or-from a ground station by way of the TDRSS link as illustrated in Figure 5-2. Full duplex (two way) communication combines two simplex communication, one receive and one transmit, that allows a two way communication to a single user location.

In the simplex receiver mode (return link: user-to-AMPA), the received signal is demodulated and detected, conditioned, and recorded on the on-board Payload Recorder and/or relayed to the ground by way of the TDRSS link.

In the simplex transmit mode (forward link: AMPA-to-user), the signal origination point is always at the ground and its signal is relayed (in digitized format) by way of the TDRSS link, detected on the Spacelab and used to modulate a 70 MHz carrier, and upconverted to L-band for transmission to the ultimate user receiver.

A typical AMPA-User geometry is shown in Figure 5-3 for the Simplex/Full Duplex Communication Experiment, showing 4 user terminals and 2 instantaneous snapshots of the AMPA's instantaneous FOV. First view on the left is for the case when user terminal ① and ② are on the horizon and signal acquisition can be initiated. The second view shows the Spacelab when users ① and ② are broadside of the Spacelab.

The 4 users ① to ④ are located -2, +3, +10 and -15 degrees relative to the flight path as seen from the horizon (left view of Figure 5-3); and in particular, users ① and ② are separated in azimuth by 5 degrees. This geometry is selected so that the angular separation is approximately equivalent to the first natural null of the AMPA array with an ASF of 4.23, but represents about one-third the HPBW for a filled array (ASF=1). This will allow evaluation of the scenario as a function of the array HPBW.

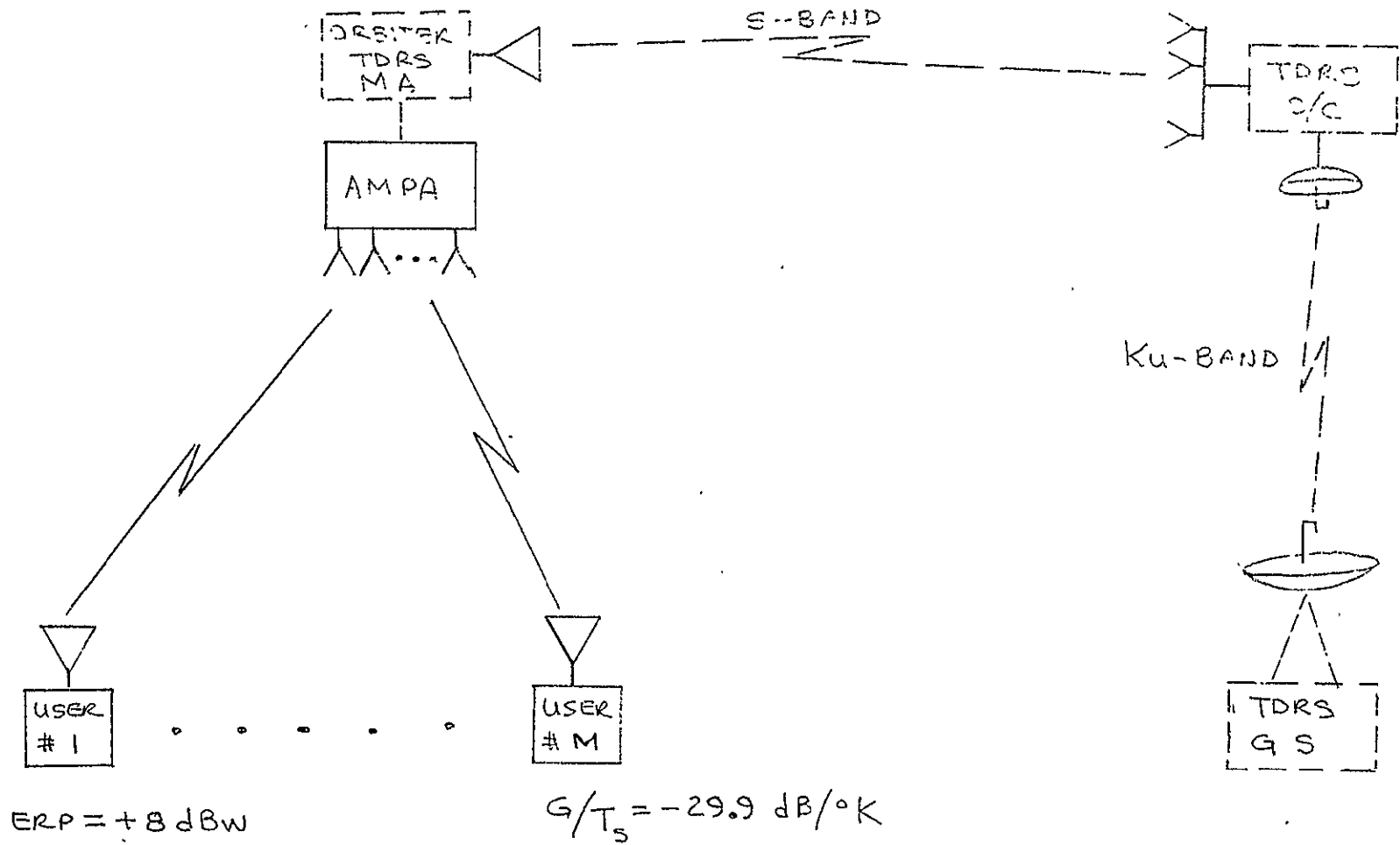


FIGURE 5-2 COMMUNICATION EXPERIMENT SIMPLEX MODE

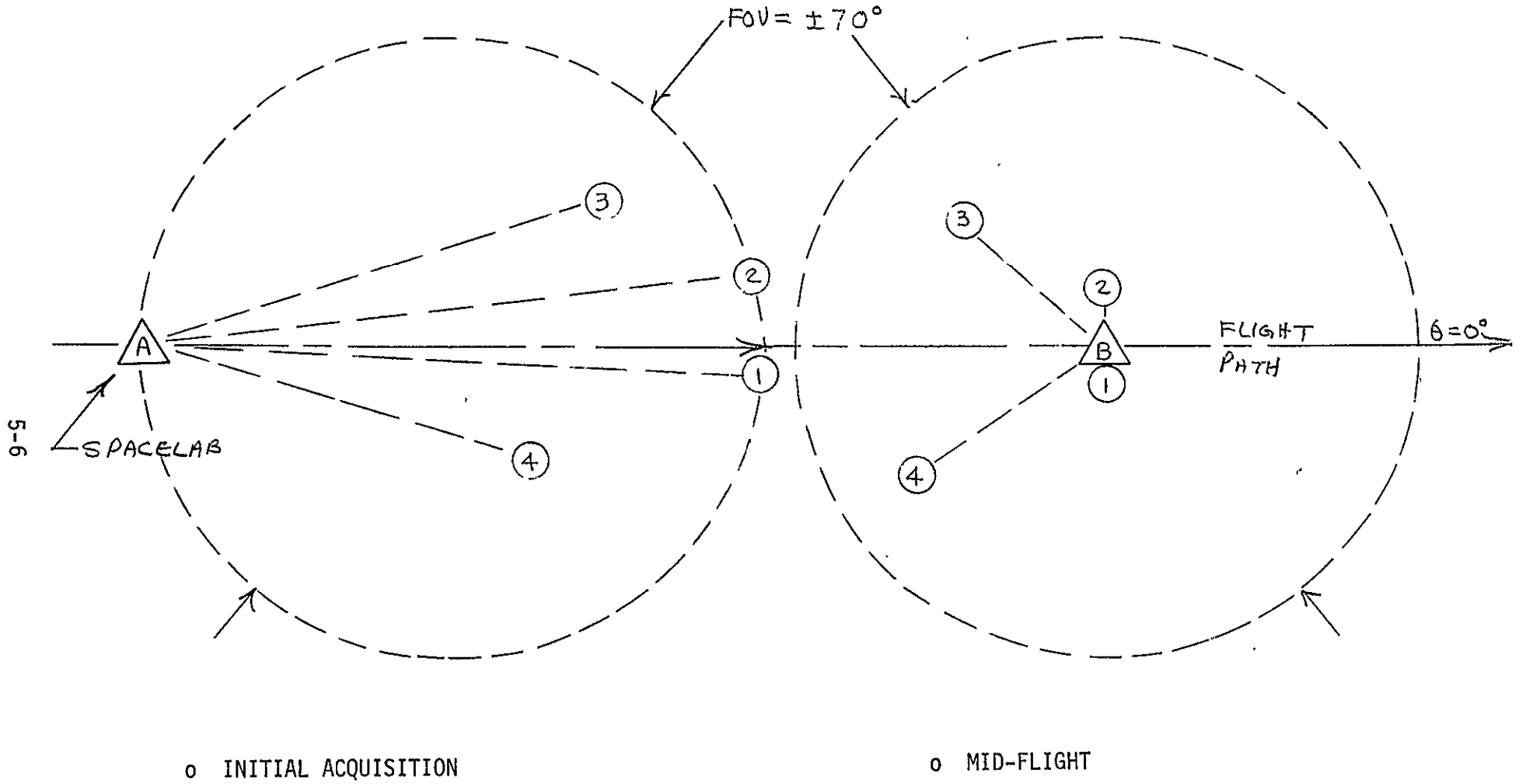


FIGURE 5-3 TYPICAL AMPA USER SIGNAL SCENARIO FOR COMMUNICATION EXPERIMENT

Using this signal scenario, the following Table 5-1 shows typical simplex and full duplex communications experiments that can be conducted with just the 4 user terminals. Referring to Case A in Table 5-1, as an example, two return beams have been formed to users ① and ③ where the "○" represents that the user terminal is a desired user. The comments column shows that the beam to user ① is in the fully adaptive mode and to user ③ can be either in the directed-adaption or pointed modes. When flying over other similar scenario's on the same orbital pass a pointed beam can be used on one scenario and the directed-adaption on the other. Referring back to Case A, the forward link is pointed or open loop to both users ② and ④. Case A represents a scenario without RFI's.

Referring to Case B as another example, users ① and ③ have both transmit and receive capability. In the return, a fully adaptive beam is formed on user ① and user #2 has become a co-channel RFI to user ① and is shown as \triangle_1 . Similarly, user #4 is an RFI to ③ that is operating in the directed adaption mode. On some similar passes, a pointed mode should be used to demonstrate the effectiveness of the adaptive system to place the interferers into spatial nulls.

In the forward link direction for Case B, an open loop beam and null forming (OLB & NF) is used on user ① with user #2 becoming a co-channel user operating in the same channel as user \triangle_1 . Therefore, it is desirable to form a null in the direction of user #2. Since he is in a sense, a co-channel RFI to user ① in the transmit direction, he is shown as an interferer \triangle_1 . Similarly, user #4 is an RFI to desired user ③ and is shown as \triangle_3 . An open loop pointed beam is used on user ③.

Case C is in the simplex return link mode with user #2 and #4 used as RFI's for users ① and ③, respectively.

Case D is also in the simplex return link mode, but users #2, #3 and #4 are all used as RFI's to desired user ①, resulting in a 3 RFI signal scenario. This signal scenario can be demonstrated in all 3 adaptive modes, pointed, directed-adaption and fully adaptive.

TABLE 5.1. LIST OF SIMPLEX AND FULL DUPLEX COMMUNICATION EXPERIMENTS

CASE #	TYPE	LINK DIRECTION	SPACELAB		USER		COMMENTS
			#1	#2	#3	#4	
A	SIMPLEX	RETURN	①		③		o Fully Adaptive ① o Directed - Adaption or Pointed ③
		FORWARD		②		④	o Pointed ② and ④
B	FULL DUPLEX	RETURN	①	△1	③	△3	o Fully adaptive ① o Directed - adaption or pointed ③
		FORWARD	①	△1	③	△3	o Pointed ③ o OLB & NF ①
C	SIMPLEX	RETURN	①	△1	③	△3	o Fully adaptive ① o Directly-adaption ③
D	SIMPLEX	RETURN	①	△1	△1	△1	o Fully adaptive ① o Directed-adaption or Pointed ①
E	SIMPLEX	FORWARD	①	△1	△1	△1	o Pointed ① or o OLB & NF ①

Notes:

- ○ indicate desired signal
- △ indicate interference sources

Case E is similar to Case D but for the forward link - transmit direction; and both pointed beam and open loop beam and null forming modes will be evaluated.

Similar scenarios as shown in Figure 5-3 can be set-up in various areas on CONUS, so that similar cases as shown in Table 5-1 can be repeated many times per orbital pass. Some set-ups may be used many times without moving on different orbital passes, and/or the scenario can be readily varied by moving one or more of the user terminals for the subsequent orbital passes.

5.2.3 Bentpipe Mode

The AMPA Experiment System has been designed for operation in the Bentpipe Mode where direct user-to-user communication can be established. In this mode, the experiment system is a frequency translation repeater and provides no modem functions.

Link calculations have shown that the sufficient system margin is available for this tandem link operation to support an output C/N_0 requirement of +46 dB-Hz to user's within a 1200 km range without RFI. A typical signal scenario is shown in Figure 5-4 which shows two typical users ① (transmitter) and ② (receiver) at a maximum range of 1200 km from the Spacelab. This signal scenario provides an available experiment time of approximately 5 minutes which will be adequate to demonstrate performance.

5.2.4 Frequency Reuse Experiment

The Frequency Reuse Experiment is similar to the Simplex and Full Duplex experiments described in Section 5.2.2., and only its ultimate application differs. AMPA Experiment System exploits spatial isolation between co-channel users (receiver and/or transmit) rather than polarization discrimination as the generally accepted approach for frequency reuse.

To illustrate the frequency reuse concept by spatial isolation, refer to a typical spatial geometry of users in Figure 5-5. Assume that the available field-of-view is typically divided into 4 quadrants and that within each quadrant the same frequency spectrums are reused. This concept is referred to herein as Frequency Reuse by Zone. The adaptive system will simply

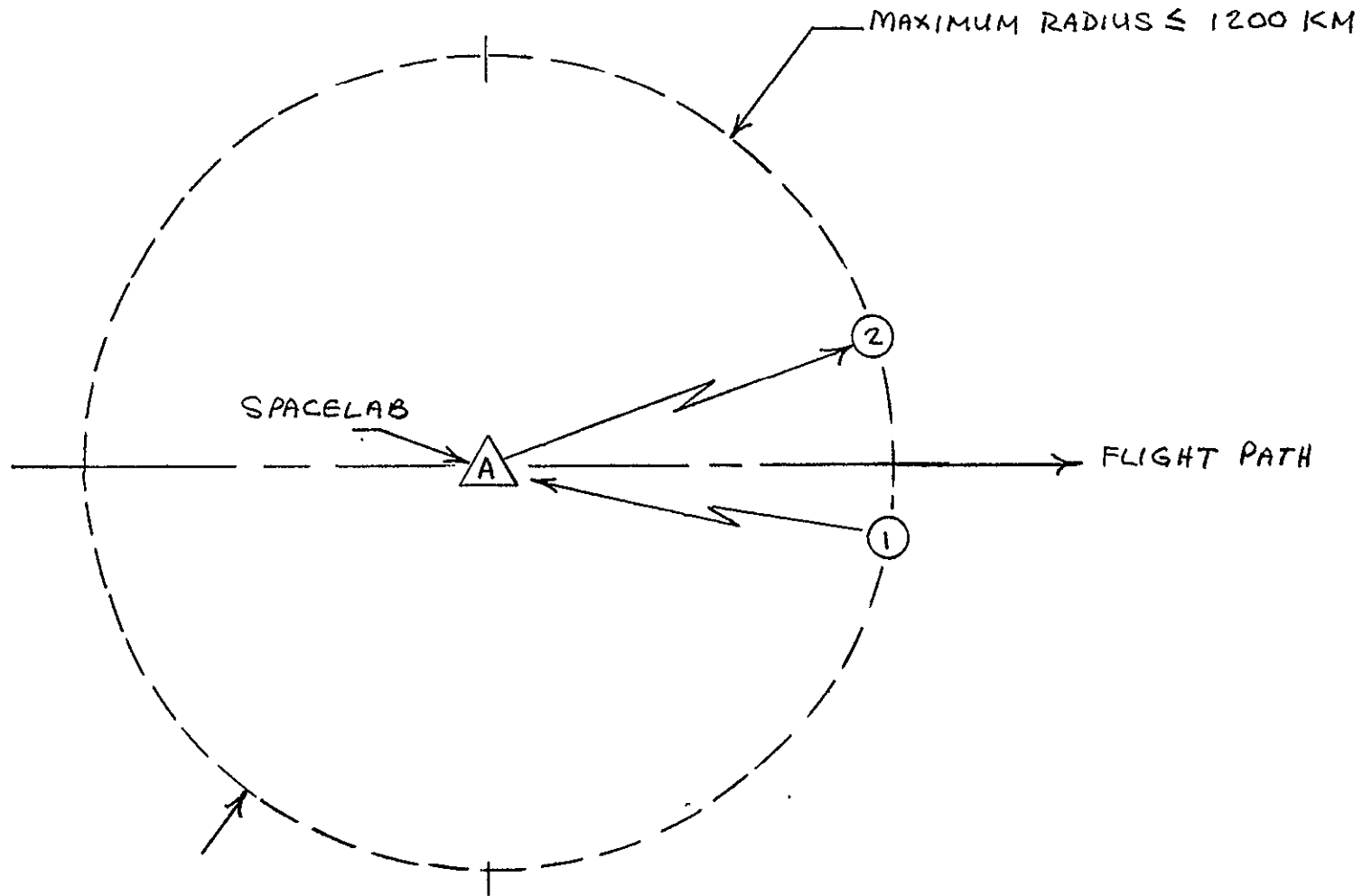
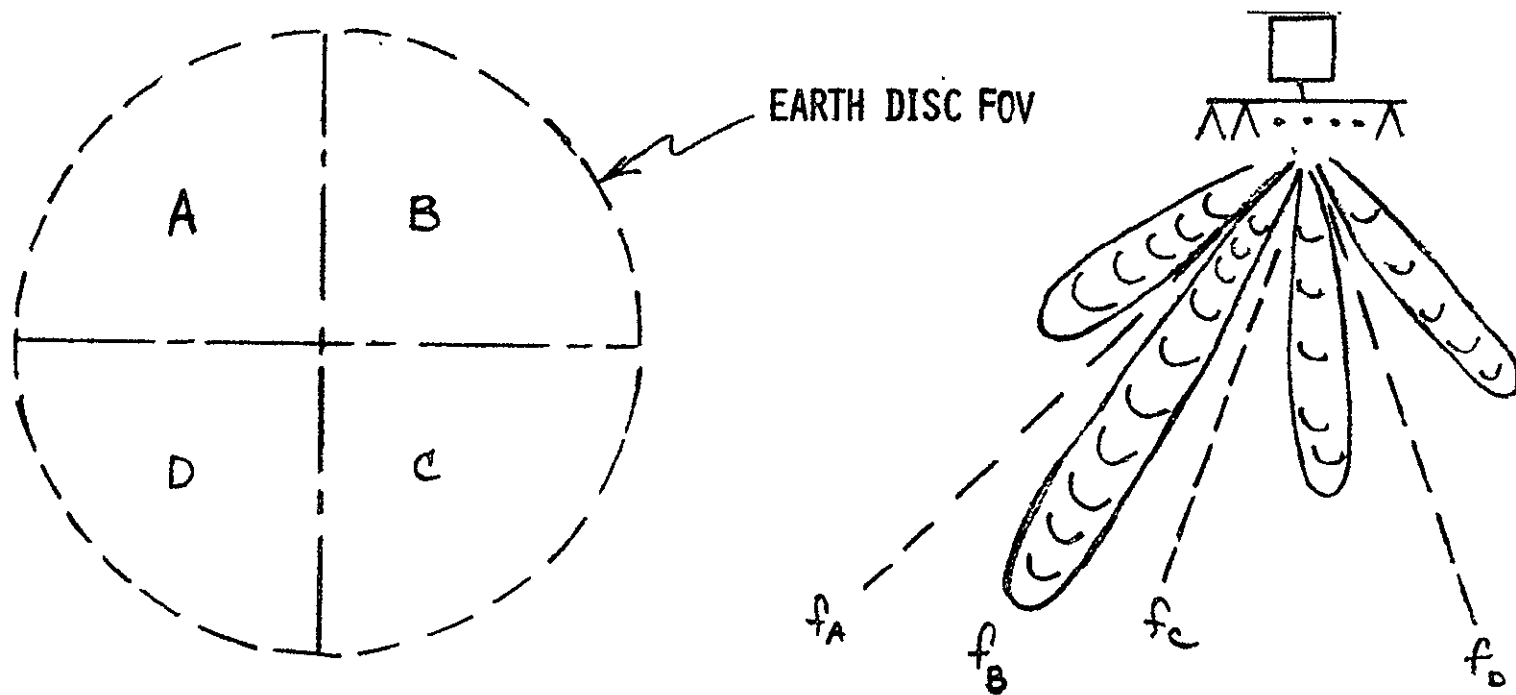


FIGURE 5-4 SIGNAL SCENARIO FOR BENTPIPE MODE EXPERIMENT



- CO-CHANNEL USERS IN ALL FOUR ZONES
- DESIRED USER IDENTIFICATION BY:
 - LOCATION (ZONE)
 - CODE ADDRESS
- ADAPTIVE SPATIAL NULLING OF OTHER USERS ON RECEIVE
- TRANSMIT BEAM:
 - POINTED
 - OPEN LOOP BEAM AND NULL FORMING
- TOTAL CHANNEL CAPACITY INCREASED FOUR TIMES

FIGURE 5.5. FREQUENCY REUSE BY ZONES

treat the other co-channel users in the other zones as RFI's and place them into deep nulls. The directed-adaptation mode is well suited to this zone concept, and the beam will be initially pointed to the desired zone with a pseudo-signal (by software) and then the adaptive algorithm will null the other co-channel users.

In principle, this frequency reuse by zone concept can be applied in both receive and transmit directions. On receive, adaptive process is closed loop and deep nulls can be readily achieved. This has been well synthesized by computer simulations and demonstrated by several hardware systems*. However, on transmit, beam steering and null forming is conducted open loop using the Omniscient Solution to compute the inputs required in the weighting network based upon known signal locations and array parameters. The achievable null depths are dependent upon the accuracy with which the signal and array parameters are known, and upon the amplitude and phase errors in each channel following the weighting network that cannot be eliminated by calibration.

This experiment will provide an excellent basis to determine the achievable performance based upon open loop beam and null forming.

Referring back to Figure 5-5, if we assume a total frequency spectrum of 2.5 MHz, fifty 50 kHz channels are available per zone. With frequency reuse by zone, the number of channels has been quadrupled to 200. Obviously, with more zones, the number of available channels can be increased even more.

5.2.5 IM Spatial Dispersion Experiment

Spatial dispersion of IM products with phased arrays has been synthesized by computer simulation and shown to be very effective, readily providing 10 dB or more IM suppression, dependent upon the signal environment, number of beams and the aperture size factor (size relative to a fully filled array). This experiment will be conducted to empirically evaluate and corroborate the achievable IM suppression as a function of aperture size.

- * (1) NASA - Contract No. NAS5-21653
- (2) Applied Physics Laboratory of John Hopkins University - Contract No. 372285
- (3) Navy - Contract No. N62269-75-C-0079

The AMPA Experiment System has been designed to provide 8 fixed beams from an IM Simulator, in addition to the two independently steerable transmit beams. The 10 beams will be operating on adjacent 50 kHz channels with the variable beams located in the middle. The selection of contiguous channels impose a very severe case that would normally cause large IM products to fall in some channels. Usually, IM suppression in channels is avoided by carefully selecting the operating channels (as in the Babcock channel selection criteria) to avoid these channels. In this experiment, these channels are deliberately included (by using contiguous channels) such that the achievable spatial dispersion of IM products can be better evaluated.

The spatial dispersion of IM products not only minimizes the IM suppression requirements in the L-band amplifier (i.e., less back-off) but can also increase the number of available channels, as well as provide better spectrum utilization.

Figure 5-6 shows a typical experiment set-up for the IM experiment.

One terminal will be instrumented to measure the spectral content of the received signal, and monitor their power level. This receiving terminal will be equipped with 10 calibrated receivers, each of which are tuned to the 10 transmit frequencies used for the 8 fixed and 2 variable beams. The outputs of the 10 receivers*will be recorded and compared continuously during the contact time period. The ratio of the average power levels of the other nine channels-to-the desired channel power represents the achievable spatial dispersion. A spectrum analyzer can also be added to the set-up in order to provide real time comparison of the received signals.

As the 2 steerable beams are varied throughout the flight (the other steerable beam is assumed to be transmitting to another user), the achievable spatial dispersion will also vary, since the performance is a function of the spatial distribution of the signals.

*Alternatively, a sampling receiver can be used that rapidly samples the ten frequency channels.

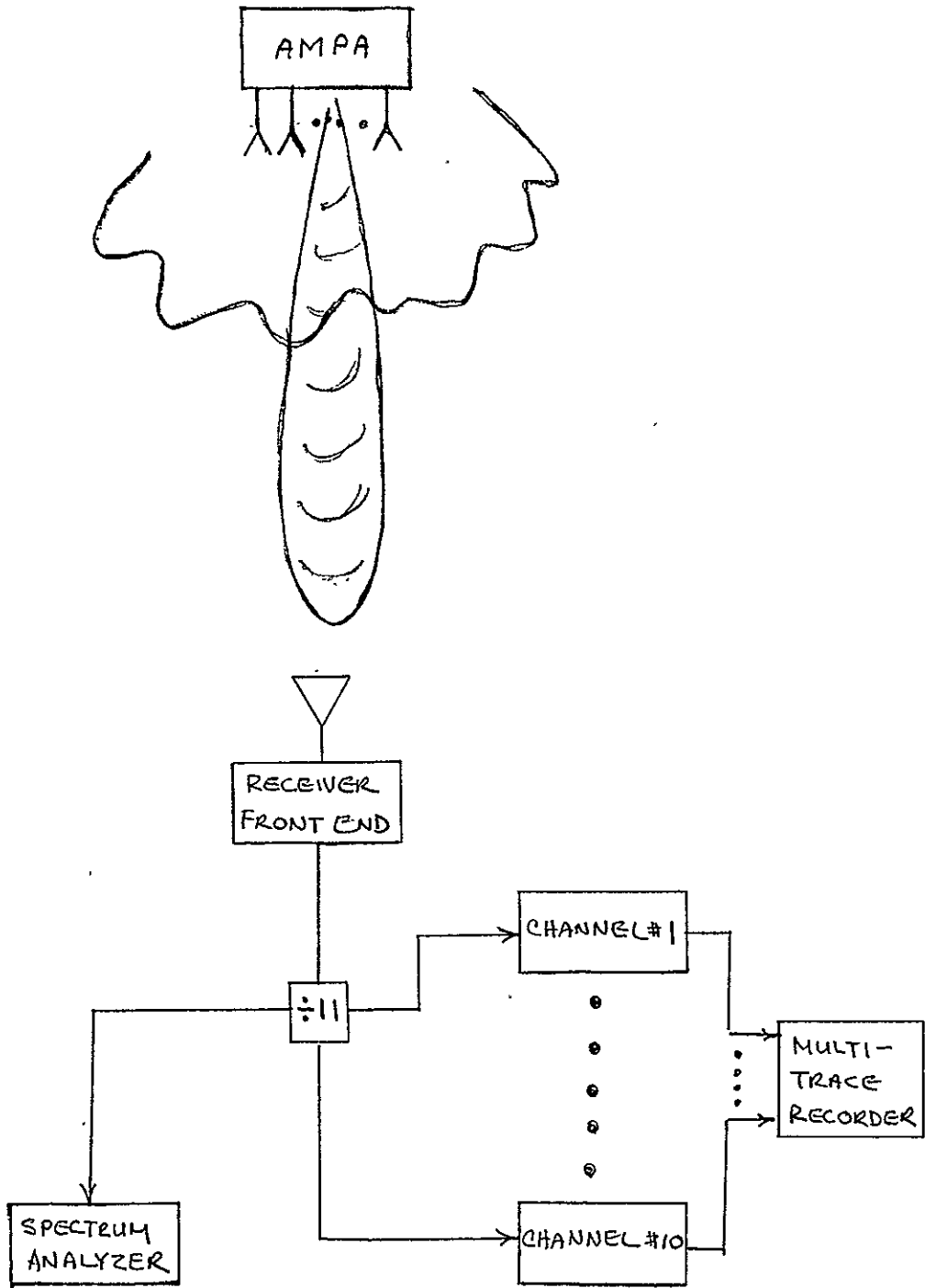


FIGURE 5-6 IM EXPERIMENT

5.3 DIRECTION FINDING EXPERIMENT

The AMPA Experiment from the Spacelab offers an excellent opportunity to evaluate the direction finding (DF) capability of a phased array. A spaceborne platform provides from a single vantage point, the direction finding of signal sources over a large field-of-view, as typically desired for search and rescue missions. Candidate users such as small vessels or aircraft can be implemented with small transmitters that transmit coded distress messages. The AMPA array can search and lock-on to this coded signal and determine their geoposition.

The major concern then is the accuracy to which this DF function can be performed from the Spacelab platform. The accuracy with which DF can be achieved is a function of knowing the geoposition of the Spacelab, the array geometry and phase errors (errors that cannot be compensated for with calibration) in each channel.

Assuming perfect knowledge of the array geometry and Spacelab geoposition, and with an average error of 6 degrees for the 32 receive channels, the resolvable location accuracy of signals at slant ranges of 400, 1000 and 2000 kilometers were computed as a function of the aperture size factor as shown in Figure 5-7. The resolution is plotted as a function of equivalent CEP in kilometer, where the equivalent CEP is defined as the diameter of a circle equivalent in area to the area intercepted by the earth with a beam having the achievable angular resolution. The achievable angular resolution is not the array HPBW, but defined by the relative phase measurement between several elements as in an interferometer system. Combining this concept with the angular resolution of the array allows the signal source to be determined to fractional parts of the array HPBW, limited primarily by the average rms phase errors in the receive channel that cannot be eliminated by calibration. For example, if we assume an average rms phase error of 6 degrees, then we could measure the relative phase between two or more elements (closely spaced so that there will be no ambiguous sidelobes) as in a short baseline (e.g., 1 wavelength) interferometer. The relative phase measurement will allow angular resolution accuracy of $6/360$ or $1/60$ of its HPBW. With several similar measurements with other baselines lengths, the achievable angular resolution can be reduced to

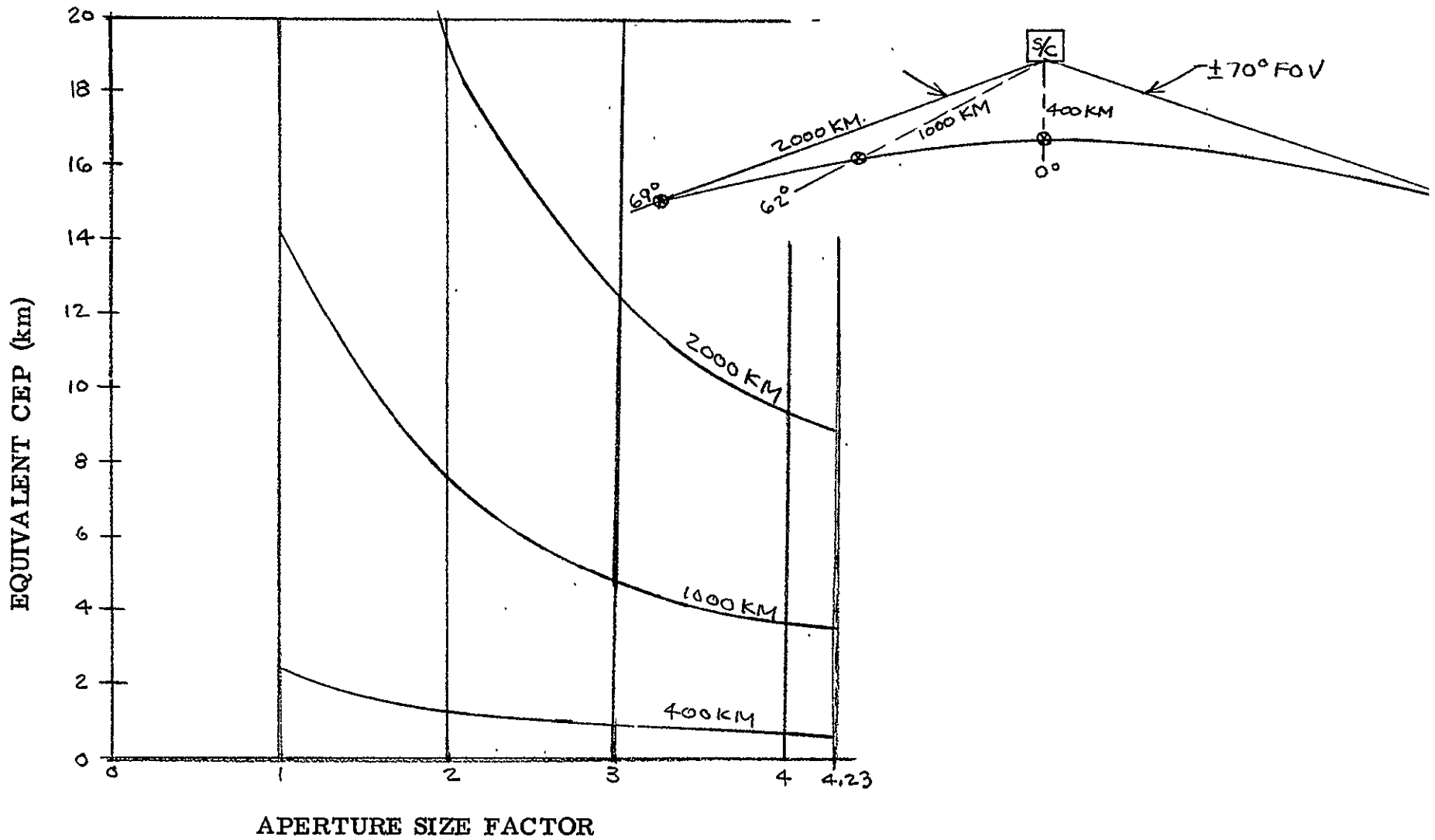


FIGURE 5.7. SEARCH AND RESCUE

1/60 of the HPBW of the AMPA array or approximately 4/60 or 0.0067 degrees or 3.8 milliradians. These measurements must be conducted in at least two orthogonal array directions in order to geoposition the signal location, the more cuts the better the accuracy. Doppler frequency (plus or minus from carrier) is used to resolve spatial ambiguity (i.e., whether the signal is fore or aft of the Spacelab).

Referring back to Figure 5-7 it is noted that the accuracy to which we can locate a source is excellent. Even for targets 2000 kilometers away and near the horizon, the equivalent CEP is approximately 10 kilometers with an aperture size factor of 4.23. Again, it is evident that the variable aperture size is a significant experiment parameter in determining performance capability, and adds to the justification to include it in the AMPA Experiment System design.

5.4 RESOLUTION EXPERIMENT

Resolution Experiment is aimed toward future application, such as for sensor read-out in a dense environment, as in Data Collection, or for personal wrist radio transceiver concept*. In this experiment, several sequential signal scenarios will be tested with two closely spaced equal powered transmit terminals located as shown in Figure 5-8 having different angular separation angle, α_n . Signal ① will be the desired signal of interest, and signal ② will be its co-channel RFI. The purpose of the experiment will be to determine achievable resolution when the desired signal ① can be resolved.

When the Spacelab is in position $\triangle A$, it will receive the first two pair of signals ① and ② with angular separation α_1 . When the Spacelab moves to position $\triangle B$, it will receive the next two pair of signals ① and ② with angular separation α_2 , and etc. In order to provide good data, the angular separation will be initiated with very close spacing of approximately 0.1 HPBW and increased in steps of 0.1 until the angular separation is equivalent to the natural first null of the array.

It is to be noted that the angular separation (α_n) varies rapidly as the Spacelab approaches the signals; consequently, the results of using several sequential pairs will have overlapping experiment results which must be carefully scrutinized to eliminate ambiguities.

*Beckey, I., and Mayer, H., Raising Our Sights for Advanced Space Systems, Astronautics and Aeronautics, July/August 1976

5-18

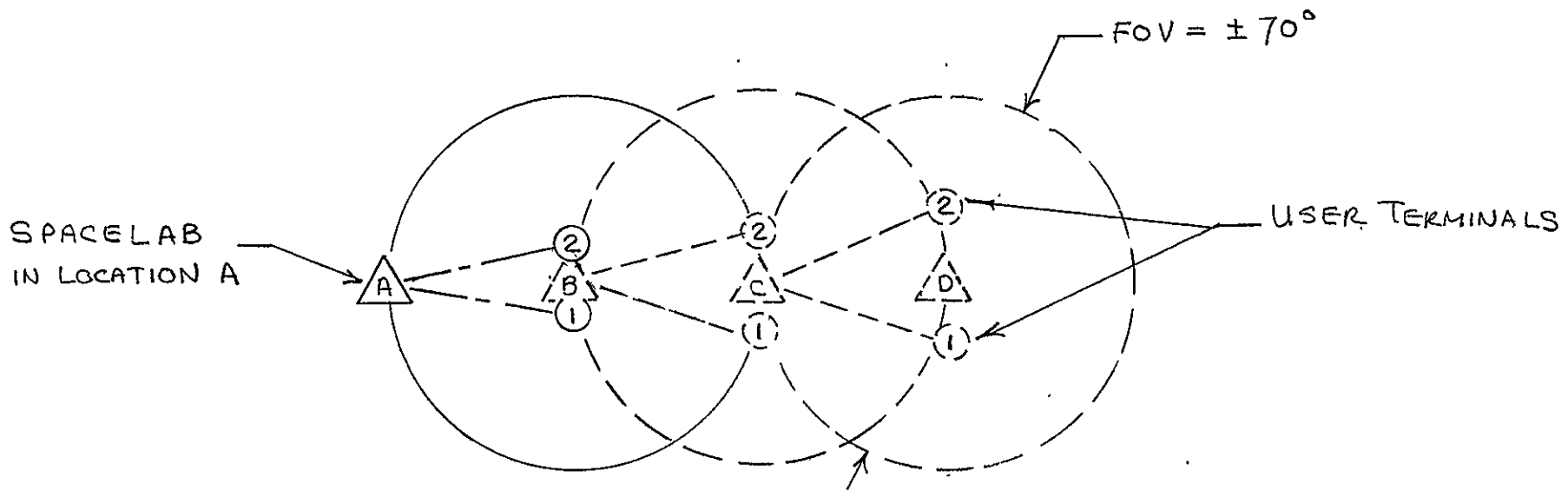


FIGURE 5-8 RESOLUTION EXPERIMENT WITH AMPA

5.5 ORBITAL ANTENNA TEST RANGE EXPERIMENT

The highly mobile Spacelab platform provides an excellent platform for antenna performance measurements of large ground based antennas. Testing of large antenna (e.g., > 100 ft. in diameter) always creates a problem of finding suitable test sites with adequate ground clearance (without obstructions) as well as adequate range to meet the far field range criteria of $2D^2/\lambda$, where D is the aperture diameter and λ is the wavelength.

The AMPA Experiment System is used in this experiment only as a conveniently instrumented test source or as a conveniently instrumented test receiver. In this experiment, the adaptive multibeam capability is not utilized. Typical test set-up is shown in Figure 5-9.

Typically, an L-band signal may be transmitted from the ground antenna, and the signal received and recorded on the payload. A plot of the relative received power will then be a measure of the ground transmit antenna radiation pattern in the plane of the Spacelab flight path.

If the AMPA simultaneously transmitted an L-band signal, the signal can be received and recorded on the ground, and provide an antenna radiation pattern at the receive frequency.

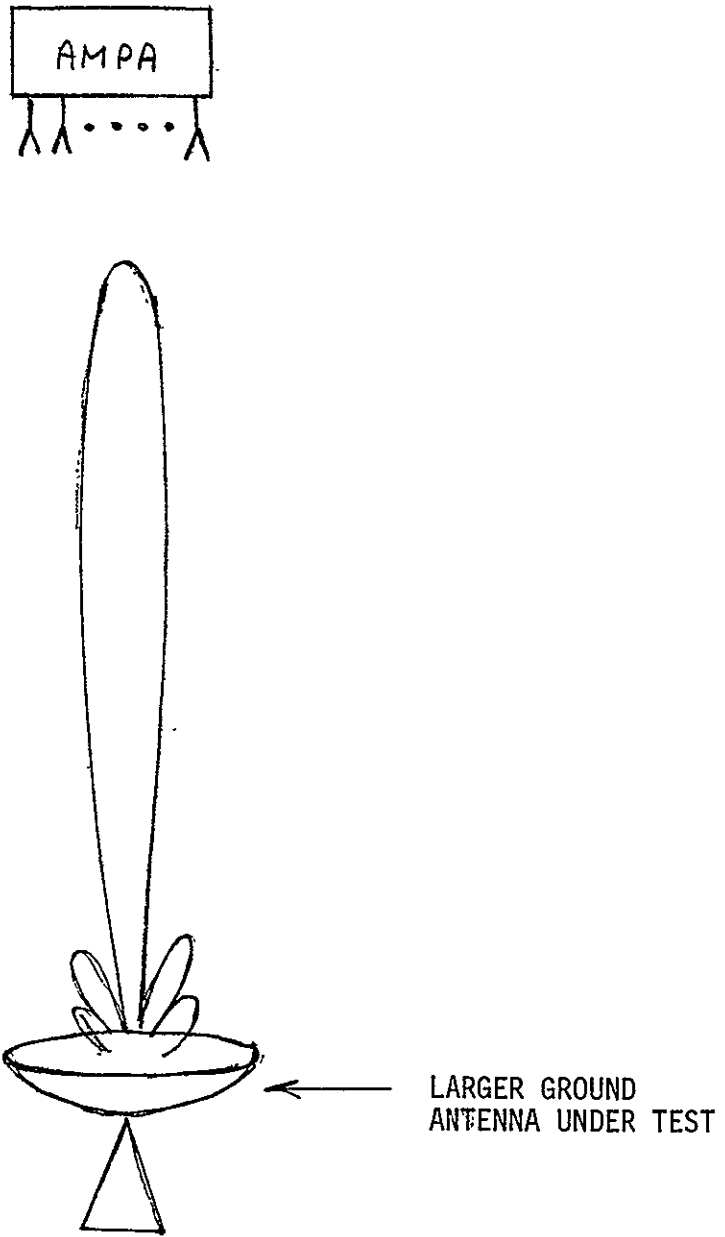


FIGURE 5-9 ORBITAL ANTENNA TEST RANGE EXPERIMENT

6.0 IDENTIFICATION OF PROBLEM AREAS

The AMPA Experiment System is based upon several hardware feasibility systems that have adequately demonstrated on receive the applicable adaptive algorithms and Beam Process on Ground Approach. The AMPA experiment applies the adaptive algorithm and Beam Process on Ground approach to the transmit or forward link directions as well. This concept is new and has not been demonstrated; however, it does not represent a problem. The only unknown is how well it can be done.

An area not clearly defined in the study is the choice in the digital processor for the AMPA Experiment System. The study has shown that the on-board Spacelab Experiment Computer (as we currently understand its characteristics) is inadequate to meet the high speed computation time required to meet the AMPA requirements. However, the Spacelab Experiment computer can be enhanced with an external add-on processor to meet the AMPA requirements; however, the computer must be available full time during the AMPA Experiment phases in order to meet the AMPA requirements.

Alternatively, a separate dedicated digital processor could be used which would be available full time and have the required computation capability to meet the AMPA requirement. Candidate digital processors meeting the AMPA requirements are:

- ROLM 16/64
- IBM AP-101
- NASA Spacecraft Computer #2

as shown previously in Table 4.3-7.

7.0 ESTIMATED SCHEDULE AND COST FOR THE HARDWARE EXECUTION PHASE

Figure 7-1 shows a schedule of the hardware execution phase, based upon the switched aperture phased array configuration for the AMPA Experiment System as recommended herein. The schedule is very short, requiring an overall schedule of 18 months at the contractor, and 3 additional months for integration with the Spacelab. A summary of the 18 months are:

- 1 month to prepare system, subsystem and subassembly design specs
- 1 to 2 months to complete design (no further design tradeoffs are assumed)
- 1 to 2 months for drafting
- Fabricate and qualify one prototype of "like" modules by the end of 7 months
- Fabricate and test flight units of "like" modules by the end of 10 months
- Complete all fabrication and qualification test of singular units in 8 months.
- Complete all subsystem integration tests by the end of the 13 1/2 months after go-ahead.
- Complete all subsystem performance test by the end of the 15 1/2 months after go-ahead.
- Complete AMPA Experiment System integration and performance test at the contractor by the end of the 18th months after go-ahead.

The rapid schedule is based on considerable similarity of subassemblies and modules of the AMPA Experiment System with those previously built by AIL on other adaptive systems.

The overall estimated cost for the hardware execution phase for the recommended AMPA Experiment System design and the previously described schedule is 3900K dollars, exclusive of fee and excluding the digital processor network. The components of the cost estimate are shown in Table 7-1.

TABLE 7-1
ESTIMATED COST FOR THE AMPA EXPERIMENT SYSTEM*

● Program Management	420K
● System Engineering/Analysis	440K
● Design and Fabrication	2500K
● System and Subsystem Test	330K
● System Integration at AIL	110K
● Field Integration Support	100K
<hr/>	
ESTIMATED Rough Order Of Magnitude COST (No fee included)	3900K

 * Does not include digital processor network.

8.0 PROGRAM RECOMMENDATION AND SUMMARY

Since the analytical study has shown the feasibility, practicality and worth of conducting AMPA experiments from the Spacelab, it is recommended that a hardware system be developed and flight tested to verify the achievable performance to demonstrate the viability of employing a multiple beam adaptive phased array in space to support austere Maritime and Aeronautical users or any other austere users located on land, sea or air. The hardware system will develop and establish a design concept for an advanced operational Maritime and/or Aeronautical satellite system(s) that can significantly increase the channel capacity as compared to the current MARISAT or planned AEROSAT systems, and at considerable cost savings to the user terminals. Although no effort has been expended in this study to design the user terminal, it is expected that the savings can extend into tens of thousands of dollars per user. This is so because the user terminal can operate with low gain hemispherical coverage elements that require minimal mounting surface or structure, no stabilization mounts and electronics as well as minimum radome for weather protection. The reduced implementation and cost impacts allow the operational satellite relay system to be available to all Maritime and Aeronautical users that can more effectively service and support the expected increased traffic.

In addition, the hardware system will provide a design basis for selecting an aperture size that can best meet the resolution requirement, as well as the achievable spatial dispersion of IM products with a phased array in the presence of a realistic Maritime and/or Aeronautical user environment. Achieving spatial dispersion of IM products with a phased array will allow the AMPA transmitter to be operated more efficiently, resulting in more efficient use of the prime power which in turn increases the channel capacity of the operational satellite repeater system.

Although the Spacelab test platform provides a unique array environment (high dynamic angular motion between the Spacelab and the user terminal), unlike the geostationary operation orbit, the Spacelab experiment offers an excellent opportunity to evaluate the achievable performances of an adaptive phased array in the dynamic environment. This required a very high speed adaptive process time and convergence speed to acquire, lock-on and track a

desired user while simultaneously nulling interference emitters. This will provide a technology advancement and a base to design future systems requiring high speed adaption in the presence of interference emitters.

In addition, the hardware system can be used to evaluate the use of an adaptive phased array for other application, such as:

- Search and Rescue
- Direction Finding
- Spaceborne antenna test range to evaluate large ground based antennas.

In summary, the Spacelab platform provides a unique opportunity to design, develop and evaluate an adaptive multibeam phased array, but also provides a precursor that minimizes the risk for an advanced operational MARISAT and Aeronautical Satellite System having a greatly increased capacity to service and support future users at a tremendous overall system cost savings.

APPENDIX A

Design Guidelines Used for an Advanced Operational AMPA System in Geostationary Orbit

The existing or planned mobile user communications requirements for the Maritime and Aeronautical Satellite system as summarized in Table A-1 are used as a basis to establish the design requirements for the advanced conceptual system. The Maritime services (MARISAT, MAROTS and INMARSAT) require transmission of high quality voice ($C/N_o = 52$ dB-Hz) and user antenna gain-to-system noise temperature ratio (G/T_s) of -4 to -10 dB/ $^{\circ}$ K and ERP of +31 to +37 dBW; whereas the Aeronautical (AEROSAT) service transmits voice at 46 dB-Hz with user G/T_s of -26 dB/ $^{\circ}$ K and effective radiated power (ERP) of +23 dBW. These known requirements are then used as a basis to forecast the design requirements for an advanced operational conceptual system of the 1980's to support future Maritime and Aeronautical users, as shown in Table A-1, with particular emphasis to maximize channel capacity, and to minimize the implementation and cost impacts on the user terminals. In particular, the operational system will be used to support Maritime users with a C/N_o of 53 dB-Hz, G/T_s of -20 dB/ $^{\circ}$ K and ERP of +21 dBW; and to support Aeronautical users with a C/N_o of 46 dB-Hz, G/T_s of -26 dB/ $^{\circ}$ K and ERP of +23 dBW. Both ERP and G/T_s requirements can be met with a single hemispherical coverage antenna ($G = 0$ dBi) on the user terminals.

In addition, design guidelines were included as secondary design goals for other array related operational applications such as:

- Direction Finding for Search and Rescue
- Multiuser Resolution (i. e., future Data Collection and personalized wrist radios)
- Orbital Antenna Test Range

where these capabilities could be obtained with minimal impact and cost to the primary Maritime and Aeronautical applications.

TABLE A-1. MOBILE COMMUNICATIONS REQUIREMENTS

System	Launch Date	C/N ₀ (dB-Hz)	USER TERMINAL				SATELLITE	
			Gain (dB)	Power (Watts)	ERP (dBW)	G/T _s (dB/K)	Return Channels	Forward Channels
MARISAT	1976	50(F) 52(R)	23	25	37	-4	14	2-14*
MAROTS	1977	52	17	25	31	-10	12	12
AEROSAT	1979	43 46	4	80	23	-26	17	7 4
INMARSAT	1981	52	17	25	31	-10	14	14
ADV. MARITIME SAT. SYSTEM	1985	53	7	25	21	-20	100+	50**
ADV. AERONAUTICAL SAT. SYSTEM	1985	46	4	80	23	-26	100+	50**

*Dependent on Navy usage of UHF channels

**1.1 kW average power source

APPENDIX B
SYSTEM ANALYSES FOR AN ADVANCED OPERATION SATELLITE RELAY
SYSTEM TO SUPPORT FUTURE MARITIME AND AERONAUTICAL USERS

B.1 GENERAL

This appendix includes a detailed tradeoff analysis for an advanced operational multiple access satellite relay system in geostationary orbit to support future Maritime and Aeronautical users. The requirements for the future Maritime and Aeronautical users were estimated as shown in Appendix A, assuming low gain, hemispherical coverage elements on each user.

This appendix includes:

- Link Analysis
- Operational System Tradeoffs
- Computer Simulation of Performance for a fully adaptive and omniscient solution algorithms
- Operational system design

B.2 LINK ANALYSIS FOR OPERATIONAL SYSTEM

Detailed link analyses for the return (user-to-AMPA) and forward (AMPA-to-user) links were conducted for an operational conceptual system located in geostationary orbit to support multiple access Maritime and Aeronautical users. The link budgets are shown in Tables B-1 and B-2, and uses the key user design guidelines established in Appendix A as summarized below:

PARAMETER		MARITIME USER	AERONAUTICAL USER
• C/N_0	dB-Hz	+53.0	+46.0
• ERP	dBw	+21.0	+23.0
• G/T_S	dB/°K	-20.0	-26.0

The link budgets show the calculations for voice transmission of +53 and +46 dB-Hz to support the Maritime and Aeronautical users, respectively. The link budgets are used to size the array (number of elements) requirements as a function of user effective radiated power (ERP) and satellite transmit power as plotted in Figures B-1 and B-2 for the return and forward link, respectively.

TABLE B-1. L-BAND RETURN LINK BUDGET - GEOSYNCH

PARAMETER		VOICE - C/N ₀ IN DB-HZ	
		53.0	46.0
$\Delta Q^{(5)}$	DB	1.0	1.0
C/N ₀ REQ'D ,	DB-HZ	54.0	47.0
K ,	DB/HZ/°K	-228.6	-228.6
ERP ,	DBW	ERP	ERP
α_S (2) ,	DB	193.8	193.8
SYS. MARGIN,	DB	3.0	3.0
G_R/T_S (4) ,	DB/°K	22.2 - ERP	15.2 - ERP
N(3)		32.8 - ERP	25.8 - ERP

NOTES: (1) $C/N_0 = \frac{ERP}{(K)} \frac{(G_R)}{T_S} \frac{\alpha_S}{M}$

(2) α_S = SYSTEM LOSSES (FREE SPACE, ATMOSPHERIC, SCAN LOSS, POLARIZATION, MULTIPATH, DEMODULATION)

= 189 + 0.16 + 2.6 + 0.5 + 0.5 + 1.0

FOR MAXIMUM SLANT RANGE OF 41,132 KM AND $F_0 = 1640$ MHZ

(3) $N = \frac{G_R}{G_{EL}}$ WHERE $G_{EL} = 18.4$ DBI (PEAK)

(4) $T_S = 29$ DB - °K (NF = 2 DB AND LOSSES AHEAD OF PREAMP = 2.25 DB)

(5) ΔQ = CNR DEGRADATION IN SPACEBORNE REPEATER

TABLE B-2. L-BAND FORWARD LINK BUDGET - GEOSYNCH

PARAMETER		VOICE - C/N ₀ IN DB-HZ	
		53.0	46.0
$\Delta Q^{(4)}$	DB	1.0	1.0
C/N ₀ REQ'D,	DB-HZ	54.0	47.0
K	DB/HZ/°K	-228.6	-228.6
G _R /T _S	DB/°K	G _R /T _S	G _R /T _S
$\alpha_S^{(2)}$	DB	193.3	193.3
M	DB	3.0	3.0
ERP	DBW	21.7 - G _R /T _S	14.7 - G _R /T _S
N ⁽³⁾		3.3 - $\frac{G_R}{T_S} - P_T$	-3.7 - $\frac{G_R}{T_S}$

Notes: (1) $C/N_0 = \frac{ERP}{(K)} \frac{G_R}{(T_S)} \frac{\alpha_S}{M}$

(2) α_S = SYSTEM LOSSES (FREE SPACE, ATMOSPHERIC, POINTING, POLARIZATION, MULTIPATH, DEMODULATION).

= 188.5 + 0.16 + 2.6 + 0.5 + 0.5 + 1.0 = 193.3 DB
FOR MAXIMUM SLANT RANGE OF 41,132 KM and F₀ = 1540 MHZ

(3) $N = \frac{G_R}{G_{EL}}$ WHERE G_{EL} = 18.4 DBI (PEAK)

(4) ΔQ = CNR DEGRADATION IN SPACEBORNE REPEATER

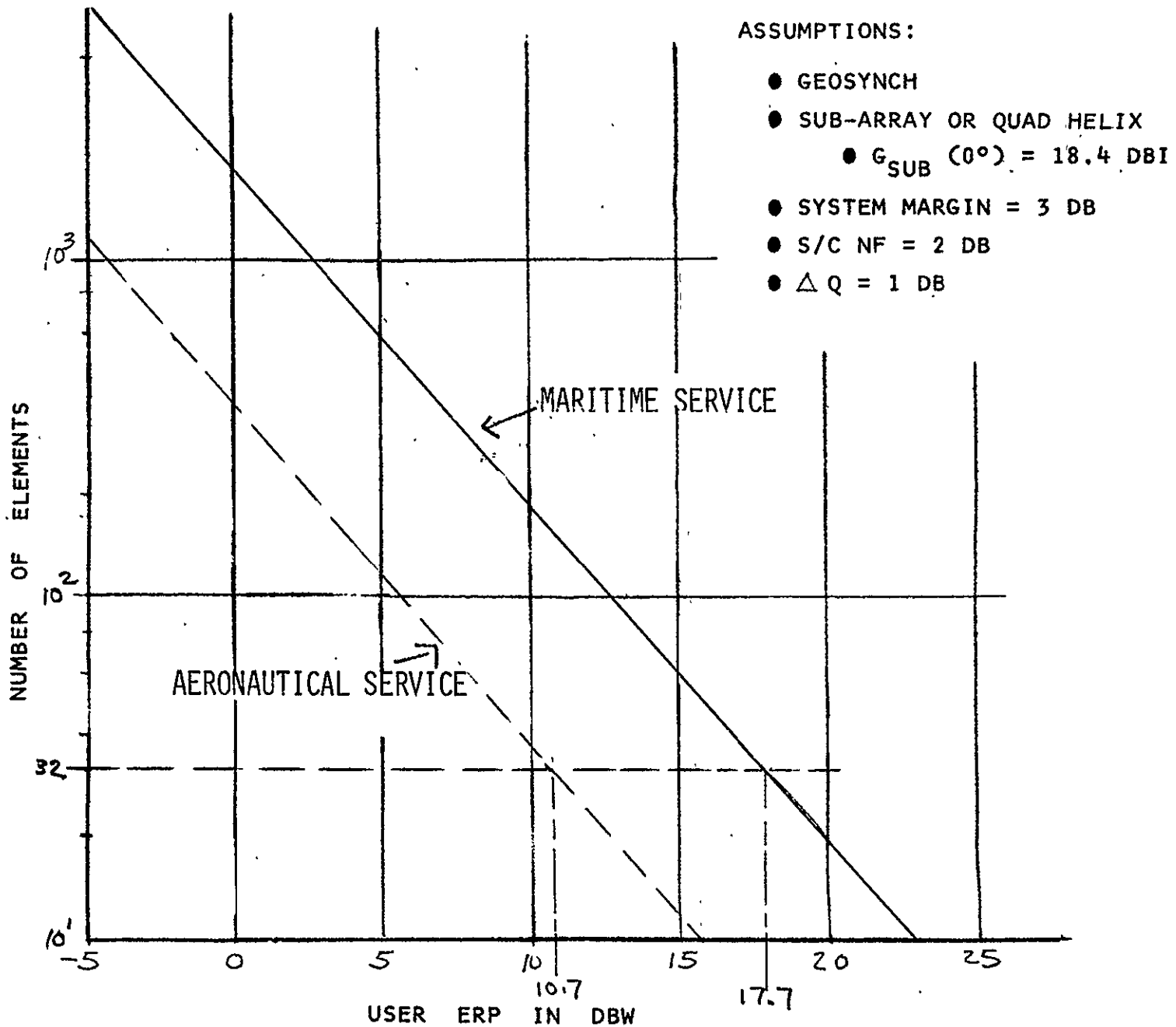


FIGURE B-1. . NUMBER L-BAND ELEMENTS REQUIRED VS: RETURN LINK ERP

B-5

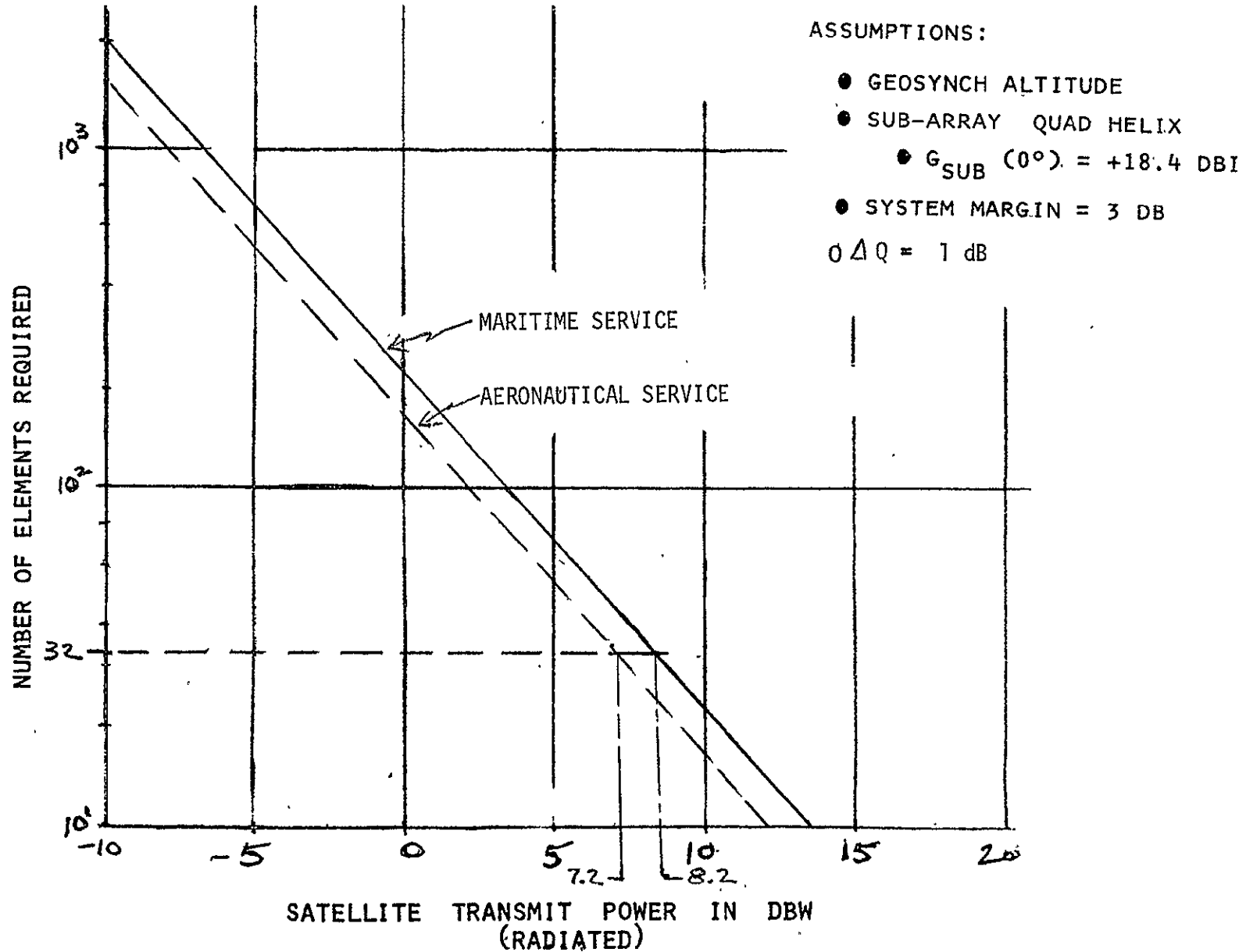


FIGURE B-2. NUMBER L-BAND ELEMENTS VS. SPACE DOWNLINK TRANSMIT POWER

The link budget shows that a spaceborne array of 32 high gain elements ($G_{el} = +18.4$ dBi) can readily support the user requirements including a +3 dB system margin in the forward link (AMPA-to-user) as well as in the return link (user-to-AMPA). In the return link, a user ERP of +17.7 dBw is required for Maritime users, and an ERP of +10.7 dBw for Aeronautical users as shown in Figure B-1. In the forward link, a satellite transmit power of +8.2 dBw is required to service Maritime users with a G/T_S of -20 dB/°K and a satellite transmit power of +7.2 dBw for the Aeronautical users with a G/T_S of -26 dB/°K, using a 32 element array in space. To meet both service requirements, the satellite transmitter will be sized to radiate a transmit power of +8.2 dBw.

In summary, the key operational system requirements are:

PARAMETER		MARITIME	AERONAUTICAL
● Voice C/No	dB-Hz	+53	+46
● User			
● ERP	dBw	+17.7	+10.7
● G/T_S	dB/°K	-20	-26
● Satellite			
● P_T /beam	dBw	+8.2	+7.2
● G/T_S (element)	dB	-10.6	-10.6
● # Elements		32	32
● Array Gain (peak)	dBi	33.5	33.5
● Element Gain (peak)	dBi	18.4	18.4

B.3 OPERATIONAL SYSTEM TRADEOFFS

B.3.1 Overall Operational System Tradeoff Tree

The key tradeoffs to be conducted in the design of the advanced operational conceptual system for geostationary orbit application employing the adaptive multibeam phased array (AMPA) concept, is summarized in Figure B-3 and are

- Adaptive approach
- Location of the beam processor
- Array type

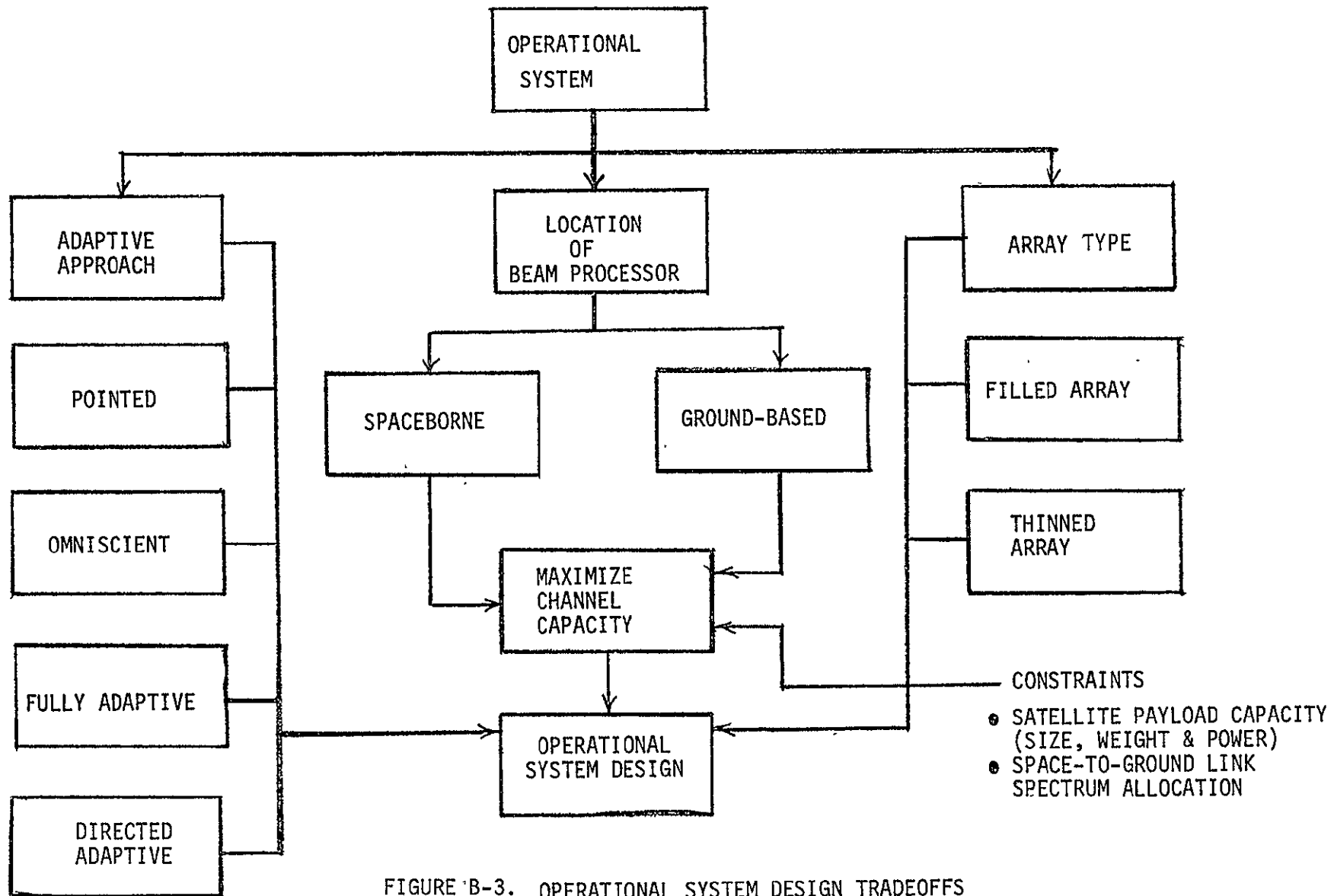


FIGURE B-3. OPERATIONAL SYSTEM DESIGN TRADEOFFS

The results of these tradeoffs are then used to maximize the channel capacity (number of users that can be supported simultaneously) and to design the advanced operational system to support future Maritime and Aeronautical users.

Detailed discussions of the Adaptive approaches are included in Section 3.0 of the report. This appendix however includes computer simulations of performances for the fully adaptive and omniscient solution algorithms conducted for several signal environments.

B.3.2 Computer Simulation of Performance for the Fully Adaptive Algorithm

The selection between competing algorithms requires a definite means of predicting their performance under a variety of operating scenarios. To provide this evaluation tool, AIL has developed computer simulations of all of the preceding candidate algorithms. Of these, the fully adaptive algorithm is the one most suited for the AMPA Experiment System and will be described in greater detail herein.

Referring to the block diagram in Figure B-4, assume that the adaptive antenna has N radiating arbitrarily displaced elements. The combined output of the array is

$$V(t) = \sum_{j=1}^N V_j(t) \cdot W_j$$

where W_j is the complex weighting factor to be updated at the end of each iteration. The signal picked up by the j^{th} element, $V_j(t)$, is a function of the environment which may consist of one desired signal and M RFI's and the thermal noise introduced at the j^{th} element. Assume that the signal, RFI's and the noise are uncorrelated with each other. The mathematical model for the signal-to-interference plus noise ratio $[S/(I+N)]$ can be easily formed. Assuming that reasonable signal processing gain is available and separation of the signal and RFI's is possible, the components of the gradient may be computed according to the following equation:

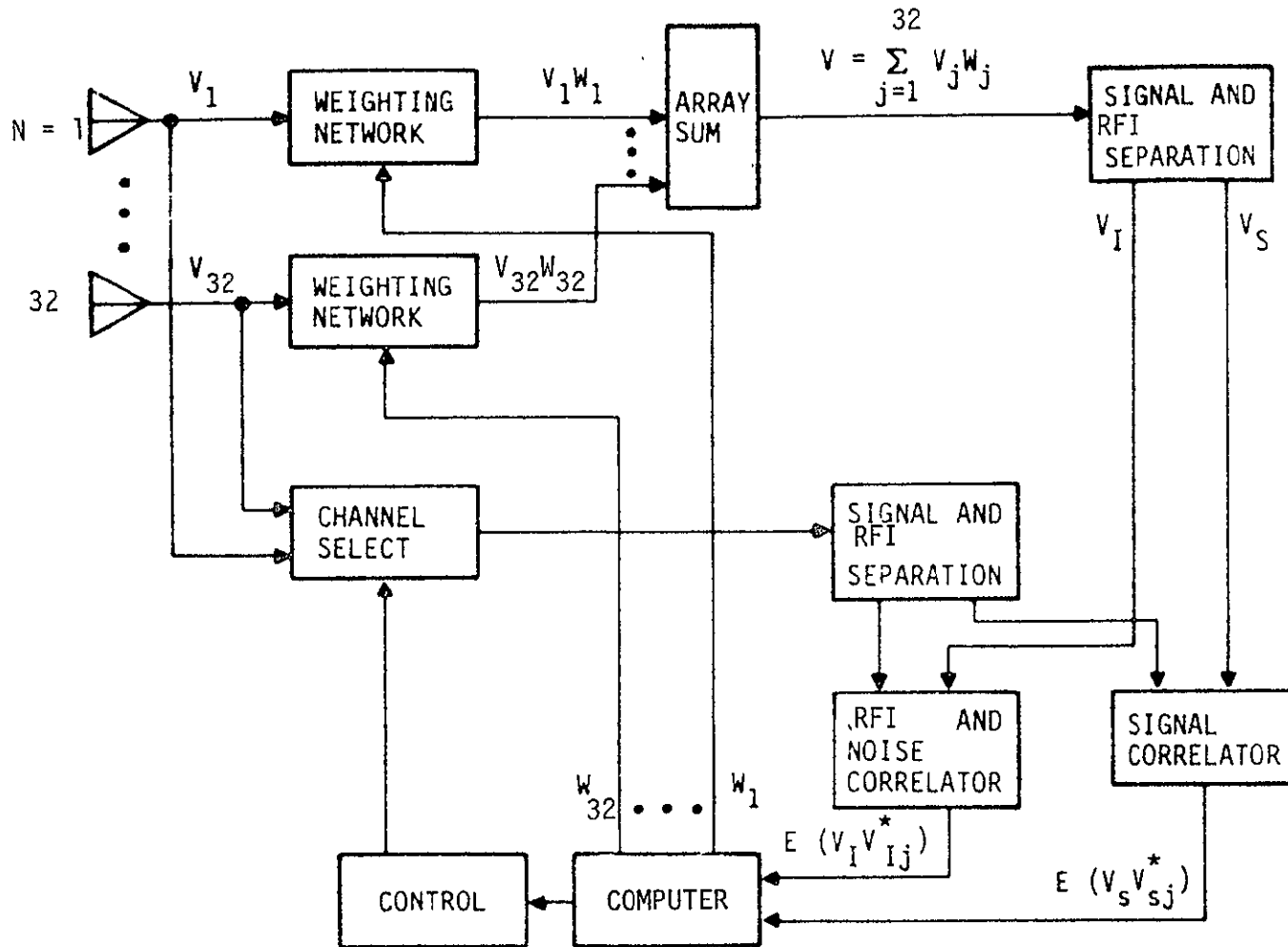


FIGURE B-4. SIMPLIFIED 32 ELEMENT GRADIENT ADAPTIVE PROCESSOR

$$q_j(i) = \frac{E(V_s V_{sj}^*)}{E(|V_s|^2)} - \frac{1}{K_0} \cdot \frac{E(V_I V_{Ij}^*)}{E(|V_I|^2)} \quad j=1, 2, 3 \dots N$$

where $E(V_s V_{sj}^*)$ is the expected value from the signal correlator and $E(V_I V_{Ij}^*)$ is the expected value from the RFI and noise correlator. $Q_j(i)$ denotes the calculated gradient for the j^{th} element, at i^{th} iteration cycle in the adaption process. $E(|V_s|^2)$ and $E(|V_I|^2)$ are the expected signal power and interference power, respectively. K_0 is a weighting factor, used to scale the interference plus noise relative to the signal power.

With the initial weight $[W_j(0)]$ chosen arbitrarily, a set of N new weights is calculated at the end of each iteration as follows:

$$W_j(i+1) = W_j(i) + \beta(i) \cdot q(i), \quad j=1, 2, \dots, N$$

where β is called the step size. Usually, if a small fixed step size is chosen, the convergent time tends to be very long, and if β is too large, the system could be unstable. Therefore, variable step size approaches have to be investigated. One of the solutions is to calculate the dot product of the present gradient $q(i)$ and the previous gradient $q(i-1)$:

$$\cos \theta = \frac{\langle q(i-1), q(i) \rangle}{|q(i-1)| \cdot |q(i)|}$$

where θ is the angle between the two gradients in hyperspace. The resulting cosine function is used to determine an appropriate step size $\beta(i)$ to be chosen for this iteration. The simulation and the experiment shows in many cases this approach can speed up the convergence by a factor of ten.

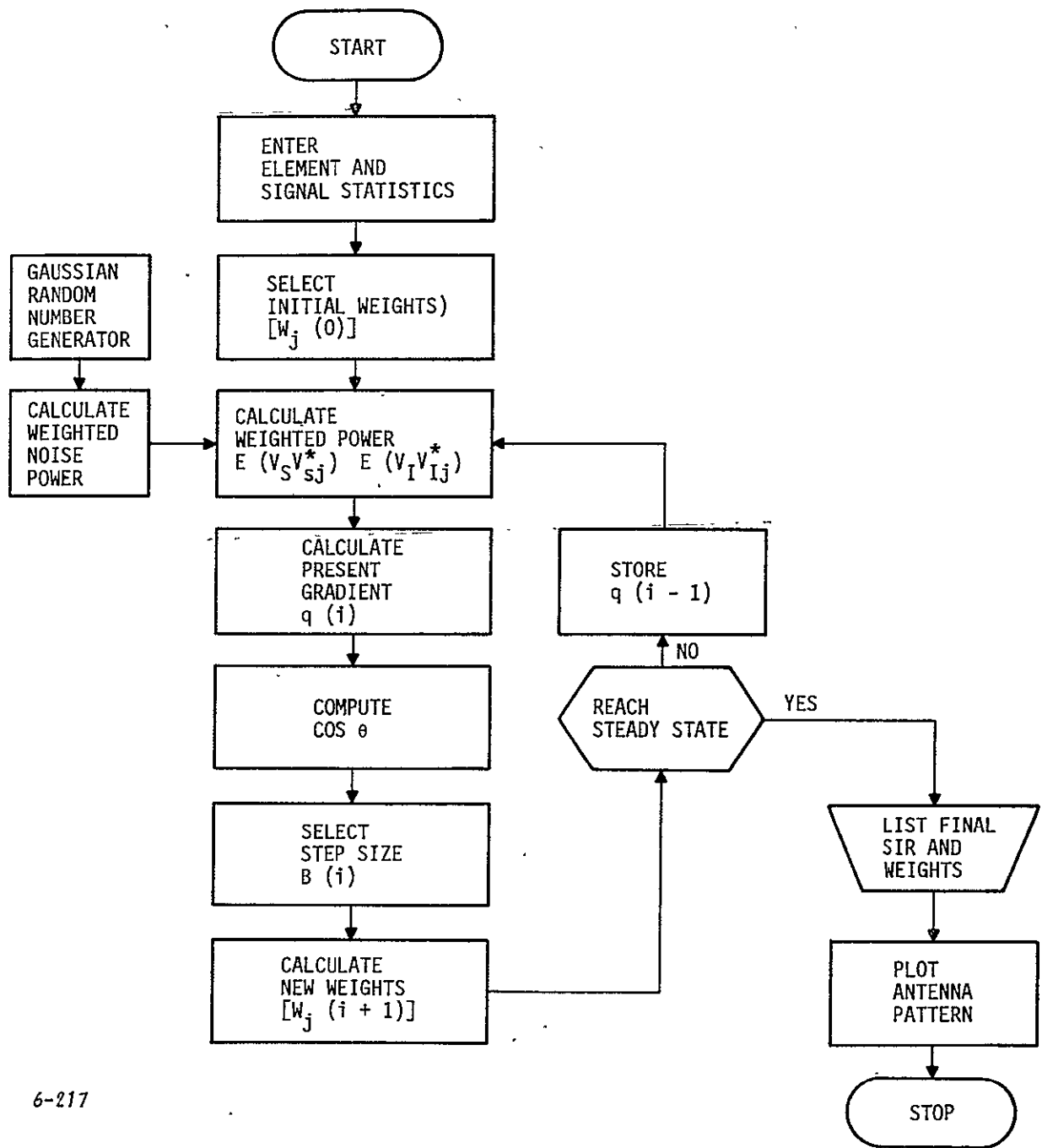
The simplicity of this system model has led itself to system simulation by digital computer. The results of the simulation program are a step-by-step performance evaluation of the adaptive array antenna. The resulting antenna patterns can be plotted directly from the steady-state weights.

Figure B-5 shows the flow chart describing the procedure of the simulation program. At the beginning of each simulation, the correlator outputs were set to zero and the initial weights $[W_j(o)]$ on the array were all the same (for example, $W_j = 1 + j0$ for all $j = 1, 2 \dots N$). During each iteration, noise samples are drawn from a zero-mean fixed variance Gaussian random number generator. The simplest way of generating a sequence of pseudo-random numbers that are Gaussian distributed is to use the Central Limit Theorem, which states that, in the limit, as "n" tends to infinity, the sum of N identically distributed, independent, random variables tend to a Gaussian distribution. Thus, one can convert a sequence of Gaussian distributed numbers $[y(n)]$ by the rule:

$$y(n) = \frac{1}{N} \sum_{i=0}^{N-1} X(nN-i)$$

when N is sufficiently large. For all practical cases, a value of N on the order of 10 yields a reasonably good approximation to Gaussian distribution. Figure B-6 shows a measured distribution from a uniformly distributed random number generator.

As an example of the performance of the system, a simulated response is depicted in two array patterns. The first pattern (Figure B-7) shows the signal (denoted by "S") clearly experiencing the full gain of the array with two RFI's (denoted by "J") being maintained in deep array-nulls as the result of the adaption process. The second pattern (Figure B-8) denotes the impact of directing the adaptive array to a new location, the position of another desired signal "S". Note that the location of the new signal has been positioned within a null of the original adapted array to simulate the case of not only maximizing $S/(I+N)$ but maintaining RFI's within very narrow null patterns.



6-217

Figure B-5. Flow Chart of Simulation Program

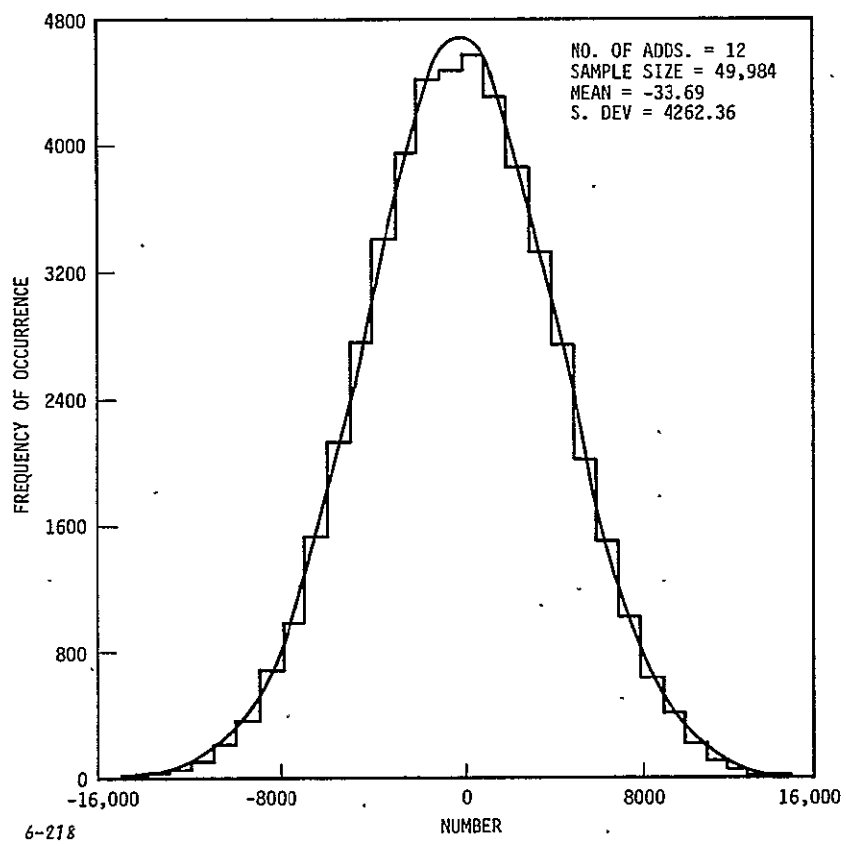


Figure B-6. Histogram of Gaussian Random Number Generator

() = 0 TO 3 DB . = 3 TO 6 DB + = 6 TO 10 DB
 e = 10 TO 15DB \$ = 15 TO 20DB X = >20 DB

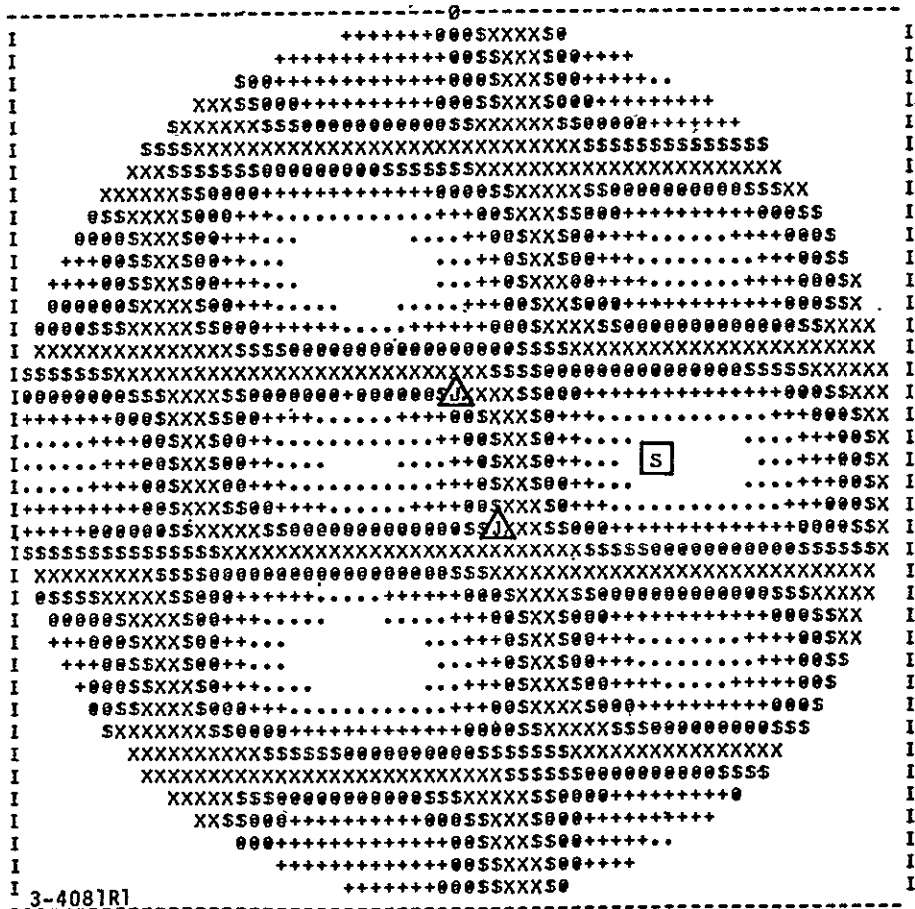


Figure B-7. Typical Array Pattern

To implement a particular set of algorithms, the adaptive processors must supply the command and control functions for the array combining networks and the interface to other systems. All of these factors, together with the desired speed of operations, must be considered in the selection of system components. A digital processor is the center of this activity. During adaptive mode processing, the digital processor must perform the following functions:

- Selection of signal and interference correlator outputs, and blanking of each correlator between readings
- Selection of the unweighted channel input to the signal and interference correlators
- Monitoring of AGC voltages to determine the number of operable channels
- Processing the adaptive algorithm to optimize the $S/(I+N)$
- Scaling of all output weights by normalizing to the strongest signal channel
- Performing directed transmit beamforming as input position vector is updated.

B.3.3 Omniscient Solution Algorithm Computer Simulation

To illustrate computer simulation of the Omniscient Solution, the optimum solution for the 32 element AMPA experiment array has been synthesized under several candidate signal scenarios. The optimum, or ideal, solution is referred to hereafter as the Omniscient Solution and provides the maximum signal-to-interference plus noise $[S/(I+N)]$ solution that is achievable for the given array and signal environment. The candidate signal scenarios used were:

- Single RFI scenario as a function of the angular separation between the desired signal and RFI for RFI's ratios of 0, +10, +20 and +30 dB
- Multiple RFI scenarios as a function of angular separation between the desired signal and RFI #1 (others remained fixed), and with RFI #1/S varied from 0 to +30 dB in steps of 10.

In these scenarios, the input signal levels into the array were selected to provide output carrier-to-noise (CNR) of +7 dB at the scan limits (+70 degrees). With an element gain of +4.2 dBi, this provides a maximum achievable output CNR of +11.2 dB without interference signals when the beam is on boresight.

The AMPA Experiment System array used in this analysis is shown in Figure B-9 in its fully expanded position (aperture size factor of 4.23). For this array geometry, the principal cardinal plane pattern is shown in Figure B-10, and the intercardinal plane is shown in Figure B-11. The resultant half power beamwidths (HPBW) are approximately 4.0 and 3.8 degrees and the angles off boresight to the first null ($\theta_{1st\ null}$) are approximately 4.5 and 4.7 degrees for the principal and intercardinal planes, respectively.

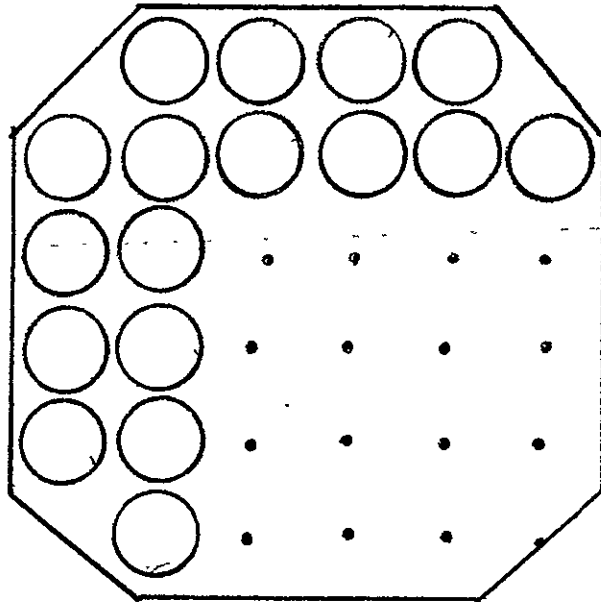
• Signal RFI Scenario

The spatial geometry used for the single RFI scenario is shown in Figure B-12 with the desired signal located on the array boresight (\equiv Spacelab nadir) and the RFI emitter is sequentially moved off boresight. The results of the Omniscient Solution are summarized also in Figure B-12 for interference-to-signal power ratios (RFI/S) of 0, +10, +20 and +30 dB. The results show that the $S/(I+N)$ for all RFI/S are approximately within 2 dB of the maximum achievable SNR (without RFI) at all angular separation greater than one half of the HPBW. It is also seen that the RFI is suppressed to noise level at approximately one-eighth of the HPBW for RFI/S of 0 dB, and depth of RFI suppression for all RFI/S greater than 0 dB is directly proportional to the RFI/S. At approximately 4.5 degrees, the RFI is suppressed by the natural first null of the array pattern.

• Multiple RFI Scenario

To evaluate the array under multiple RFI's, a 3 RFI and 6 RFI scenario as shown in Figures B-13 and B-14, respectively, has been used. In both scenarios, the desired signal is located on boresight and the angular separation between the desired signal and RFI #1 has been varied as shown. All other RFI's have been deployed over the +70 degree field-of-view (FOV) as shown. All RFI/S are initially equal as angular separation is varied; then subsequently repeated for RFI #1/S of +10, +20 and +30 dB. The results are summarized in Figures B-15 and B-16 for the 3 and 6 RFI scenarios, respectively. It is interesting to note in both cases that the resultant $S/(I+N)$

● ELEMENT



● 32 ELEMENT ARRAY

FIGURE B-9. 32 ELEMENT AMPA ARRAY CONFIGURATION

PRINCIPAL CARDINAL PLANE PATTERN

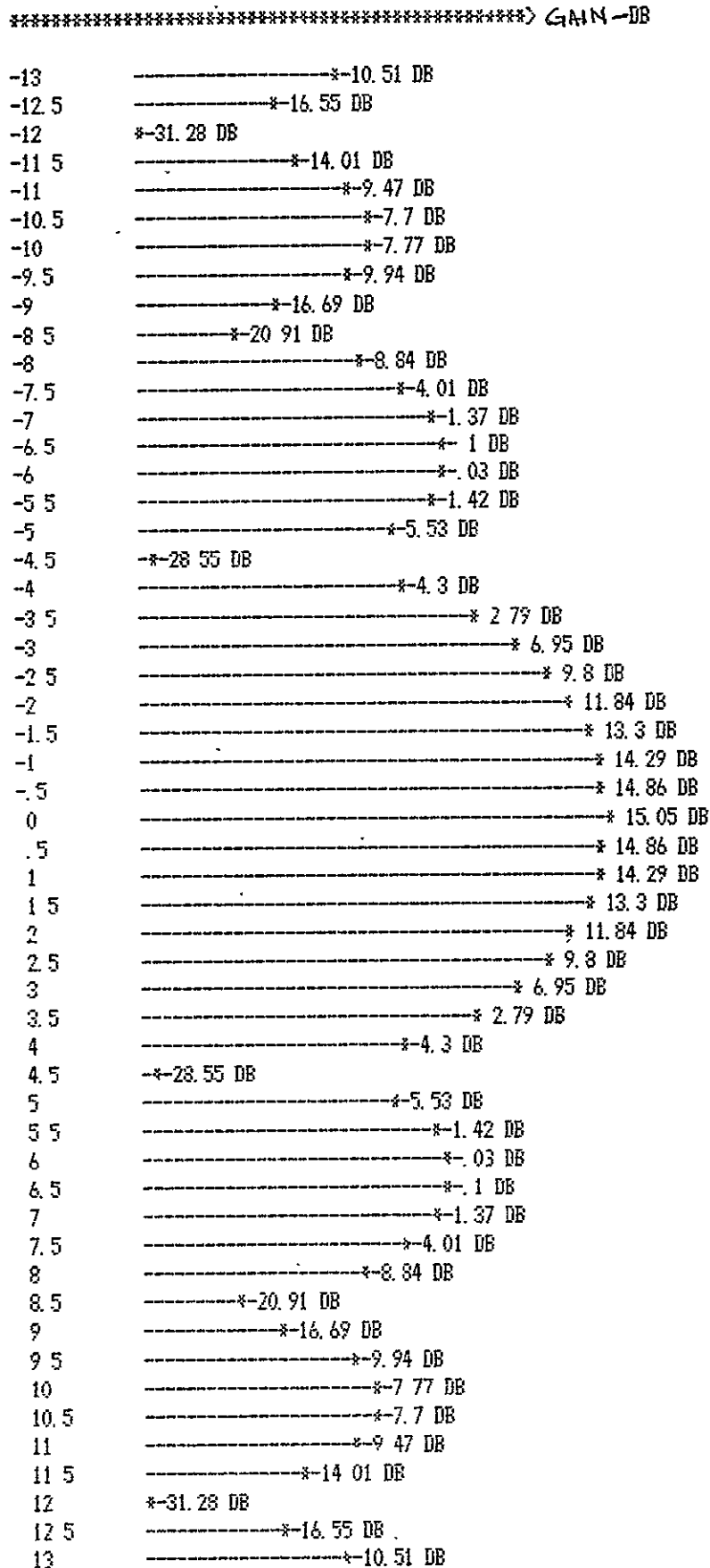


FIGURE B-10. AMPA 32 ELEMENT ADAPTIVE ARRAY
 (APERTURE SIZE FACTOR=4.23 EL HPBW=140 DEG EL GAIN = 4.2 DBI)

INTERCARDINAL PLANE PATTERN

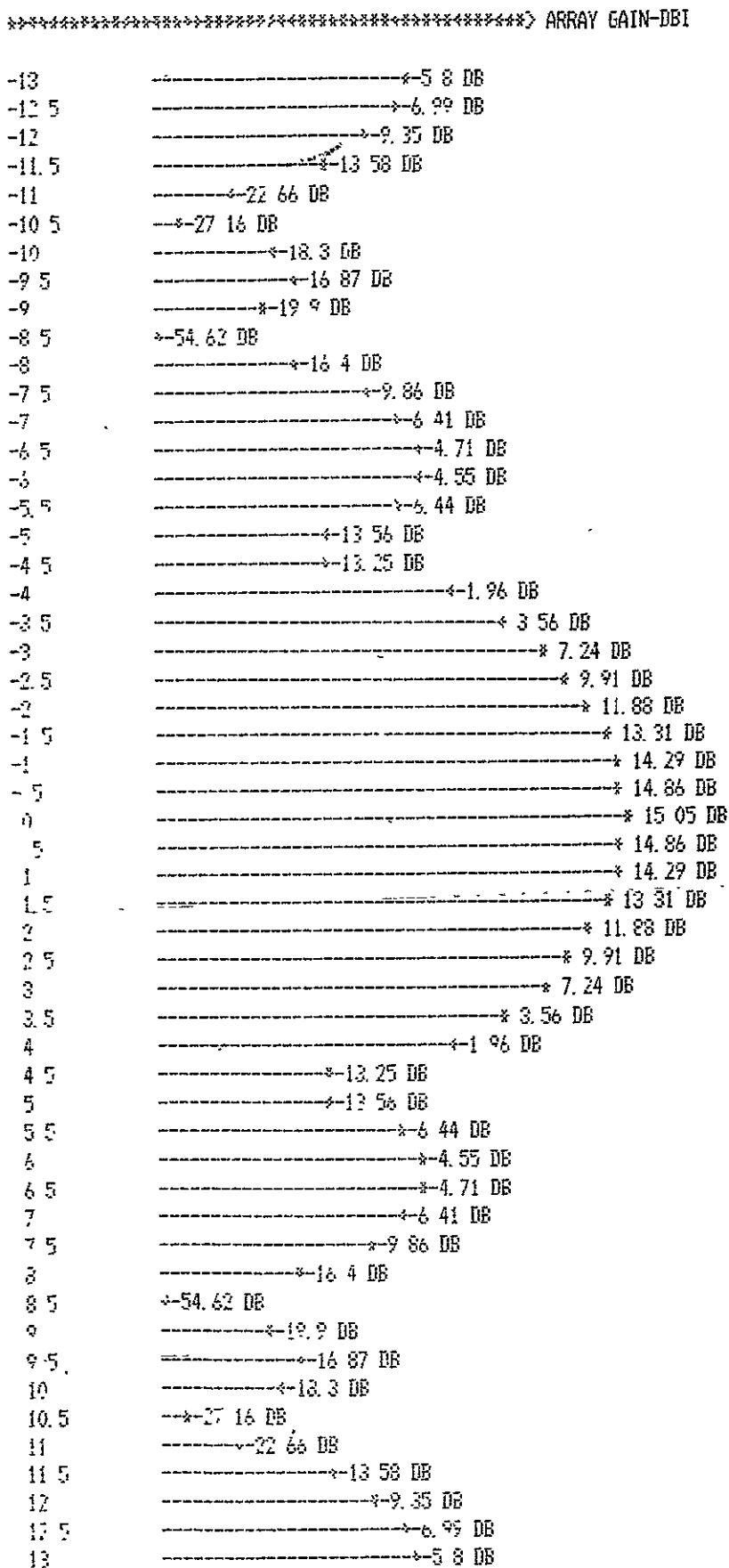


FIGURE B-11. AMPA 32 ELEMENT ADAPTIVE ARRAY
 (APERTURE SIZE FACTOR=4.23 EL HPBW=140 DEG EL GAIN = 4.2 DBI)

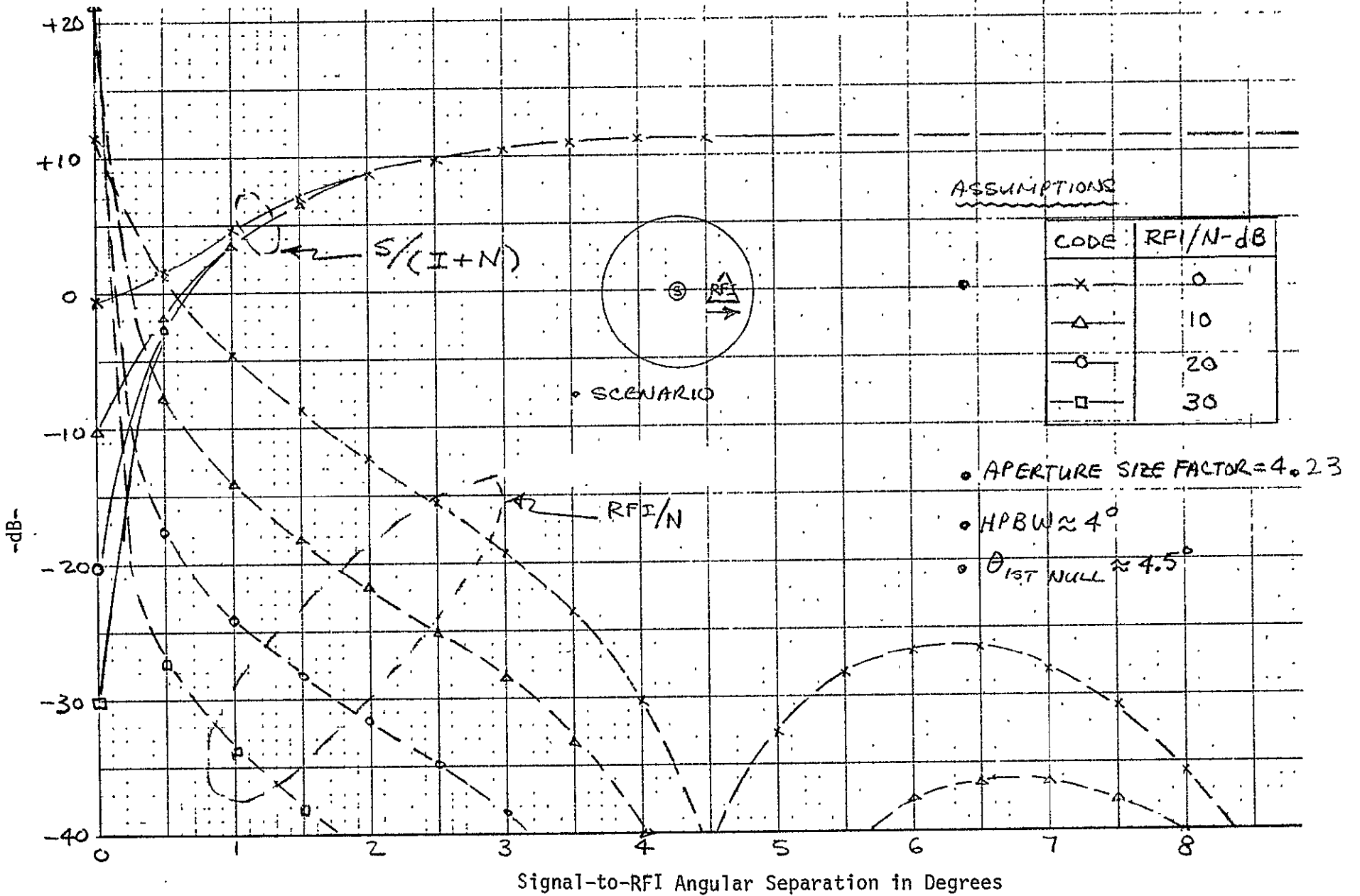
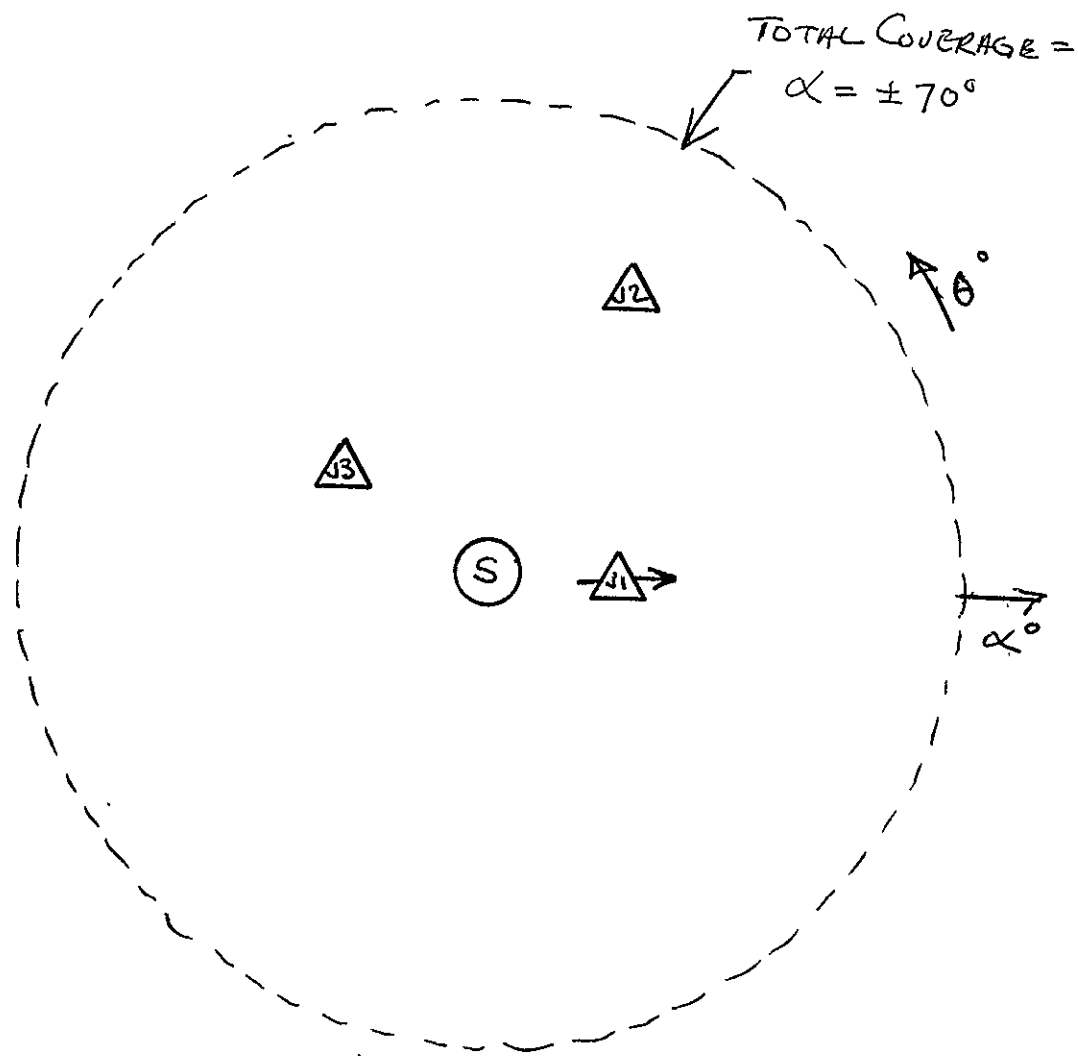


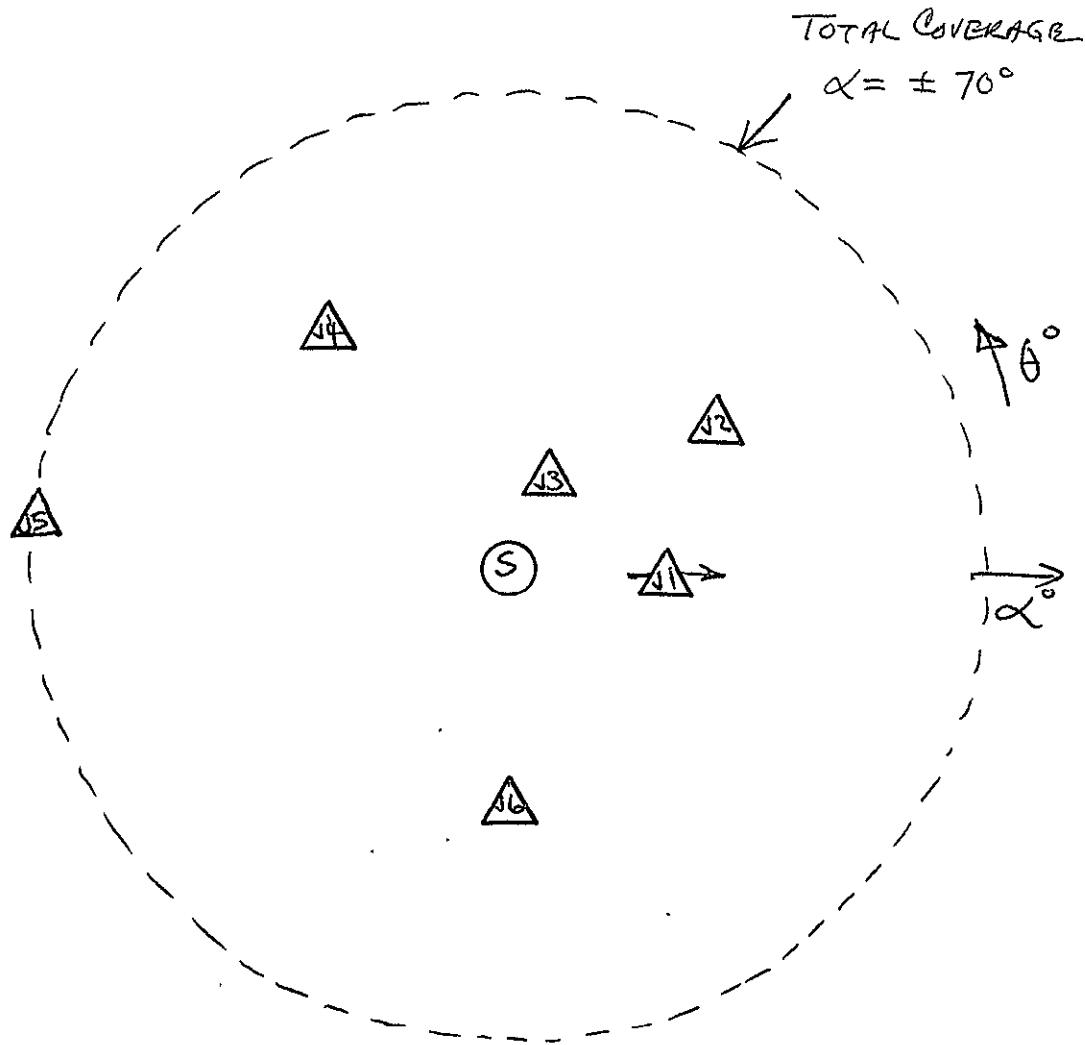
FIGURE B-12. ADAPTIVE PERFORMANCE VS. SIGNAL-TO-RFI SEPARATION
(OMNISCIENT SOLUTION - SINGLE RFI)

B-22



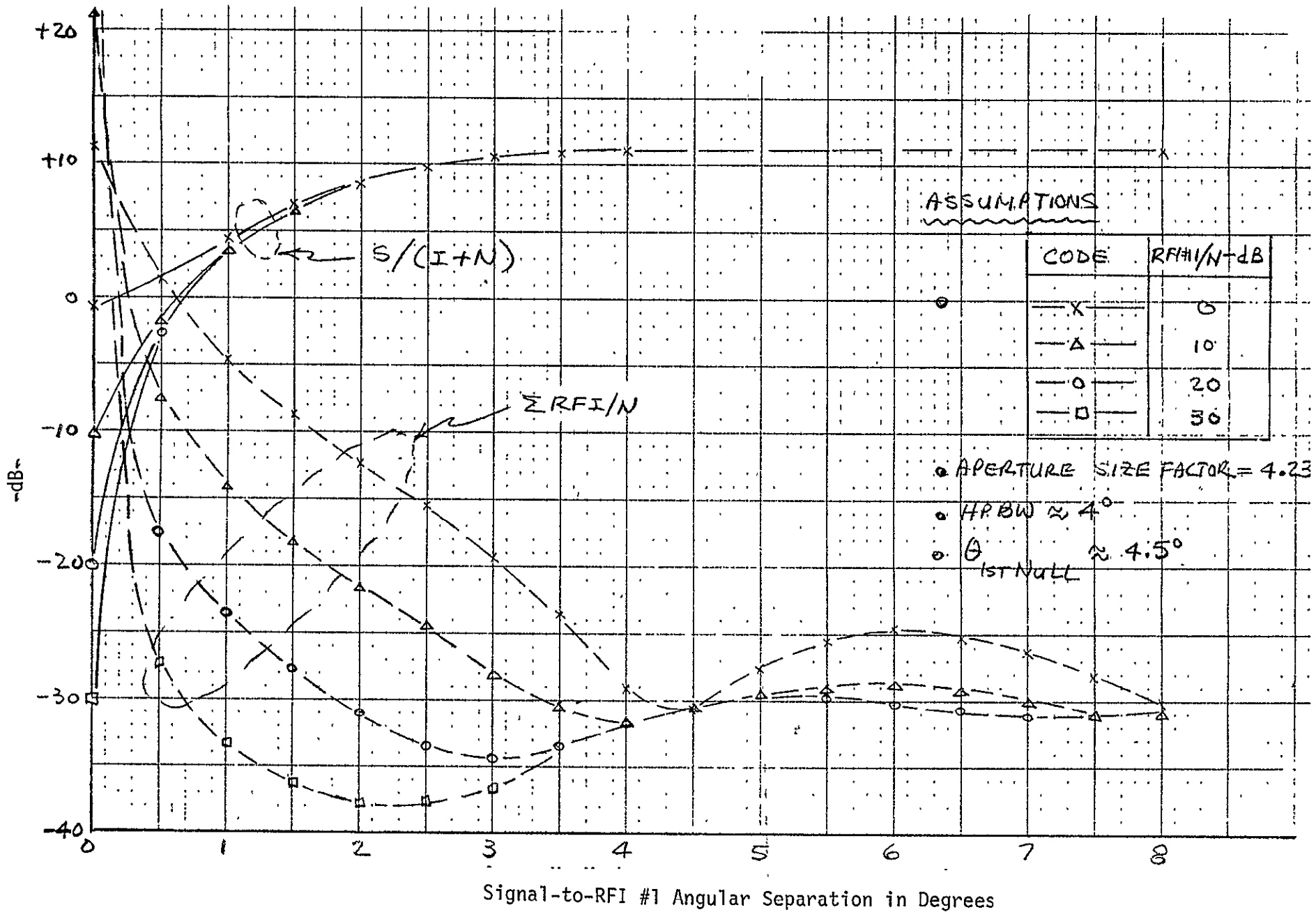
SIGNAL	PWR/EL-DBM	α°	θ°
NOISE	-123		
DESIRED	-131	0	0
JAM #1	-131	Var.	0
JAM #2	-131	60	60
JAM #3	-131	30	150

FIGURE B-13. FREQUENCY REUSE SCENARIO - #1



SIGNAL	PWR/EL-DBM	α°	θ°
NOISE	-123		
DESIRED	-131	0	0
JAM #1	-131	Var.	0
JAM #2	-131	40	30
JAM #3	-131	10	75
JAM #4	-131	50	120
JAM #5	-131	70	170
JAM #6	-131	40	140

FIGURE B-14. FREQUENCY REUSE SCENARIO - #2



Signal-to-RFI #1 Angular Separation in Degrees
 FIGURE B-15. ADAPTIVE PERFORMANCE VS. SIGNAL-TO-RFI #1 SEPARATION
 (OMNISCIENT SOLUTION - 3 RFI EMITTERS)

B-25

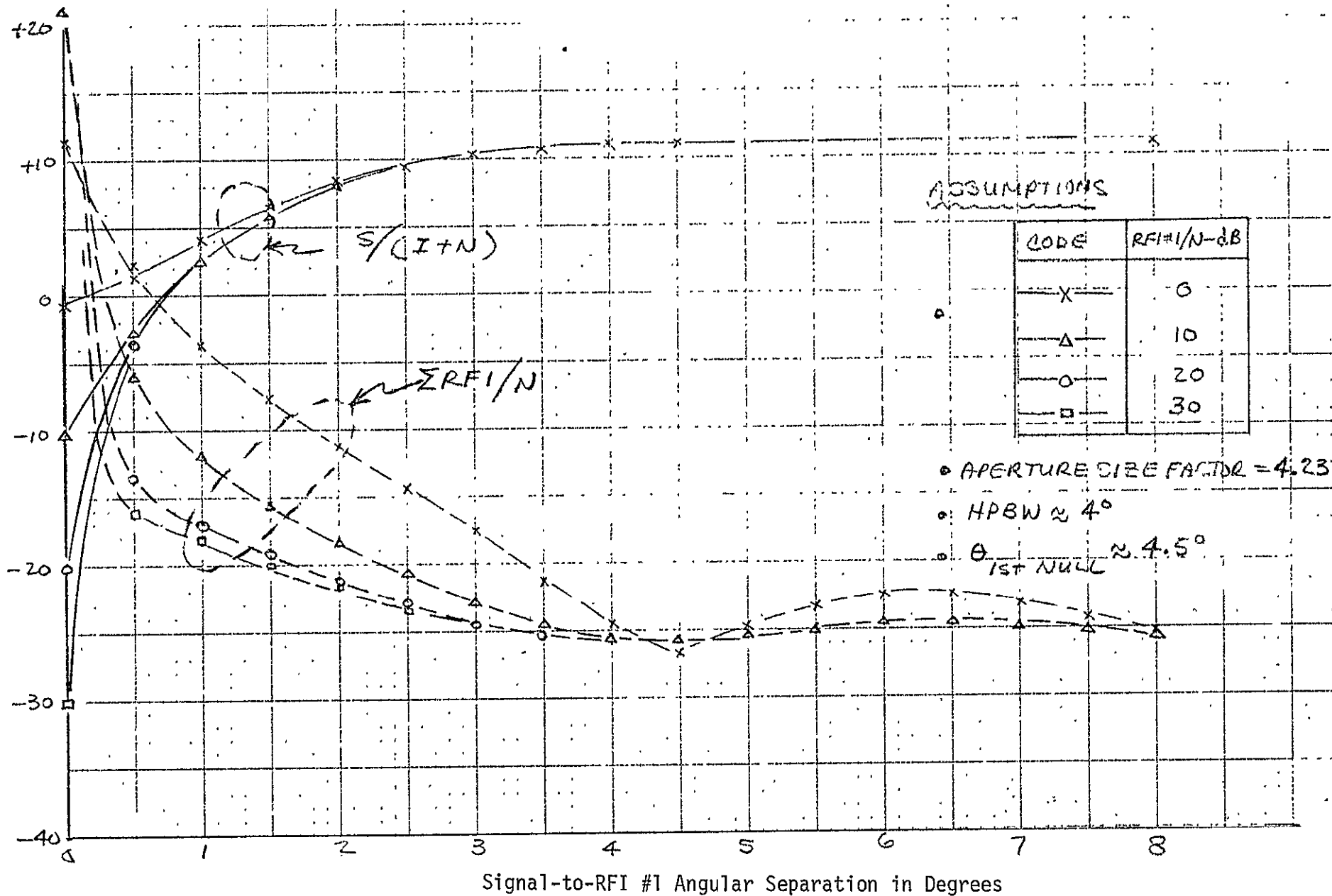


FIGURE B-16. ADAPTIVE PERFORMANCE VS SIGNAL-TO-RFI #1 SEPARATION (OMNISCIENT SOLUTION - 6 RFI EMITTERS)

performance curves remain essentially the same as for the single RFI case, indicating that the fixed RFI's are in deep nulls and the variable RFI #1 is the main contributing interference emitter. However, it is noted that the total sum of RFI/N suppression level (Σ RFI/N) has leveled in at approximately minus 30 and minus 25 dB, respectively.

To more effectively illustrate the performance of an adaptive array, two dimensional antenna radiation patterns were synthesized using computer simulations for the cases with single and multiple RFI environments. In both cases, RFI#1 was varied in angle relative to the desired signal. Typical results are shown in Figures B-17 and B-18 for the single and multiple RFI cases, respectively. In comparing the array patterns with Figure B-10 (no RFI case), the adapted pattern is shown to vary considerably in shape and beam pointing angle (main beam angle toward the desired signal) in order to maximize the output $S/(I+N)$. It is to be noted that the desired signal is frequently pulled off the peak of the main beam, in the $S/(I+N)$ optimization process.

The Omniscient Solution shows how well an adaptive array can null RFI's. For RFI's beyond the 0.25 times the HPBW, the RFI's have been suppressed below the receiver thermal noise level for the signal scenarios synthesized. The Omniscient solution will be used as a reference to evaluate solutions obtained with adaptive algorithms and under the Spacelab dynamic-moving environment.

B.3.4 Space Vs. Ground Based Beam Processing

B.3.4.1 General

The number of multiple access users that can be simultaneously supported is primarily impacted by the AMPA implementation approach and by the satellite payload weight and prime power capacity. The implementation approaches considered are:

- Beam Process on the ground
- Beam Process in Space

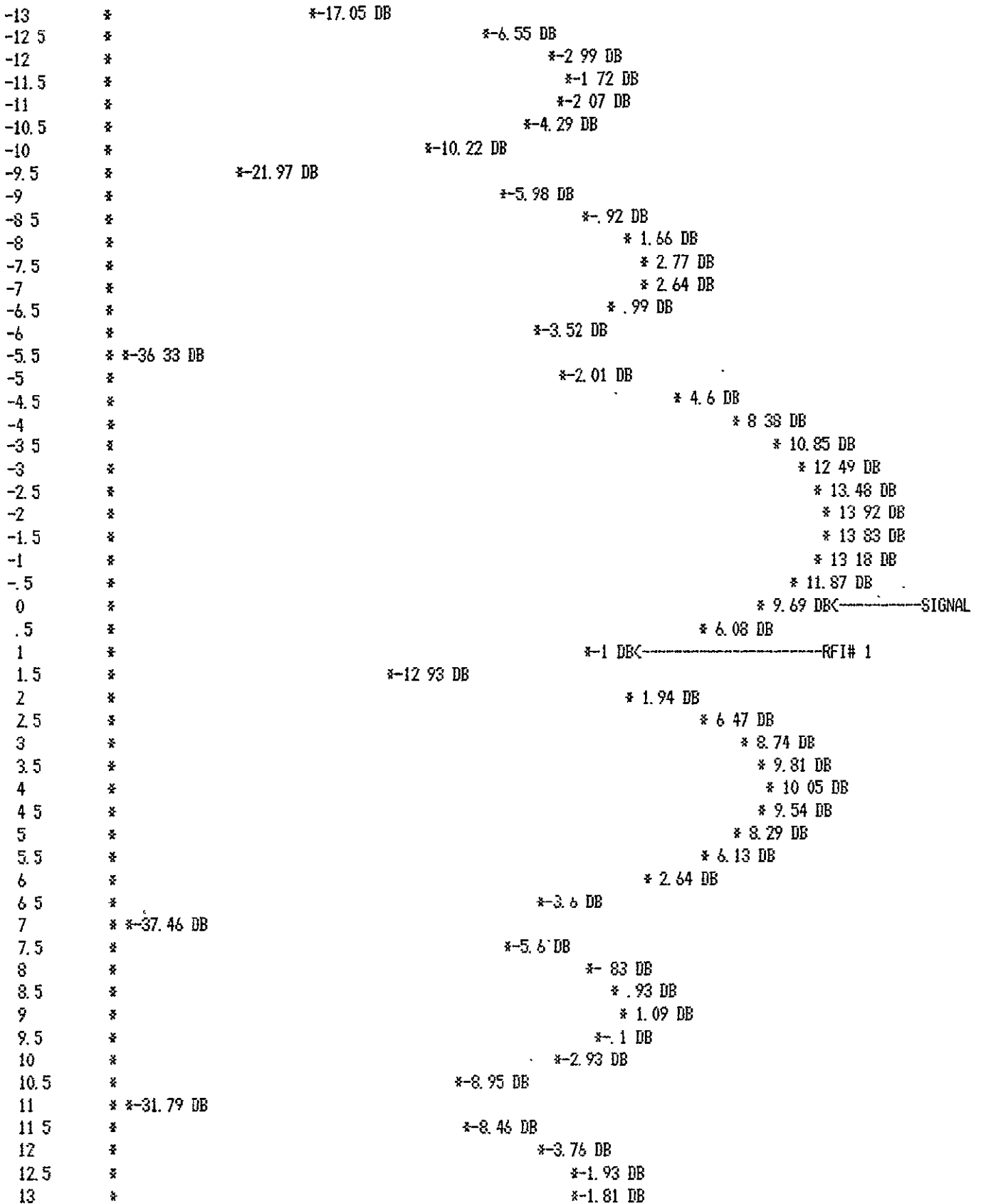
as illustrated in Figure B-19.

The first approach utilizes multi-channel repeaters in space for the return and forward links that simply relays the signal from each element to-and-from a ground station where all beam and signal process functions are

PRINCIPAL CARDINAL PLANE PATTERN

*****> ARRAY GAIN-DBI

FIGURE B-17. TYPICAL ADAPTED ARRAY PATTERN WITH SINGLE RFI EMITTER



PRINCIPAL CARDINAL PLANE PATTERN

*****> ARRAY GAIN-DBI

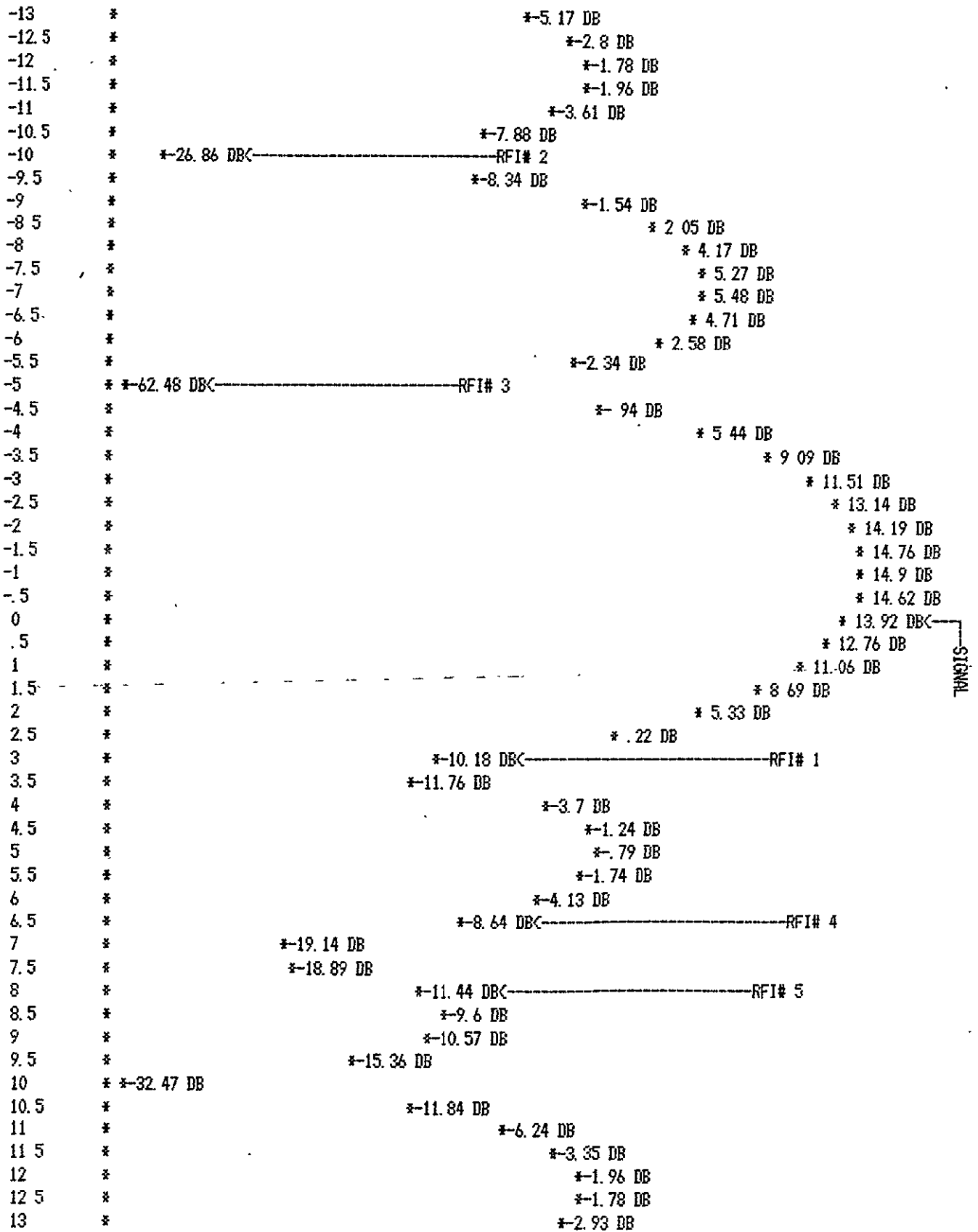
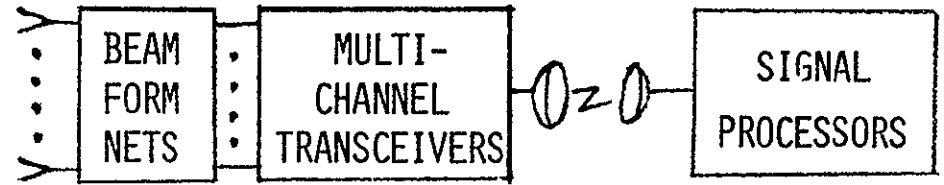
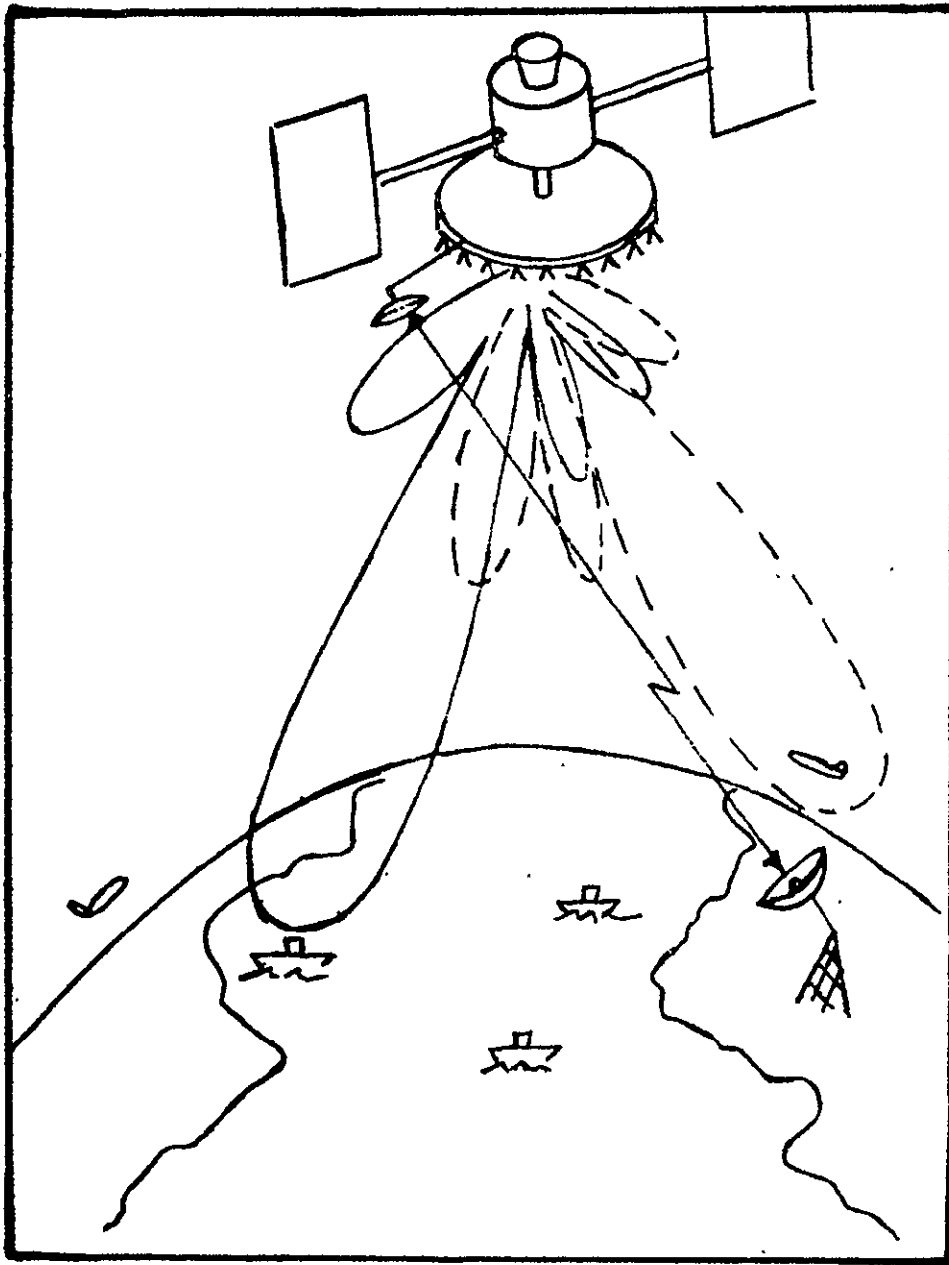
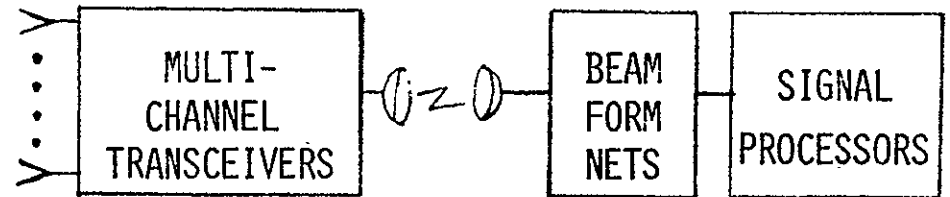


FIGURE B-18. TYPICAL ADAPTED ARRAY PATTERN WITH FIVE RFI EMITTERS



● BEAM PROCESS IN SPACE



● BEAM PROCESS ON GROUND

FIGURE B-19. AMPA SYNCHRONOUS SATELLITE CONCEPT

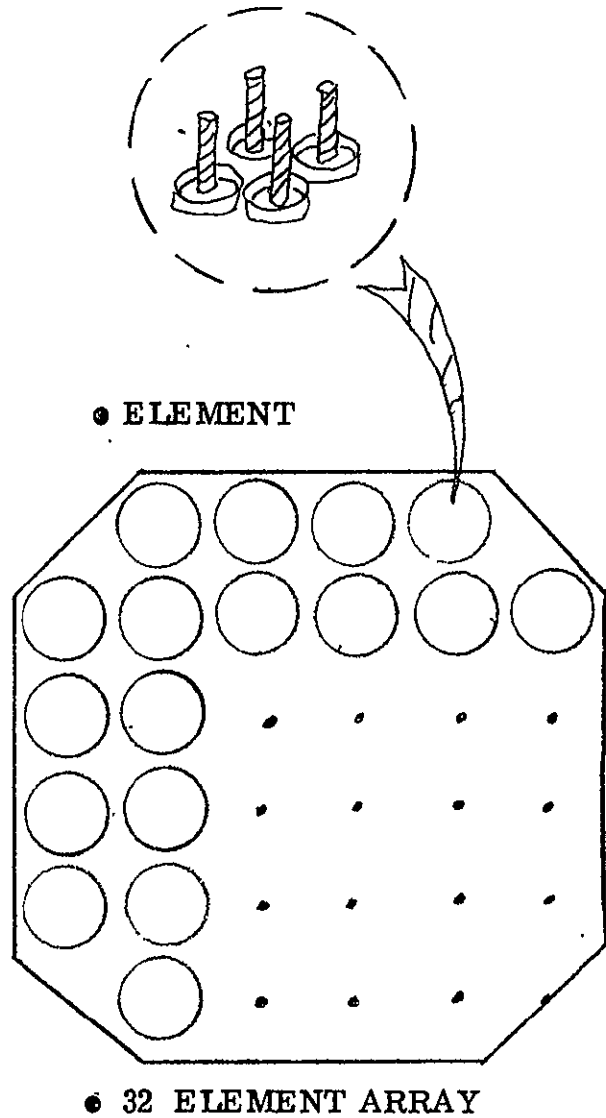
performed. As a result, the implementation impact is essentially independent of the number of beams formed; only the size of the L-band transmit amplifiers must be increased to handle more simultaneous beams. For example, in order to radiate 6.6 watts per beam each amplifier must be increased to handle $6.6 \times M/N$ watts where M is the number of transmit beams and N is the number of elements.

On the other hand with beam processors located in space, the implementation hardware required in space increases with the number of receive and transmit beams formed. The hardware which is directly impacted as a function of the number of beams are the adaptive receive processors, transmit beam processors, frequency synthesizer, L-band transmit amplifiers, digital processor network and power supplies. These additional hardware requirements add considerable weight and complexity (with commensurate decrease in reliability) to the Beam Process in Space approach.

In both approaches, a common transmit/receive 32 element array as shown in Figure B-20 has been used. Typically, the array element consists of a subarray of quad-helices and provides a peak gain of +18.4 dBi (dB above an isotropic radiator) and a half power beamwidth (HPBW) of approximately 18 degrees. (Alternatively subarrays of crossed dipoles, spirals, etc., could be considered). The array is a filled array with an aperture of 4.1 meter by 4.1 meter, providing a peak gain of 33.5 dBi and approximate HPBW of 3 degrees.

Link analyses in Section 3.2 showed that a relatively small array of 32 high gain elements ($G_{e1} = 18.4$ dBi) could adequately support high quality voice (C/N_0 of +53 dB-Hz) transmission between a spaceborne satellite system in geostationary orbit and many mobile Maritime and Aeronautical multiple access users with an ERP of +17.7 dBw and G/T_S of -20 dB/°k. This section describes the implementation tradeoffs to evaluate the candidate system approaches. For the Beam Process on ground approach, two configurations have been considered, differing primarily by its space-to-ground link bandwidth requirement. The three approaches are shown in Figure B-21 and described below:

B-31



● ELEMENT CHARACTERISTICS

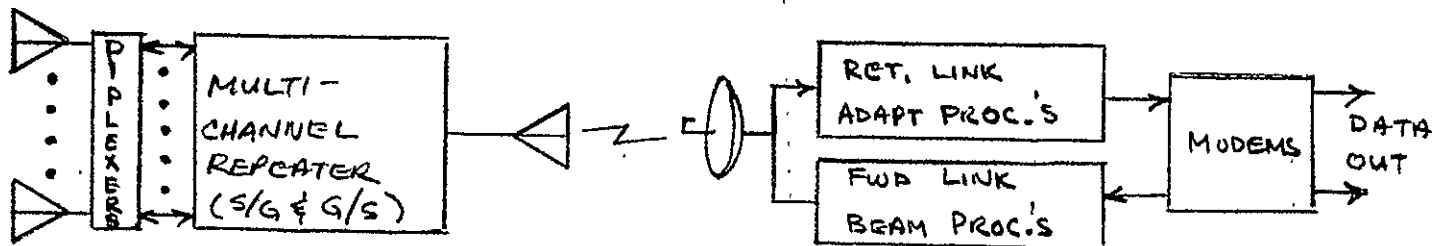
- HPBW $\approx 18^\circ$
- GAIN = 18.4 dBi (PEAK)
= 15.8 dBi ($\pm 8.5^\circ$)

● ARRAY CHARACTERISTICS

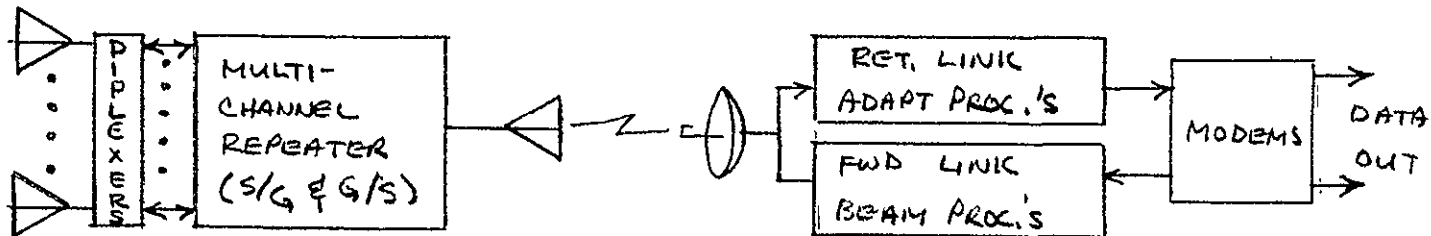
- HPBW $\approx 3^\circ$
- GAIN = 33.5 dBi (PEAK)
= 30.8 dBi ($\pm 8.5^\circ$)
- 4.1 METER x 4.1 METER

FIGURE B-20. . . ARRAY CHARACTERISTICS FOR SYNCH ORBIT

A. ULTIMATE GROUND PROCESSING SYSTEM (UNLIMITED S/G BANDWIDTH)



B. LIMITED GROUND PROCESSING SYSTEM (S/G LINK BANDWIDTH = 100 MHz)



C. BEAM PROCESS IN SPACE

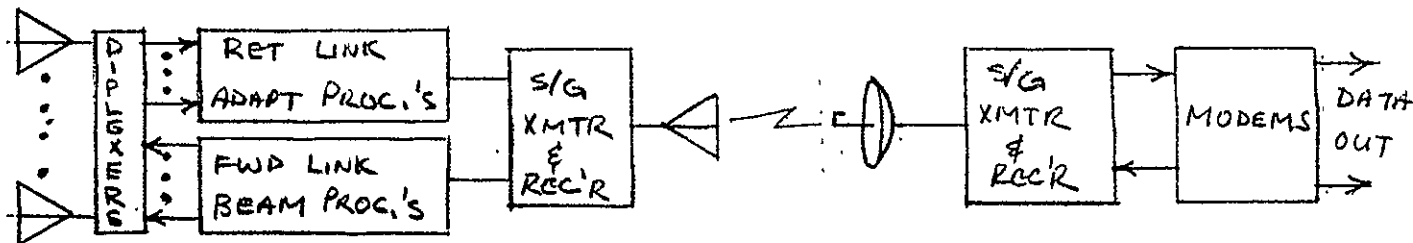


FIGURE B-21. BEAM PROCESS APPROACHES

- Beam Process on Ground

- Ultimate Ground Processing System with all beam and signal processor functions located on the ground. This system relays the full spectral bandwidth (~10 MHz) from each element to the ground, and requires approximately 320 MHz for space-to-ground link, and 320 MHz for the ground-to-space link.

- Limited Ground Processing System with all beam and signal processor functions conducted on the ground, but with the space-to-ground link bandwidths limited to 100 MHz for each of the up and down links. This limits the spectral coverage to approximately 2.5 MHz.

- Beam Process in Space with all beam processor functions located in space but with all signal processor functions located on the ground. The space-to-ground link bandwidth required is a function of the number of simultaneous receive and transmit beams that are formed.

In order to determine the number of simultaneous receive and transmit beams that can be supported, a parametric tradeoff analysis of weight and prime power requirement was conducted for each of the above system alternatives. Therefore, for a given payload capacity, the number of beams that can be employed for the three candidate approaches can be readily estimated.

The selected configuration is arrived at by considering the result of a tradeoff between providing beam processing in space or at the ground. The tradeoff is analyzed within the constraints of system bandwidth and number of beams to be processed along with satellite payload weight and power limitations. The satellite to ground station and receive functions are accomplished at Ku-band.

B.3.4.2 Ultimate System With Ground Processing

The Ultimate System performs all beam and signal processor functions on the ground, and in addition relays the full spectral RF bandwidth (~10 MHz with guard band) from each element to the ground station.

A block diagram of the space segment of the Ultimate System is shown in Figure B-22. The space segment is simply a multi-channel repeater that returns the signal from multiple access users to a ground based terminal referred to herein as the return link, and from the ground terminal to the users (referred to as the forward link). In the return link, the repeater frequency division multiplexes and amplifies the user signals and retransmits the received signals at Ku-band to the ground station. In the forward link, the information to be transmitted to users is received at Ku-band from the ground station and demultiplexed and amplified at L-band to generate the required ERP for user reception. Simultaneous service is provided by forming customized narrow beams at the ground for each user.

Referring to Figure B-22 each of the 32 array elements has a separate transmit/receiver module. The received L-band signal from each element is individually amplified by a low noise transistorized front end and multiplexed into a 32 channel FDM spectrum. The channel bandwidth is set by the filter after the first conversion which is centered at 100 MHz. This bandwidth is fixed at 10 MHz including guard band* for the 32 channels, resulting in a total of 320 MHz downlink bandwidth. The second conversion utilizes 8 offset LO's to provide a sub-group of four channels with eight frequencies each. The next conversion makes use of four super-group LO's to arrive at 32 distinct channels making up the FDM spectrum. The multiplexing is accomplished in two steps to minimize spurious responses.

The receiver channel noise figure is determined primarily by the L-band low noise amplifier and the insertion loss of the filter preceding the amplifier. The amplitude and phase response of the channel is established by the 100 MHz bandpass filter (BPF) following the initial conversion. All other components are sufficiently wideband so as to be negligible in their contribution of amplitude and phase distortions.

*To provide spectral coverage for both Maritime and Aeronautical bands, 3 satellites (envisioned for the future) can be used.

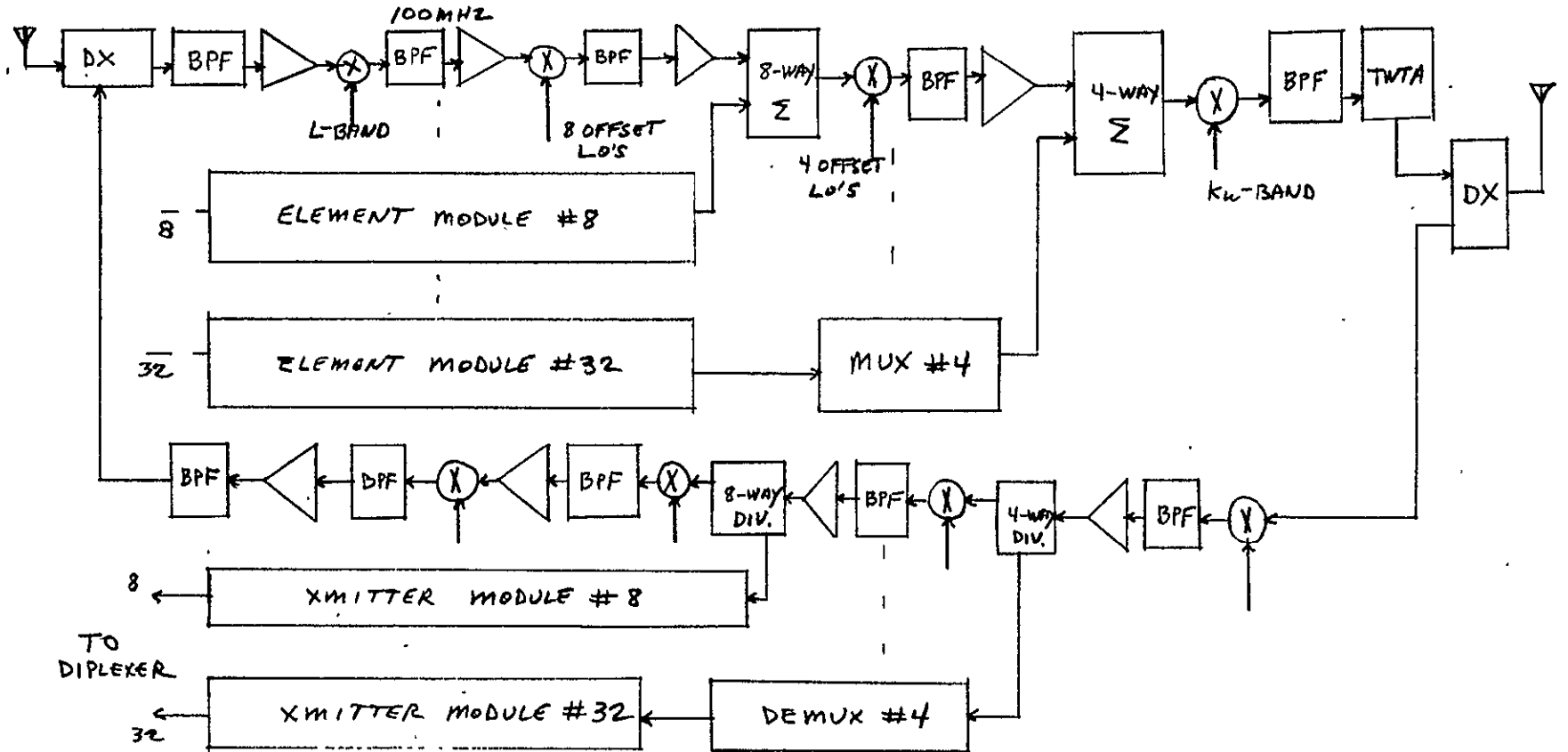


FIGURE B-22. ULTIMATE SYSTEM WITH GROUND PROCESSING (SPACE SEGMENT)

The composite FDM signal is upconverted to Ku-Band, filtered and fed to a TWT amplifier. The TWT provides linear amplification to an output level suitable for transmission to the ground via the diplexer and Ku-band antenna. The TWT is operated with backoff to reduce the generation of intermodulation distortion products. The diplexer in-band insertion loss is kept to a minimum in both the transmit and receive directions to minimize dissipative losses at the transmitter output and to maximize the uplink receiver sensitivity.

The diplexers (DX) connected to the 32 element array must prevent the L-band transmission from entering the receiver and producing spurious responses. In addition, the diplexer must prevent the transmitter noise from degrading the receiver sensitivity.

A detailed functional block diagram for the forward link spaceborne repeater is shown in Figure B-23. The received Ku-band signal is a 32 channel FDM signal which contains the signals for "M" pre-formed transmit beams. The received signal is then demultiplexed to provide the required 32 output signals. Each of these signals are upconverted to L-band, power amplified and fed to the diplexers for subsequent transmission to the users.

The choice of the 32 power amplifiers are critical to the overall system performance in terms of:

- DC Power
- Intermodulation distortion
- Phase Linearity

The link budget (Section 2 of Appendix B) has shown that a transmit power of 6.6 watts per beam must be radiated from the 32 element array. If we assume 50 beams to be transmitted at 6.6 watts per beam, the total radiated power is 330 watts. Allowing for amplifier backoff and 1.5 dB for diplexer and RF losses, the total RF power required by the amplifiers is 587 watts. Thus, each amplifier provides an output of approximately 18.3 watts or +42.6 dBm. The efficiency of 40% was assumed for these Class C amplifiers, thus requiring 1467 watts of peak DC power for 50 beams being simultaneously transmitted. Each amplifier consists of four stages to provide the required gain and output power. The first two stages are operated Class A and the last two stages are operated Class C. The third stage utilizes an MSC 3003 transistor with the last stage being an MSC 1417. The last two stages provide 17.5 dB of gain and an output of 18.3 watts.

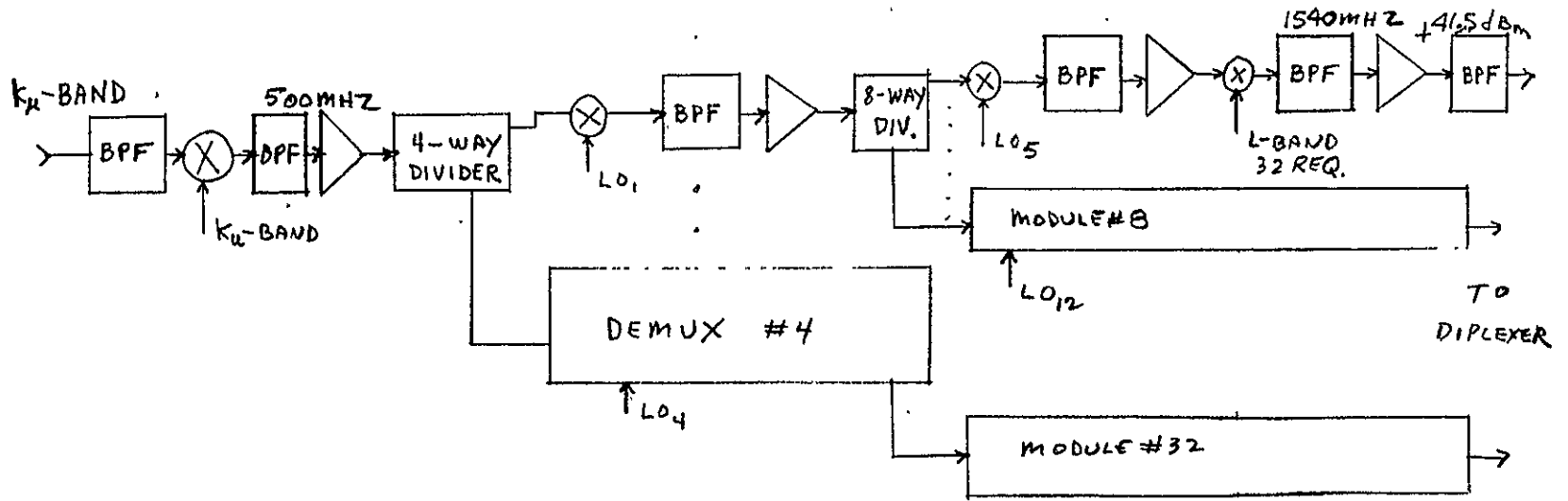


FIGURE B-23. . FORWARD LINK SPACEBORNE REPEATER

The amplifier provides 15 dB of rejection to the second harmonic. A bandpass filter at the output of the amplifier provides an additional rejection of 35 dB so that the output level of the second harmonic will be 50 dB below the fundamental output.

The total weight of the system for the configuration where all beam and signal processor functions are accomplished at the ground is 77.2 KG. This weight includes the antenna array, frequency source and power supply. With the L-band transmitter requirement of 6.6 watts per beam, the number of beams selected for transmission impacts the overall system prime power requirements. Figure B-24 shows the effect of system power as a function of the number of beams formed. If it is assumed that 1.6 KW of prime power is available approximately 50 beams can be supported with the Ultimate System. In arriving at the DC power 1 dB backoff was used for the L-band amplifiers.

B.3.4.3 Ground Processing System with Reduced Satellite-to-Ground Bandwidth

This system is the same as the previously described Ultimate System with the exception that the spectral bandwidth has been reduced to 2.5 MHz in order to limit the satellite-to-ground bandwidth to 100 MHz. In addition, this system has reduced channel capacity (≈ 37 channels with guard band), due to the reduced spectral coverage. However, this merely limits the portion of the spectrum that is usable in one satellite. Assuming a 3 satellite system (typically located over the Atlantic, Pacific, and Indian Oceans), each satellite system can be assigned a different 2.5 MHz band to provide a total of 7.5 MHz and up to 111 channels.

The overall block diagram of the space segment is functionally the same as shown previously in Figures B-22 and B-23. The major implementation impact is the satellite-to-ground Ku-band TWT transmitter which can be reduced to handle the reduced 100 MHz bandwidth. The resultant system weight is reduced approximately 2.3 KG and the total prime power requirement is reduced by approximately 30 watts as compared to the Ultimate System as shown in the graph of Figure B-24.

B.3.4.4 System with Beam Processors in Space

This system locates all receive and transmit beam processors in space, but locates all signal processor (MODEM) functions on the ground. A functional block diagram of the space segment is shown in Figure B-25.

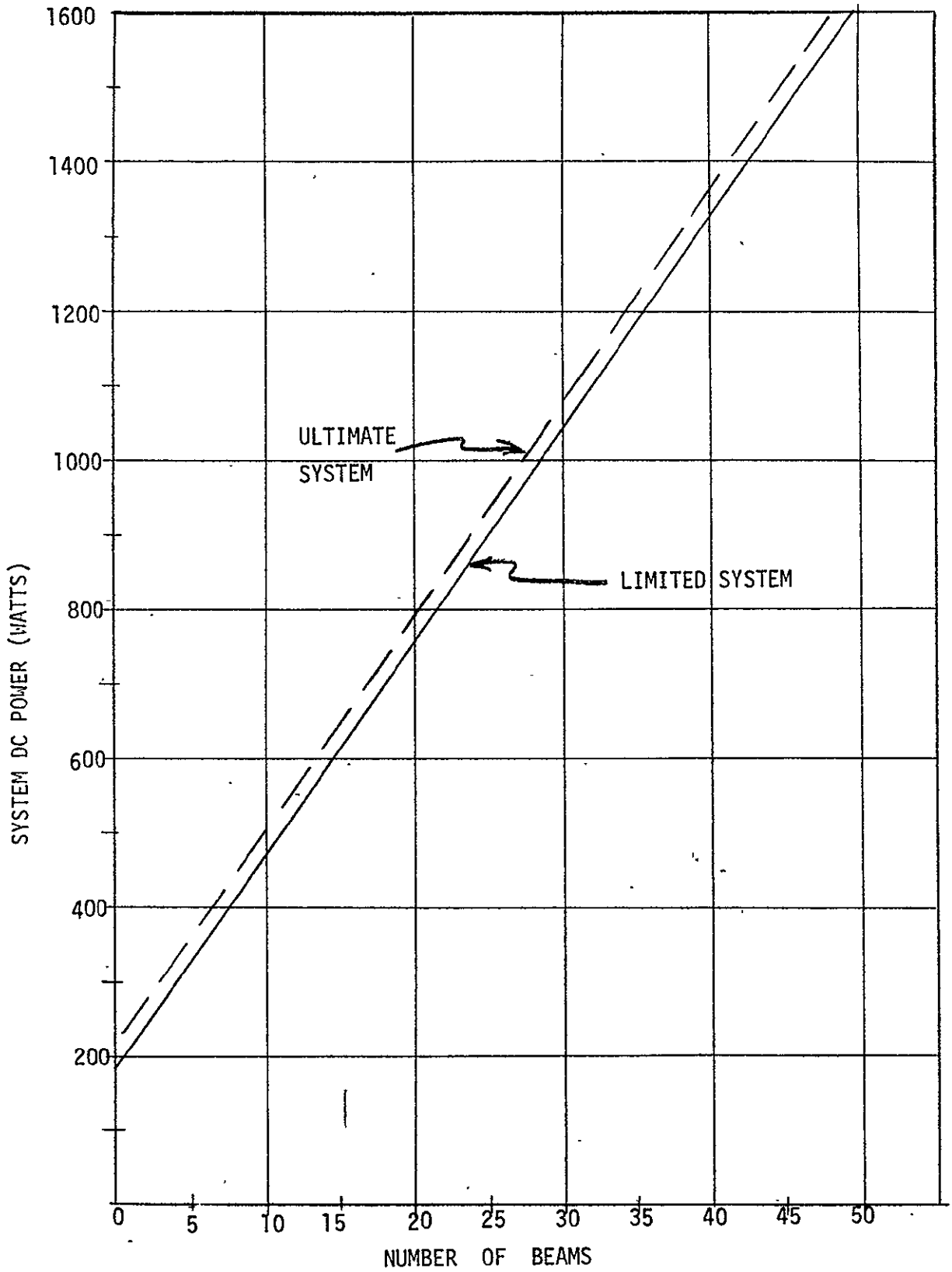


FIGURE B-24. PRIME POWER REQUIREMENT VERSUS NUMBER OF BEAMS FOR BEAM PROCESS ON GROUND APPROACH

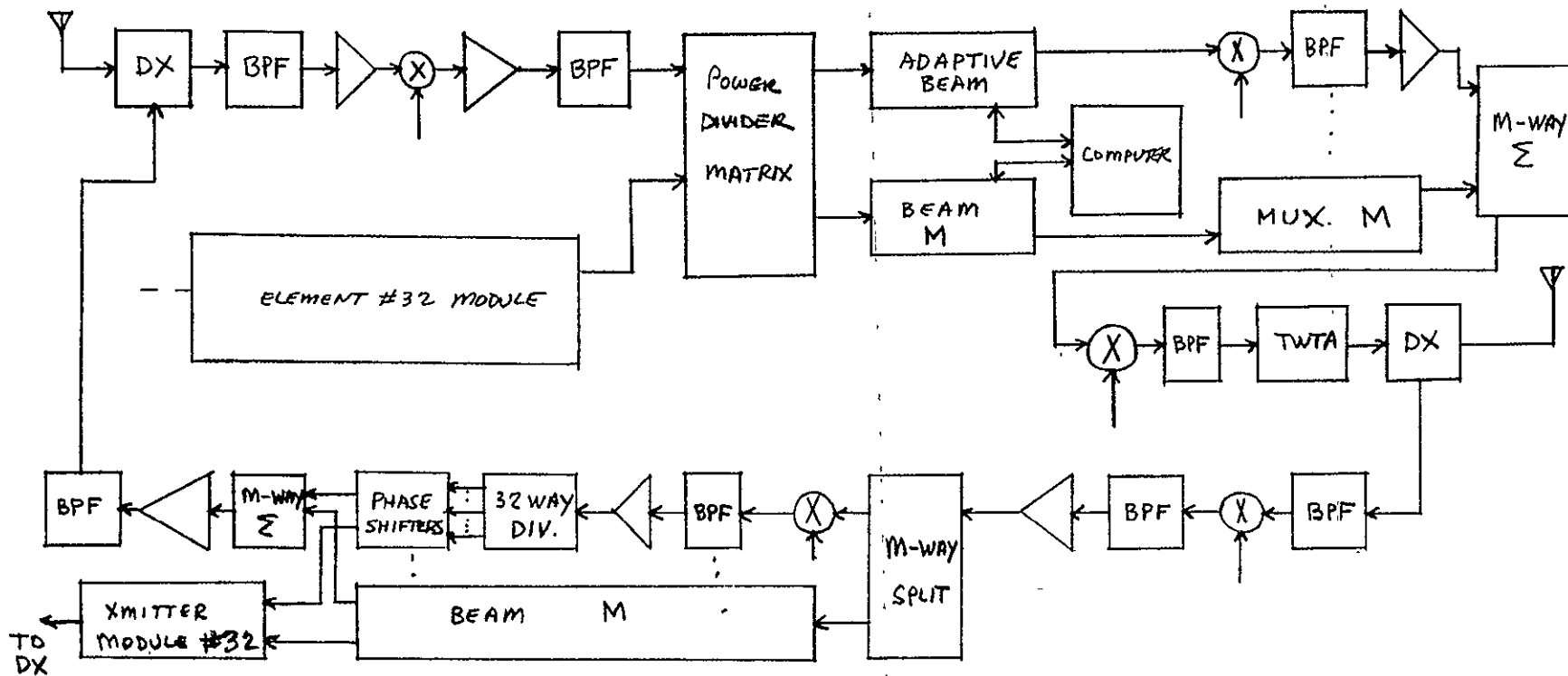


FIGURE B-25. SYSTEM WITH BEAM PROCESSORS IN SPACE

The 32 element L-band array is identical to that used for the ground processing systems. Each receiver channel consists of a diplexer, bandpass filter and low noise amplifier. Each amplifier output signal is downconverted to 100 MHz where it is filtered, amplified and fed to a power divider matrix. The matrix connects the 32 channels of information to a number (M) of adaptive processors. A separate processor is required for each independent antenna beam required. The processor consists of weighting networks which adjust amplitude and phase to optimize the array output signal. The adaptive processor operates in conjunction with an on-board computer. The output from each adaptive processor is the final array beam. These M outputs are then multiplexed and combined into a single line which is upconverted to Ku-band. The composite signal is then amplified by a TWTA and fed to the diplexer and antenna for transmission to the ground.

For the forward link, the received Ku-band signal is downconverted and demultiplexed to form the required number of beams for user transmission. The beam forming is accomplished by 32 individual phase shifters for each beam to be formed, working in conjunction with the on-board computer. However, since the transmit beam is steered open-loop, beam pointing data to change the phase shifters must be transmitted from the ground station by way of the on-board Telemetry, Track and Command Subsystem. The L-band transmitter is identical to that used for the configuration where beamforming is accomplished at the ground station.

With the implementation of beam processors in space, both the payload weight and power become a function of the number of beams to be processed. Figure B-26 indicates the weight and power as a function of the number of beams formed. Thus, it is seen that a 1.6 KW system could process 18 beams and would weigh 332 kg, (730 lbs.) as compared to the ground processing configurations which can provide 50 beams, and weighs only 77.2 KG. If a weight constraint of 182 kg (400 lbs.) is used, only 7 beams can be formed with the beam process in space approach.

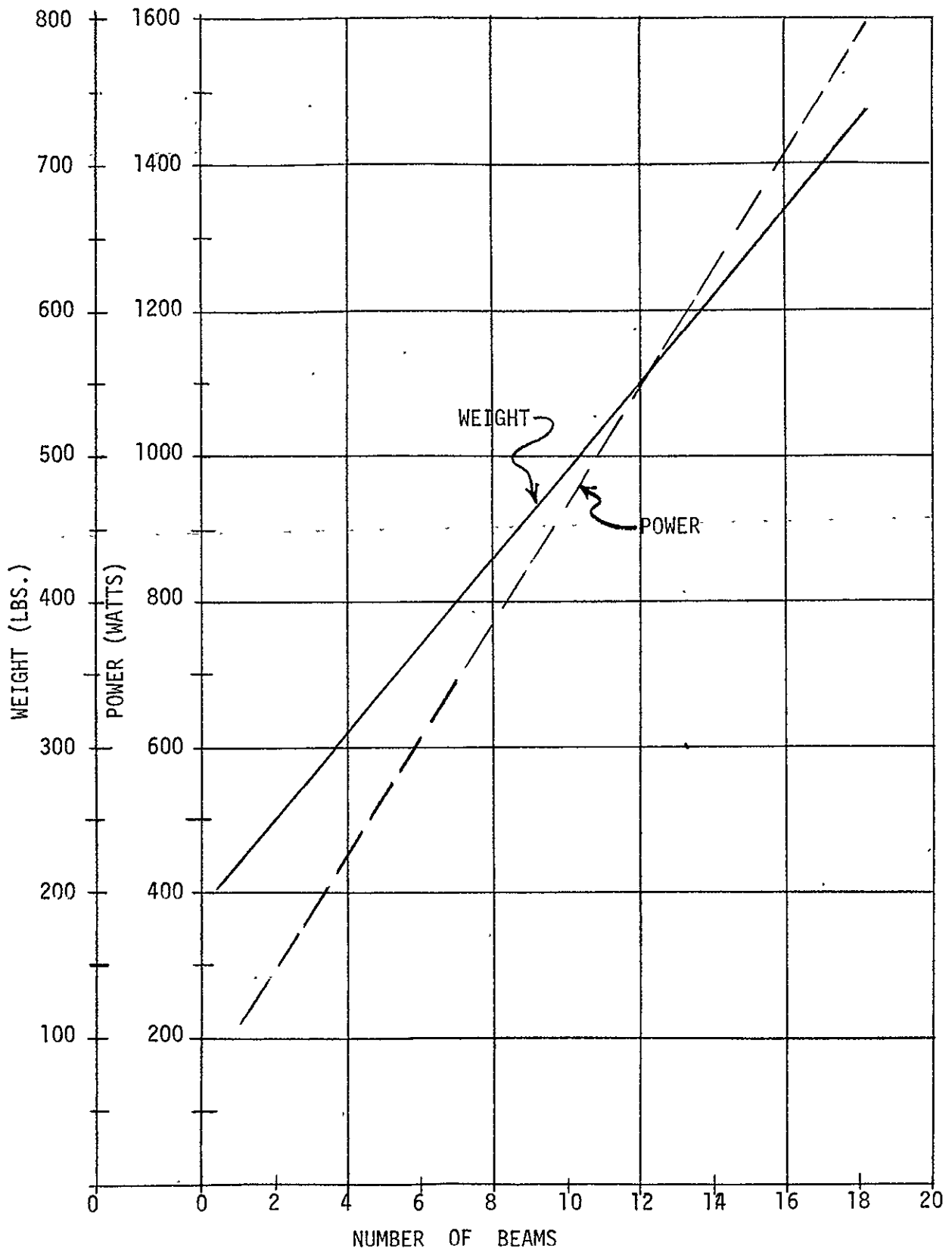


FIGURE B-26. WEIGHT AND PRIME POWER REQUIREMENT VERSUS NUMBER OF BEAMS FOR BEAM PROCESS IN SPACE APPROACH

B.3.4.5 Comparison Of Beam Process On Ground Vs. Space

In order to compare the ultimate beam capacity of the two candidate approaches, a spacecraft having a payload weight and prime power capacity of 182 kg and 1.6 kw has been assumed. For this case, the number of beams that can be supported by the two candidate approaches are:

APPROACH	# BEAMS	WT-KG	PWR-KW
● Beam Process on Ground	50	77	1.6
● Beam Process in Space	7	182	0.69

The Beam Process on ground approach is limited by the power constraint, whereas the Beam Process in Space is limited by the weight constraint. If, however, the unused weight and/or the unused power are used to increase the number of beams at a nominal power-to-weight conversion factor of 4.15 watts per kg, the beam capacity increases to:

APPROACH	# BEAMS	WT-KG	PWR-KW
● Beam Process on Ground	63	182	2.04
● Beam Process in Space	14	182	1.6

In summary, the implementation tradeoff analyses have clearly shown that an operational system with all beam and signal processor functions located on the ground can more than quadruple the number of beams and the number of multiple access users that can be supported simultaneously. Furthermore, the ground processing approach:

- Minimizes complexity in space and locates complexity on ground
- Improves reliability (due to reduced space hardware complexity)
- Provides flexibility to grow with needs
- Provides versatility to make changes to beam and signal process networks.

Therefore, it is recommended that an array of 32 high gain elements with ground processing be used to support the multiple access users of an advanced operational Maritime and Aeronautical Satellite System.

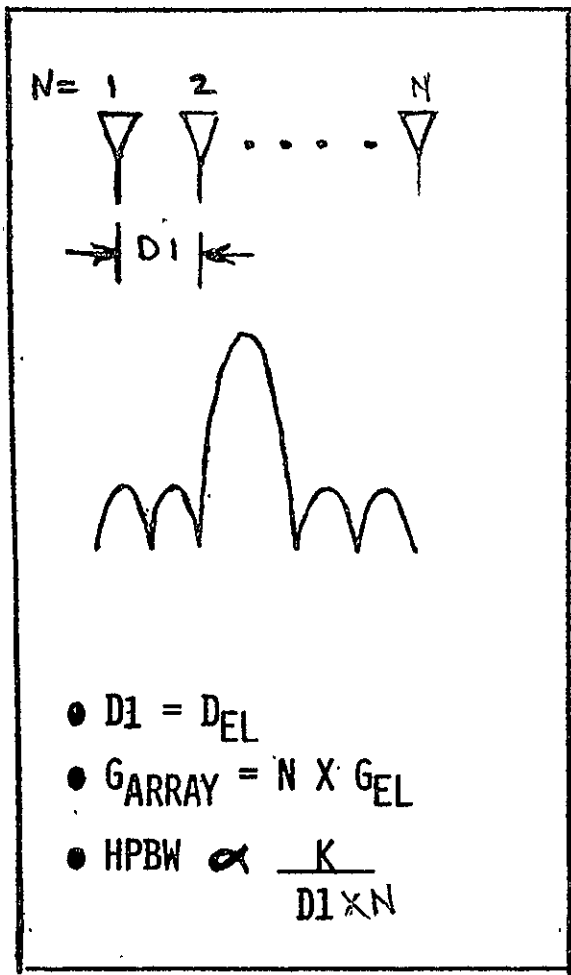
B.3.5 Thinned Vs. Filled Array

The thinned array concept uses the same elements as the filled array, but its element spacing is increased as compared to a filled array, as illustrated in Figure B-27. Thinning of the array has no impact on the array gain; however, its sidelobe levels increase rapidly as the aperture size factor is increased. In an adaptive array, however, the high sidelobe does not present a problem since interference signals are simply placed in spatial pattern nulls. In addition, thinning of the array decreases the array half power beamwidth (HPBW) that provides improved resolution to spatially null interference emitters that are closely spaced to the desired signal.

In order to compare the achievable performances of thinned and filled arrays, their adaptive performance was synthesized in a 10 signal environment of airport emitters as listed in Figure B-28 for a 32 element array located in geostationary orbit at 76 degree west longitude. This scenario is a very severe environment, representing two emitters at the Dulles and Baltimore airports that are only 0.1 degree apart as seen from geostationary altitude. The 10 signals are assumed to be equal power, resulting in an input signal-to-noise (S/N) into each element of 15 dB. This provides a maximum achievable array output signal-to-interference plus noise $[S/(I+N)]$ of +30 dB.

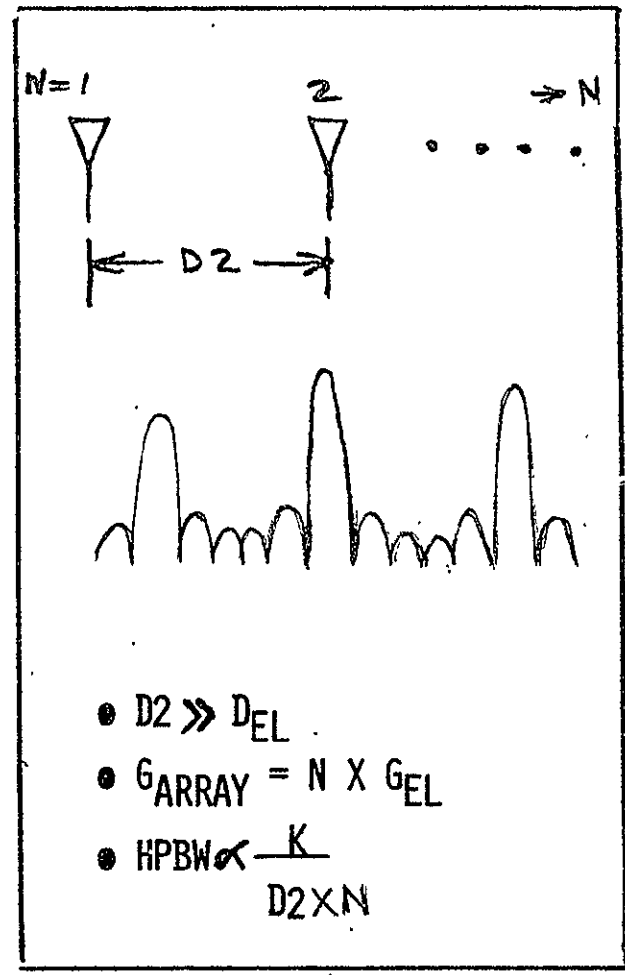
Three cases were examined, viz, the desired signal in (I) Baltimore, (II) Dulles and (III) Dulles without Baltimore, and with all other signals becoming interference signals (or RFI's). Figure 3.3-26 shows the resultant adapted $S/(I+N)$ as a function of the aperture size factor over a range of 1 to 20. The adapted performance in cases I and II are nearly identical, requiring an aperture size factor of 20 before their closest RFI emitter (≈ 0.1 degree) is completely nulled and the maximum achievable $S/(I+N)$ of +30 dB has been attained. For this case, it means that the aperture size has

FILLED ARRAY



VS

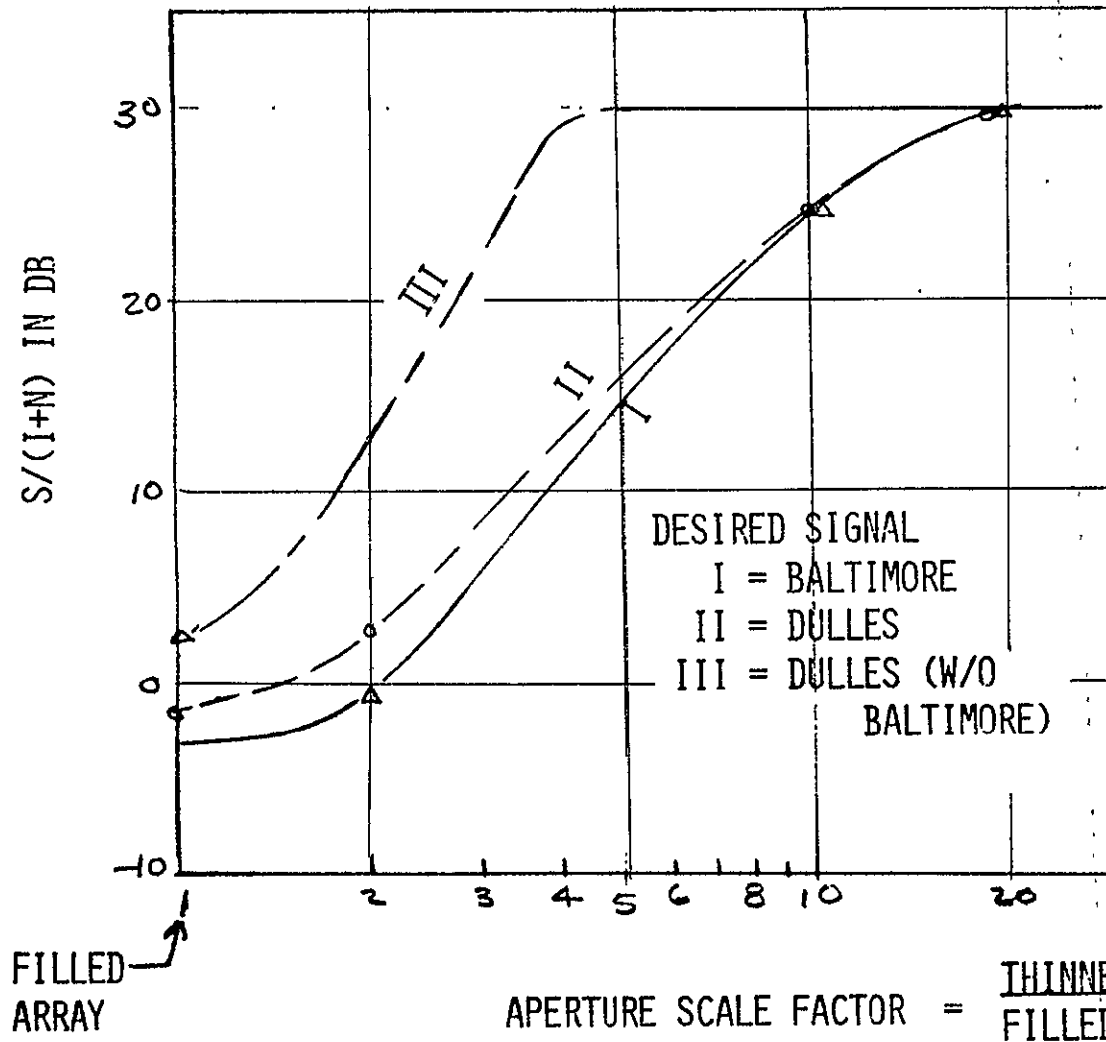
THINNED ARRAY



* D_{EL} = EFFECTIVE APERTURE OF ELEMENT
 $K \propto$ APERTURE ILLUMINATION TAPER

FIGURE B-27. FILLED VS. THINNED ARRAY TRADEOFF

B-46



SIGNAL SCENARIO

● 10 SIGNALS AT:

- BOSTON
- NEW YORK
- BALTIMORE
- DULLES
- CHICAGO
- MIAMI
- ATLANTA
- DALLAS
- DENVER
- SEATTLE
- LOS ANGELES

● INPUT S/N = 15 dB/ELEMENT

● SATELLITE @ 76° W LONGITUDE
(GEOSTATIONARY)

FIGURE B-28. ADAPTIVE PERFORMANCE WITH 32 ELEMENT ARRAY

been sufficiently increased to place all RFI's into spatial nulls while maintaining the peak of the beam on the desired signal. However, it is to be noted that adequate performance can be attained with smaller aperture size factor, depending upon the threshold $S/(I+N)$ required. For example, for a typical threshold $S/(I+N)$ of +10 dB, aperture size factor of 3.5 to 4 would be adequate to meet the threshold level.

Case III represents a less severe case with the desired signal at Dulles airport, and its closest RFI emitter at Baltimore airport removed. The adapted performance has improved significantly where the maximum attainable performance has been achieved with an aperture size factor of only 4, and the typical $S/(I+N)$ threshold of +10 dB has been achieved with an aperture size factor of approximately 1.8.

On the other hand, however, the reduced HPBW and sharper (narrower) null increases the beam and null pointing accuracy requirement to place the main lobe on the desired signal and RFI's into spatial nulls. However, subsequent simulation results will show that 8 bit quantization levels provide adequate resolution to meet the AMPA requirement.

Comparisons of the key parameters for the thinned and filled array are summarized in Figure B-29. The most significant impact of using a thinned array is the improved resolution to operate more efficiently near closely spaced RFI's and the improved spatial dispersion of IM products that ultimately makes it possible to operate more efficiently in the L-band transmitter amplifier.

B.4 OPERATIONAL SYSTEM DESIGN

An overall functional block diagram of the advanced operational system concept is shown in Figure B-30, including a spaceborne and a ground based segment. The space segment is merely a 32 channel transceiver that relays the signal components to-or-from each array element to the ground segment where all adaptive beamforming and beam steering functions are performed. The signals to-or-from the 32 channel transceiver are multiplexed and demultiplexed and relayed to-or-from the ground, typically at Ku-band. All of the beam and signal processing functions for both receive and transmit are performed at the ground segment.

PARAMETER	FILLED ARRAY	THINNED ARRAY
● BEAMWIDTH	WIDE	NARROW*
● ARRAY GAIN (PEAK)	SAME	SAME
● SIDELOBES	LOWER	HIGH GRATING LOBES**
● SPATIAL NULLING OF RFI'S	GOOD	EXCELLENT
● TRACKING REQUIREMENTS	SIMPLER	MORE DIFFICULT***
● SPATIAL DISPERSION OF IM	SOME	BETTER

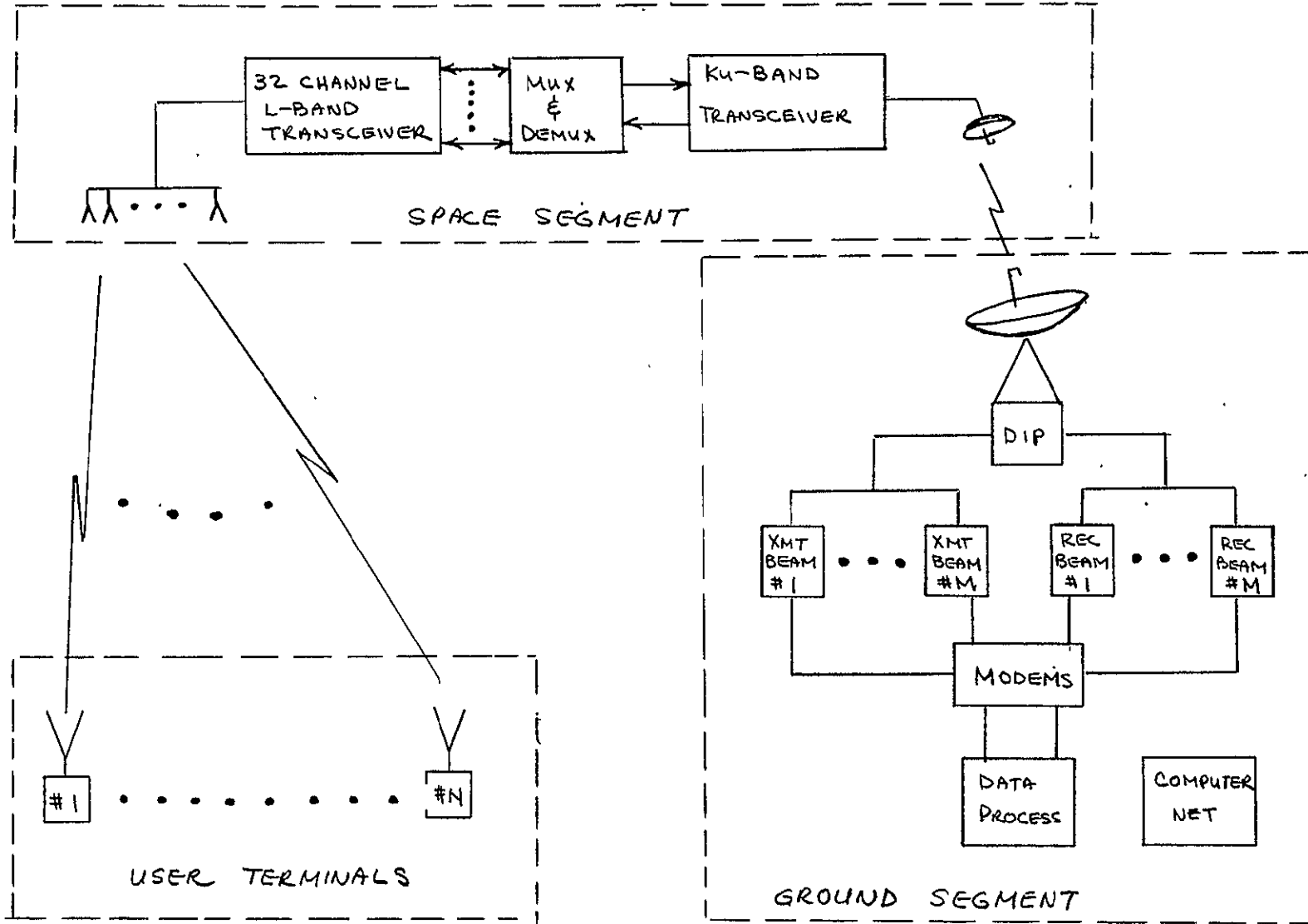
NOTE:

* NARROW BEAMWIDTH IMPROVES SPATIAL RESOLUTION TO NULL CLOSE-IN INTERFERERS

** HIGH GRATING LOBES NOT A PROBLEM WITH ADAPTIVE SPATIAL NULLING OF INTERFERERS

*** INCREASED TRACKING REQUIREMENTS ON RECEIVE AND TRANSMIT TO BE INVESTIGATED FOR EXPERIMENT

FIGURE B-29. SUMMARY OF FILLED VS. THINNED ARRAY



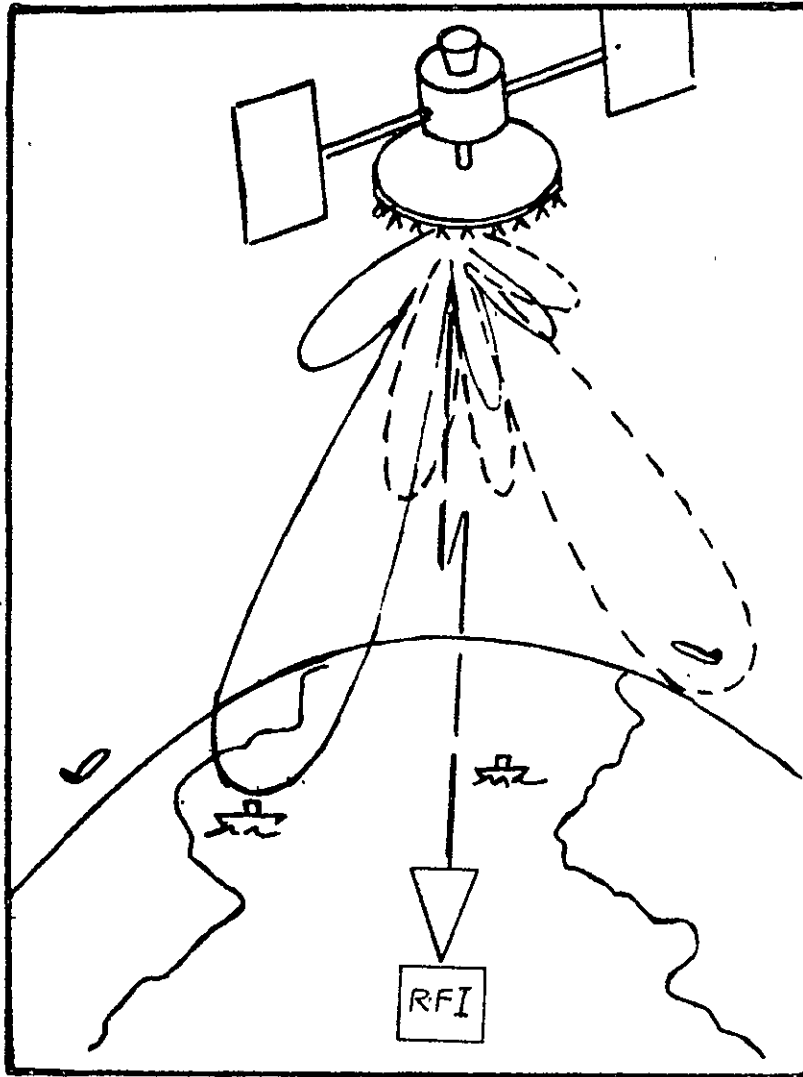
B-49

FIGURE B-30. ADVANCED OPERATIONAL SYSTEM CONCEPT

In the return link, the received signal is demultiplexed to recover the independent signals from each of the 32 elements. The space segment has essentially become a long RF transmission link between the array elements and the beam processors located at the ground segment. On the ground, the signal from each element is divided M-way, where M is the number of adaptive receiver processors to be used or the number of users to be supported simultaneously. Each adaptive processor then forms and steers a customized beam with the aid of a computer network that points a beam to the desired user and places spatial nulls on RFI emitters.

In the forward link, the inverse procedure is followed. All transmit beam forming functions are conducted on the ground with the aid of the computer network. The beam is formed at an IF frequency, multiplexed for transmission to the space segment at Ku-band, demultiplexed and transmitted to the appropriate user at L-band.

A summary of the operational system concept is shown in Figure B-31. It is to be noted that the space segment is essentially independent of the number of beams formed with the exception that the L-band transmitter must be sized to handle the maximum number of beams (M) to be transmitted at one time. Otherwise, all of the complexity has been removed from the space segment and located on the ground.



- MULTIPLE CUSTOMIZED BEAMS TO SERVICE MANY USERS
- HIGH SATELLITE ANTENNA GAIN TO MINIMIZE USER COST BY MINIMIZING USER REQUIREMENTS:
 - ERP = +20 TO +23 dBW
 - $G/T_S = -20$ TO -26 dB/°K
- SPATIAL NULLING OF RFI'S FOR:
 - FREQUENCY REUSE
 - MAXIMIZE CHANNEL CAPACITY
- MINIMIZE SPACEBORNE IMPLEMENTATION IMPACT WITH BEAM PROCESS ON GROUND
- THINNED ARRAY IMPROVES RFI REJECTION AND IM DISPERSION BUT INCREASES TRANSMIT BEAM POINTING REQUIREMENT

FIGURE B-31. SUMMARY OF KEY OPERATIONAL SYSTEM REQUIREMENTS

APPENDIX C

Weight and Power Tradeoff Analysis for the AMPA Experiment System as a Function of the Number of Beams and Number of Array Elements

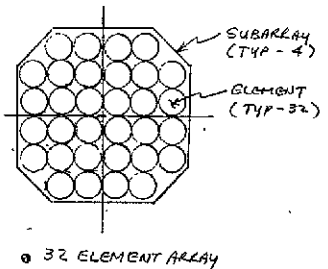
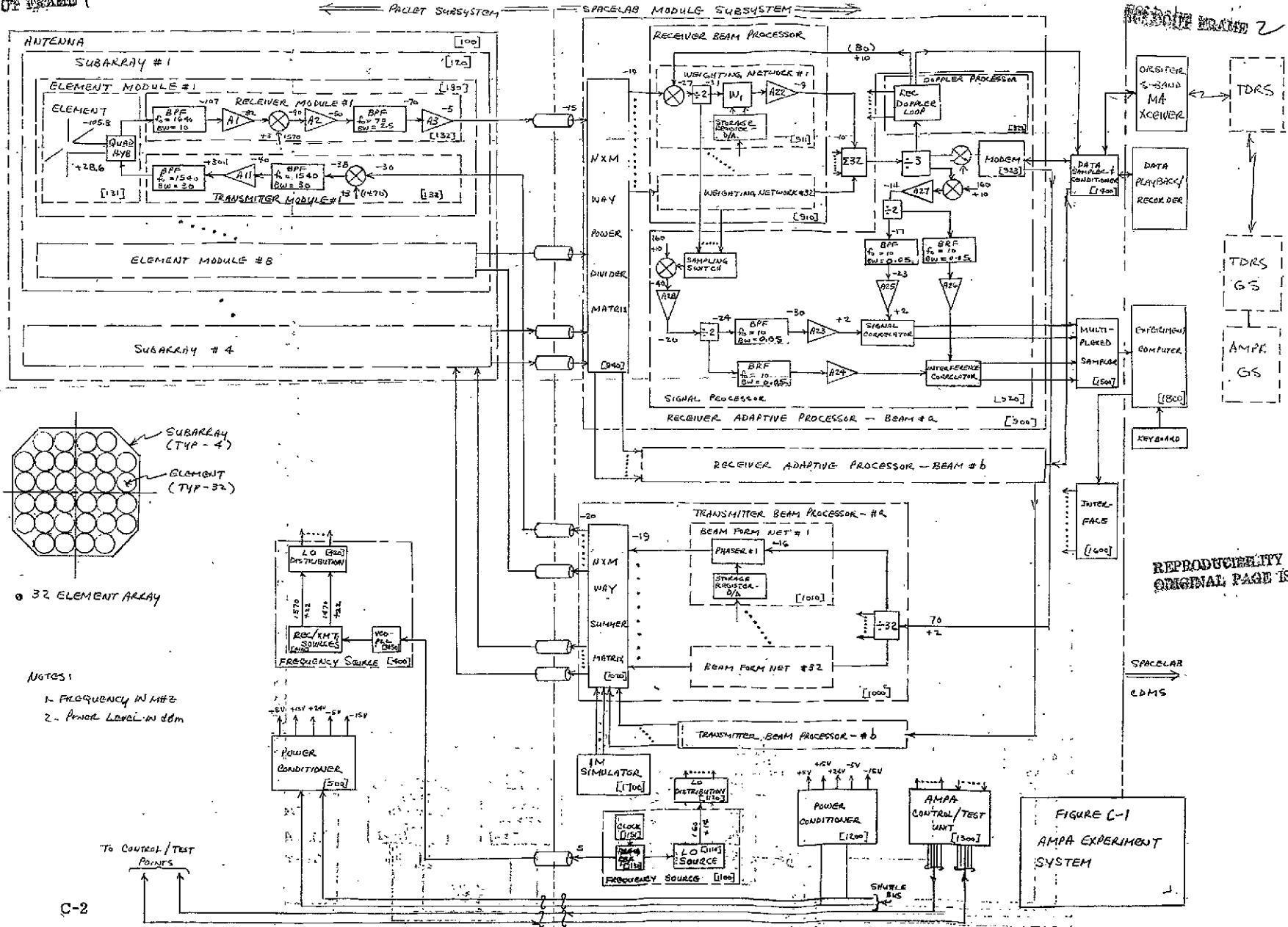
This appendix includes the results of a preliminary analyses of the implementation impact on the Experiment system as a function of the number of beams and number of array elements. A simplified functional block diagram of the Experiment system is shown in Figure C-1, showing the major modules/subassemblies that are mounted on the Pallet and Spacelab module subsystems. This analysis assumes a filled array, and does not include:

- IM Simulator
- Data Conditioner
- Control Unit
- Digital Processor Network

This appendix provides a weight and power breakdown for the cases with 2, 4, and 8 simultaneous independently steerable receive and transmit beams. In addition, this appendix includes alternate array configurations with 64 and 128 elements.

Initially, a weight and power relationship has been developed as a function of the number of array elements (N) and number of beams (M) as shown in Table C-1 for the major module/subassemblies for the AMPA Experiment system. Table C-2 summarizes the total weight and power for the AMPA Experiment system as a function of N and M .

From the weight and power summary, as presented in Table C-2, a 32 element array with two independently steerable receive and two independently steerable transmit beams is well within the estimated weight and power that can be allocated for the AMPA experiment, and is the most cost effective configuration that meets the intent of the AMPA program to test and evaluate an adaptive multibeam phased array in space. There would be nothing to be gained from the experiment by using more than 32 elements and two beams would adequately demonstrate the concept of beam processing.



32 ELEMENT ARRAY

- NOTES:
1. FREQUENCY IN MHz
 2. Power Level in dbm

C-2

FIGURE C-1
AMPA EXPERIMENT SYSTEM

Table C-1. Weight/Power Relationship Vs. Number of Beams and Array Size for AMPA Experiment System

Items	Relationship	
	Weight - KG	Power Watts
A. Pallet Subsystem		
● Antenna Structure	29.55	
● Element Module	29.09K	10+25 (BO/K)
● Frequency Source	6.8+2.3K	5+3K
● Power Conditioner	4.5+4.5K	20K+5M

● Sub-Total	40.85+35.89K	5+33K+5M+25M(BO/K)
B. Module Subsystem		
● Adaptive Processor	10M+11.1KM	10M+23KM
● Transmit Beam Processor	3M+3KM	2M+2KM
● Frequency Source	6.8+2.3K	5+5K
● Power Conditioner	6+5K	30+22M
● Digital Processor Interface	11.8KM	23KM

● Sub-Total	12.8+7.3K+13M+25.9KM	35+5K+34M+48KM
C. Intra-Subsystem Harness	27.3K	
Total	53.7+70.5K+13M+25.9KM	40+38K+39M+48KM+25M(BO/K)

Notes:

(1) K = Array size relative to 32 elements

(2) M = Number of beams

(3) $\frac{M}{2}$ B.O.
 $\frac{M}{4}$ 3 dB = (2)
 $\frac{M}{8}$ 5 = (3.17)
7 = (5)

Table C-2. Total Weight and Power Summary for
AMPA Experiment Subsystem

N	K	M = 2		M = 4		M = 8	
		Wt- (KG)	Pwr-Watts	Wt- (KG)	Pwr-Watts	Wt- (KG)	Pwr-Watts
32	1	202.0	352	279	743	435	1774
64	2	324.0	436	454	814	713	1696
128	4	569	679	802	1195	1269	2290

Notes:

- (1) N = Number of elements
- (2) M = Number of simultaneous receive and transmit beams
- (3) K = Array size relative to 32 elements